

University of Windsor

## Scholarship at UWindor

---

Electronic Theses and Dissertations

Theses, Dissertations, and Major Papers

---

1-1-1970

### An experimental investigation into non-isothermal flow of air in a horizontal pipe.

Muhammad Abbas  
*University of Windsor*

Follow this and additional works at: <https://scholar.uwindsor.ca/etd>

---

#### Recommended Citation

Abbas, Muhammad, "An experimental investigation into non-isothermal flow of air in a horizontal pipe." (1970). *Electronic Theses and Dissertations*. 6844.  
<https://scholar.uwindsor.ca/etd/6844>

This online database contains the full-text of PhD dissertations and Masters' theses of University of Windsor students from 1954 forward. These documents are made available for personal study and research purposes only, in accordance with the Canadian Copyright Act and the Creative Commons license—CC BY-NC-ND (Attribution, Non-Commercial, No Derivative Works). Under this license, works must always be attributed to the copyright holder (original author), cannot be used for any commercial purposes, and may not be altered. Any other use would require the permission of the copyright holder. Students may inquire about withdrawing their dissertation and/or thesis from this database. For additional inquiries, please contact the repository administrator via email ([scholarship@uwindsor.ca](mailto:scholarship@uwindsor.ca)) or by telephone at 519-253-3000ext. 3208.

AN EXPERIMENTAL INVESTIGATION  
INTO THE NON-ISOTHERMAL FLOW  
OF AIR  
IN A HORIZONTAL PIPE

A Thesis  
Submitted to the Faculty of Graduate Studies through the  
Department of Mechanical Engineering in Partial  
Fulfillment of the Requirements for the  
Degree of Master of Applied Science  
at the University of Windsor

by

MUHAMMAD ABBAS

B.E.(MECHANICAL), PESHAWAR UNIVERSITY, PAKISTAN, 1966.

Windsor, Ontario, Canada

1970

UMI Number: EC52782

### INFORMATION TO USERS

The quality of this reproduction is dependent upon the quality of the copy submitted. Broken or indistinct print, colored or poor quality illustrations and photographs, print bleed-through, substandard margins, and improper alignment can adversely affect reproduction.

In the unlikely event that the author did not send a complete manuscript and there are missing pages, these will be noted. Also, if unauthorized copyright material had to be removed, a note will indicate the deletion.

**UMI**<sup>®</sup>

---

UMI Microform EC52782

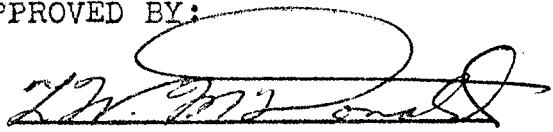
Copyright 2008 by ProQuest LLC.

All rights reserved. This microform edition is protected against unauthorized copying under Title 17, United States Code.

ProQuest LLC  
789 E. Eisenhower Parkway  
PO Box 1346  
Ann Arbor, MI 48106-1346

AAV4276

APPROVED BY:



St. Liduan.

Henry J. Tucker

Robert A. Stager

324390

## ABSTRACT

A comprehensive experimental investigation into the nonisothermal heat transfer from air in a horizontal circular tube under the condition of constant ambient temperature is reported. Radial temperature profiles both along horizontal and vertical diameters, and axial wall and air mean temperatures were measured. The range of inlet air temperature  $t_1$  was from 200°F to 560°F and the range of Reynold's number  $N_{Re_1}$  was from 800 to 18000. The temperature and velocity profiles initially uniform at the entrance developed simultaneously along the tube length. The effect of increasing inlet air temperature on local Nusselt number was seen to be insignificant. Nusselt number varied approximately linearly with inlet Reynolds number for  $N_{Re_1} > 6000$ . At  $N_{Re_1} > 6000$ , the phenomenon of laminar, transition and turbulent boundary layer was encountered which had pronounced effects on the axial distribution of wall temperature and the local Nusselt number. The effects of free convection were observed to be dominant over Reynolds numbers approximately up to 6000.

## ACKNOWLEDGEMENTS

Grateful acknowledgement is made to Professor W. G. Colborne for his help regarding the design and direction of this study. The constant encouragement and thought provoking discussions of Professor T. McDonald have contributed much to this work.

Technical assistance of Messers R. Myers and O. Brudy is sincerely appreciated.

The part of the research sponsored by the National Research Council of Canada is gratefully acknowledged.

## TABLE OF CONTENTS

	Page
ABSTRACT	111
ACKNOWLEDGEMENTS	iv
TABLE OF CONTENTS	v
LIST OF FIGURES	vii
NOTATION	1x
CHAPTER	
1 INTRODUCTION	1
1.1 Background to the Problem	1
1.2 Specific Objectives of the Investigation	3
2 SUMMARY OF PREVIOUS WORK	7
3 APPARATUS AND INSTRUMENTATION	22
3.1 Basic Description	22
3.2 Air Supply System	23
3.3 Flowmeters	23
3.4 Heating System	23
3.5 Mixing Chamber	24
3.6 Thermal Jacket	25
3.7 Test Section	25
3.8 Exhaust Arrangement	26
3.9 Leakage	26
3.10 Temperature Measurement	27
3.11 Traversing Mechanism	28
3.12 Pressure Measurement	28
4 EXPERIMENTAL PROCEDURE AND RESULTS	29
4.1 Procedure	29
4.2 Experimental Results	30
4.3 Experimental Uncertainty	32
5 DISCUSSION	119
5.1 Axial Variation of Mean Fluid Temperature	119
5.2 Axial Variation of Wall Temperature	119
5.3 Radial Temperature Profiles	124
5.4 The Secondary Flow	125
5.5 Circumferential Temperature Distribution	126

	Page
5.6 Effect of Increasing $t_1$ on $N_{Nux}$	127
5.7 Effect of Increasing $N_{Re1}$ on $N_{Nux}$	127
5.8 Effect of X/D Ratios on $N_{Num}$	128
5.9 Comparison with Previous Investigations	128
5.10 Reliability of the Experimental Results	130
 6 CONCLUSIONS	 132
 BIBLIOGRAPHY	 134
 APPENDIX A	 140
 APPENDIX B	 188
 VITA AUCTORIS	 193

## LIST OF FIGURES

- Figure
- 1 SCHEMATIC LAYOUT OF EQUIPMENT
  - 2-4 TYPICAL VARIATION OF AIR MEAN AND WALL TEMPERATURES FOR  $N_{Re_1} < 3000$
  - 5-9 AXIAL VARIATION OF AIR MEAN TEMPERATURE FOR VARIOUS INLET AIR REYNOLDS NUMBERS AND TEMPERATURES ( $200 \leq t_1 \leq 560$  and  $N_{Re_1} < 3000$ ).
  - 10-14 AXIAL VARIATION OF WALL TEMPERATURES CORRESPONDING TO THE AXIAL VARIATION OF AIR MEAN TEMPERATURES SHOWN IN FIGURES 5 TO 9.
  - 15-30 AXIAL VARIATION OF AIR MEAN AND WALL TEMPERATURES FOR HIGHER INLET REYNOLDS NUMBERS ( $4000 < N_{Re_1} < 18000$  AND  $300 \leq t_1 \leq 500$ ).
  - 31-32 GROUPED AXIAL VARIATION OF WALL TEMPERATURES SHOWN IN FIGURES 15 TO 30: FOR  $t_1 = 300$  AND  $500^\circ\text{F}$  RESPECTIVELY.
  - 33-48 RADIAL HORIZONTAL AND PERPENDICULAR TEMPERATURE PROFILES AT VARIOUS  $X/D$  RATIOS AND FOR VARIOUS INLET REYNOLDS NUMBERS AND TEMPERATURES.
  - 49-52 TYPICAL CIRCUMFERENTIAL AND AXIAL VARIATION OF WALL

## TEMPERATURES

- 53-63 EFFECT OF INLET AIR TEMPERATURE ON THE AXIAL VARIATION OF LOCAL NUSSELT NUMBER
- 64-72 EFFECT OF INLET REYNOLDS NUMBER ON THE AXIAL DISTRIBUTION OF LOCAL NUSSELT NUMBER
- 73-74 VARIATION OF LOCAL NUSSELT NUMBER WITH INLET REYNOLDS NUMBER FOR  $t_1 \approx 300$  AND  $500^\circ\text{F}$ .
- 75-76 INFLUENCE OF X/D RATIOS ON THE VARIATION OF  $N_{\text{Num}}$  WITH  $N_{\text{Re}_1}$ 's.
- 77-79 COMPARISON OF THE RESULTS OBTAINED IN THIS INVESTIGATION WITH THE EXPERIMENTAL DATA OF HALL AND KHAN.
- 80 COMPARISON OF THE RESULTS OBTAINED IN THIS INVESTIGATION WITH THE EXPERIMENTAL RESULTS OF MCCOMAS ET AL. AND THE ANALYTICAL PREDICTION OF SIEGEL ET AL.
- 81-82 COMPARISON OF THE PRESENT RESULTS WITH THE NUMERICAL SOLUTIONS OF KAYS FOR VARIOUS WALL BOUNDARY CONDITIONS
- 83-84 REPRODUCIBILITY OF THE EXPERIMENTAL RESULTS
- 85-86 EFFECT OF THE EXTERNAL FORCED DRAFT ON THE REPRODUCIBILITY OF THE EXPERIMENTAL RESULTS

## NOTATION

A	= surface area of pipe, $L^2$
$C_p$	= specific heat at constant pressure, $Q/Mt$
d	= sectional position measured from the wall of the pipe, L
D	= diameter of pipe, L
f	= functional relation
g	= acceleration due to gravity, $L/\theta^2$
h	= film coefficient, $Q/L^2\theta t$
k	= thermal conductivity of air, $Q/L\theta t$
x	= axial distance from the entrance of the pipe, L
q	= rate of heat transfer through pipe wall, $Q/\theta$
$\bar{U}$	= mean or average velocity, $L/\theta$
t	= temperature in degrees Fahrenheit, t
T	= temperature in degrees absolute
w	= mass flow rate, $M/\theta$
$N_{Gr}$	= Grashof number = $\frac{\rho^2 \cdot D^3 \cdot g \cdot \beta \cdot \Delta t}{\mu^2}$
$N_{Gz}$	= Graetz number = $\frac{w C_p}{kX}$
$N_{Nu}$	= Nusselt number = $\frac{hD}{k}$
$N_{Pr}$	= Prandtl number = $\frac{C_p \mu}{k}$
$N_{Re}$	= Reynolds number = $\frac{\bar{U} \rho D}{\mu}$
$N_{Ra}$	= Rayleigh number = $N_{Gr} \cdot N_{Pr}$
$N_{St}$	= Stanton number = $N_{Nu} / N_{Re} \cdot N_{Pr}$

- $N_{Pe}$  = Peclet number =  $N_{Re} \cdot N_{Pr}$   
 $\beta$  = coefficient of thermal expansion =  $\frac{1}{T_0}, \frac{1}{t}$   
 $\mu$  = absolute viscosity, M/L $\theta$   
 $\Delta t$  = difference between bulk mean and wall temperatures  
 $\Delta$  = difference between two values, or small increment  
 $\rho$  = density of air, M/L $^3$   
 $L$  = length, feet  
 $M$  = mass, pounds  
 $Q$  = heat, British Thermal Units  
 $t$  = temperature, Fahrenheit degrees  
 $\theta$  = time, seconds

#### Subscripts

- $b$  = bulk mean, evaluated at bulk mean temperature  
 $i$  = at inlet or entrance  
 $m$  = mean  
 $o$  = ambient  
 $w$  = condition at the wall or evaluated at wall temperature  
 $lm$  = based on logarithmic-mean-temperature difference  
 $a$  = based on arithmetic average temperature  
 $x$  = local axial value

Number within the brackets indicates the reference

## CHAPTER I

### INTRODUCTION

The rate of heat transfer from or to fluids flowing in pipes is of great commercial interest and has been the object of hundreds of investigations over the past eighty years.

#### 1.1 BACKGROUND TO THE PROBLEM

One of the practical problems in heat transfer in horizontal ducts is that the fluid properties vary along all the axes. Neither the wall temperature nor the wall heat flux is constant and uniform. Temperature and velocity profiles keep changing (34) and thus the flow is never thermally or hydrodynamically fully established. The pressure gradients in the radial and axial directions may or may not be constant depending upon the fluid and thermal conditions inside the system. When a fluid flowing in a horizontal circular pipe is heated or cooled at a sufficiently high rate, the radial and axial density gradients, cause a secondary flow of the fluid which is symmetrical about a vertical plane passing through the axis of the pipe. Because this secondary fluid motion carries the fluid from the central part of the pipe to the wall, and the fluid from the wall to the central part of the pipe, the rate of heat transfer is greatly enhanced by the presence of this natural convection.

Due to mathematical limitations, this complex situation is extremely difficult to handle analytically. Therefore, in the past, attempts have been made to simplify the problem by making use of one or more of the following assumptions:

1. Constant and uniform wall temperature.
2. Constant and uniform wall heat flux.
3. Linear variation of wall temperature.
4. Prescribed wall heat flux.
5. Constant fluid to wall temperature difference.
6. Fully developed velocity and temperature profiles at the entrance of the heat transfer section.
7. Simultaneous development of velocity and temperature profiles.
8. Uniform temperature and velocity distributions at the entrance of the heat transfer section.
9. Uniform velocity profiles throughout the test-section.

Some of the above mentioned assumptions have been duplicated experimentally to check the theoretical solutions.

It is apparent that most of these assumptions are not justified for an actual situation. Therefore, an experimental study under the boundary conditions which match the real situation is left as the alternate solution to the problem. With this background in mind, the

investigation was initiated.

## 1.2 SPECIFIC OBJECTIVES OF THE INVESTIGATION

### 1. Buoyancy Effects

The effect of buoyancy together with frictional forces produces the radial and longitudinal pressure gradients, and as a result, velocity and heat transfer characteristics of the basic forced convection will be modified. The presence of natural convection may increase the rate of heat transfer from or to a fluid having a Reynolds number less than 3000 by a factor of three or four (28). Design for free convection differs radically from general commercial practice since low velocity and large tube diameter are important considerations. In the application of heat transfer principles to equipment in which tube lengths are "short", as perhaps in aircraft heaters and in some petroleum refinery equipment, the free convection effect can bear appreciably on the heat transfer surface required. Therefore, the conditions under which the buoyancy effects are significant are of practical interest. To determine these conditions was one of the objectives of this investigation.

### 2. Effect of Thermal Boundary Condition

The variation of the heat transfer coefficient near the entrance of a circular pipe depends not only on the

flow in this region but also on the heat transfer boundary condition (12). The problem of heat transfer from the fluid with a non-isothermal wall operating under constant ambient conditions has never been studied before. Therefore, it was one of the objectives of this study to touch this practical problem and compare the results with hypothetical boundary conditions of (i) constant and uniform wall temperature, (ii) constant and uniform wall heat flux, and (iii) constant fluid to wall temperature difference.

### 3. Data on Local Heat Transfer Characteristics

In order to gain more insight into the effects of natural convection on forced flow, local data seems extremely necessary. Data on local heat transfer may be applied to the design of an exhaust-gas and air heat exchanger. For example, the life of an exhaust-gas and air heat exchanger may depend on the distribution of the local heat transfer rate within the exchanger. Points of high temperature may often cause metal failure, and regions of large temperature gradients cause dangerous thermal stress which decreases the life of the heater. A thorough knowledge of the distribution of the local heat transfer rate would allow a prediction of these effects, and thus a proper design could be established.

It is interesting to note that there is only one study (24) which provides temperature and velocity distributions

(only at one station) in a horizontal tube (constant wall heat flux), both along vertical and horizontal diameters.

The present investigation aims at providing an extensive amount of data on the local heat transfer characteristics at 11 X/D ratios for the cooling of air in a horizontal pipe with no restriction of the thermal boundary at the wall but operated under constant ambient conditions.

#### 4. Effect of Increasing Inlet Air Temperature and Reynolds number

The investigation also seeks to evaluate the effect of increasing inlet air temperature and Reynolds number on the local heat transfer characteristics.

#### GENERAL

Ambient air was forced into a settling chamber by a centrifugal blower. From the settling chamber, it flowed through rotameters then entered the furnace to be heated. The heated air entered the jacketed mixing chamber from which it passed through a bell mouth into the aluminum test pipe. This pipe was 2.87" inside diameter and 33' long. The air cooled and was finally discharged into the atmosphere by the exhaust arrangement. The experiments can be divided into two ranges, i.e., lower range and higher range according to the inlet Reynolds number. In the lower range (900, 1200, 1800, 2800), each value of Reynolds number was

studied against five different inlet air temperatures (200, 300, 400, 500, 550°F). In the higher range (4000, 6000, 8000, 10000, 12000, 14000, 16000, 18000), each value of inlet Reynolds number was studied against two different inlet air temperatures (300, 500°F).

The physically achieved boundary conditions of the problem were (i) uniform temperature and velocity profiles at the entrance of the test-section, and (ii) constant ambient temperature with no forced drafts in the surroundings.

## CHAPTER 2

### SUMMARY OF PREVIOUS WORK

The theoretical study of convective heat transfer with laminar flow in a tube was begun by Graetz and Nusselt. Leveque, Drew, Yamagata, etc., solved the same problem under the condition that the physical properties of the fluid were constant and the flow was axisymmetrical. The theoretical analyses are limited to fully developed laminar flow, i.e. Poiseuille flow, and the temperature distribution is obtained by putting this velocity distribution into the energy equation. These theoretical analyses are the same whether the tube axis is horizontal or vertical. The results obtained by experiments on convective heat transfer with laminar flow in horizontal tubes show higher heat transfer co-efficients than those obtained by theoretical studies as mentioned above.

Drew (9) introduced empirical formulae by correlating experimental results and pointed out that they were higher by 20-50 per cent than the values resulting from the theoretical analysis of Leveque and others.

Colburn (6) was the first one to examine the effects of natural convection quantitatively. This pioneer work led to the equation :

$$N_{Nu_{am}} = 1.75 N_{Gz_m}^{1/3} \phi^{1/3} \dots\dots\dots(2.1)$$

where

$$\phi^{1/3} = \left( \frac{\mu_b}{\mu_f} \right)^{1/3} (1 + 0.015 N_{Grf}^{1/3}) \dots\dots\dots(2.2)$$

$$N_{Nu_{am}} = \frac{h_{am}D}{k}$$

$$N_{Gz_m} = \frac{WC_p}{kX}$$

$$N_{Grf} = \frac{\beta_f D^3 \rho_f^2 g \Delta t}{\mu_f^2}$$

$\mu_b$  = viscosity of fluid at mean fluid temp.

$\mu_f$  = viscosity of fluid at film temp.

The correction factor  $\phi$ , which allowed for the radial variation of fluid properties and natural convection, was evaluated from data obtained both in vertical and horizontal tubes.

Martinelli and Boelter (20) presented the following equation for a system of superposed free and forced convection in a horizontal tube :

$$N_{Nu} = 1.75 F_1 \sqrt[6]{(N_{Gz})^2 + \left[ 0.0722 F_2 \left( \frac{N_{Gr} N_{Pr} D}{x} \right)_w^{0.84} \right]^2} \dots(2.3)$$

In equation (2.3) the Nusselt number is based on the arithmetic-mean temperature difference (the arithmetic average of the initial and final temperature differences). The Graetz number is calculated using the mean fluid temperature, and the Grashof Prandtl -  $\frac{D}{L}$  term is based on

fluid properties at the temperature of the wall. The factors  $F_1$  and  $F_2$  are functions of  $N_{Nu} / N_{Gz}$ . In the above equation, the Graetz number was squared to account for the horizontal forces influencing the heat transfer, and the Grashof Prandtl -  $\frac{D}{L}$  term was squared to take care of the vertical forces influencing the heat transfer. In other words, because these forces act at 90 deg. to each other in a horizontal tube, the term represented by the radical was considered to be the vectorial sum of two sets of forces. This equation is for fully developed flow with constant wall temperature and therefore is not suited for comparison with developing flow data.

Latzko (19) developed turbulent forced convection solutions with both hydrodynamic and thermal entrance regions with uniform wall temperature conditions. His solutions are valid for Prandtl modulus equal to unity and for systems where heat is only transferred by convection.

Boelter, Young and Iverson (3) presented experimental local heat transfer data for air in the entrance section of a uniform wall temperature circular tube for 16 different entrance conditions. In many cases their experimental values are appreciably higher than those derived from equations. The data indicated that (except for a bell mouth) the entrance lengths for the specific conditions given were about  $X/D = 17$  or greater.

Poppendick and Palmer (29,30) studied analytically the convective heat transfer in the entrance region of parallel plates and ducts. The fluid in the channel was liquid metal and the wall temperature was uniform and constant. The solutions were based on the postulate that all the heat was transferred by means of the conduction mechanism and that the fluid properties were invariant with temperature.

McAdams (21) gave the following formula for the heat transfer coefficient for the constant wall temperature case.

$$\frac{h_a D}{k} \left( \frac{\mu_w}{\mu_b} \right)^{0.14} = 1.75 \sqrt[3]{\frac{W C_{pb}}{k_b X}} + 0.04 \left[ \frac{D}{L} N_{Gr} N_{Pr} \right]_b^{0.75} \dots (2.4)$$

where  $N_{Gr}$  is based on tube diameter and  $\Delta t_a$ .

Kays (15) presented numerical solutions for laminar flow heat transfer in circular pipes using developing velocity profiles. The solution of Langhaar(18) was employed to provide velocity profiles which were introduced into the energy equation for three boundary conditions, i.e., constant wall temperature, constant wall-to-fluid temperature difference and constant heat input per unit of the tube length. The solutions are restricted to fluids with  $N_{Pr} = 0.7$  and with velocity and temperature profiles uniform at the tube entrance. His numerical solutions gave good agreement with experimental results while differing considerably from solutions based on parabolic profiles

throughout the tube. Suggested equations are :

1. Constant wall temperature, Langhaar velocity profiles

$$N_{Nu_m} = 3.66 + \frac{0.014 \left[ \frac{N_{Re} N_{Pr}}{X/D} \right]}{1 + 0.016 \left[ \frac{N_{Re} N_{Pr}}{X/D} \right]^{0.8}} \quad \dots(2.5)$$

2. Constant temperature difference, Langhaar velocity profiles

$$N_{Nu_m} = 4.36 + \frac{0.10 \left[ \frac{N_{Re} N_{Pr}}{X/D} \right]}{1 + 0.016 \left[ \frac{N_{Re} N_{Pr}}{X/D} \right]^{0.8}} \quad \dots(2.6)$$

3. Constant heat flux, Langhaar velocity profiles.

$$N_{Nu_x} = 4.36 + \frac{0.036 \left[ \frac{N_{Re} N_{Pr}}{X/D} \right]}{1 + 0.0011 \left[ \frac{N_{Re} N_{Pr}}{X/D} \right]} \quad \dots(2.7)$$

Deissler (7) investigated analytically the influence of Reynolds number, Prandtl number, initial velocity distribution, passage shapes and variable fluid properties on the turbulent heat transfer in the entrance region of smooth passages. Predictions are summarized below :

1. The thin thermal boundary layers and consequently severe temperature gradients at the wall near the entrance, produce high heat transfer co-efficients. Fully developed heat transfer was obtained in less than 10 diameters.
2. The effect of the wall boundary condition and of the

passage shape (round tube or parallel plates) on heat transfer in the entrance regions was small.

3. The use of a uniform rather than a fully developed initial velocity profile increased heat transfer co-efficients in the entrance region.

4. In general, the entrance effect for heat transfer decreased as the Prandtl number increased above 1.

Morton (26) made a theoretical analysis by setting up the equation of motion including the buoyancy term and the equation of energy simultaneously and obtained the following formula for low Rayleigh number,  $N_{Ra}$  :

$$N_{Nu} = \frac{48}{11} \left[ 1 + (0.0505 - 0.1054N_{Pr} + 0.3334N_{Pr}^2) \left( \frac{N_{Re}N_{Ra}}{4608} \right)^2 + \dots \right] \dots (2.8)$$

The formula is restricted to steady laminar motion of a fluid along a horizontal circular pipe with a fully developed velocity profile and a uniform heat flux at the wall, in a range of  $N_{Re}N_{Ra} < 3000$ . In this regards, Mori's (25) comments are noteworthy. He states, "within this range of  $N_{Re}N_{Ra}$  the effects of natural convection do not exceed several percent. As the Rayleigh number is proportional to the fourth power of the diameter, the natural convection has small effect on convective heat transfer in a horizontal tube of less than  $\frac{1}{4}$ " diameter. But in comparatively large tubes, the effect seems to be quite considerable."

Jackson, Spurlock and Purdy (13) studied heat transfer to air in a constant temperature horizontal tube, their results being well represented by the following semi-theoretical equation :

$$N_{Nu_{lm}} = 2.67 \left[ (N_{Gz})_b^2 + (0.0087)^2 + \left\{ (N_{Gr})_{lm} N_{Pr} \right\}_w^{1.5} \right]^{1/6} \dots (2.9)$$

The terms in square brackets result from the vectorial addition of the free and forced convective flows, this method originally being suggested by Martinelli and Boelter as a possible means of adapting their equation to the case of flow in horizontal tubes. The apparatus used by Jackson et al. was fitted with a sharp edge entrance and therefore was not capable of producing uniform or fully established velocity profiles at the entrance. The reader should note that in the original equation (2.3) proposed by Martinelli and Boelter, the constant outside the brackets is 1.75 while in equation (2.9) it is 2.67. Perhaps the most interesting feature of equation (2.9) is the disappearance of the ratio  $D/X$  from the natural convection term of equation (2.3).

Mills (23) determined local heat transfer characteristics experimentally for air flowing turbulently in the entrance of a circular duct over a flow Reynolds number range of 10000 to 110000. A wall boundary condition of uniform heat flux was imposed. His data for heat transfer under

fully developed conditions was correlated by the following equation :

$$N_{Nu} = 0.0397 N_{Re}^{0.73} N_{Pr}^{0.33} \dots\dots(2.10)$$

Maximum deviation of five per cent was claimed. The velocity and temperature profiles were uniform at the start of the heated section. The shape of the curves illustrated the growth of the boundary layer and the resultant phenomenon, i.e. the local heat transfer co-efficients decreased rapidly from a very high value in the laminar flow region until a point of transition to a turbulent boundary layer was reached. After passing through the minimum, the value was raised again probably to a corresponding value for the turbulent flow.

Oliver (28) attempted to investigate whether the type of equation originally proposed by Martinelli and Boelter for the vertical tubes could be adapted to work on horizontal tubes or whether the experimental evidence available suggested the need for a more elaborate correlation. His experimental work dealt with the laminar flow of relatively non-viscous Newtonian liquids through a horizontal jacketed tube with a calming section upstream of the test-section. He compared the empirical relations proposed by Martinelli et al. and McAdams with his data and relevant data from the literature. Comparison showed that the empirical relations did not represent the data adequately. He pointed out that

McAdams' relationship grossly underestimated the effects of natural convection except at the highest values of

$\left(N_{Pr_m} N_{Gr_m} \frac{D}{X}\right)$ . Oliver also compared his results for heating and cooling water with the predictions of Jackson, Spurlock and Purdy's relationship (equation 2.9). The theoretical results were higher. He pointed out that this behaviour was not caused by the "vectorial" form of the equation but by the fact that the physical properties of the fluid were evaluated under wall conditions rather than under bulk conditions. The author concluded that when the group

$\left(N_{Gr_m} N_{Pr_m} \frac{D}{X}\right)$  was taken as the factor controlling natural convection, the information obtained in the tubes of different dimensions was inconsistent, and better agreement could be obtained by omitting  $D/X$  from the group. Further improvement resulted by incorporating the ratio  $X/D$ , all data being adequately presented by the following equation :

$$N_{Nu_{am}} \left(\frac{\mu_w}{\mu_b}\right)^{0.14} = 1.75 \left[ N_{Gz_m} + 5.6 \cdot 10^{-4} \left( N_{Gr_m} N_{Pr_m} \frac{X}{D} \right)^{0.7} \right]^{1/3} \dots(2.11)$$

This equation becomes inaccurate when  $N_{Gz_m} < \pi N_{Nu_{am}}$  and the power of  $X/D$  is only provisional.

Hall and Khan (12) investigated the effects of the thermal boundary condition on the heat transfer in the inlet region of a circular pipe. They provided an experimen-

tal comparison between uniform wall temperature and uniform wall heat flux boundary conditions for the case when the velocity profile was uniform at the entrance of the test-section. They concluded from their experiments that there was little difference between the results for the two boundary conditions if the Reynolds number was greater than  $5 \times 10^4$ . At a Reynolds number of  $8 \times 10^3$  the Stanton number for the case of uniform heat flux exceeded that for uniform wall temperature by about 30 per cent. The form of variation in Stanton number was consistent with the model studied by Mills (23); that was, a laminar boundary layer giving way to a turbulent boundary layer which then grew to fill the tube.

Brown and Thomas (4) studied combined free and forced convection heat transfer in constant wall temperature horizontal tubes. Water was used as the test fluid. Their experimental data could not be reconciled with any of the existing horizontal tube formulae including those of McAdams (21) and Oliver (28). They used three test sections of  $\frac{1}{2}$ " diameter, 6' long;  $\frac{1}{2}$ " diameter, 4' long; and 1" diameter 6' long. A smooth contraction at the entrance was used to provide a flat velocity profile at entry to simulate as nearly as possible the normal heat exchanger entry conditions. For the sake of comparison they also carried out tests without the smooth contraction at the entrance. They found that the results taken with a bell

mouth entrance were practically identical with those without, indicating that the initial velocity profile had little effect on the heat transfer under the conditions of their investigation. Their experimental data gave the following equation :

$$N_{Nu} \left( \frac{\mu_w}{\mu_b} \right)^{0.14} = 1.75 \left[ N_{Gz} + 0.012 (N_{Gz} N_{Gr}^{1/3})^{4/3} \right]^{1/3} \dots (2.12)$$

They claimed that their equation correlated their data to within  $\pm 8$  per cent and the majority of the published data, irrespective of fluid, to within  $\pm 50$  per cent. They also pointed out that the best previous correlation (i.e. Oliver's (28)) correlated those same data to within  $-25$  per cent  $\checkmark$   $+110$  per cent. All the properties were evaluated at average bulk temperature.

McComas and Eckert (22) studied the effect of free convection on laminar forced flow heat transfer in a horizontal tube having uniform heat flux. Air was used as the working fluid. An unheated entrance length established the velocity profile before the air entered the heated section. Heat transfer data were obtained for the Reynolds number range from 900 down to 100. The Grashof number was varied from 1000 down to the order of one. They noted that for the same value of Reynolds number, the effect of different Grashof numbers on the tube wall temperature was considerable. For lower  $N_{Gr}$ , after a few diameters, the wall to

bulk temperature difference remained constant. On the other hand for the higher  $N_{Gr}$  runs, a decrease in the local wall to bulk temperature difference occurred after a maximum had been reached. From that observation they concluded that a considerable starting length appeared necessary for the establishment of free convection effect. They further explained that when the secondary flow was established, an increase in the heat transfer occurred causing a decrease in the required difference between the wall and the bulk temperatures.

Mori et al. (24,25) investigated experimentally and theoretically the effects of buoyancy on forced convection in horizontal tubes under the condition of constant heat flux at the wall. In their experimental study they used a brass tube of 35.6 millimeter I.D. Air was passed through a 7 meter long unheated section to have a fully developed velocity profile before it entered the test section. Velocity and temperature profiles were measured in horizontal and vertical diameters only at one station, where flow was thermally established and the wall temperature gradient was constant. Their findings are :

1. When the product of Reynolds number  $N_{Re}$  and Rayleigh number  $N_{Ra}$  is more than  $10^4$ , the secondary flow is stronger.
2. For laminar flow, measured velocity distribution is remarkably different from the velocity distribution of Poiseuille flow.

3. In laminar flow, the effect of buoyancy on local Nusselt number  $N_{Nu}$  appears at about  $N_{Re}N_{Ra} = 10^3$ , and  $N_{Nu}$  increases substantially due to the secondary flow caused by buoyancy and becomes twice as large as Nusselt number without secondary flow at  $N_{Re}N_{Ra} = 4 \times 10^5$ .
4. For turbulent flow, the effect of secondary flow on the temperature and velocity distribution is very small.

The same authors also studied the patterns of secondary flow due to buoyancy in flow visualization experiments. They noted that when the temperature of the tube was higher than that of the fluid, the fluid in the core region went down due to gravitational forces, stagnated at the bottom, went upwards along the wall and stagnated again at the top, changing its flow direction.

Shannon and Depew (32) investigated the influence of free convection on forced laminar flow of water initially at the ice point. The flow was horizontal in a circular tube with a uniform wall heat flux and a fully developed velocity profile at the onset of heating. Local measurements were made for the calculation of Nusselt number, Reynolds number and Grashof number. Reynolds number ranged from 120 to 2300. Nusselt number was not significantly affected in the thermal entry region, but increases in Nusselt number up to 150 per cent were discovered far down the tube at  $X/D \approx 700$ , when compared with the predicted equation

of Siegel et al. (31).

Back et al. (1) carried heat transfer measurement along the wall in the thermal entrance region of a high turbulent airflow through a cooled tube 5" diameter and 43" long. There was simultaneous development of velocity and temperature profiles along the tube. The measurements were made over the range of Reynolds number from  $7 \times 10^4$  to  $10^6$ , and the wall to gas temperature ratio from  $1/3$  to  $2/3$ , included natural boundary-layer transition data in laminar, transition and turbulent boundary-layer regions, and the forced transition data obtained with a trip at the tube inlet.

Newell and Bergless (27) presented an analysis to determine the effects of free convection on fully developed laminar flow in a horizontal circular tube with uniform heat flux at the wall. Solutions for heat transfer and pressure drop were obtained for water with two limiting tube wall conditions : low thermal conductivity (glass tube) and infinite thermal conductivity. At modest  $\Delta t$ , extensive stratification of the flow was predicted, with the tube wall exhibiting a large circumferential temperature gradient. Due to the secondary flow, Nusselt numbers were higher than the values predicted for constant property Poiseuille flow.

After going through the summary of "Previous work", it is not difficult to realize that the scant experimental

data available on heat transfer characteristics (both local and mean ) for the value of Reynolds number  $< 10^4$  are highly contradictory and have not up to now, received a correct physical interpretation. Consequently, a practical method for calculating the heat transfer in many real problems has not yet been developed.

## CHAPTER 3

### APPARATUS AND INSTRUMENTATION

The research facility used for this study was designed using the experience gained from previous similar studies. It consisted of a centrifugal blower, settling chamber, flowmeters, heating system, mixing chamber, bell mouth entrance, test section and exhaust arrangement. This chapter is devoted to the brief description of the principal components of the test installation and the instruments employed for various measurements.

#### 3.1 BASIC DESCRIPTION

Ambient air was forced by a centrifugal fan into the settling chamber from which it was lead to the flowmeter through a gate valve. This measured air was then piped to the furnace to be heated to any desired temperature. From the furnace, the heated air entered the jacketed isothermal mixing chamber and subsequently into the aluminum test pipe the entrance to which was a bell mouth. Heat was given up by the air as it passed through the test section. The air was then discharged into the atmosphere by means of an exhaust system. The experimental set up is shown in figures 1a.&1b.

### 3.2 AIR SUPPLY SYSTEM

Ambient air was supplied by a Canadian Buffalo centrifugal fan, size and type 4½E, driven at 3500 rpm by a 3 phase G.E. 5 HP A.C. motor. Air from the blower was discharged into a cylindrical settling chamber 2' in diameter and 2' long, fitted with a baffle at the centre to avoid direct passage. The 5" dia. outlet of the fan and the inlet to the settling chamber were joined by a flexible pipe 5" in diameter and 1' long to prevent any vibration effects being transmitted to the rest of the equipment. The exit side transition of the settling chamber was also connected by a flexible rubber pipe to a 2" I.D. copper pipe leading the air to the flowmeters.

### 3.3 FLOWMETERS

The volume of air was controlled by gate valves and measured by means of two Brooks high accuracy flowmeters whose calibrated accuracy was within 1 per cent. The low range rotameter was capable of measuring 1.0 to 10.5 SCFM and the high range from 6.0 to 54.5 SCFM at 14.7 psia and 70°F. Chromel constantan thermocouples were installed at the exit of each rotameter to determine the temperature of air for use in making corrections for density.

### 3.4 HEATING SYSTEM

The air from the rotameter entered the furnace at the

bottom through a diverging cone fitted with a conical baffle at the centre to distribute the air uniformly across the heating elements. There were seven stove heating elements of 2000 watts each. The bottom element was controlled through a variac for the purpose of fine temperature control. The remaining 6 elements were controlled independently by means of three way switches (high, low, medium). In between every two elements a perforated screen was fixed to distribute the heat uniformly in the entire section. The furnace was covered with approximately 3" thick insulation of glass wool and a special putty to reduce the heat losses to the ambient air. The top of the furnace converged conically to a  $2\frac{1}{2}$ " I.D. to provide better mixing and thus uniform temperature to the leaving air.

### 3.5 MIXING CHAMBER

The heated air from the furnace entered the isothermal mixing chamber which was 9" I.D. and 18" long. This chamber was provided with two wire mesh screens to reduce irregularities in the flow before it entered the bell mouth section. Three thermocouples were installed to measure the centre line temperature between the two screens and the wall temperatures (side and top) of the mixing chamber. The centre temperature could be compared with the wall temperature to check the stratification in the chamber. Between the test pipe and the mixing chamber was fitted the bell

mouth section designed (33) to give a uniform velocity profile at the entrance of the test-section. A thermocouple was installed at the centreline of bell mouth exit in order to know the temperature of the air entering the test section. For the use in the calculations, a ten point (centres of equal areas) temperature profile at the entrance was obtained.

### 3.6 THERMAL JACKET

The purpose of the thermal jacket was to eliminate stratification by keeping the mixing chamber and bell mouth section isothermal. The air at the test-pipe entrance would then have a uniform temperature profile. It consisted of a special Glas-Col asbestos and glass fabric cover with one circuit of 1850 watts, 208 volts - single phase. It was connected to a variac to allow for fine control of the mixing chamber wall temperature.

### 3.7 TEST SECTION

The test-section consisted of a 33' long aluminum pipe, 3.0" outside and 2.87" inside diameter. The test pipe consisted of three sections, two 12' long and one 9' long joined by removable clamps. Sixteen stations at X/D ratios of 0.0, 1.6, 4.0, 7.0, 10.0, 15.0, 22.0, 32.0, 56.5, 67.0, 77.0, 87.0, 97.0, 113.0 and 133.0 were provided for the measurement of wall temperature, temperature

and/or velocity profiles. At each station, two access slots (top, side) were made to allow for the measurements both along vertical and horizontal diameters. After careful study of preliminary data from the above mentioned 16 stations, the number was reduced to 11 X/D ratios of 0.0, 4.0, 10.0, 22.0, 32.0, 42.0, 56.5, 77.0, 97.0, 113.0 and 133.0.

### 3.8 EXHAUST ARRANGEMENT

The air from the test pipe was discharged into the atmosphere by the exhaust arrangement. This consisted of a vertical circular conduit 18" in diameter and  $4\frac{1}{2}$ ' long made of sheet metal, supported on a rectangular steel structure such that the lower end of the conduit was approximately 2' above the floor level. On the upper end of the conduit, at the top of a slanting roof type transition, a fan of 60 CFM capacity was installed to exhaust the hot air coming from the test pipe, into the atmosphere. This arrangement protected the outlet of the test pipe from room drafts.

### 3.9 LEAKAGE

To check the leakage of air at various joints in the system, the extreme end of the test pipe was blocked under full fan pressure and soap solution was used to detect the air leakage. No trace of leakage was detected along the

test pipe. There was some leakage from the furnace joints which was eliminated by using air-tight gaskets and asbestos paper packings with a special cement.

### 3.10 TEMPERATURE MEASUREMENT

Temperature measurements were made for (1) ambient air (2) air leaving the rotameters (3) air leaving the furnace (4) air at the centre line of mixing chamber (5) wall (top, side) of the mixing chamber (6) air at the exit of the bell mouth section (7) wall (top, side, bottom) of the test pipe and (8) air in the test pipe at various axial locations mentioned earlier. Ambient air temperature was measured by means of accurate thermometers positioned along the pipe and at a distance of  $1\frac{1}{2}$ ' from it. All other temperatures were measured by 24 gauge 9B4B7 type chromel constantan thermocouples.

Temperature profiles were measured by means of a 90 degree chromel constantan thermocouple probe designed for a previous investigation (2). The probe was designed with a contact point at a known distance from the thermocouple junction. This contact point completed an electric circuit when it touched the wall and thus provided a reference point from which to start the traverse.

All the thermocouples were connected to Thermovolt Instruments 24 point rotary switches. The outputs were measured with a Leeds and Northrup 8686 Millivolt Potentio-

meter. A Thermo Electric Frigistor Reference Chamber (32°F) was used for the thermocouple reference junctions.

### 3.11 TRAVERSING MECHANISM

The traversing mechanism consisted mainly of a threaded rod, probe holder and an indicating dial capable of positioning the probe with an accuracy of 0.008". The thermocouple probe could be aligned parallel to the pipe axis with the help of a pointer. The traversing mechanism was designed for previous studies (2, 10).

### 3.12 PRESSURE MEASUREMENT

The laboratory barometer, accurate to  $\pm 0.01$ "Hg. was used to measure the ambient air pressure.

## CHAPTER 4

## EXPERIMENTAL PROCEDURE AND RESULTS

## 4.1 PROCEDURE

Heat transfer data obtained in this investigation was based on 48 tests. The inlet Reynolds number and temperature ranges studied were from 800 to 18000 and 200 to 550°F respectively. The complete data is tabulated in appendix A.

The following measurements were recorded for each test after having attained a steady state :

1. Barometric pressure.
2. Ambient air temperature at various positions along the pipe length.
3. Centre line and circumferential temperature of the mixing chamber.
4. Centre line temperature at the entrance to the test-section.
5. Radial temperature profiles both along vertical and horizontal diameters at each of the X/D ratios.
6. Circumferential wall temperatures (top, side, bottom) at each of the X/D ratios.
7. Volume flow rate of air in the pipe.

In order to have a selected temperature at the inlet of the test-section with (i) steady state condition

(ii) the wall and centre line temperature of the mixing chamber approximately equal by making use of the thermal jacket, the time taken for the process was normally from 20 to 30 hours for each test depending upon the inlet temperature and Reynolds number.

Stability of each experiment was ensured by checking the key point observations periodically.

#### 4.2 EXPERIMENTAL RESULTS

1. Figures 2 to 4 show the typical variation of mean air temperatures ( $t_m$ ) and wall temperatures ( $t_w$ ) with  $X/D$  for  $N_{Re_1} < 3000$ . For various flow rates and inlet air temperatures, the axial variation of mean air temperatures are grouped in figures 5 to 9 and their corresponding axial variation of wall temperatures in figures 10 to 14. The dependence of  $t_m$  and  $t_w$  curves on the inlet Reynolds number in the range of  $4000 \leq N_{Re_1} \leq 18000$ , for  $t_1 \simeq 300^\circ\text{F}$  &  $500^\circ\text{F}$ , is shown in figures 15 to 22 and 23 to 30 respectively. In graphs 31 and 32 are shown the isolated  $t_w$  curves ( $6000 \leq N_{Re_1} \leq 18000$ ,  $t_1 \simeq 300^\circ\text{F}$  &  $500^\circ\text{F}$ ) from their corresponding  $t_m$  curves, to demonstrate the consistency of the observed trend.

2. Radial horizontal and perpendicular temperature profiles at various  $X/D$  ratios are shown in figures 33 to 48 for various inlet Reynolds numbers and temperatures.

3. The effects of free convection on circumferential

temperature variation are demonstrated in figures 49 to 52.

4. The influence of increasing inlet air temperature on the local Nusselt number along the pipe length is shown in graphs 53 to 63.

5. Figures 64 to 72 show how the rate of local heat transfer is affected when the inlet air Reynolds number is increased. These figures demonstrate such effects for both low and high Reynolds numbers at various inlet air temperatures.

6. Figures 73 and 74 illustrate the dependence of the local Nusselt number on the inlet Reynolds number when the  $X/D$  ratio is held constant.

7. Figures 75 and 76 show the results of calculating the mean Nusselt numbers for different tube lengths at various inlet Reynolds numbers.

8. The experimental results of Hall and Khan (12) for thermal boundary conditions of uniform wall temperature and uniform wall heat flux are compared with the results of the present investigation in figures 77 to 79. This shows the effect of the thermal boundary condition on the local heat transfer coefficient.

9. Figure 80 provides a comparison between the results of this study, experimental results of McComas and Eckert (22), and the prediction of Seigel et al. (31), to show the effects of free convection on the local Nusselt number.

10. Numerical solutions of Kays (14) for laminar flow heat transfer for different wall boundary conditions and Langh-

air's developing velocity profiles are compared in fig. 81 and 82 with the results of this study to shed some light on the extent of heat transfer by free convection.

11. Figures 83 and 84 show the reproducibility of the experimental results of this investigation for tests run at different times.

12. Figures 85 and 86 demonstrate the influence of forced external draft on the axial variation of wall temperature and mean air temperature; and the local rate of heat transfer respectively. The external draft was produced by a fan operating in the room so as to cause forced convection over the surface of the test section.

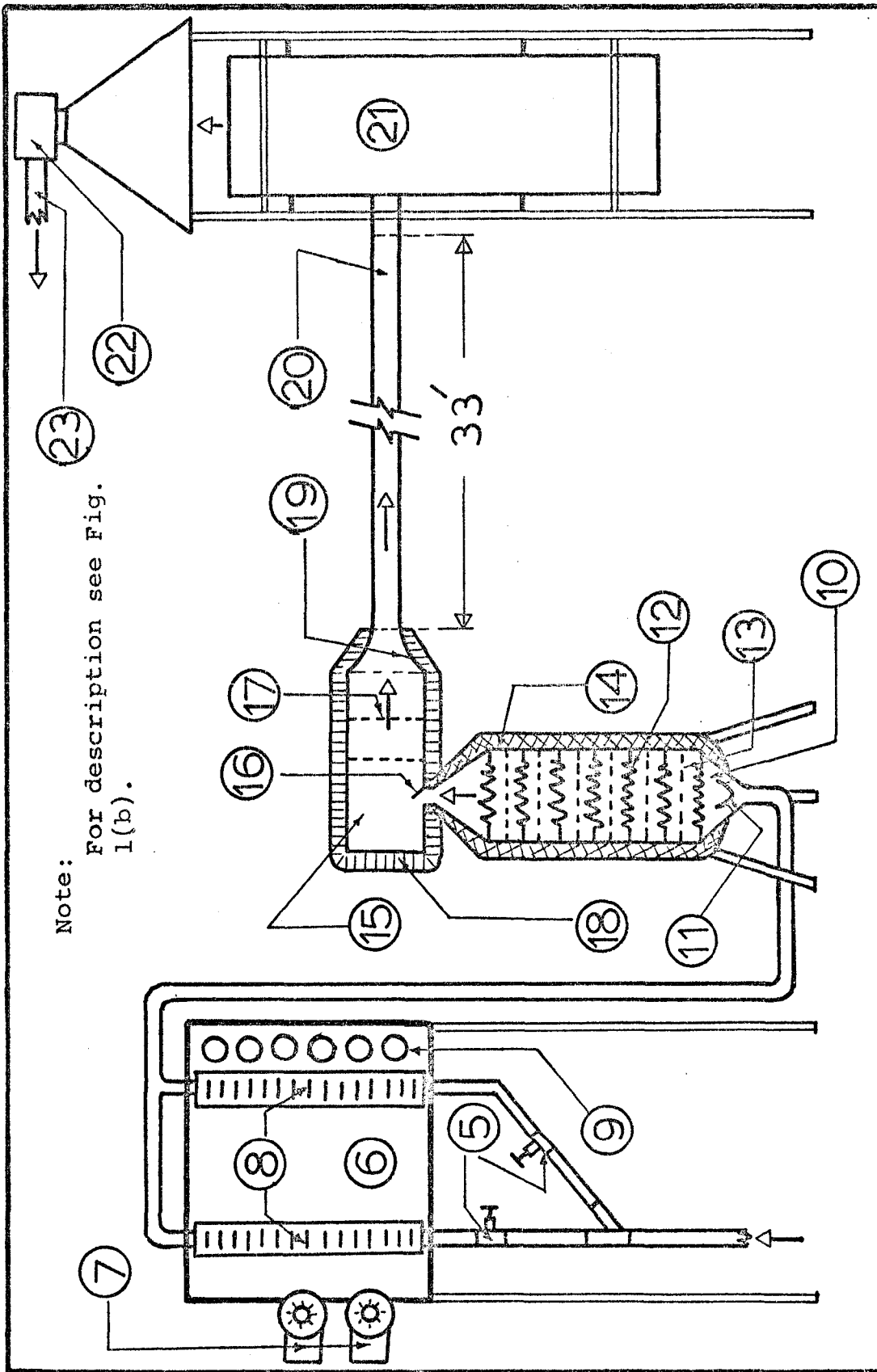
#### 4.3 EXPERIMENTAL UNCERTAINTY

1. The various measured quantities and the properties of air employed in the computation of local Nusselt numbers and other dimensionless parameters were within the limits as shown below:

Barometric pressure .....	= $\pm 0.3$ " Hg
Ambient air temperature .....	= $\pm 2.0$ °F
Rotameter readings .....	= $\pm 1.0$ %
Wall and air temperatures .....	= $\pm 0.3$ °F
Pipe diameter .....	= $\pm 0.006$ "
Thermal conductivity of air, $k$ ....	= $\pm 0.8$ %
Specific heat of air, $C_p$ .....	= $\pm 0.16$ %
Viscosity of air, $\mu$ .....	= $\pm 0.8$ %

Using the above mentioned intervals, the calculations for several representative test runs showed that the maximum possible uncertainty in the values of local Nusselt numbers was approximately  $\pm 15$  percent.

2. The calculations accounting for the heat losses due to radiation from the thermocouple probe showed that the correct values of local Nusselt numbers could be as low as 16 percent than those shown in graphs and in appendix A.



Note:  
For description see Fig.  
1(b).

Fig. 1(a). Schematic Diagram of the Test Facility. Front View.

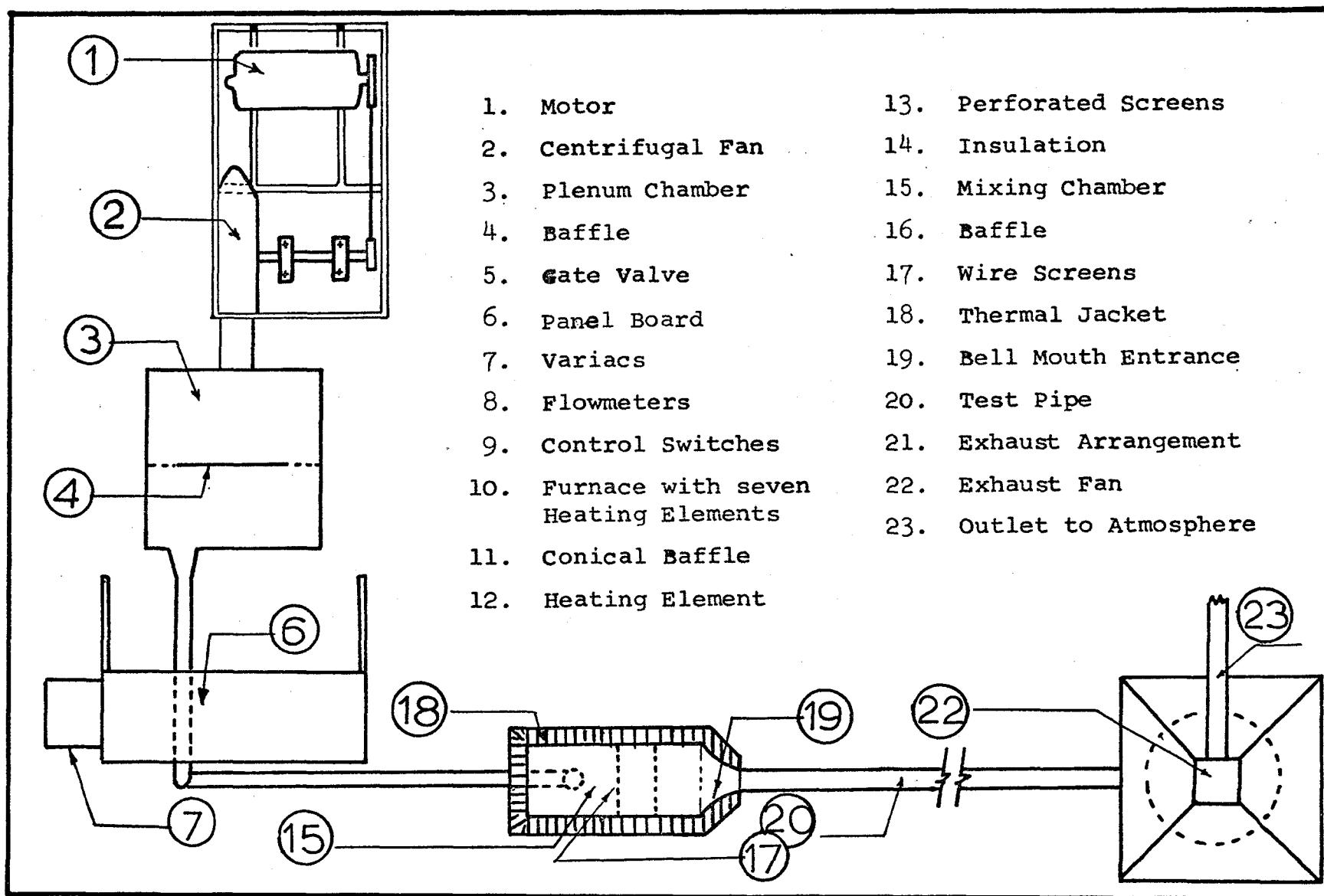


Fig. 1(b). Schematic Diagram of the Test Facility. Top View.

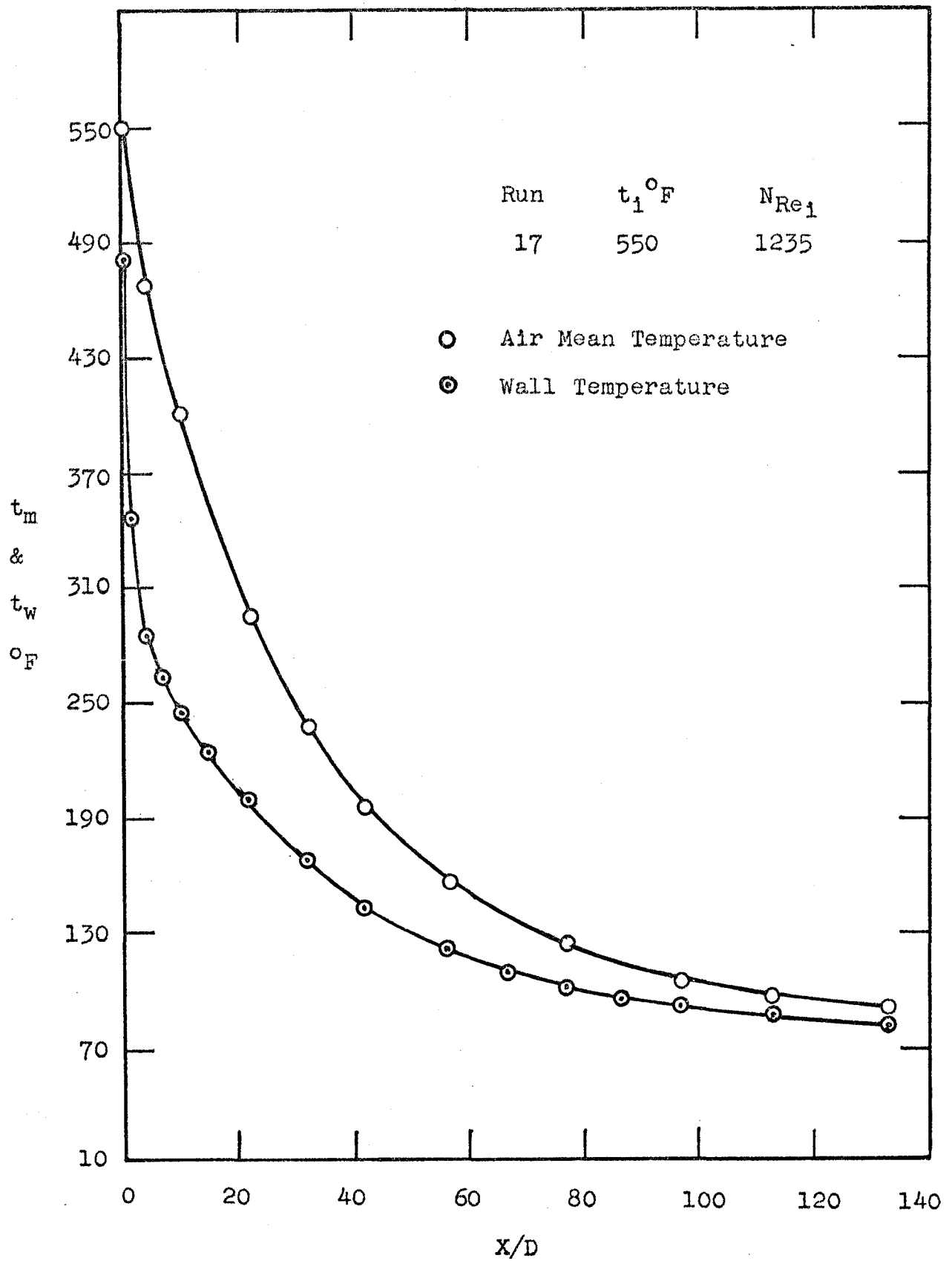


Fig. 2. Axial Variation of Air Mean and Wall Temperatures

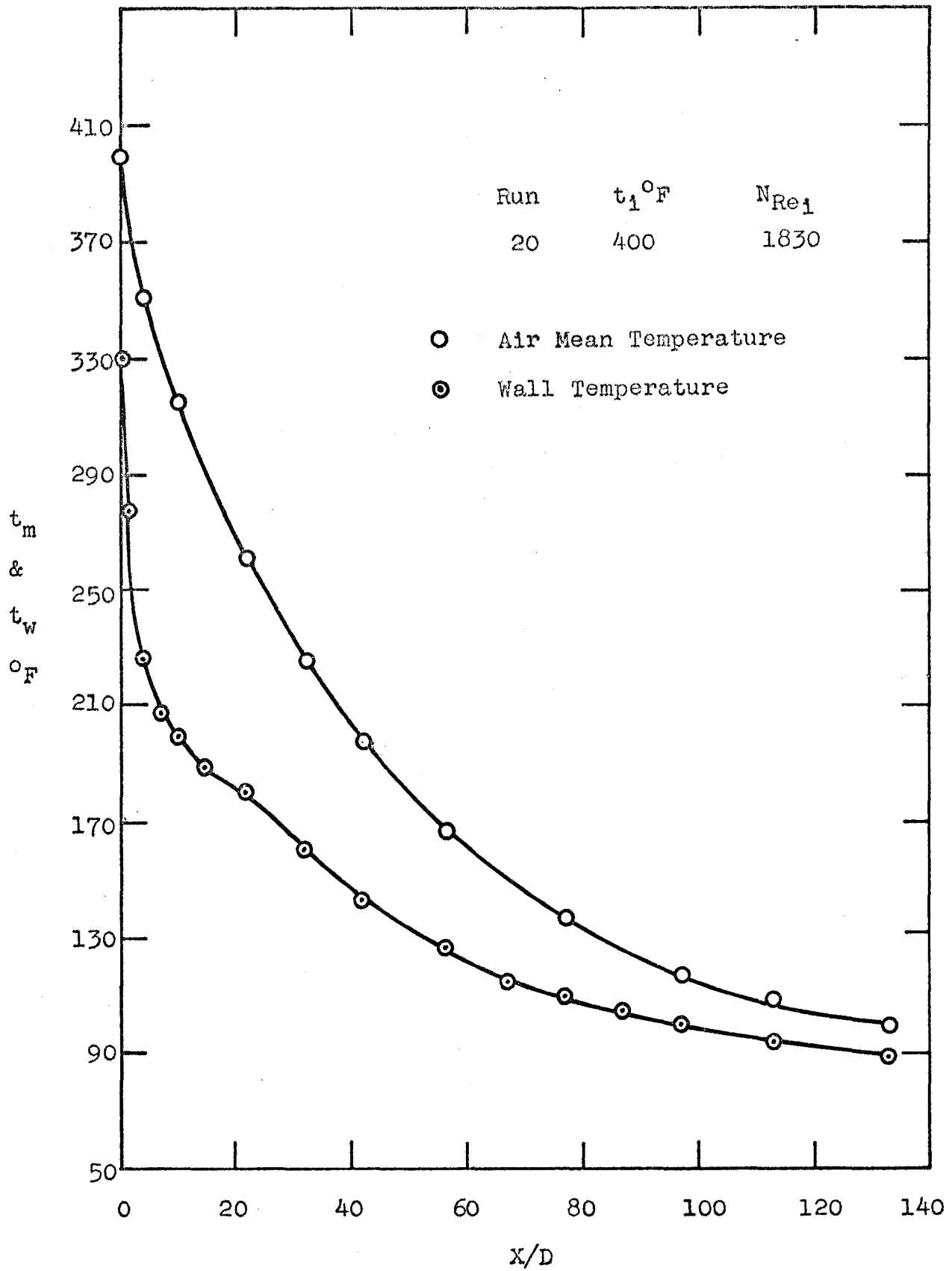


Fig. 3. Axial Variation of Air Mean and Wall Temperatures

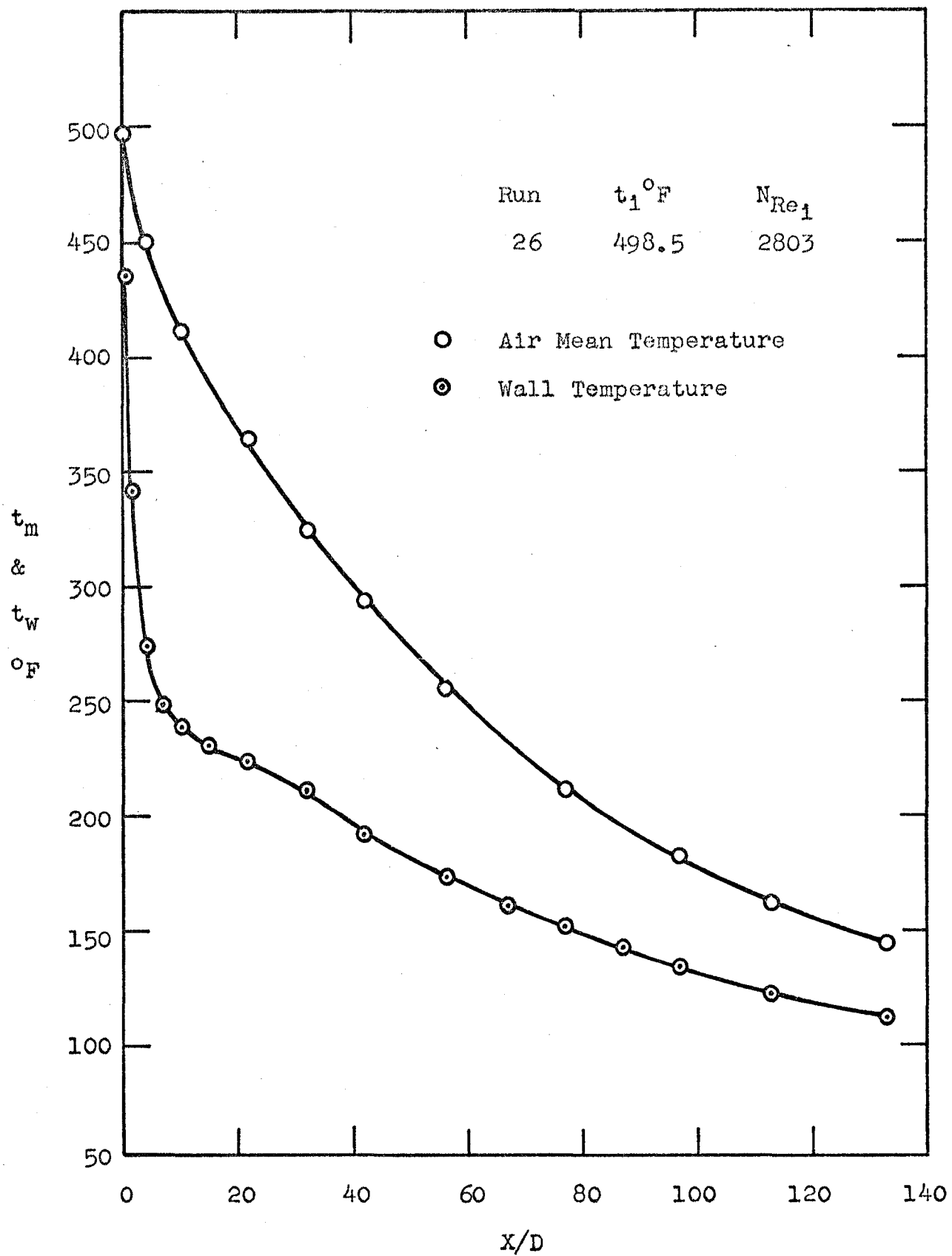


Fig. 4. Axial Variation of Air Mean and Wall Temperatures

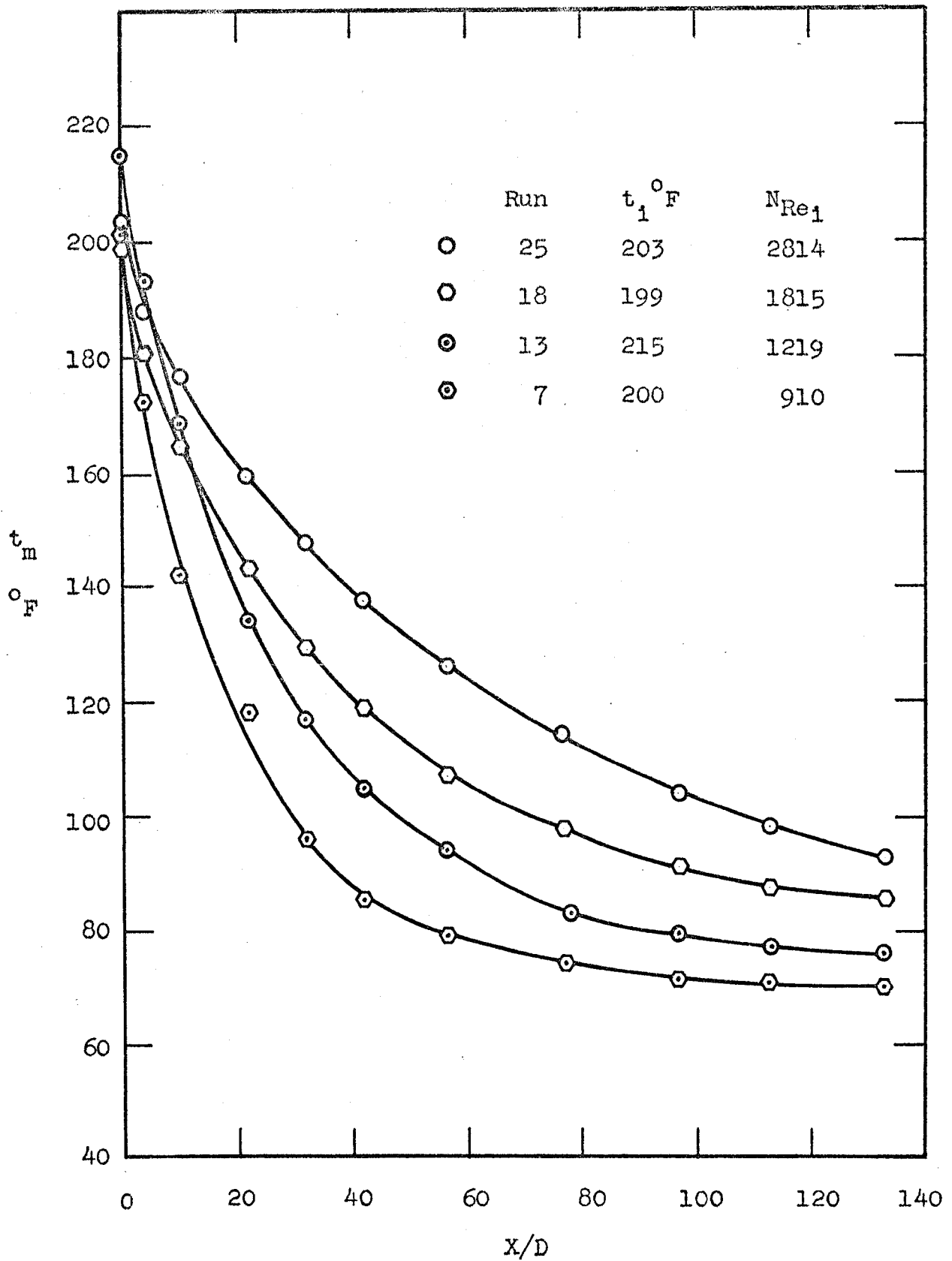


Fig. 5. Axial Variation of Air Mean Temperature for Various Inlet Reynolds Numbers.

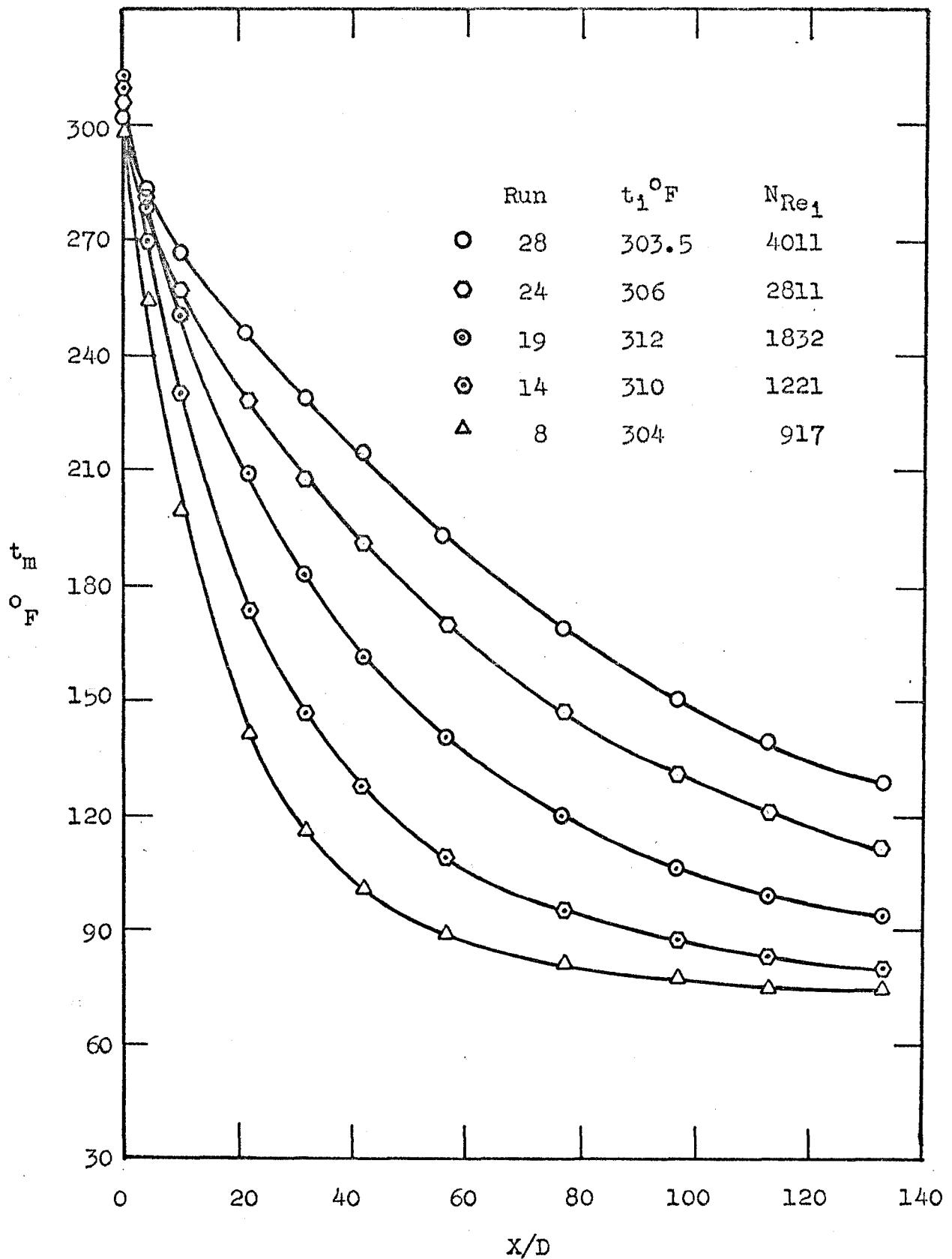


Fig. 6. Axial Variation of Air Mean Temperature for Various Inlet Reynolds Numbers.

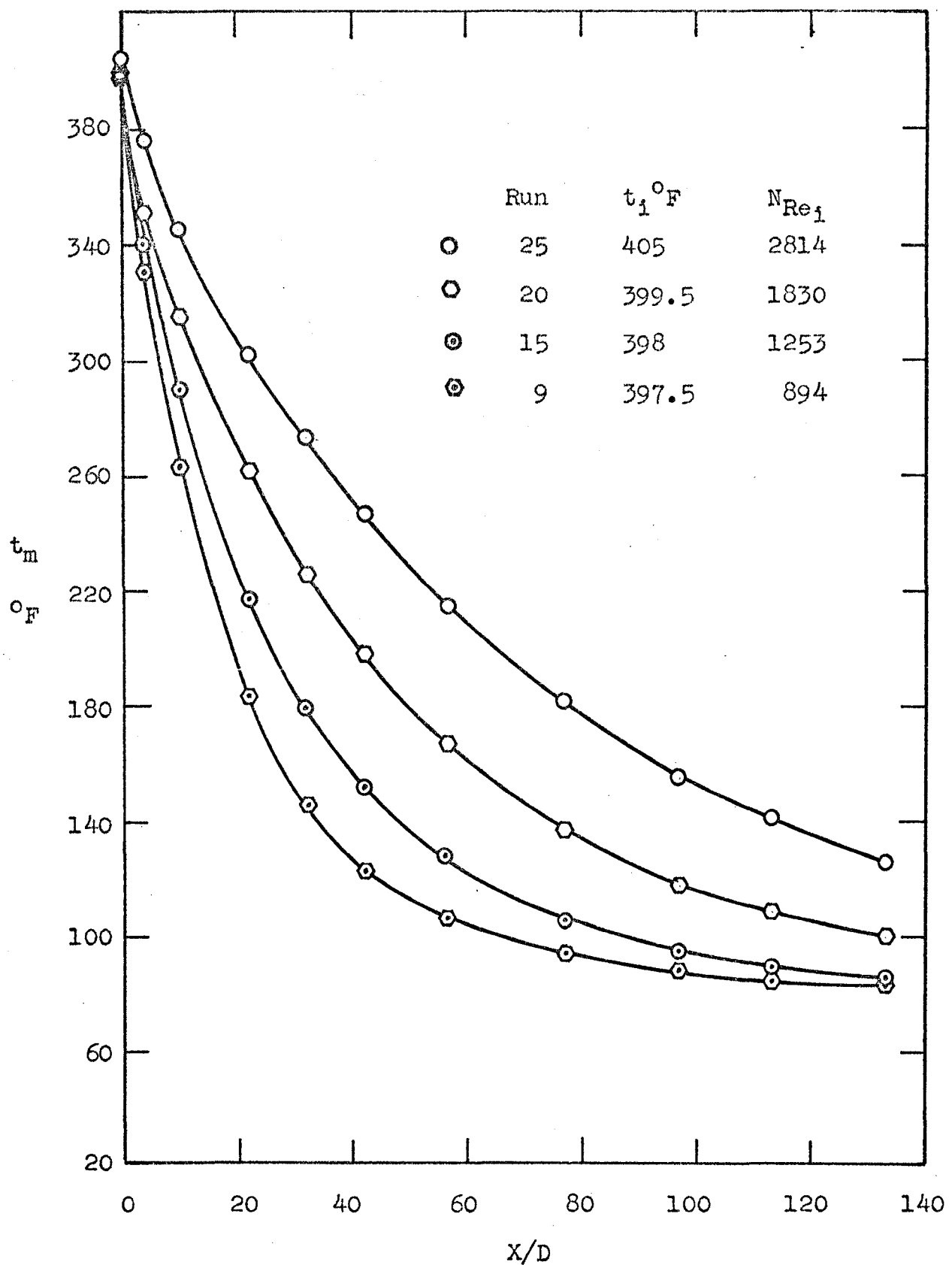


Fig. 7. Axial Variation of Air Mean Temperature for Various Inlet Reynolds Numbers

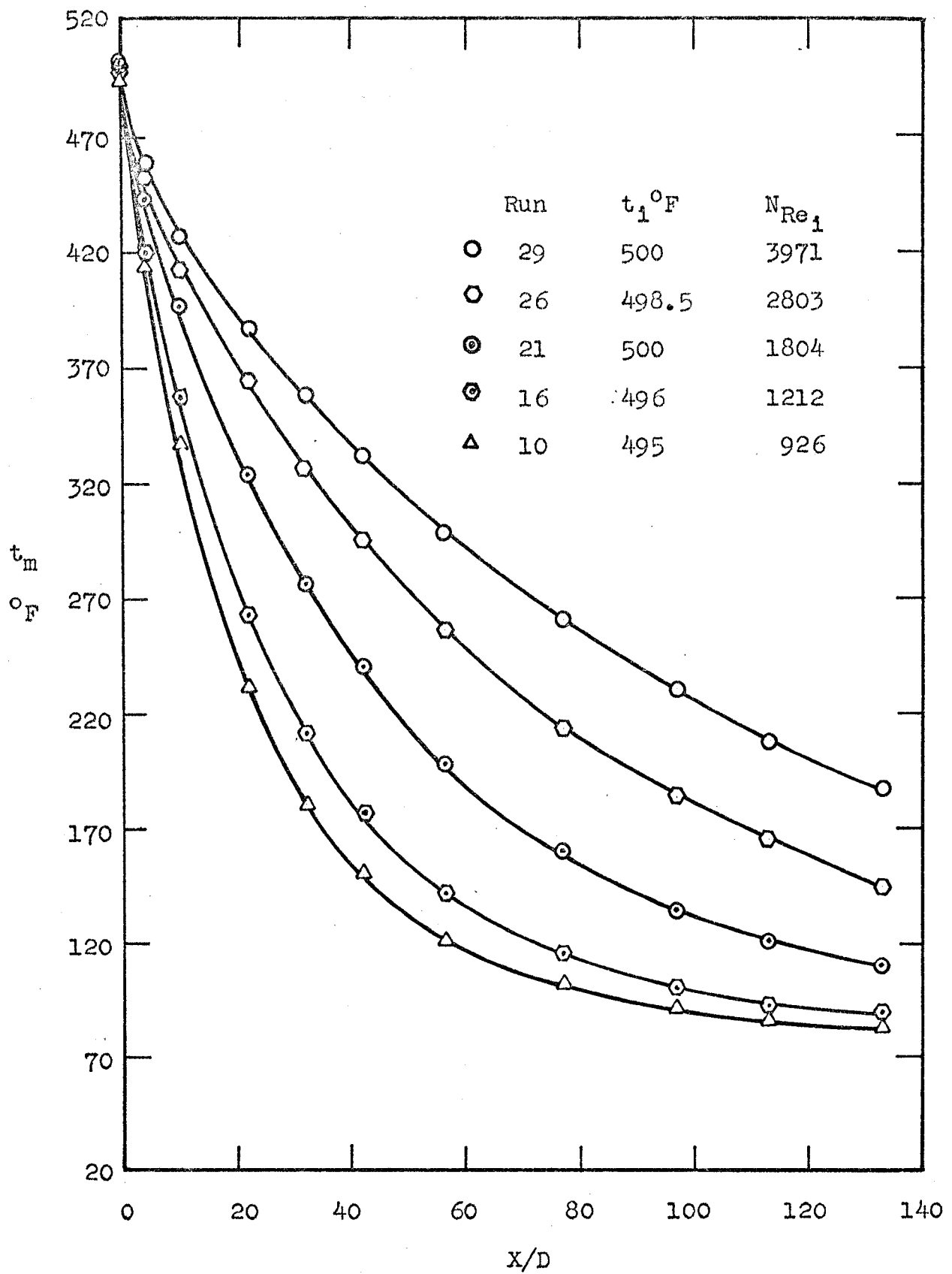


Fig. 8. Axial Variation of Air Mean Temperature for Various Inlet Reynolds Numbers.

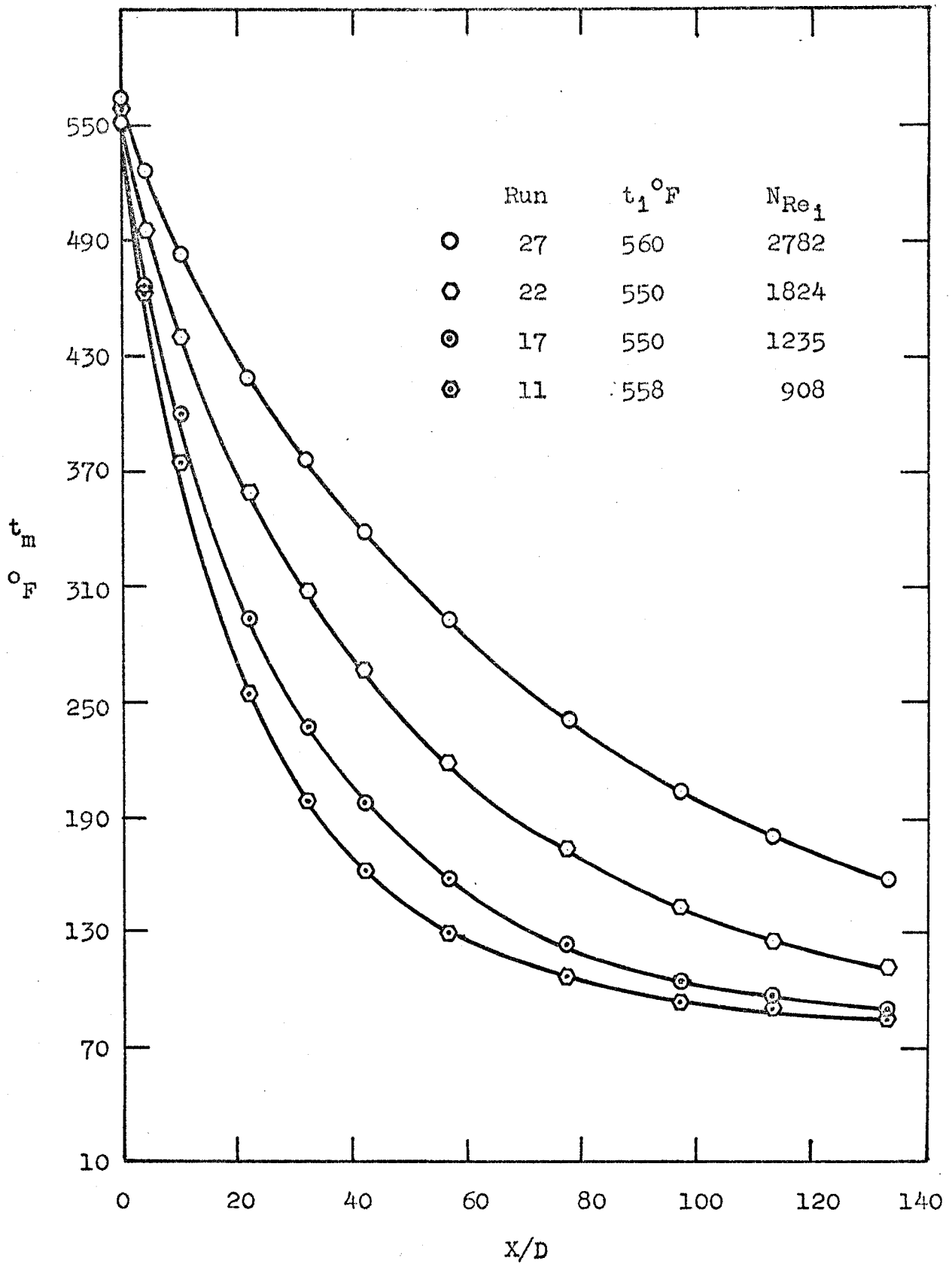


Fig. 9. Axial Variation of Air Mean Temperature for Various Inlet Reynolds Numbers.

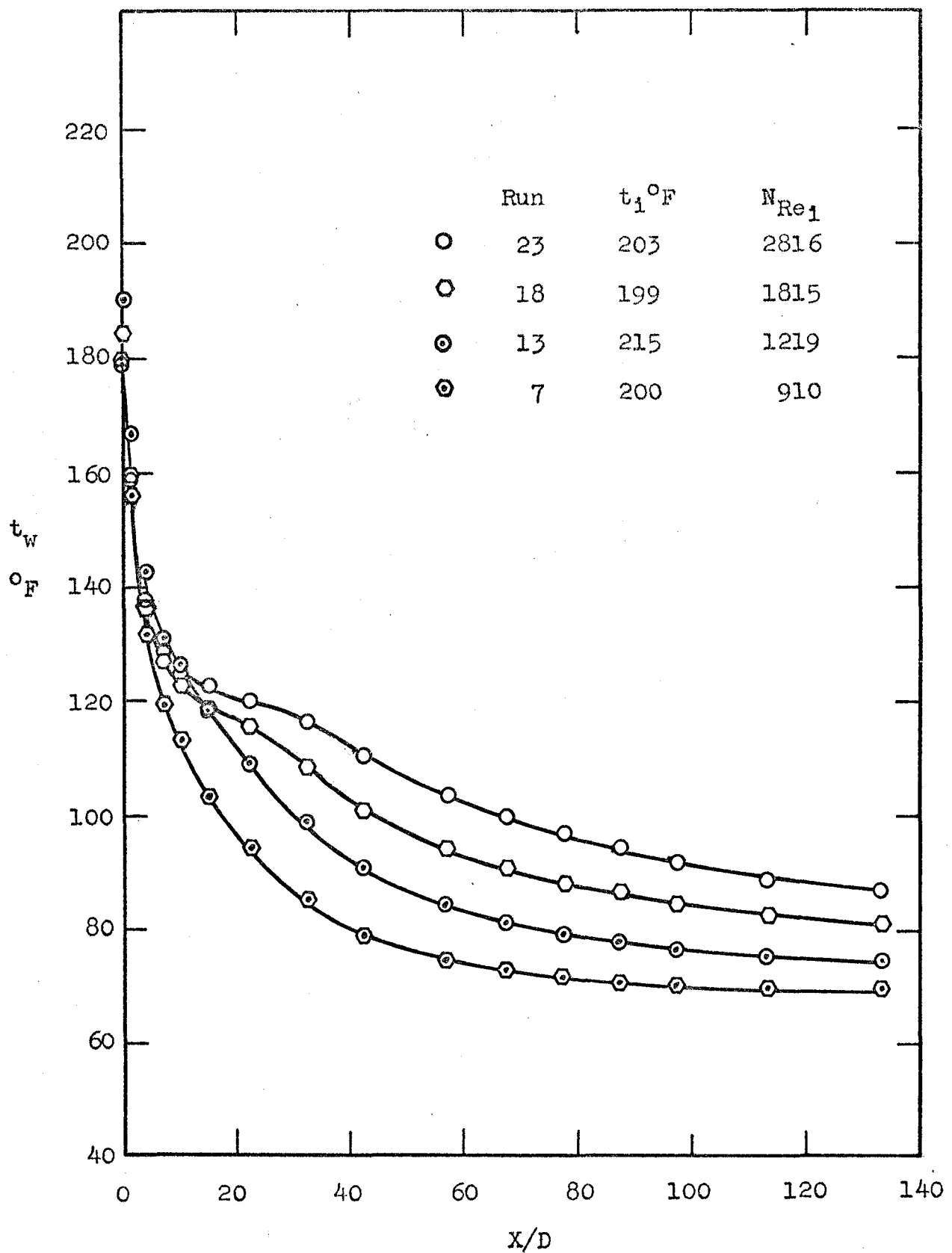


Fig. 10. Axial Variation of Wall Temperature for Various Inlet Reynolds Numbers.

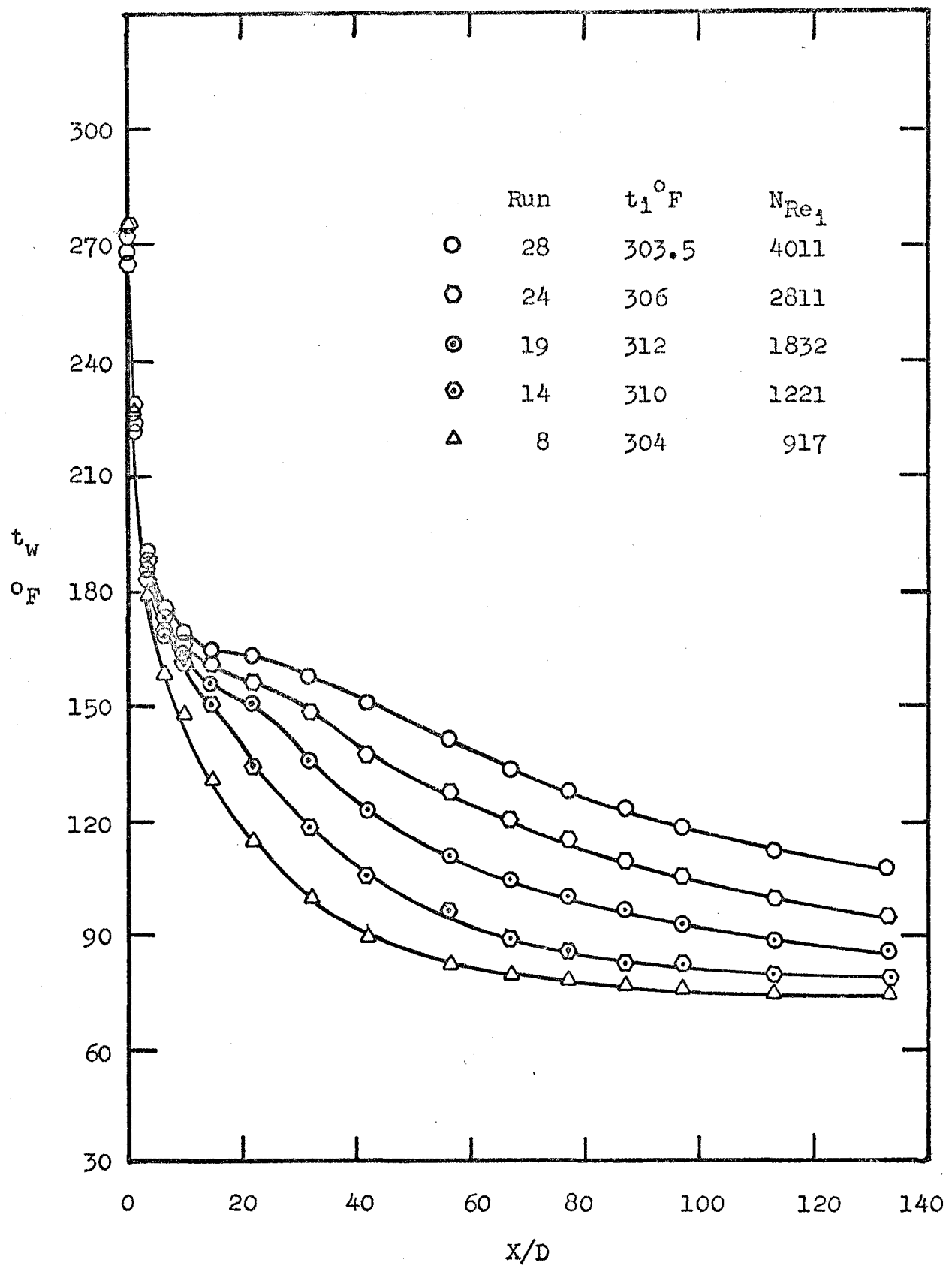


Fig. 11. Axial Variation of Wall Temperature for Various Inlet Reynolds Numbers.

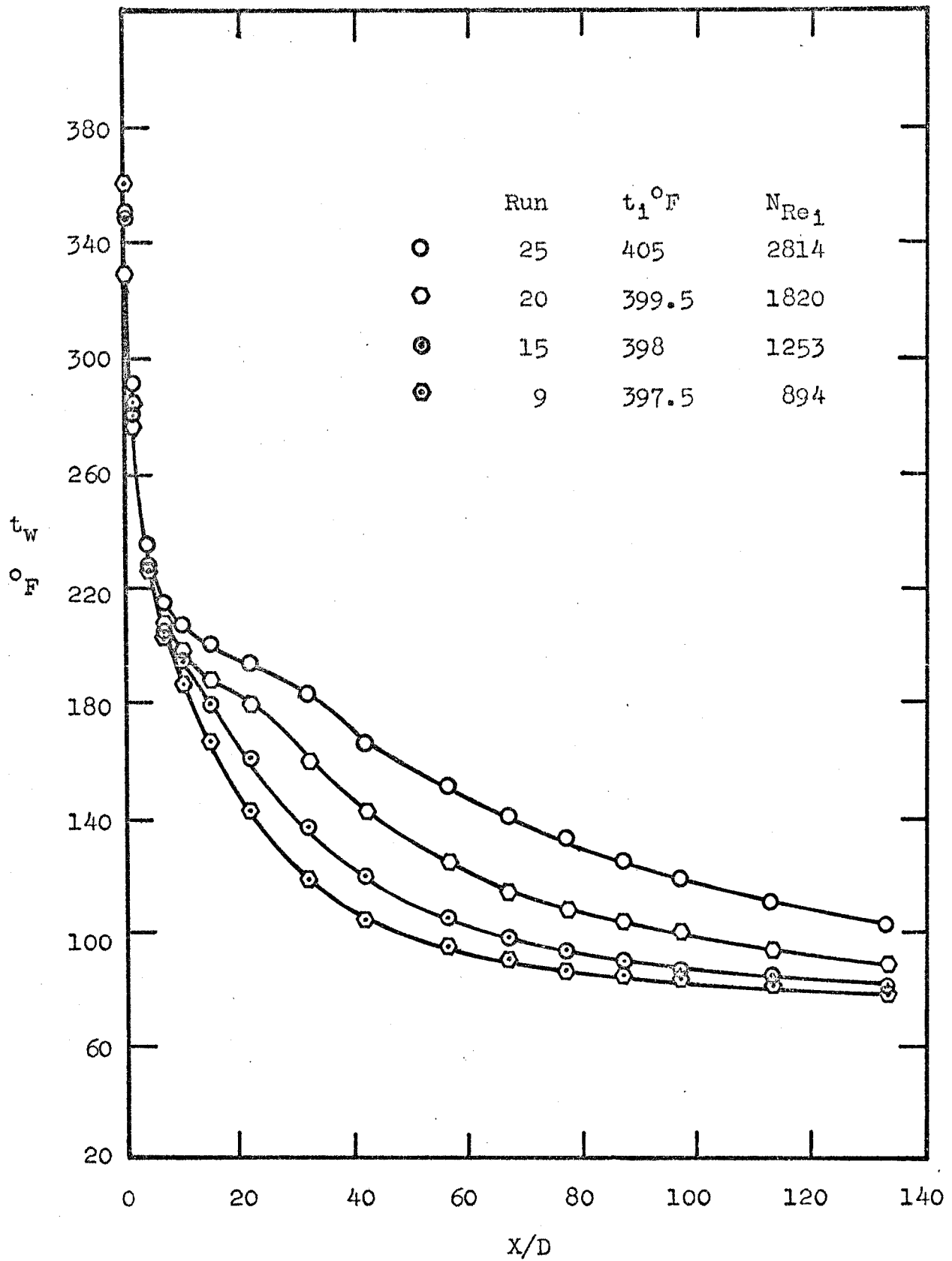


Fig. 12. Axial Variation of Wall Temperature for Various Inlet Reynolds Numbers

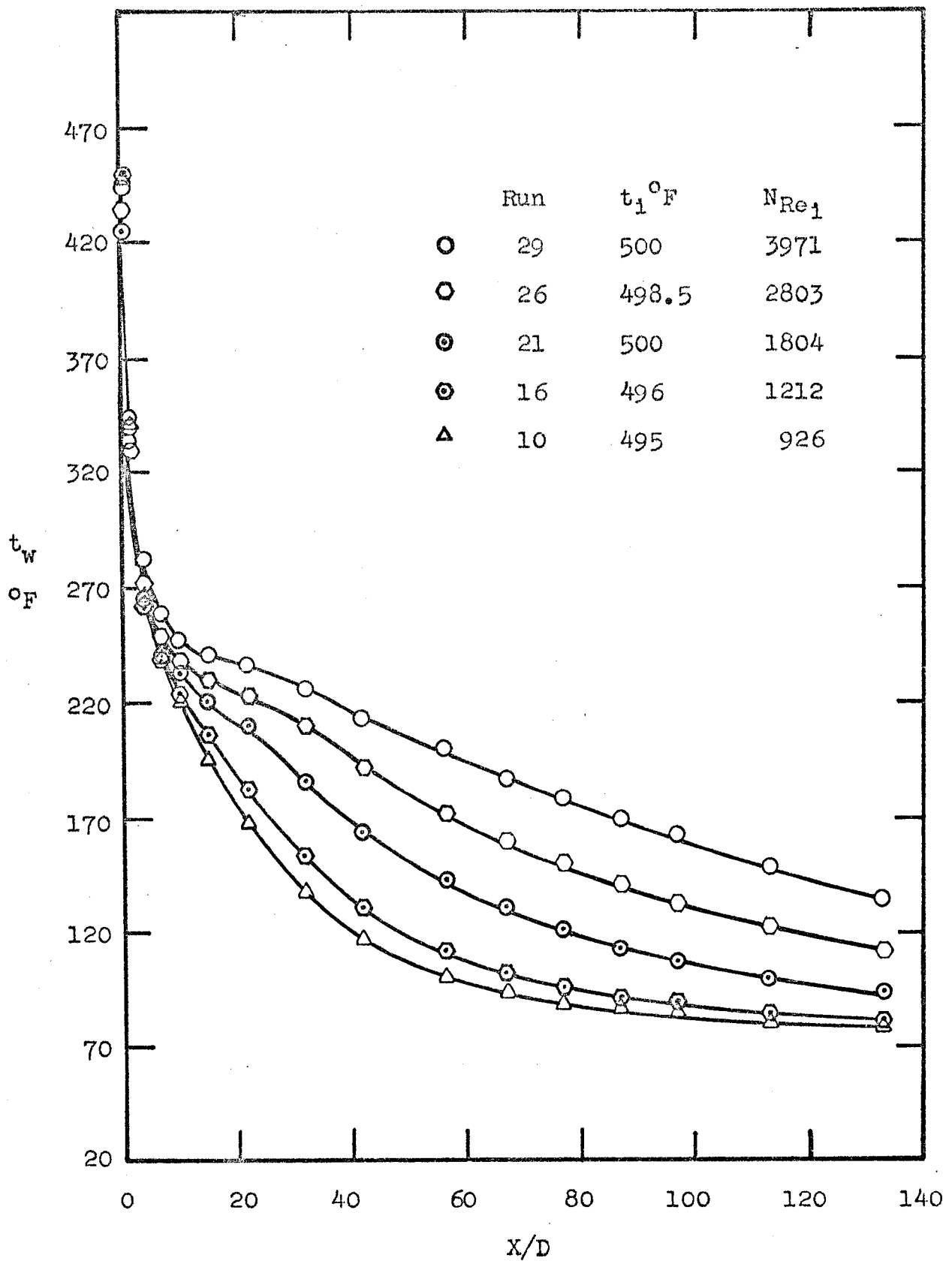


Fig. 13. Axial Variation of Wall Temperature for Various Inlet Reynolds Numbers

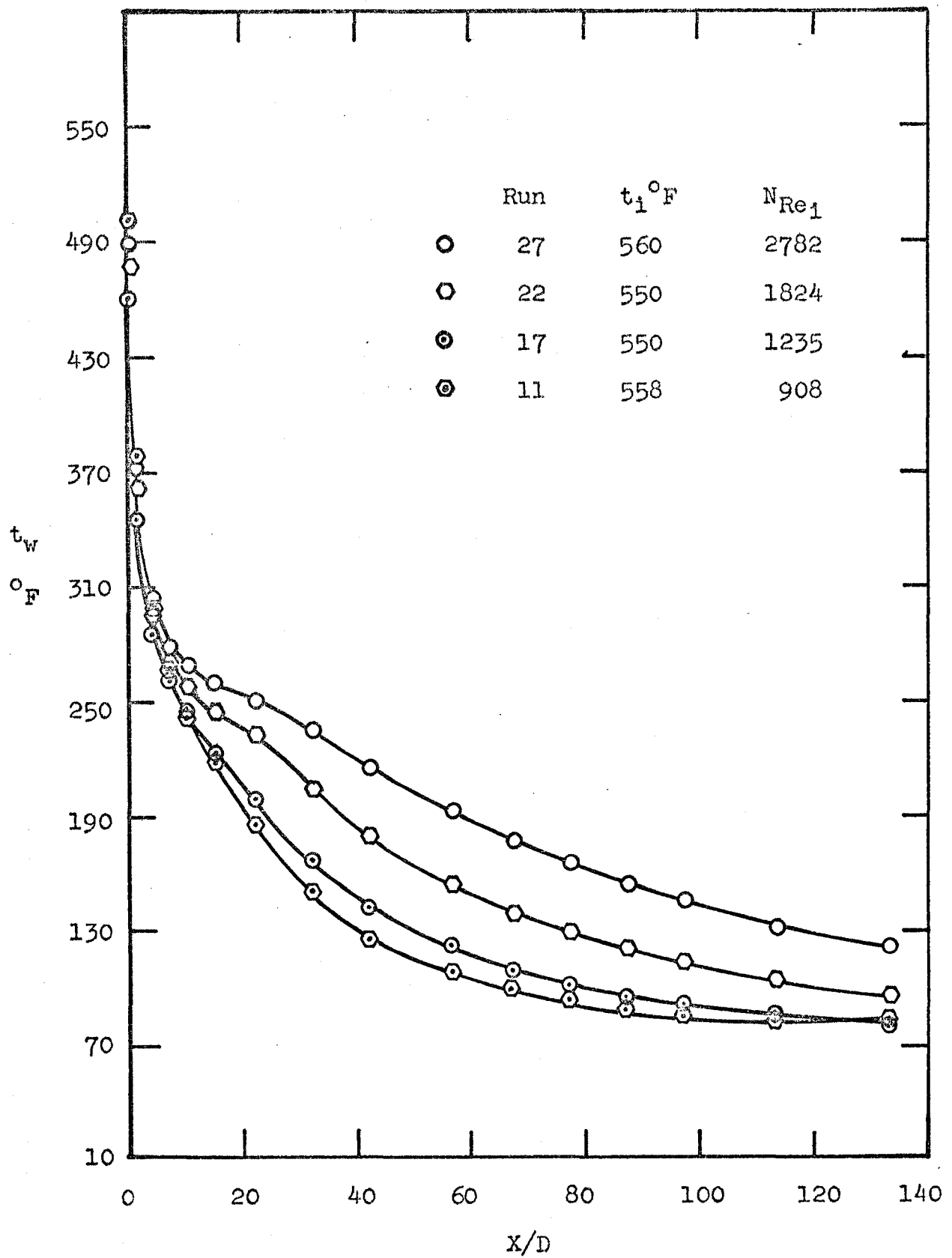


Fig. 14. Axial Variation of Wall Temperature for Various Inlet Reynolds Numbers

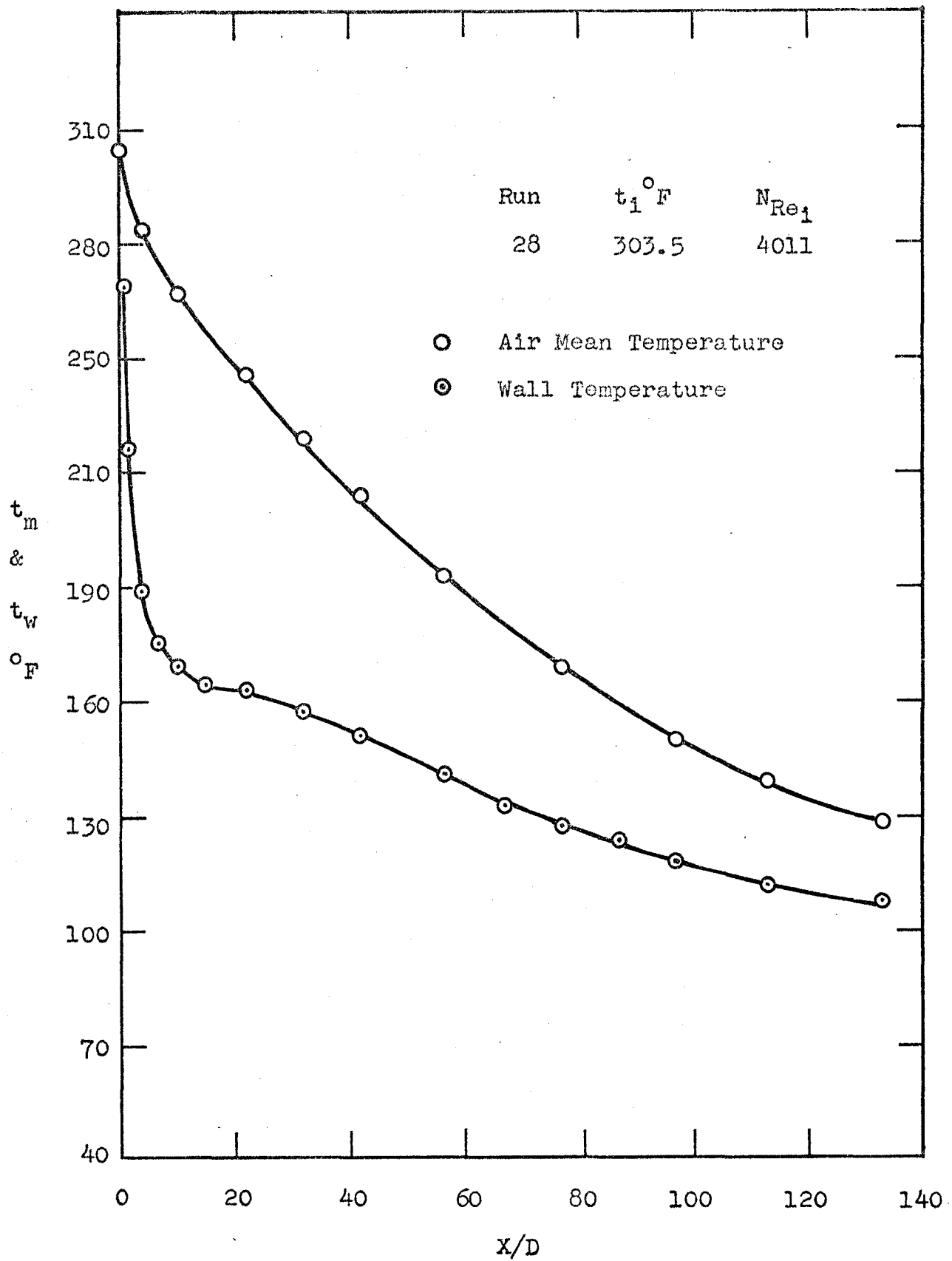


Fig. 15. Axial Variation of Air Mean and Wall Temperatures

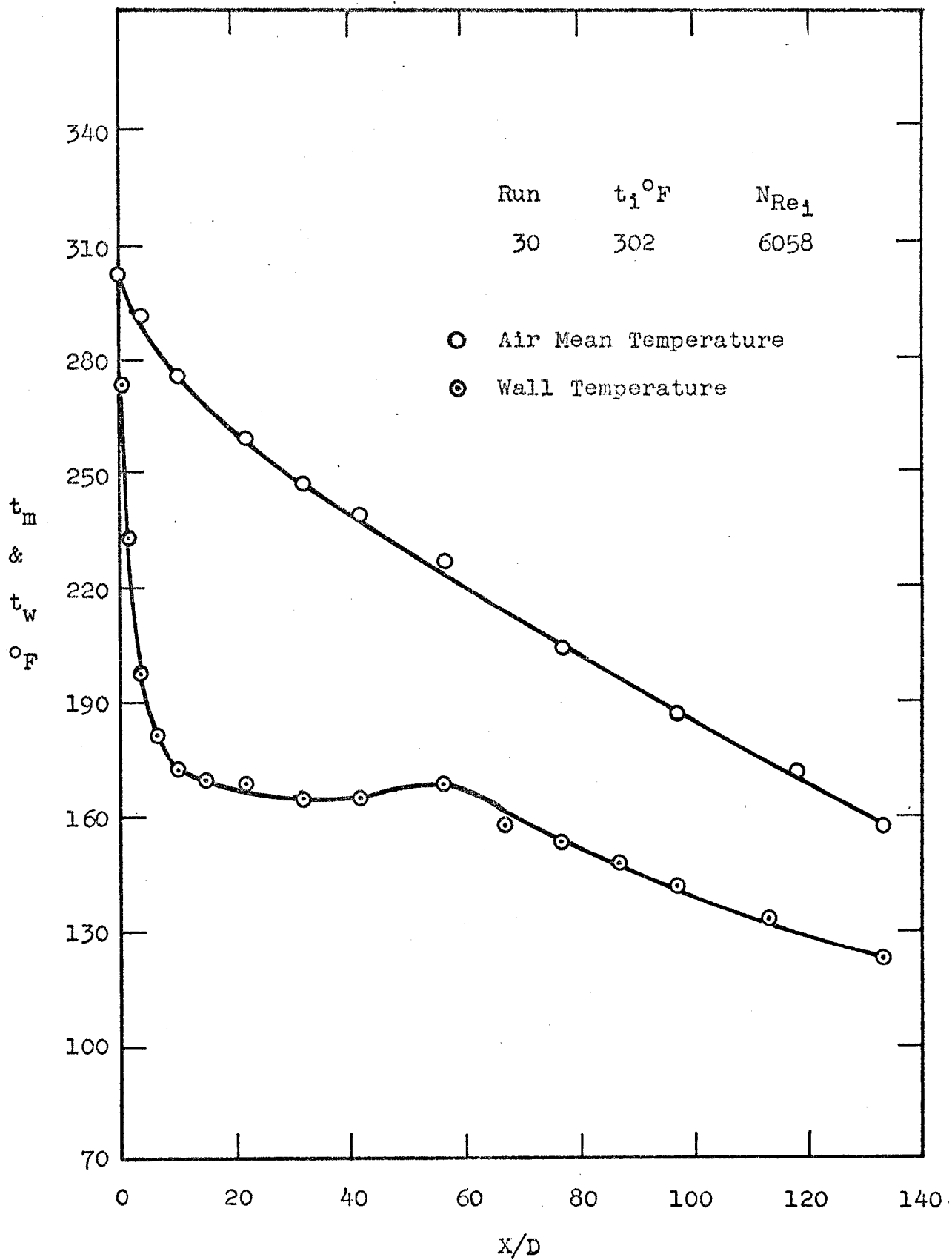


Fig. 16. Axial Variation of Air Mean and Wall Temperatures

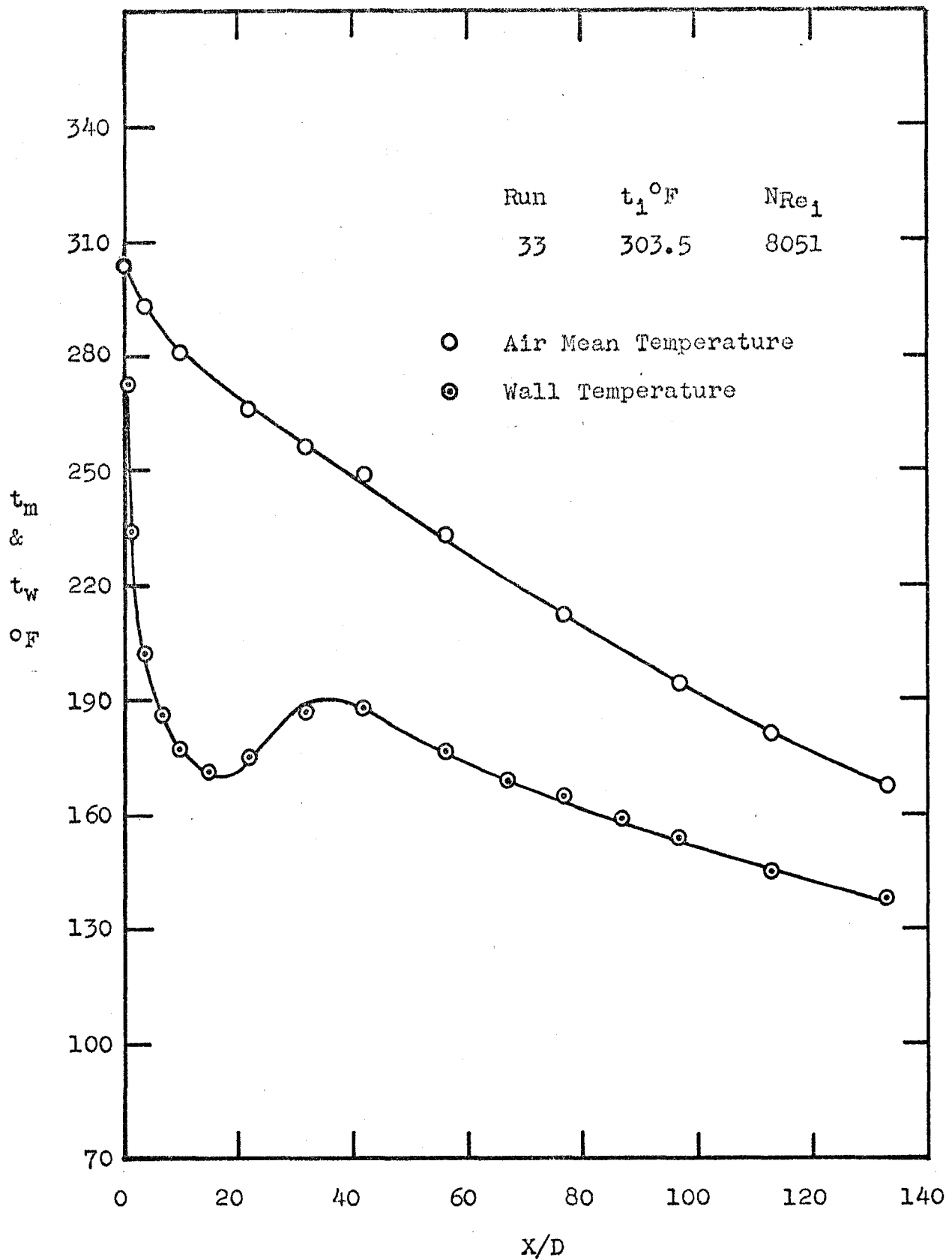


Fig. 17. Axial Variation of Air Mean and Wall Temperatures

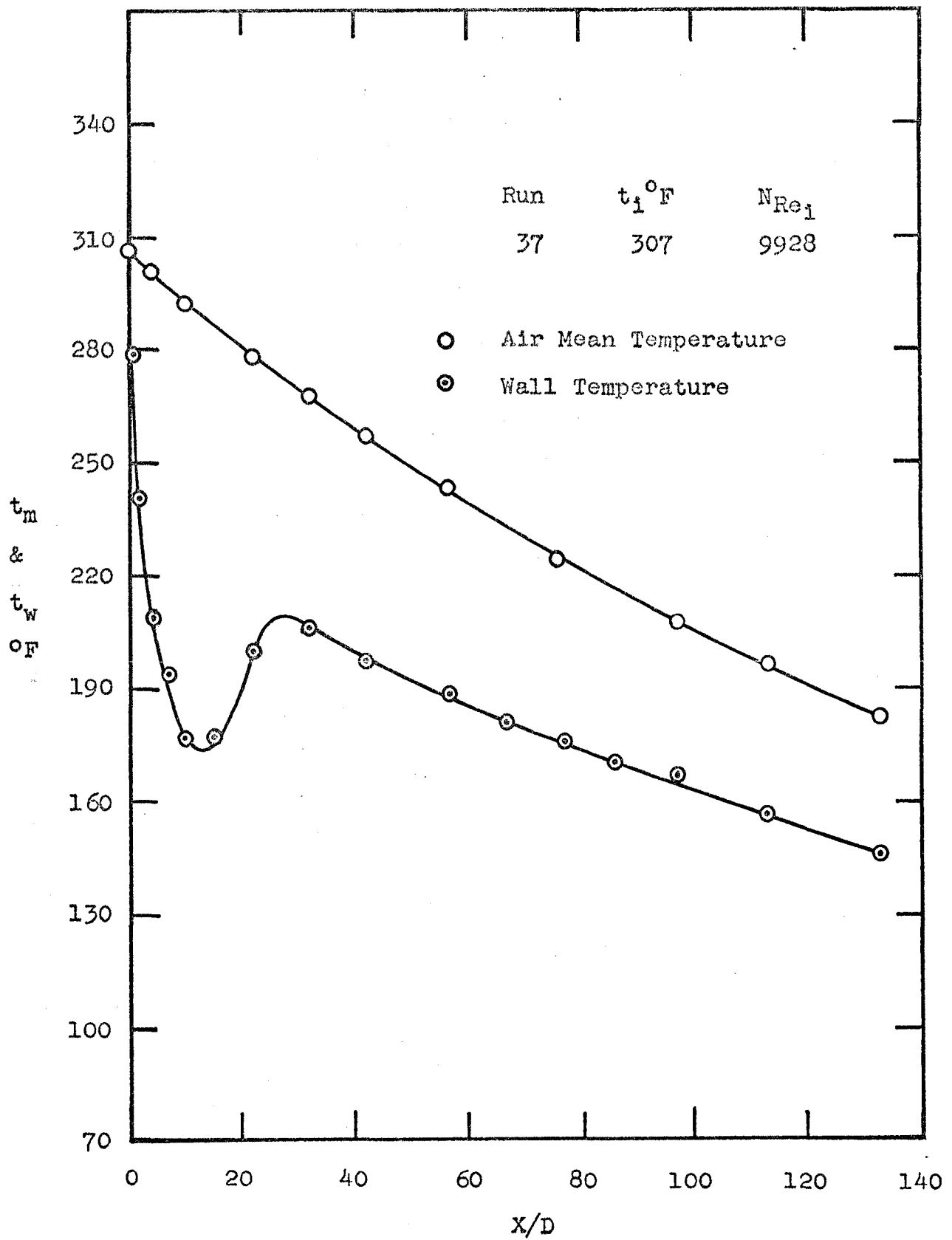


Fig. 18. Axial Variation of Air Mean and Wall Temperatures

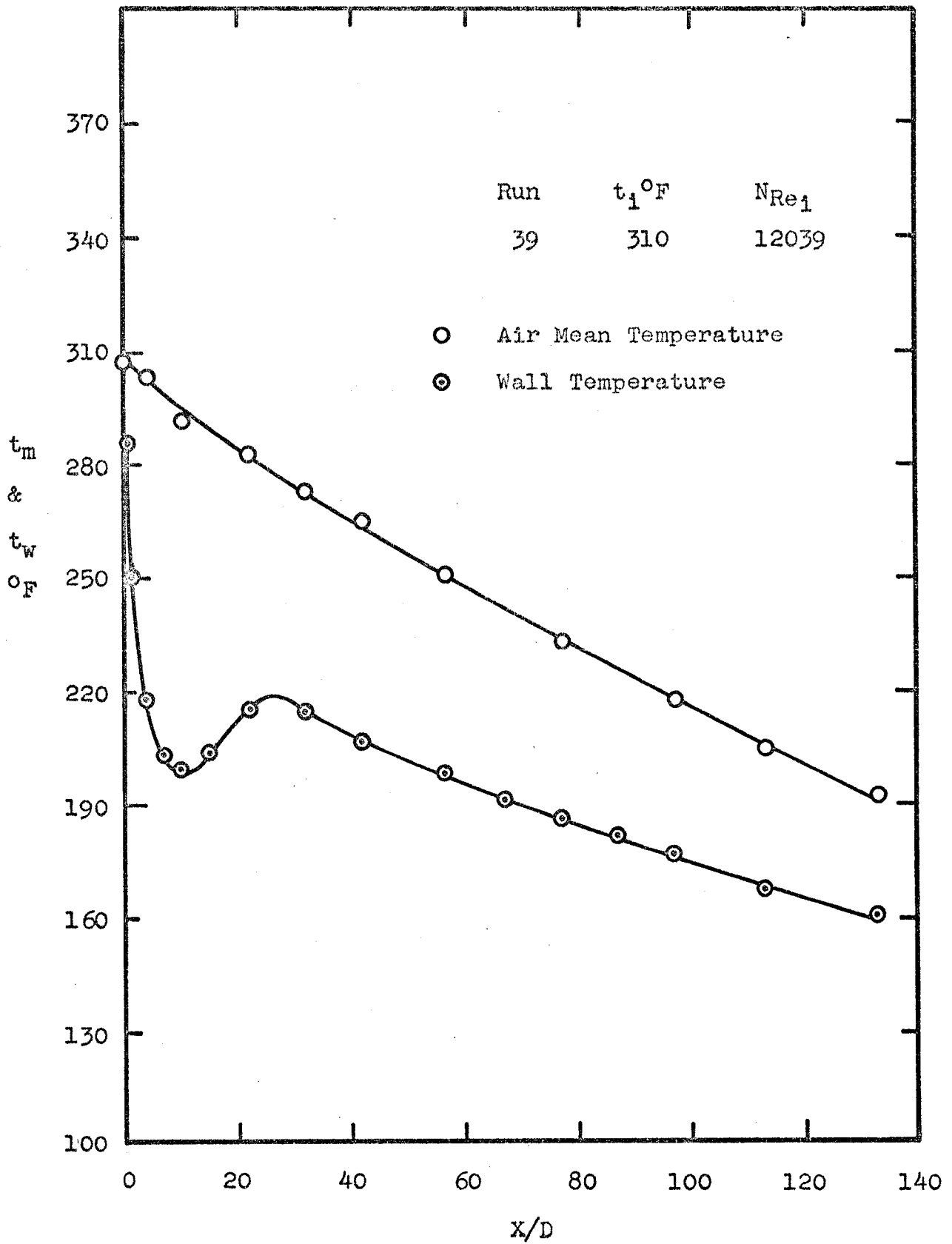


Fig. 19. Axial Variation of Air Mean and Wall Temperatures

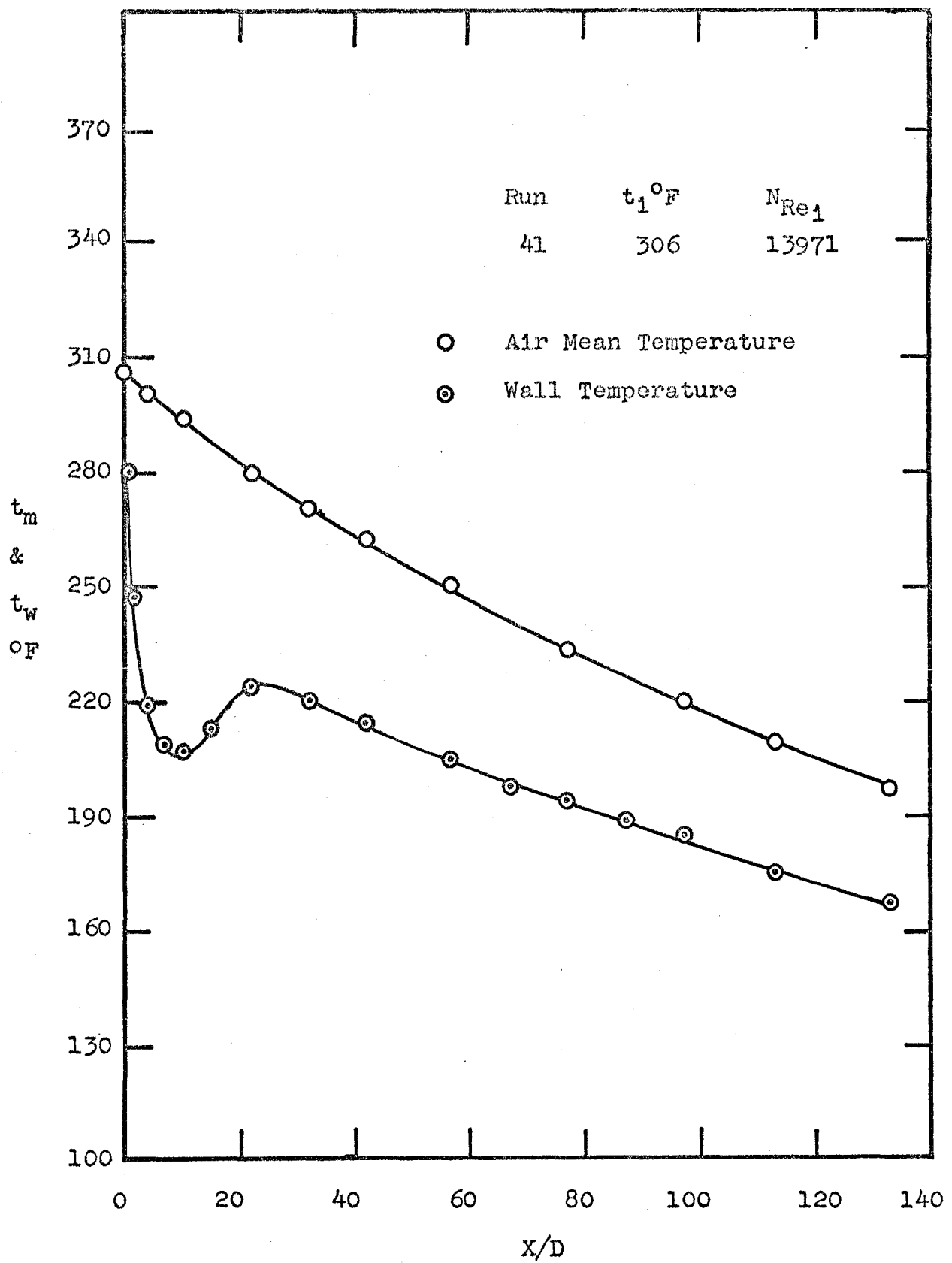


Fig. 20. Axial Variation of Air Mean and Wall Temperatures

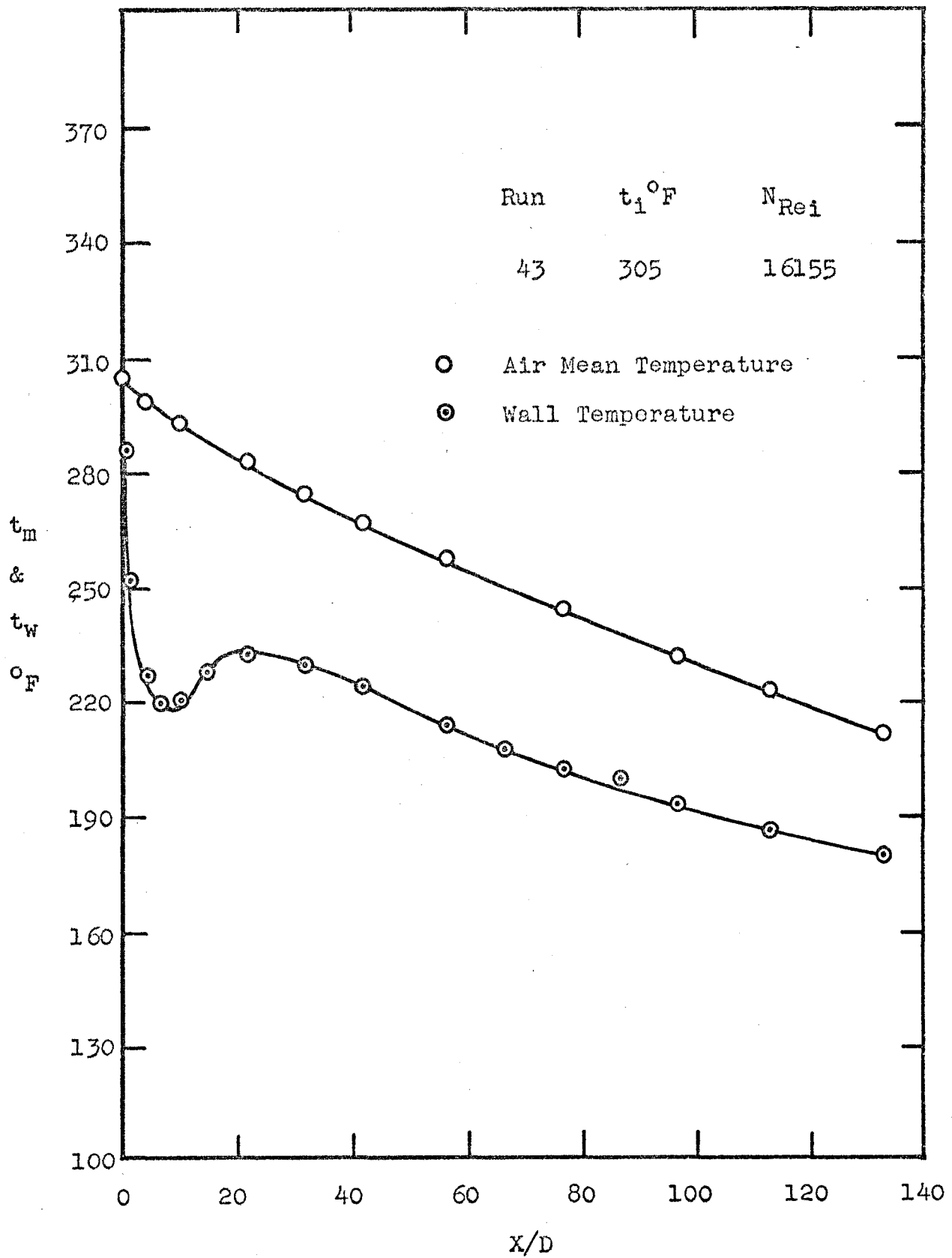


Fig. 21. Axial Variation of Air Mean and Wall Temperatures

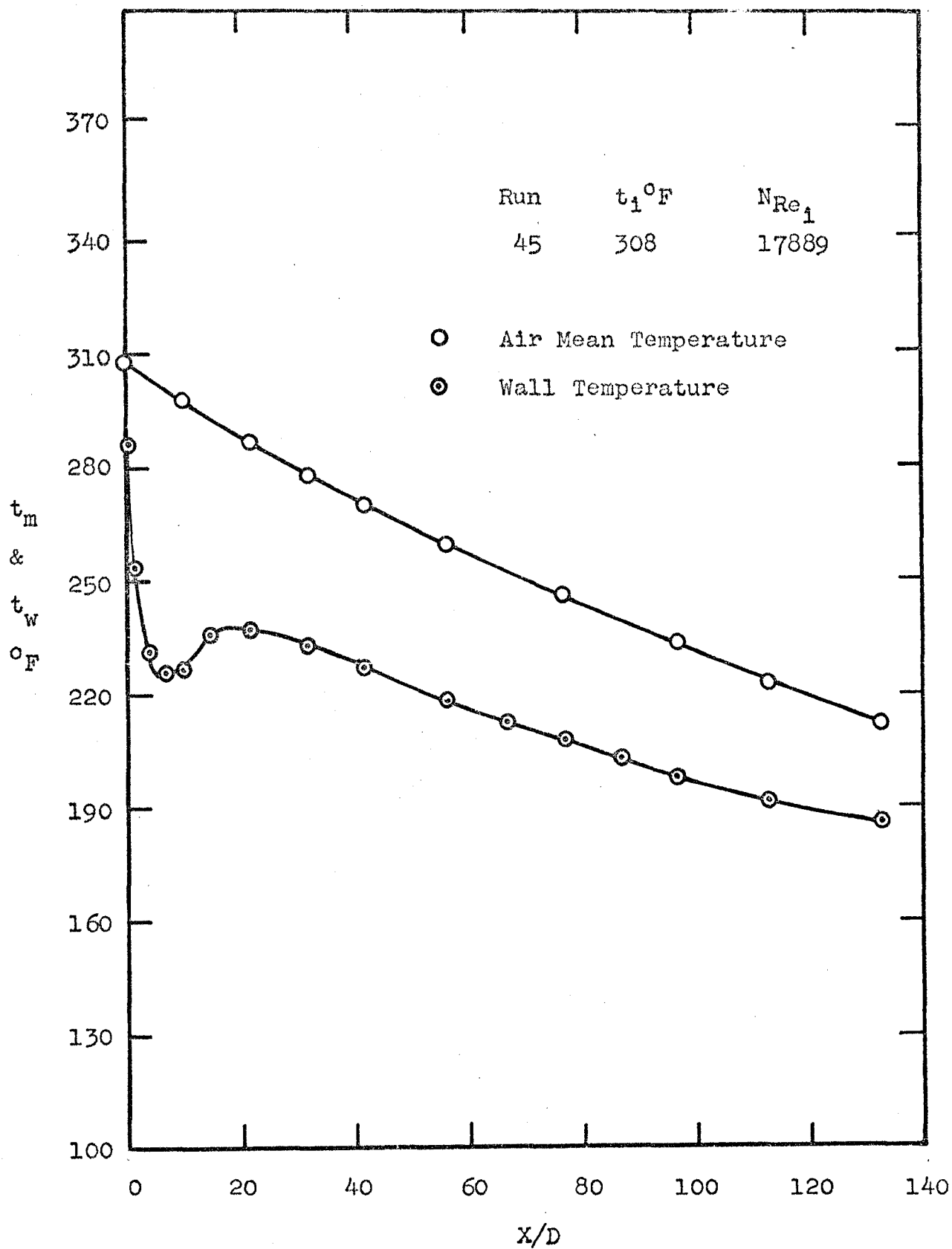


Fig. 22. Axial Variation of Air Mean and Wall Temperatures

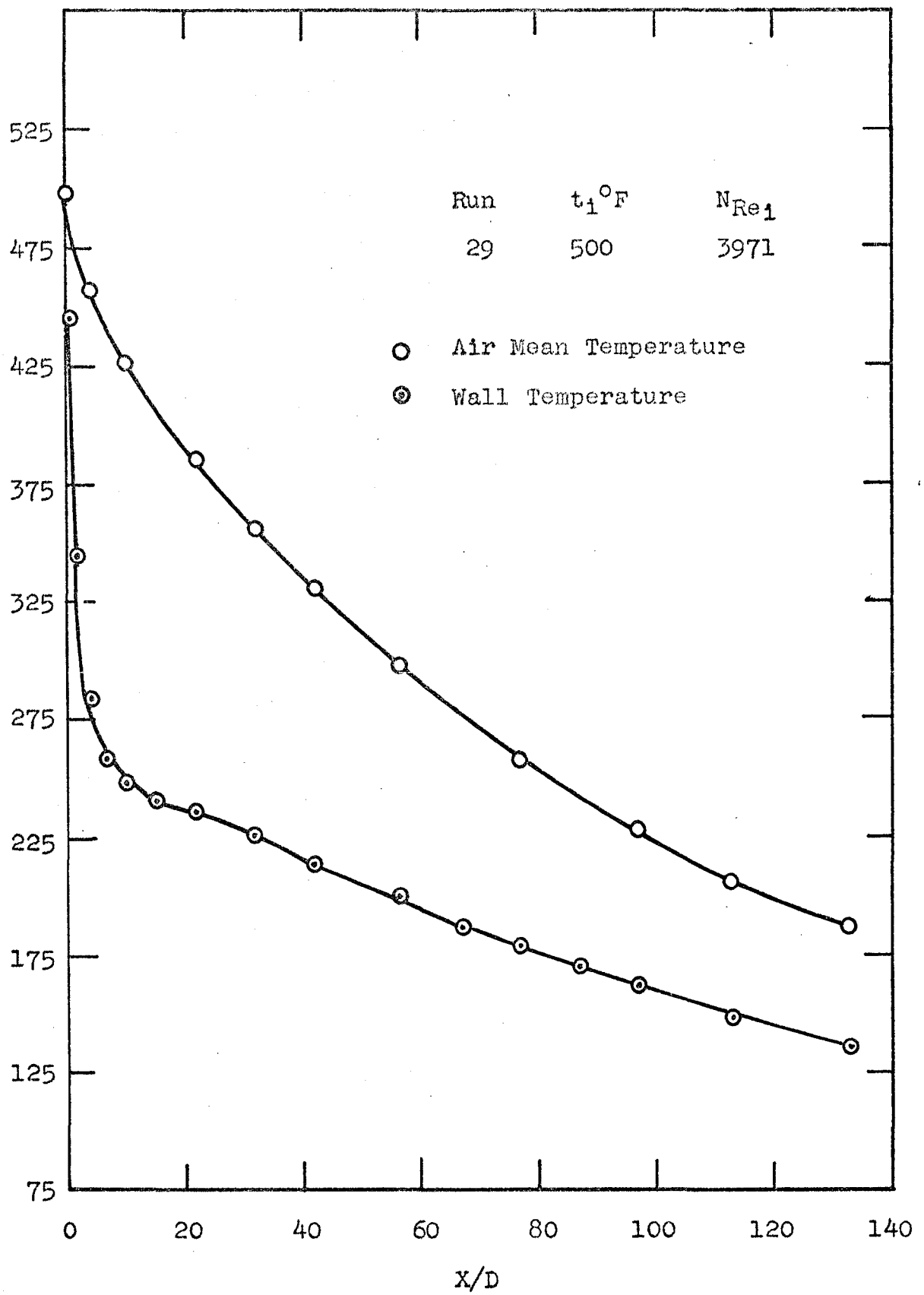


Fig. 23. Axial Variation of Air Mean and Wall Temperatures

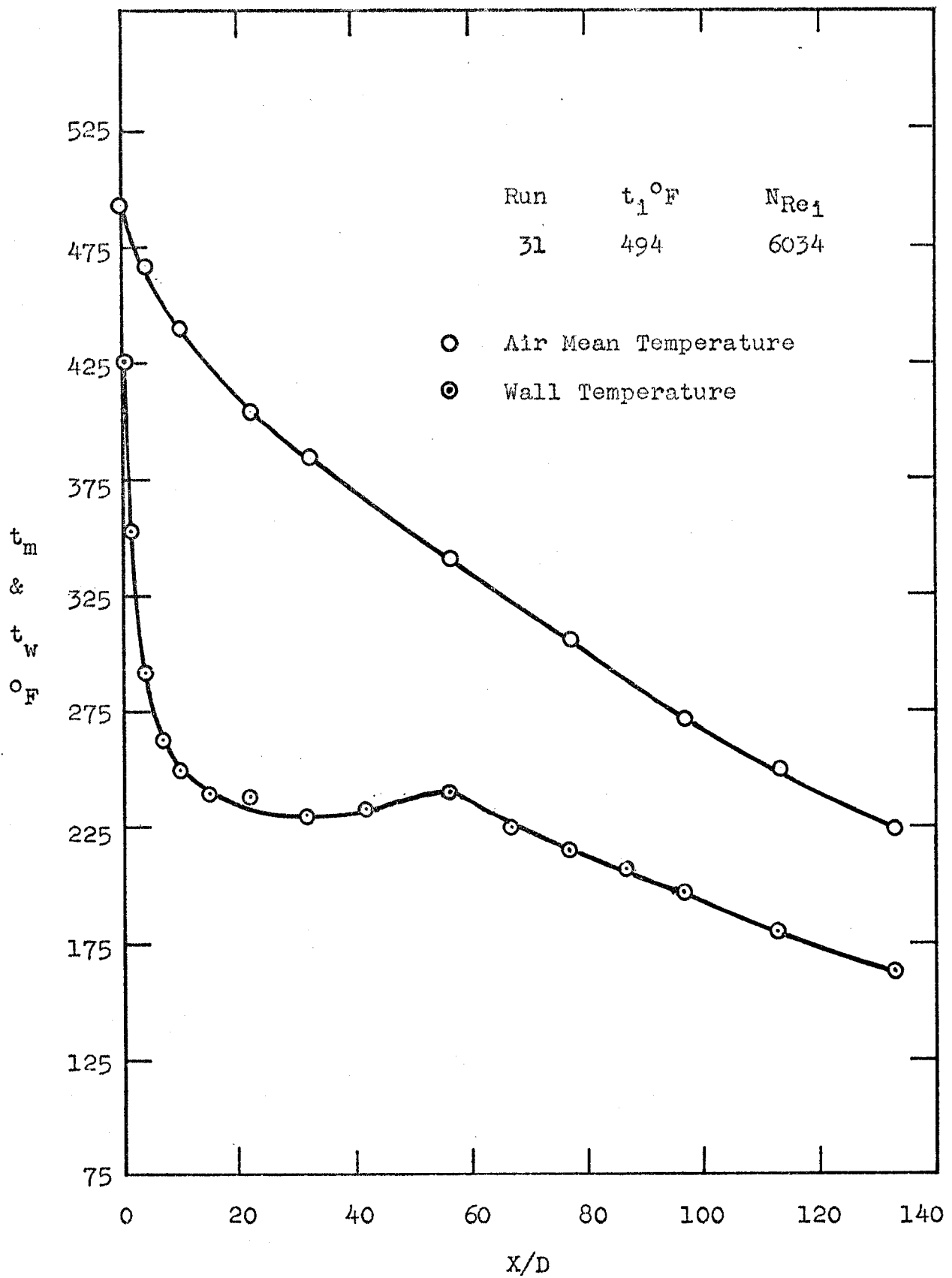


Fig. 24. Axial Variation of Air Mean and Wall Temperatures

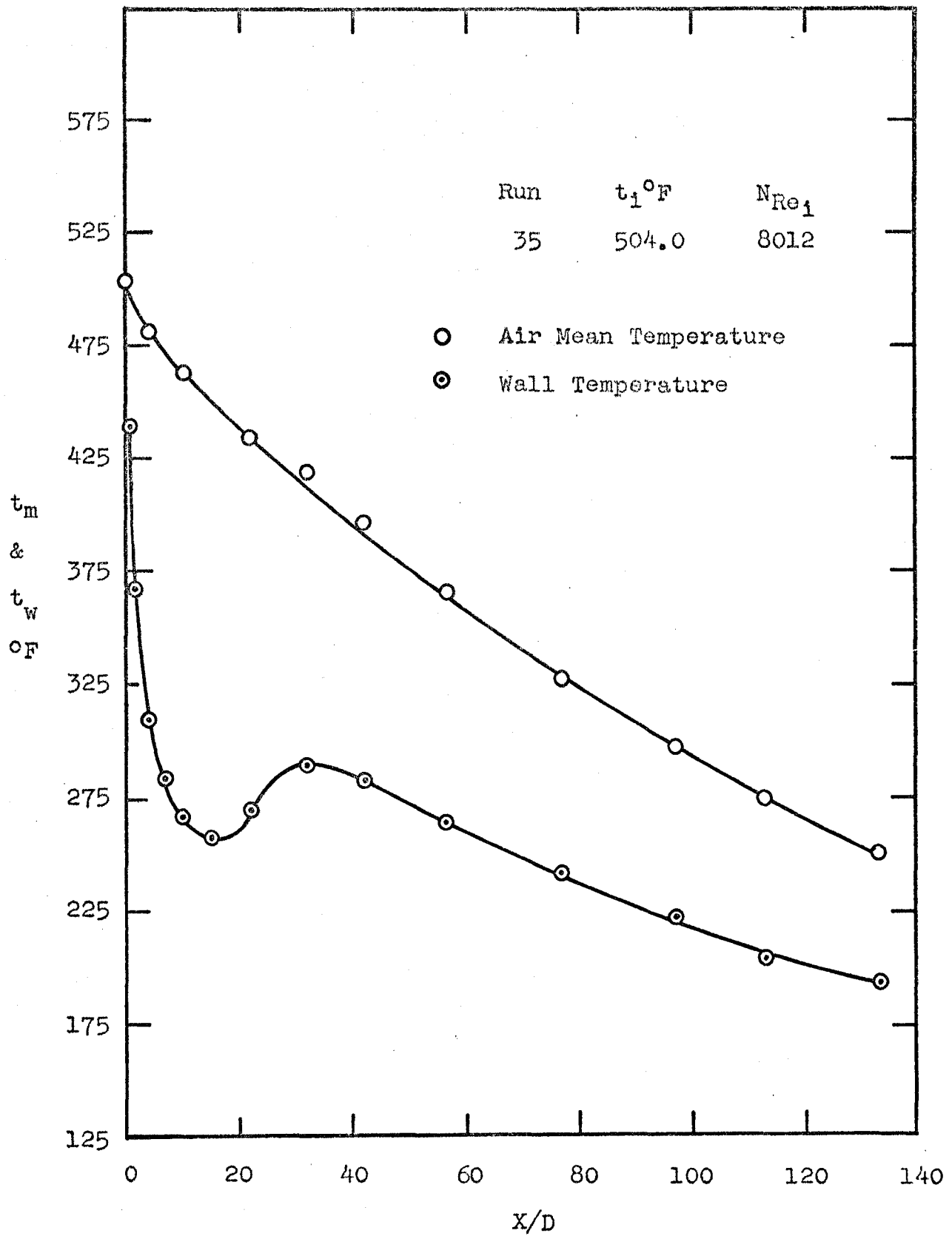


Fig. 25. Axial Variation of Air Mean and Wall Temperatures

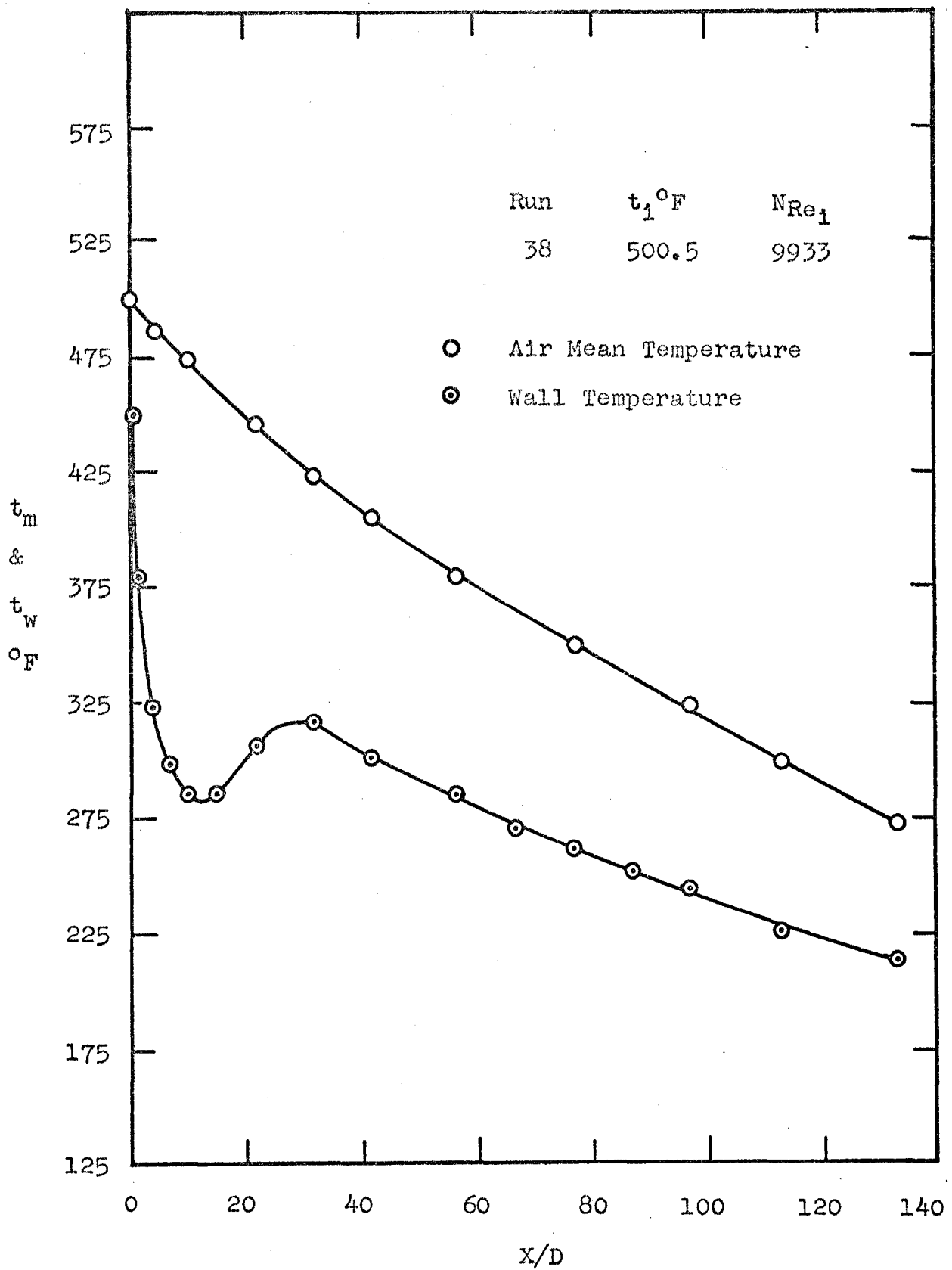


Fig. 26. Axial Variation of Air Mean and Wall Temperatures

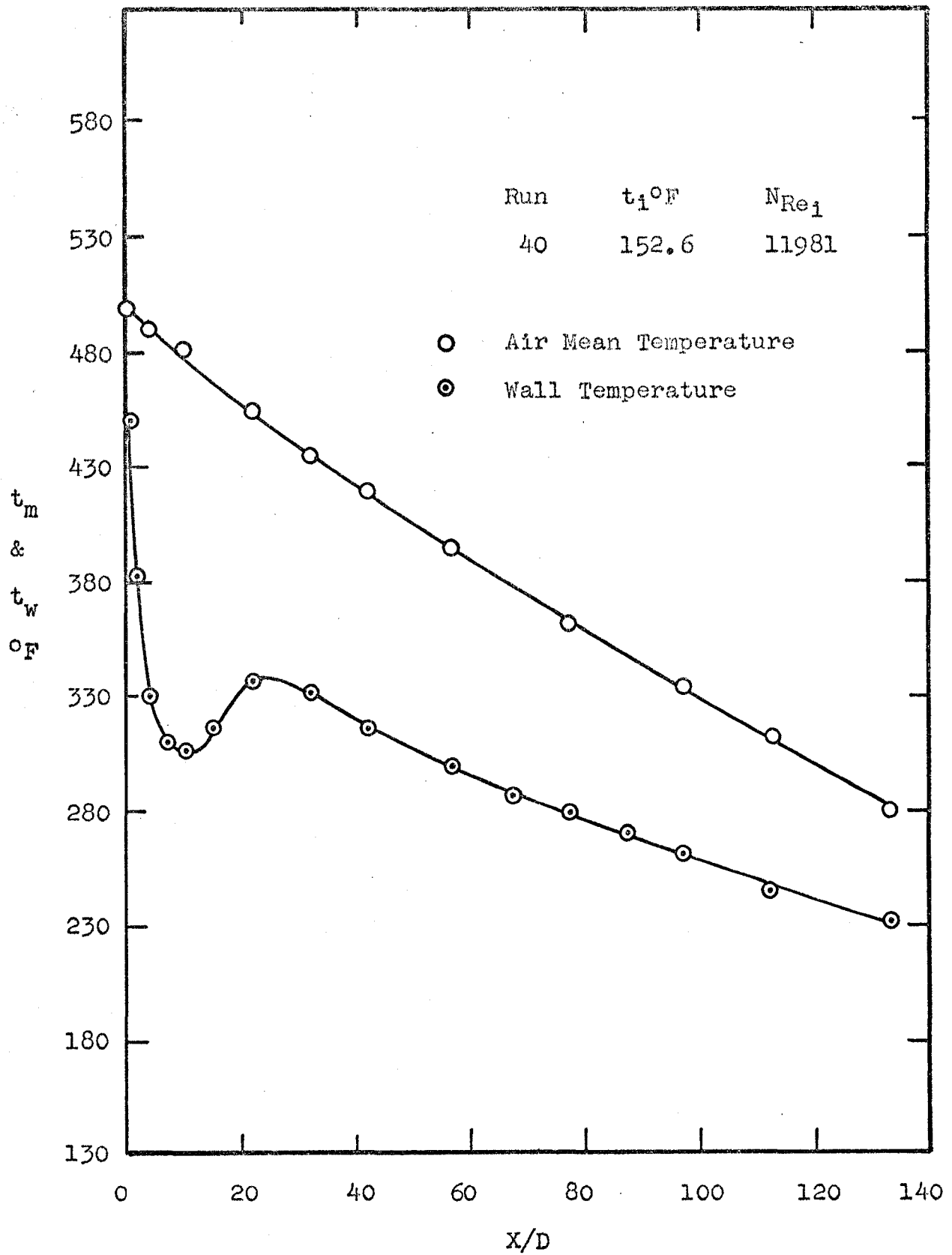


Fig. 27. Axial Variation of Air Mean and Wall Temperatures

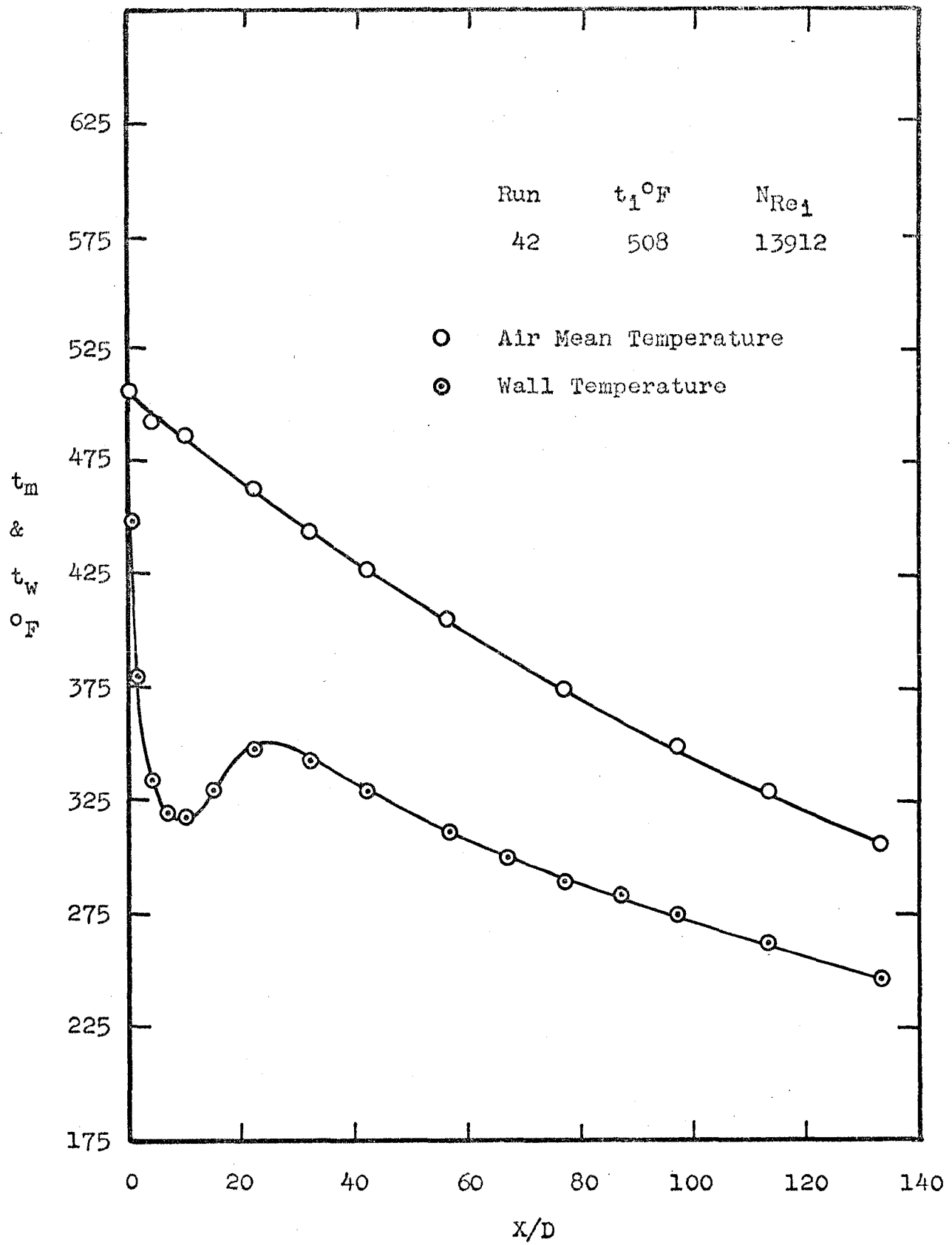


Fig. 28. Axial Variation of Air Mean and Wall Temperatures

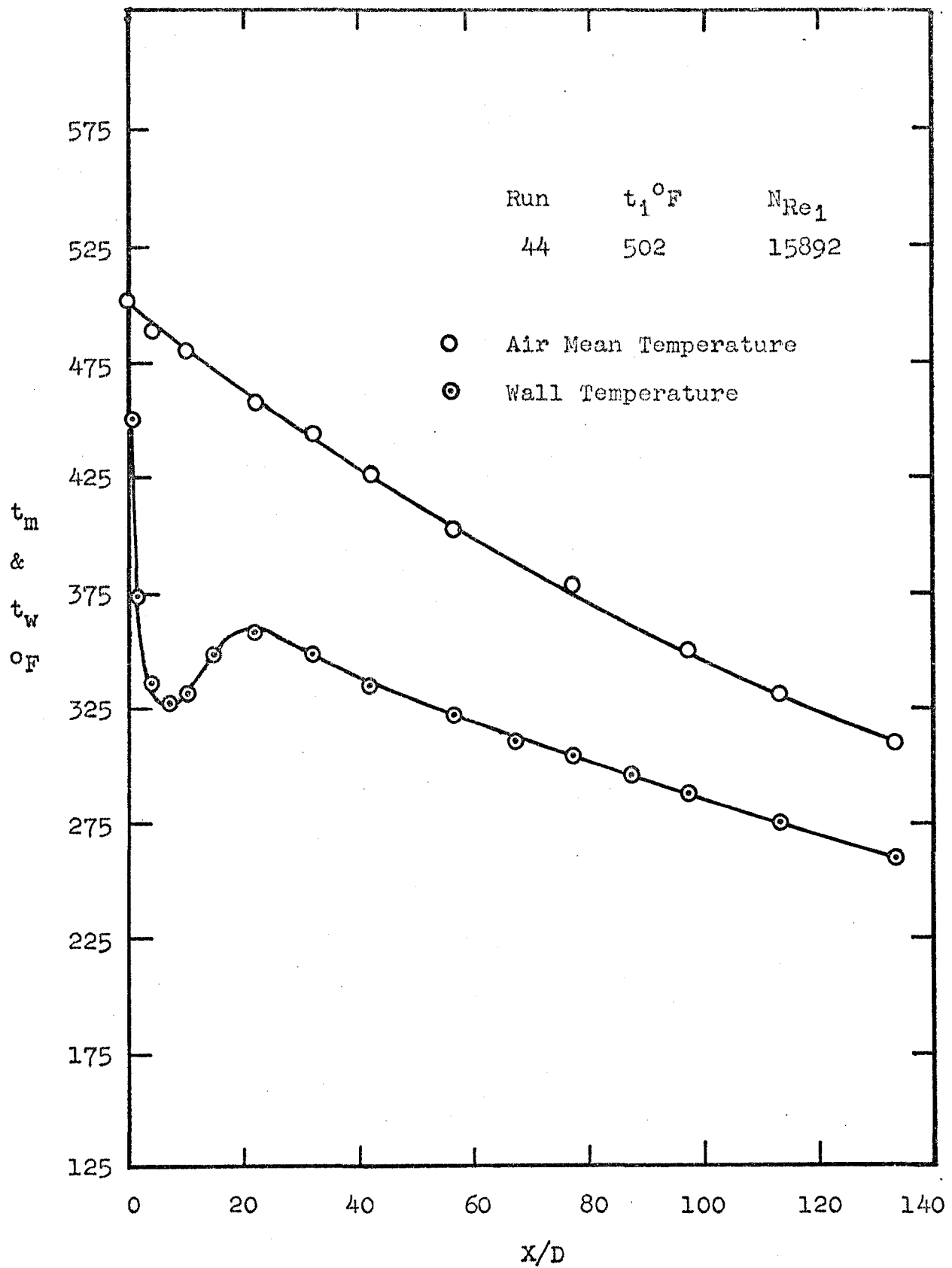


Fig. 29. Axial Variation of Air Mean and Wall Temperatures

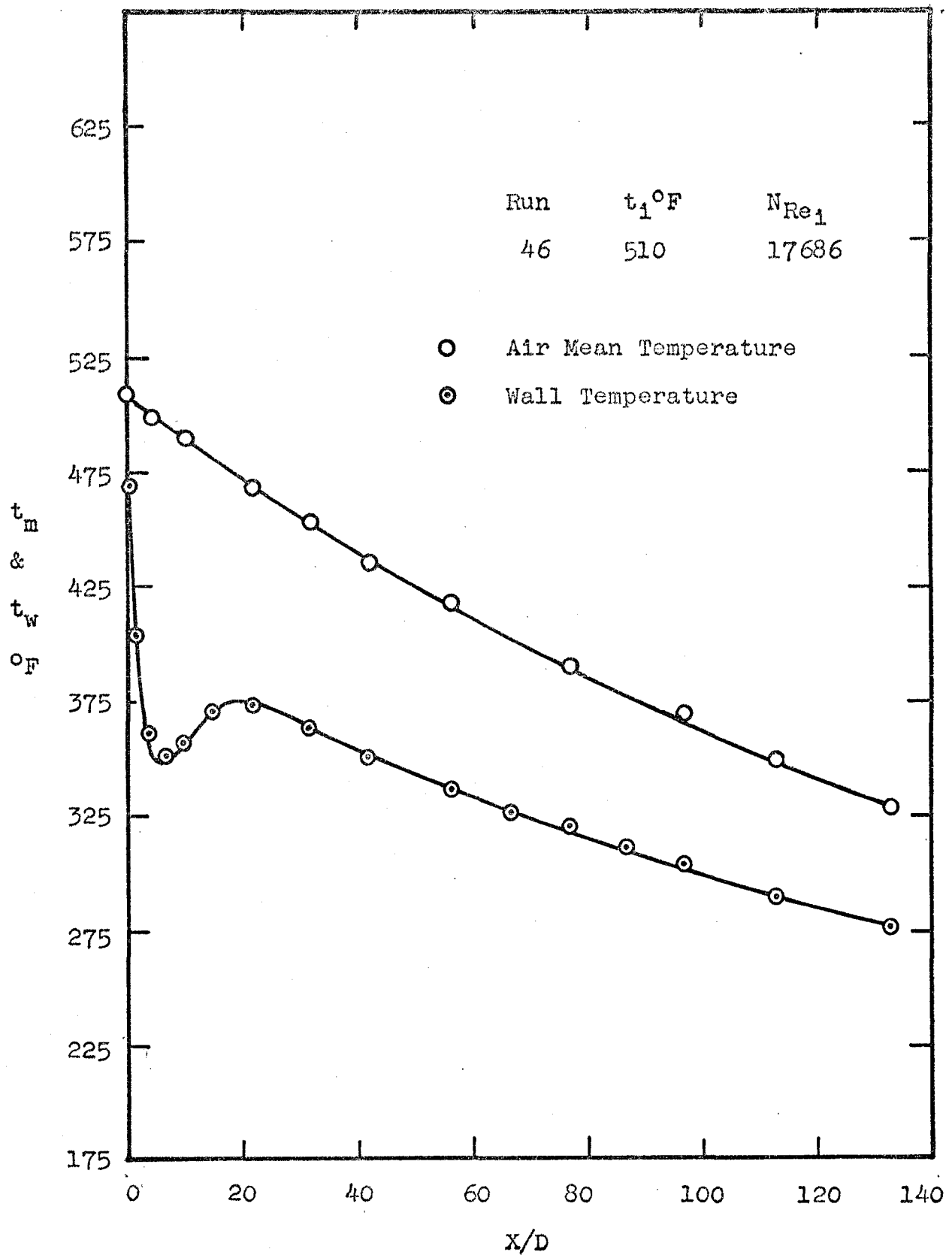


Fig. 30. Axial Variation of Air Mean and Wall Temperatures

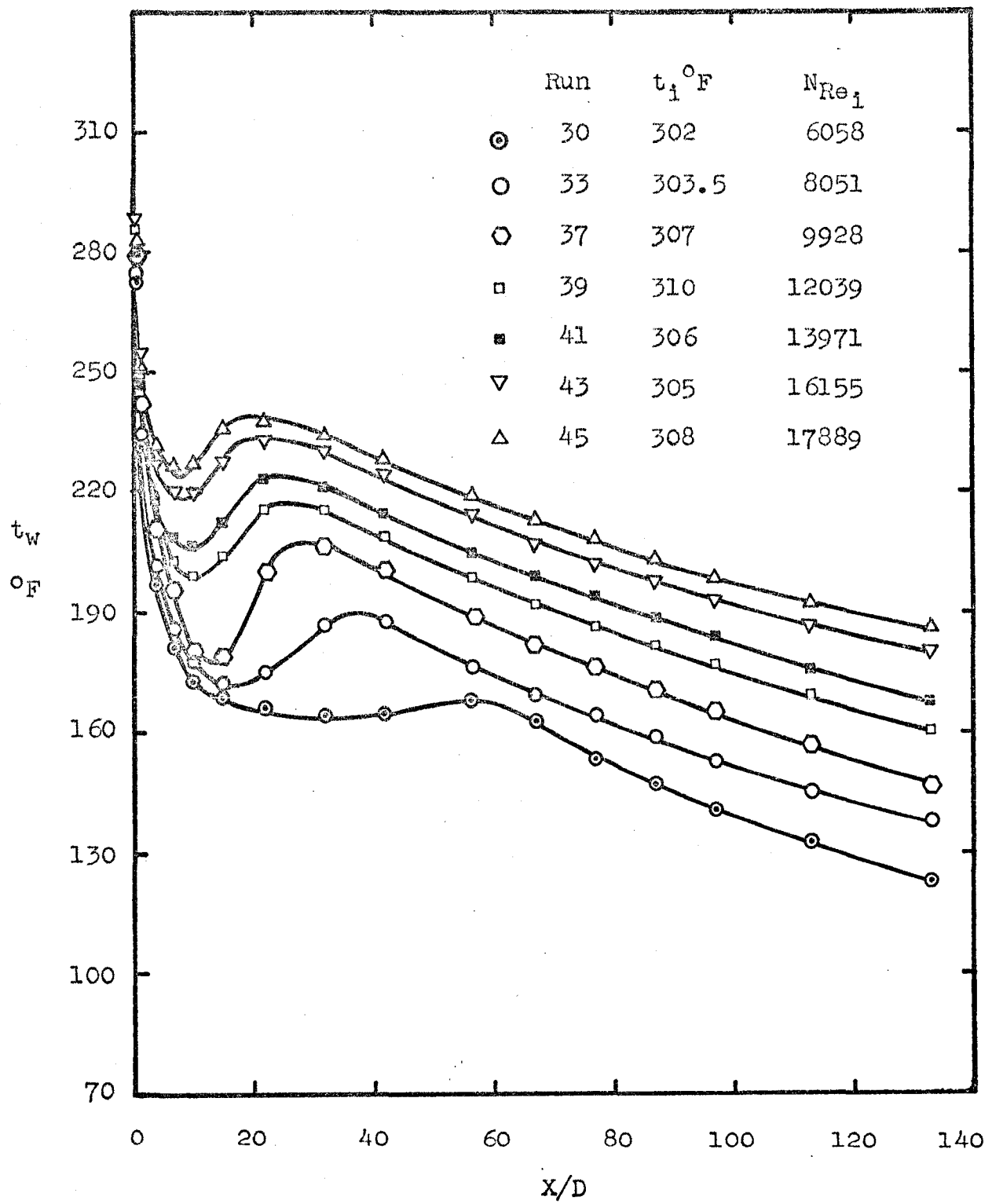


Fig. 31. Effect of Inlet Reynolds Number on the Axial Variation of Wall Temperature.

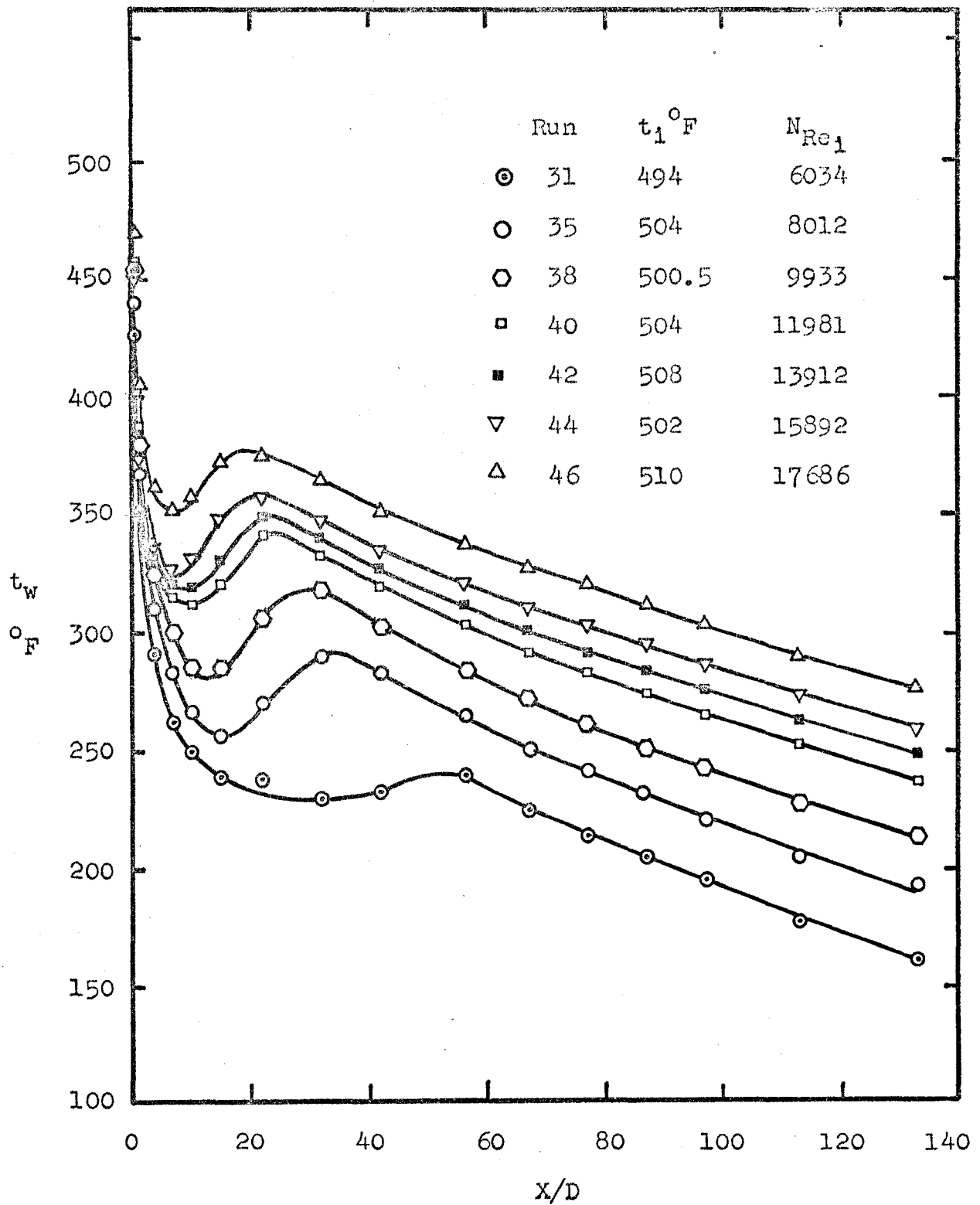


Fig. 32. Effect of Inlet Reynolds Number on the Axial Variation of Wall Temperature.

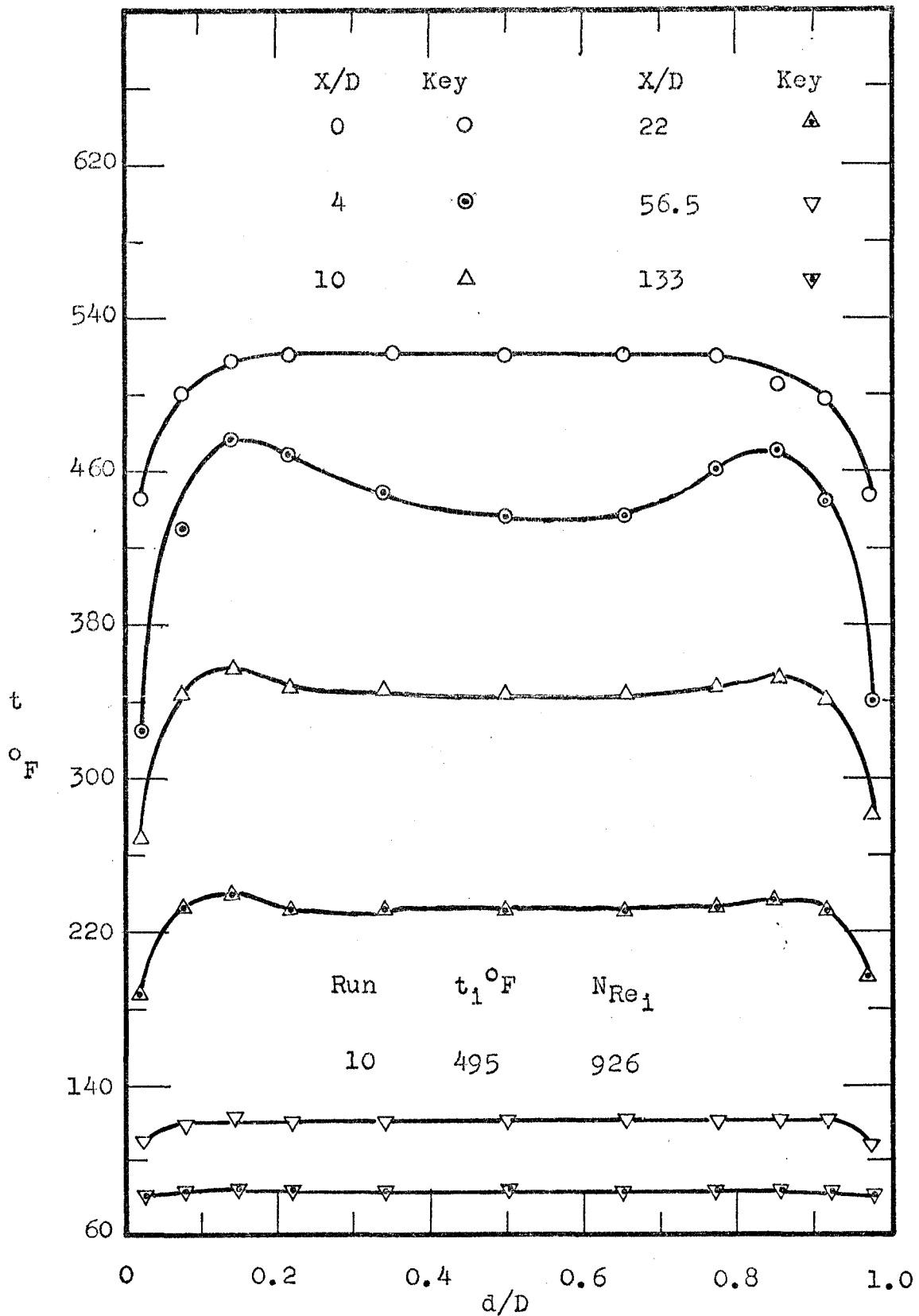


Fig. 33. Radial Horizontal Temperature Profiles at Various  $X/D$  Ratios.



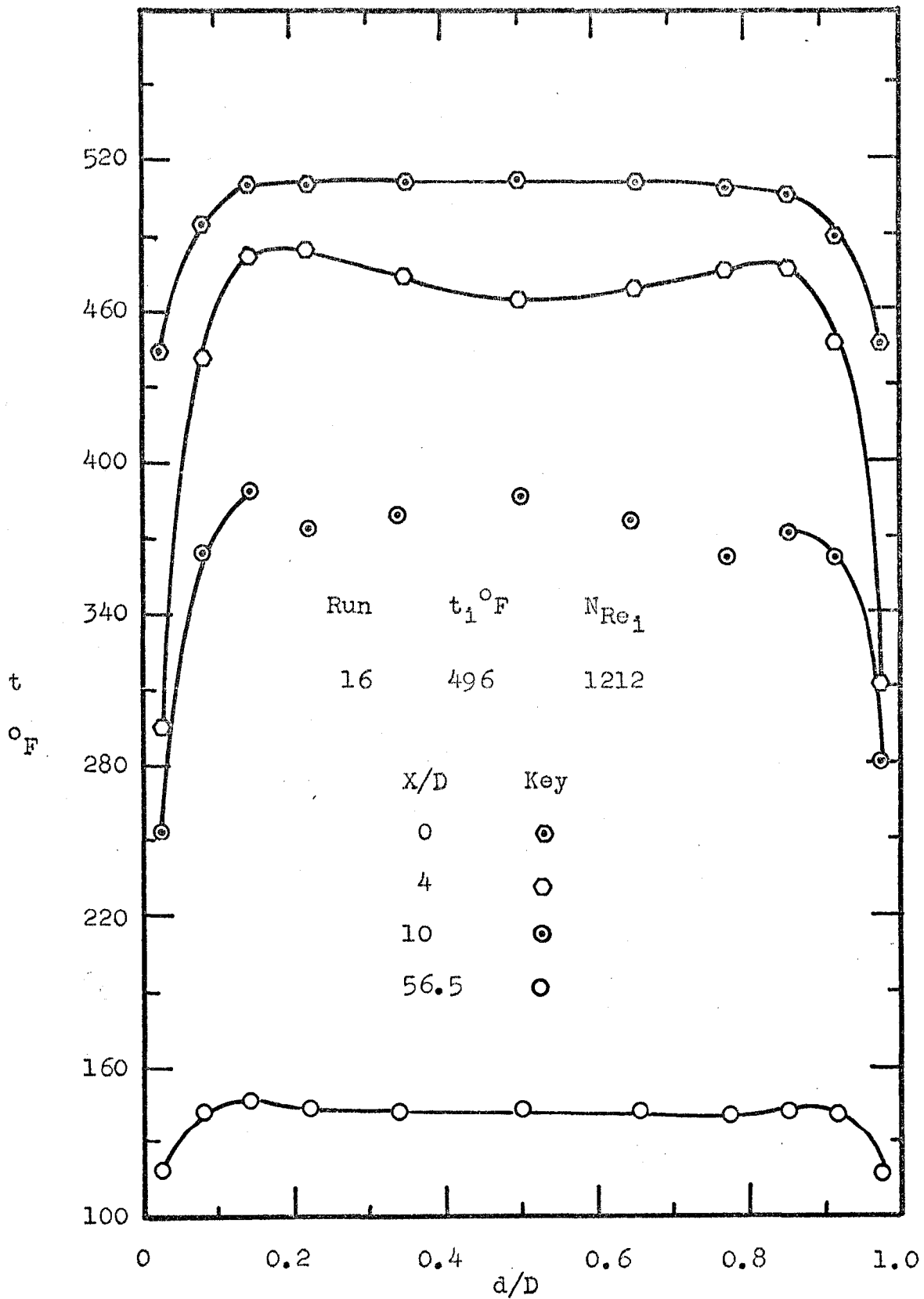


Fig. 35. Radial Horizontal Temperature Profiles at Various X/D Ratios.

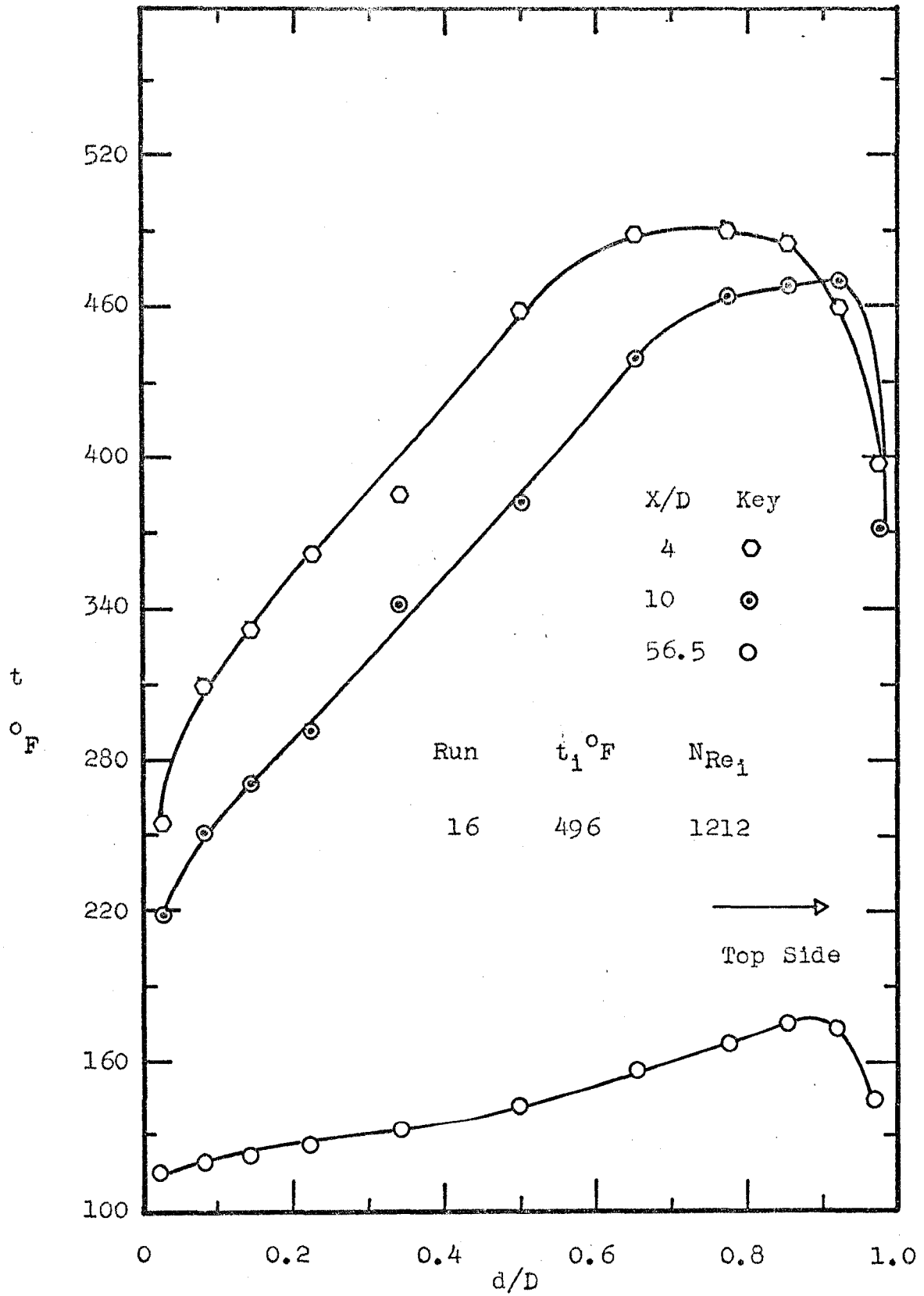


Fig. 36. Radial Perpendicular Temperature Profiles at Various  $X/D$  Ratios.

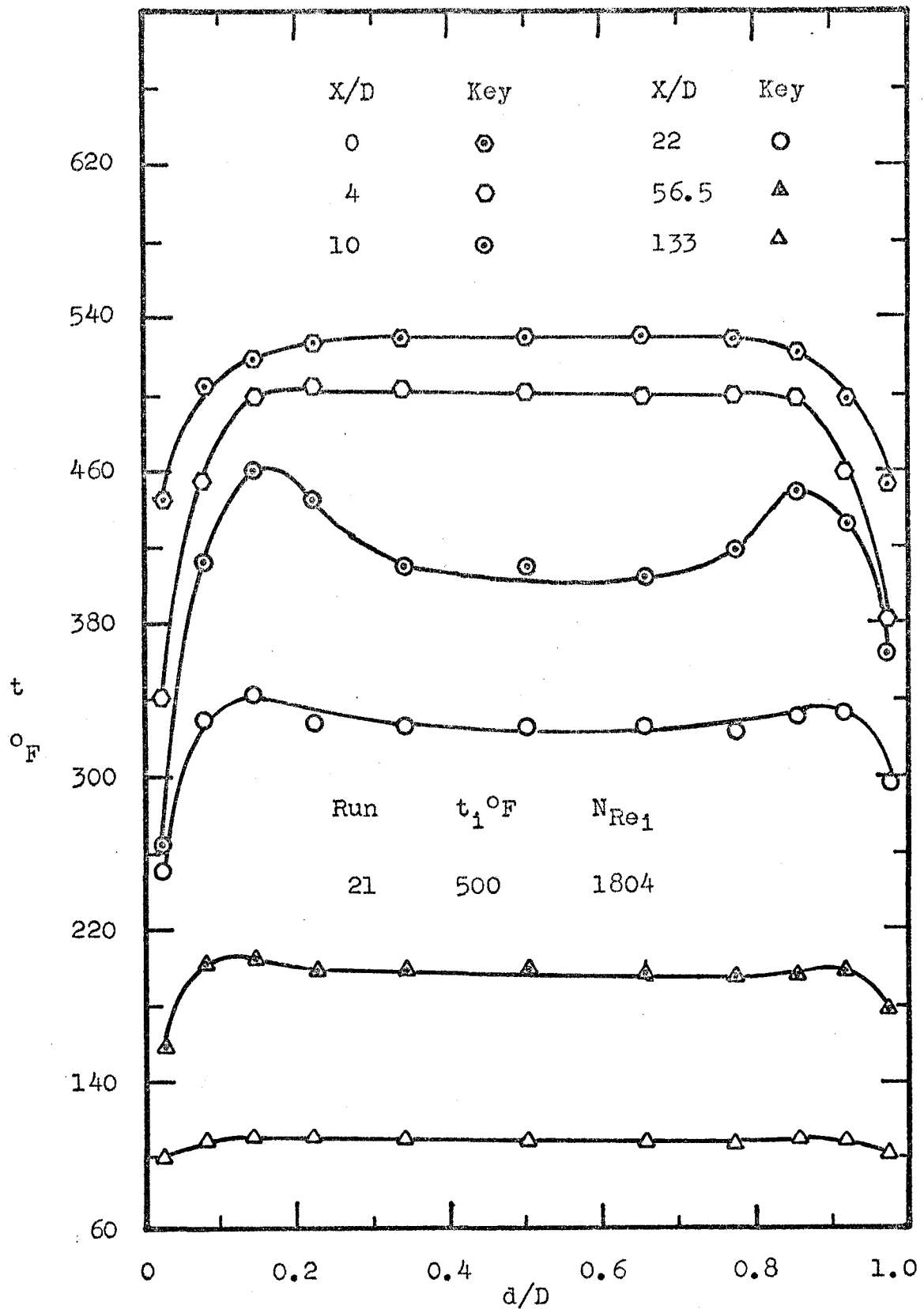


Fig. 37. Radial Horizontal Temperature Profiles at Various X/D Ratios.

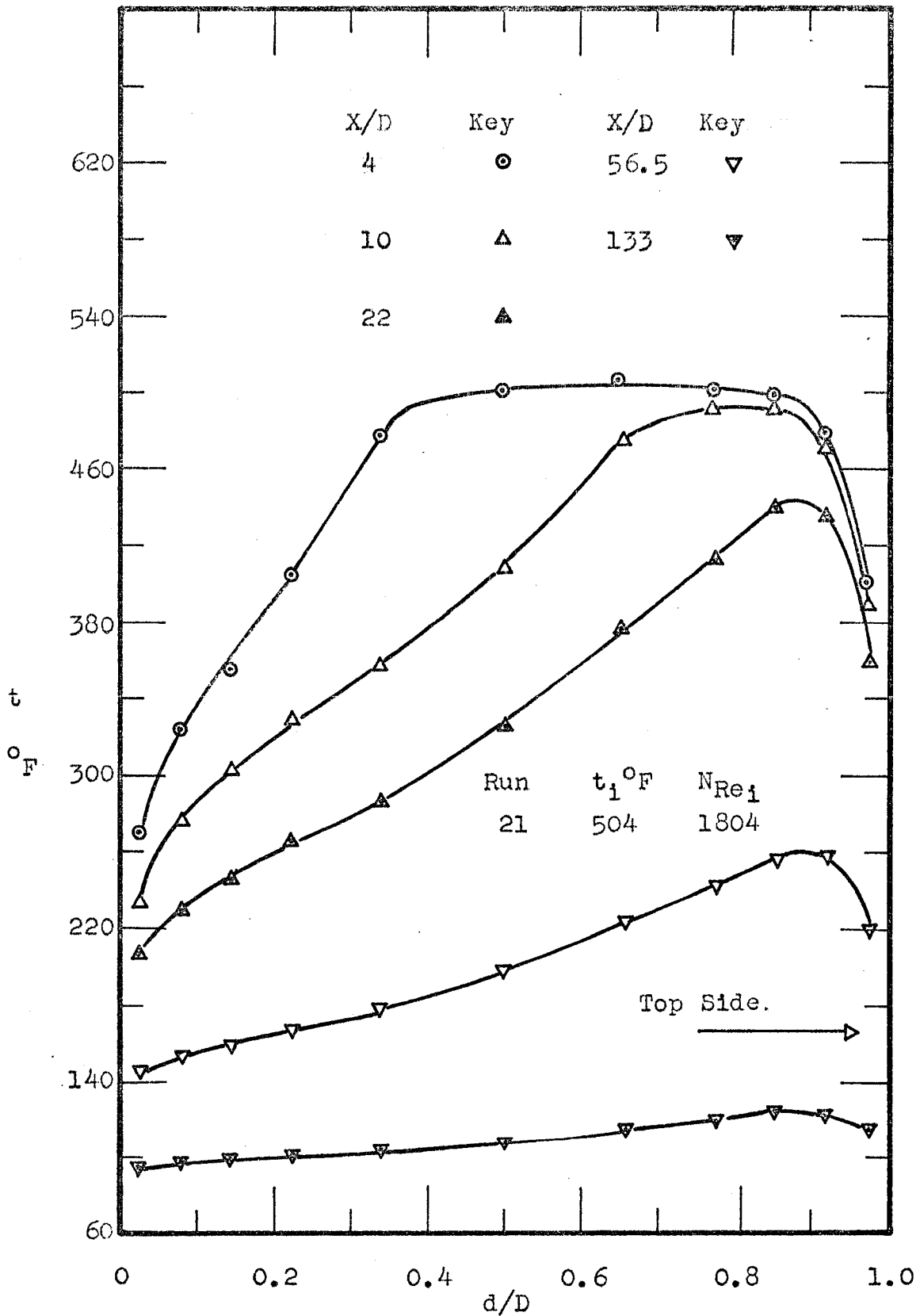


Fig. 38. Radial Perpendicular Temperature Profiles at Various X/D Ratios.

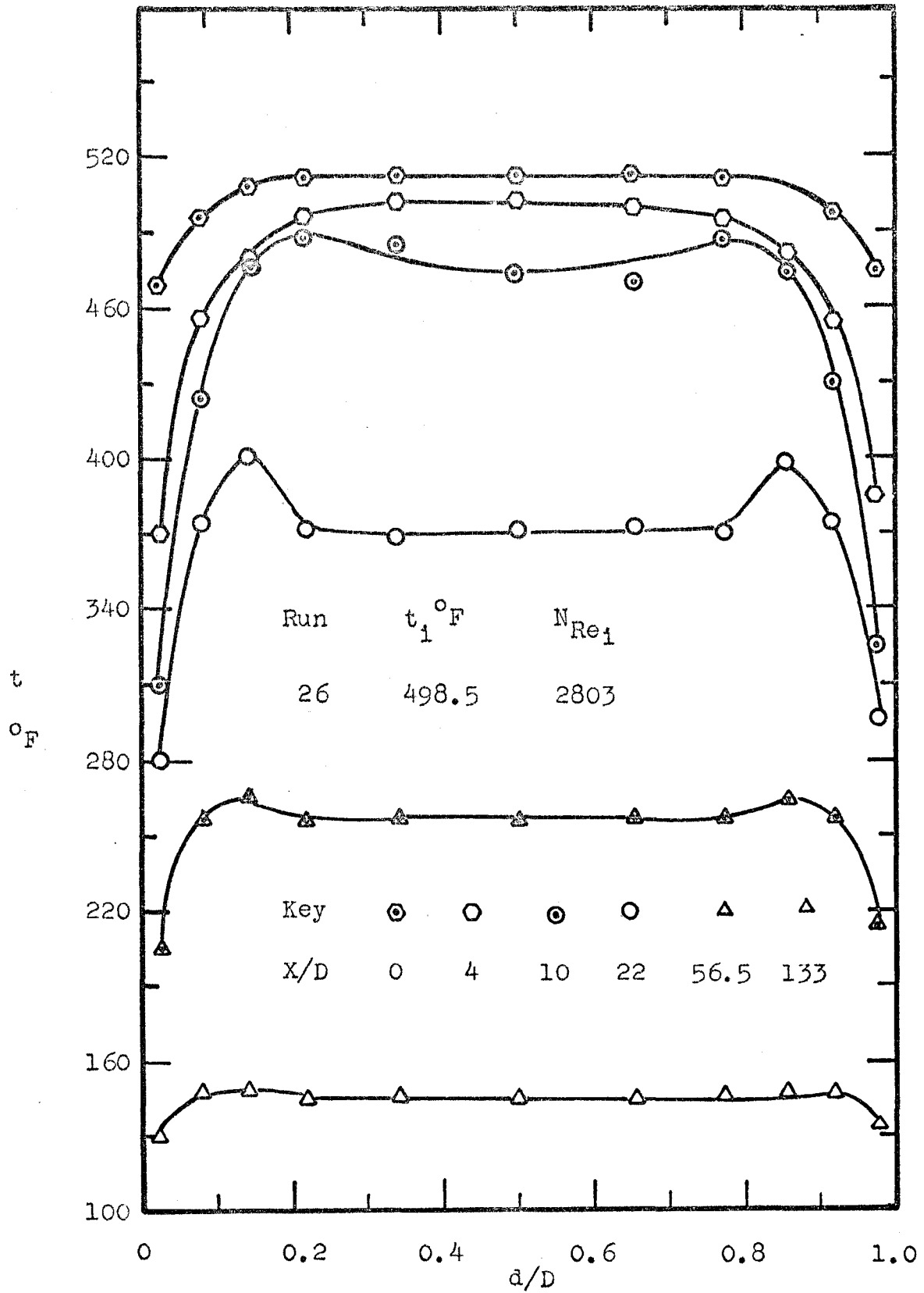


Fig. 39. Radial Horizontal Temperature Profiles at Various  $X/D$  Ratios.

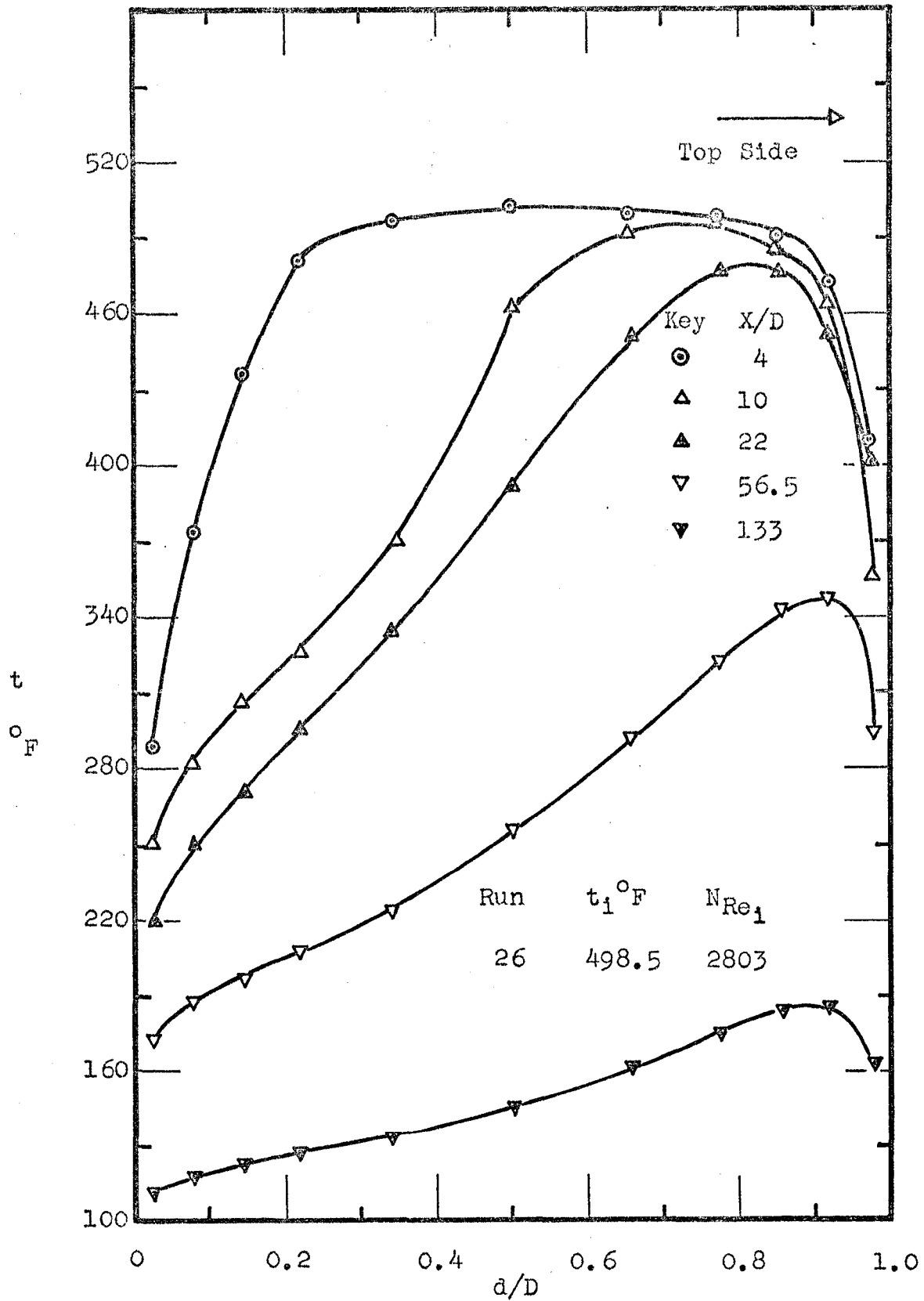


Fig. 40. Radial Perpendicular Temperature Profiles at Various X/D Ratios.

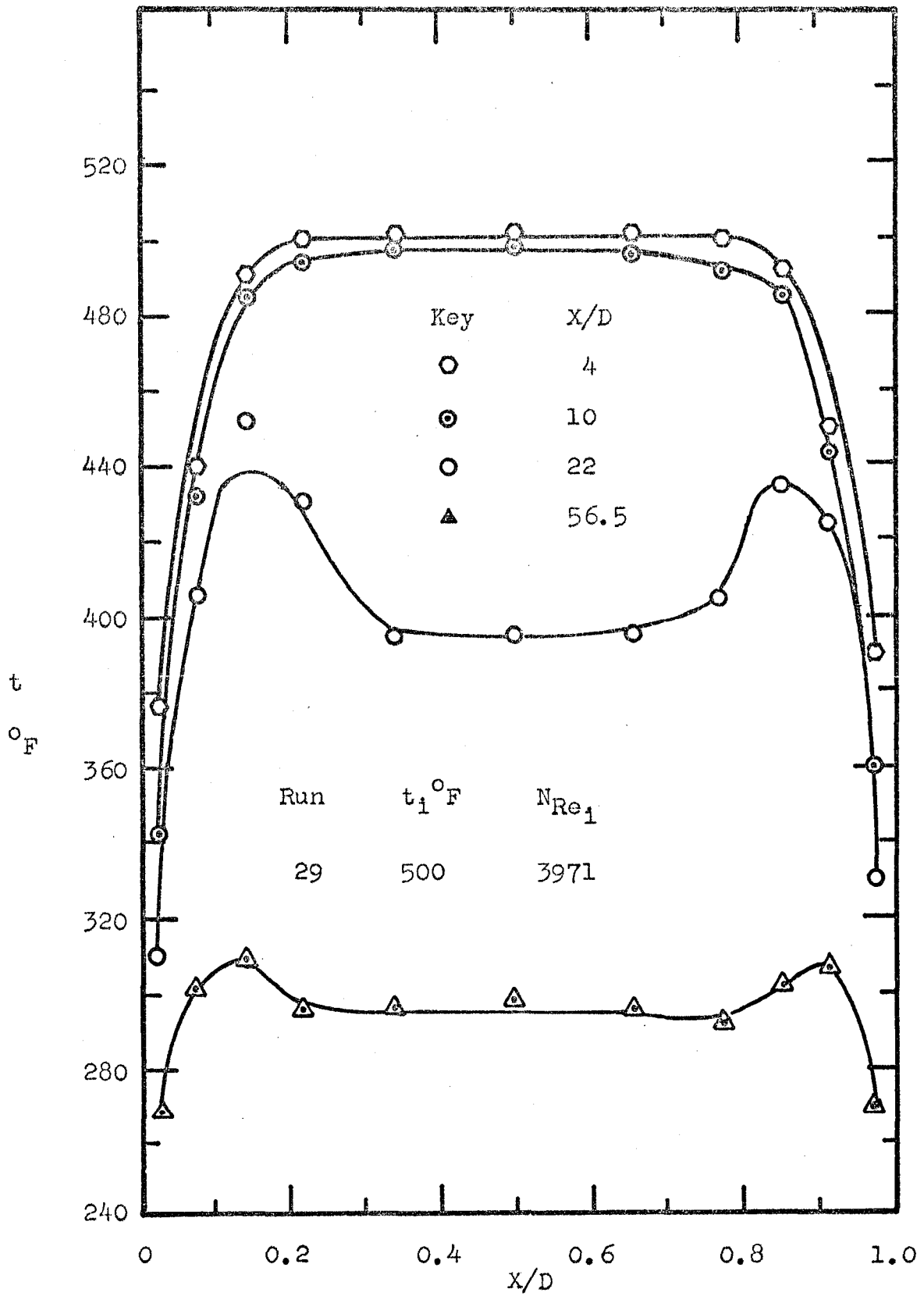


Fig. 41. Radial Horizontal Temperature Profiles at Various X/D Ratios.

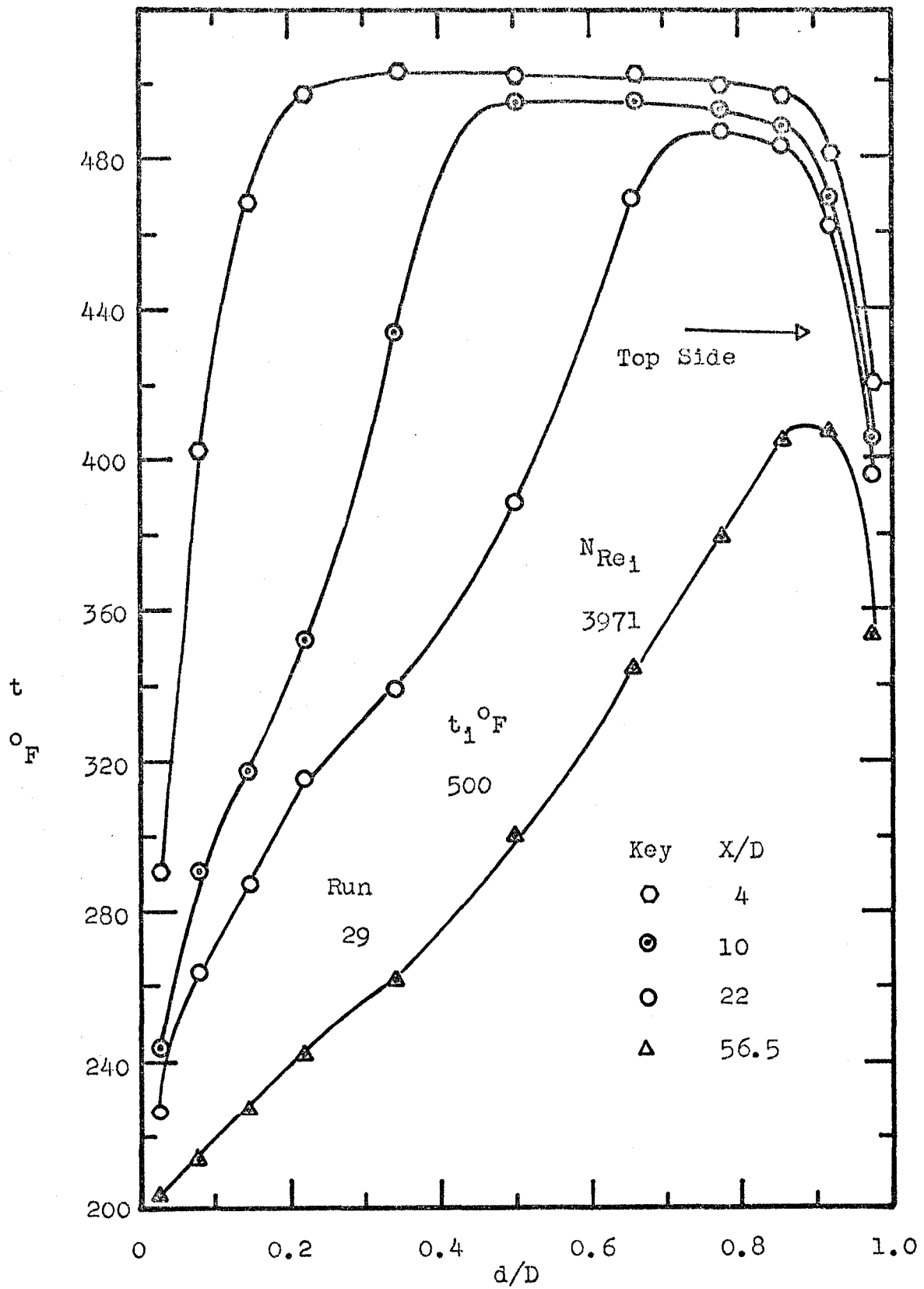


Fig. 42. Radial Perpendicular Temperature Profiles at Various X/D Ratios.

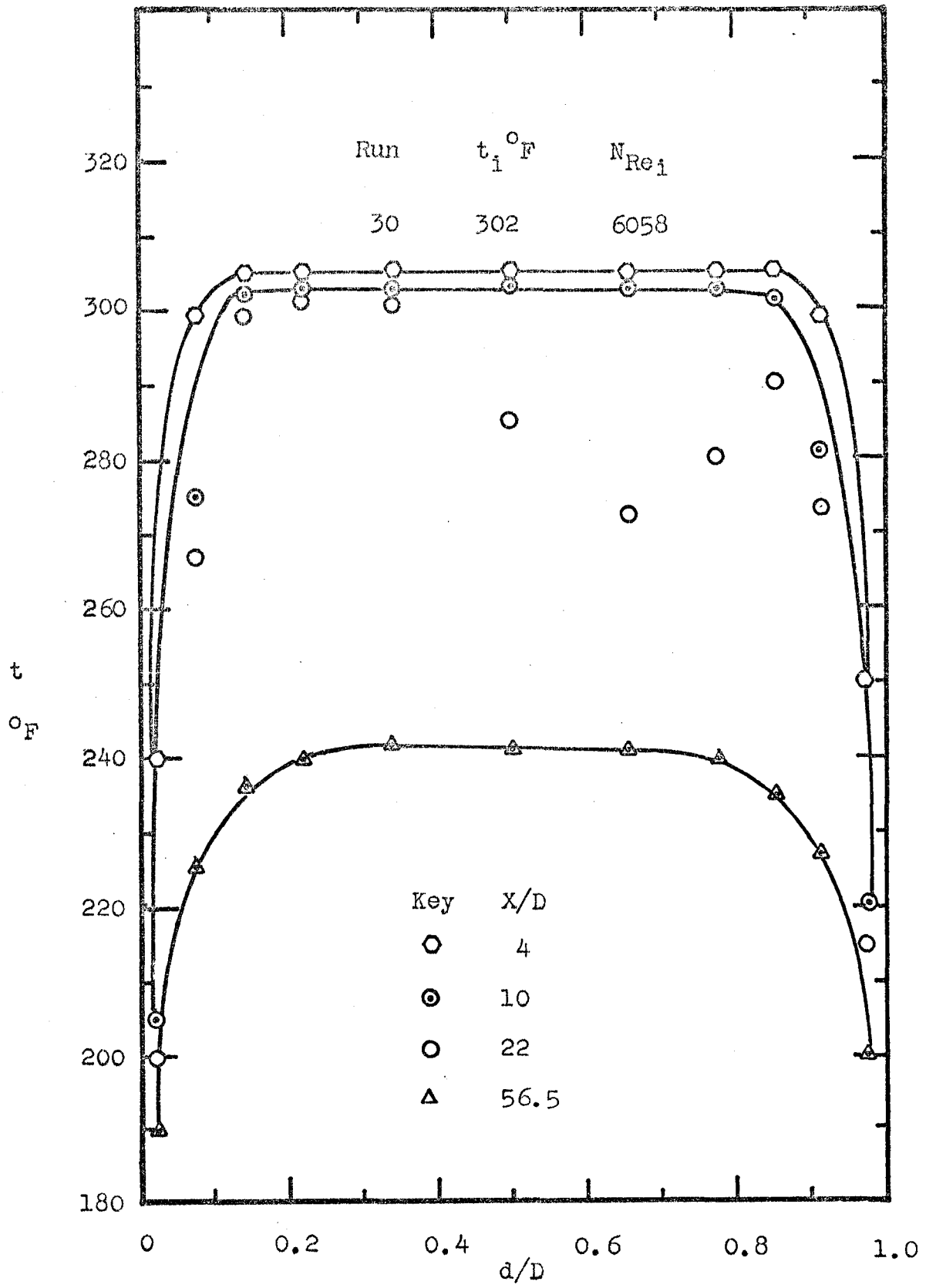


Fig. 43. Radial Horizontal Temperature Profiles at Various X/D Ratios.

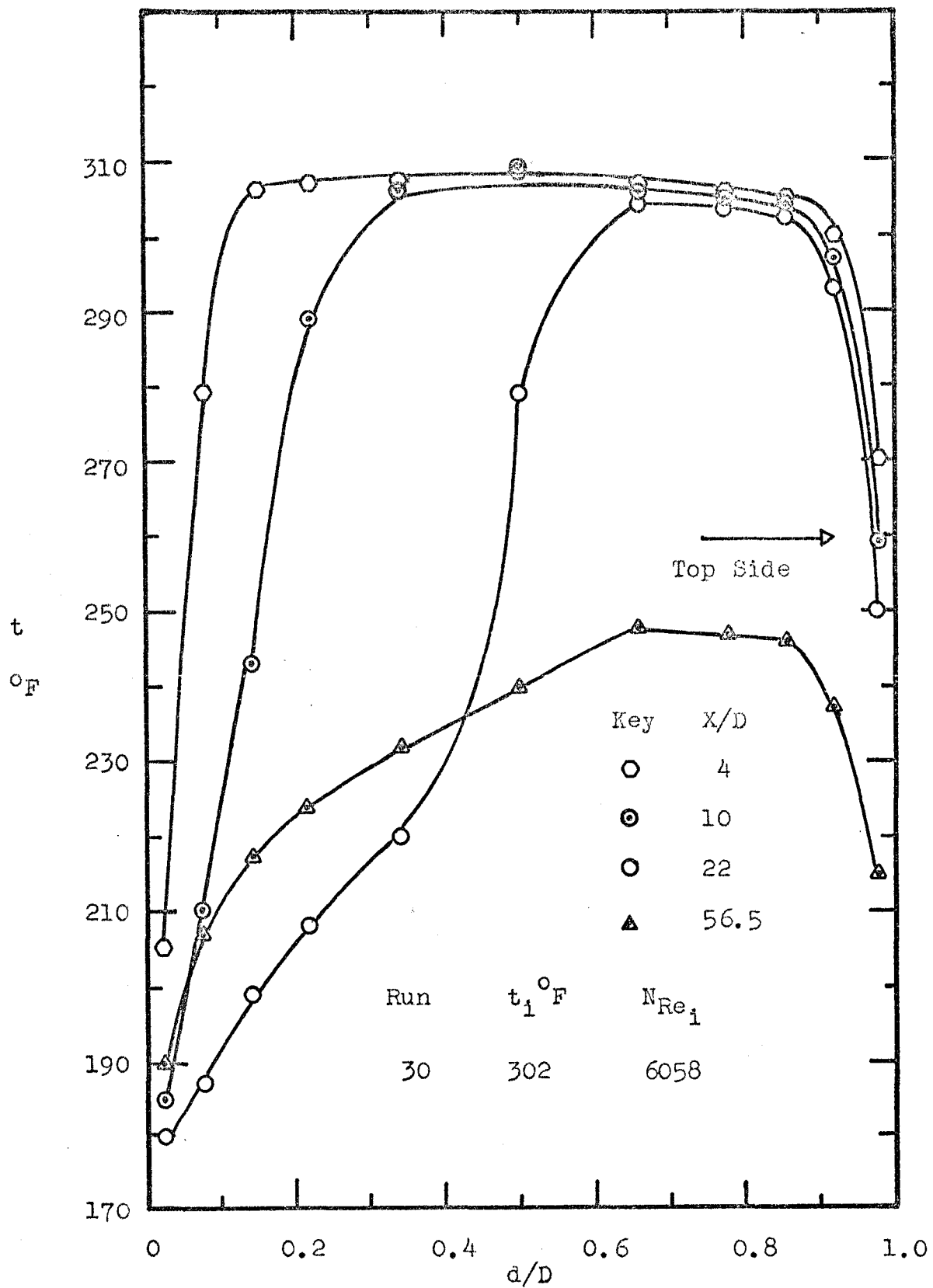


Fig. 44. Radial Perpendicular Temperature Profiles at Various X/D Ratios.

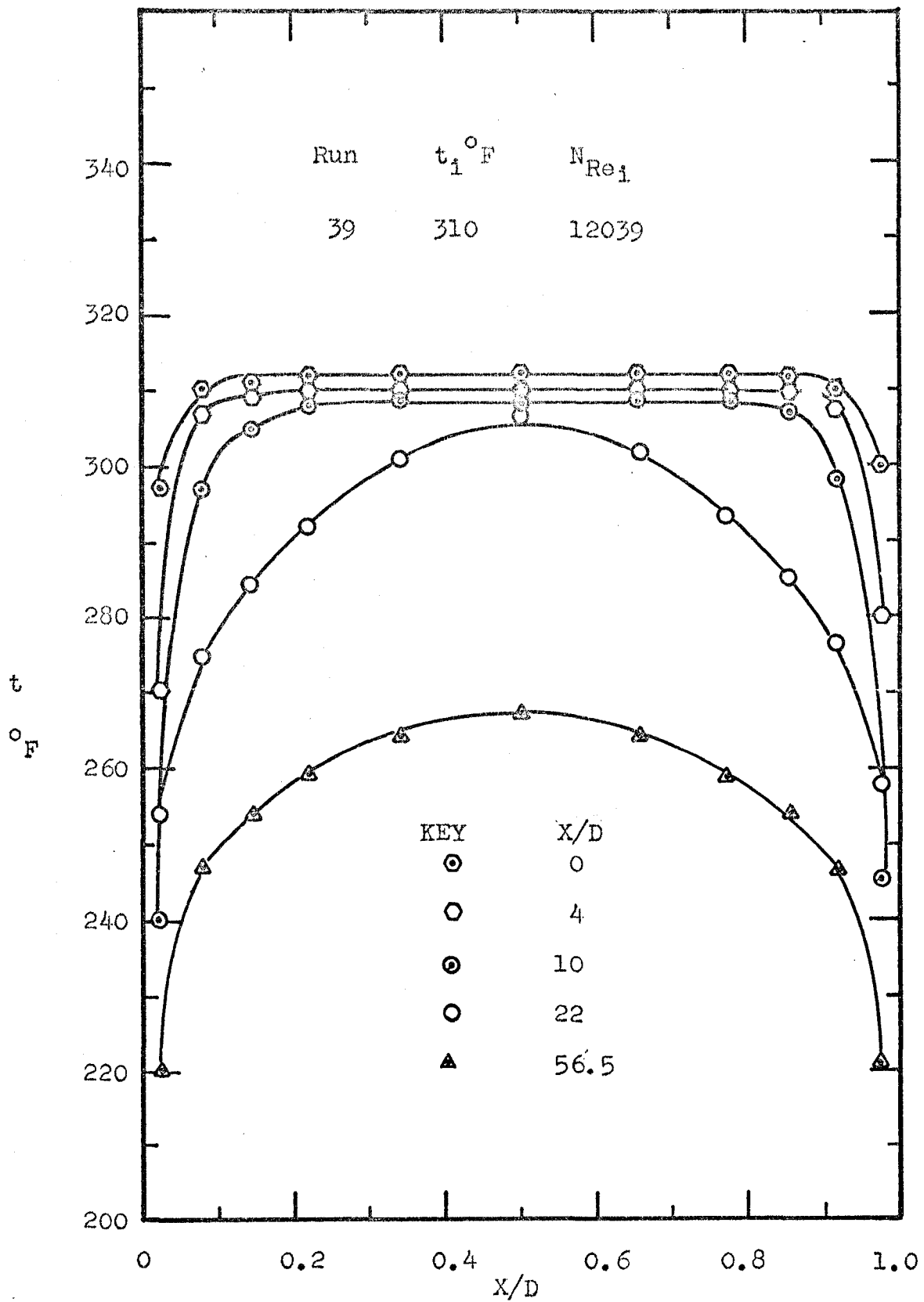


Fig. 45. Radial Horizontal Temperature Profiles at Various X/D Ratios.

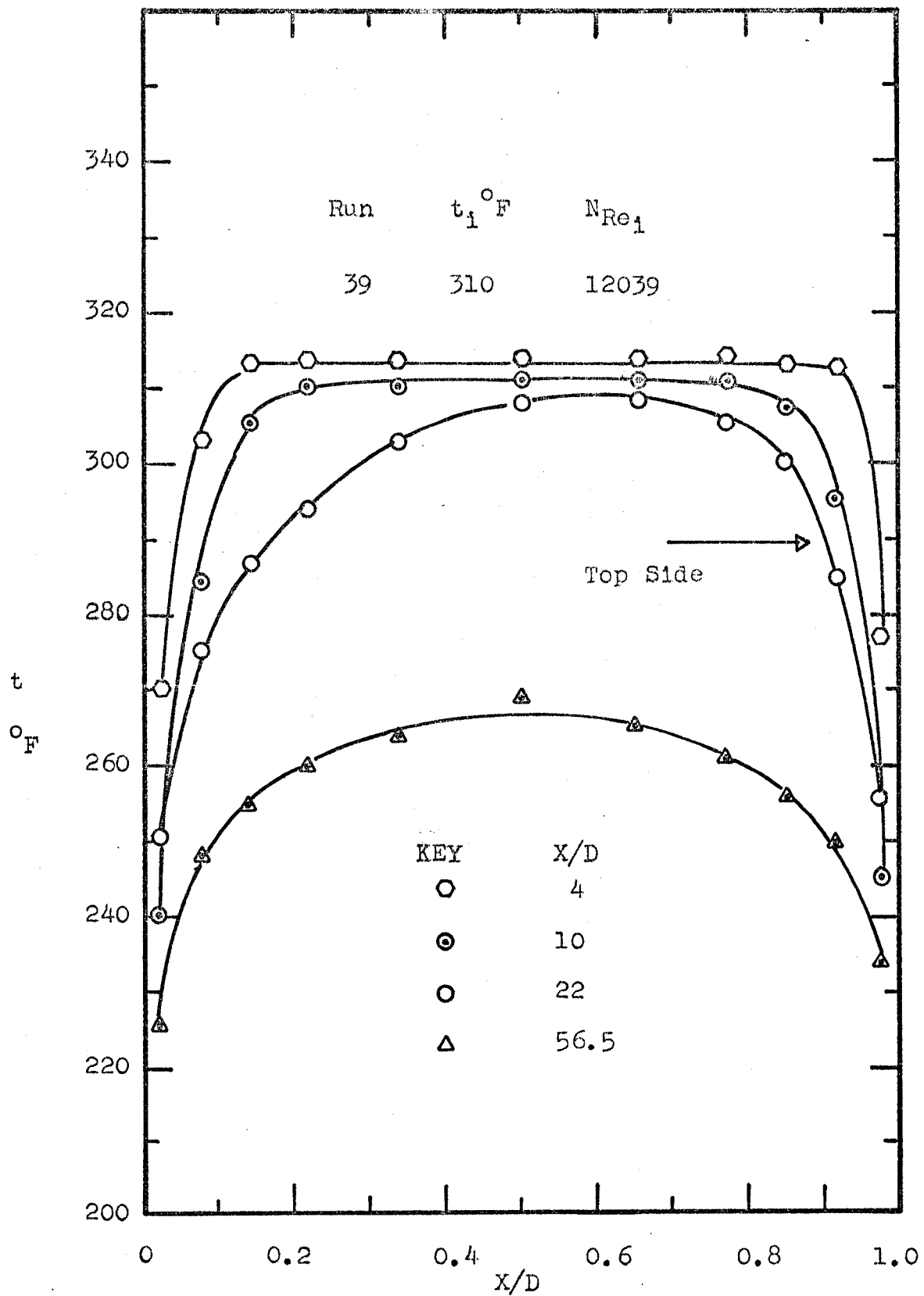


Fig. 46. Radial Perpendicular Temperature Profiles at Various  $X/D$  Ratios.

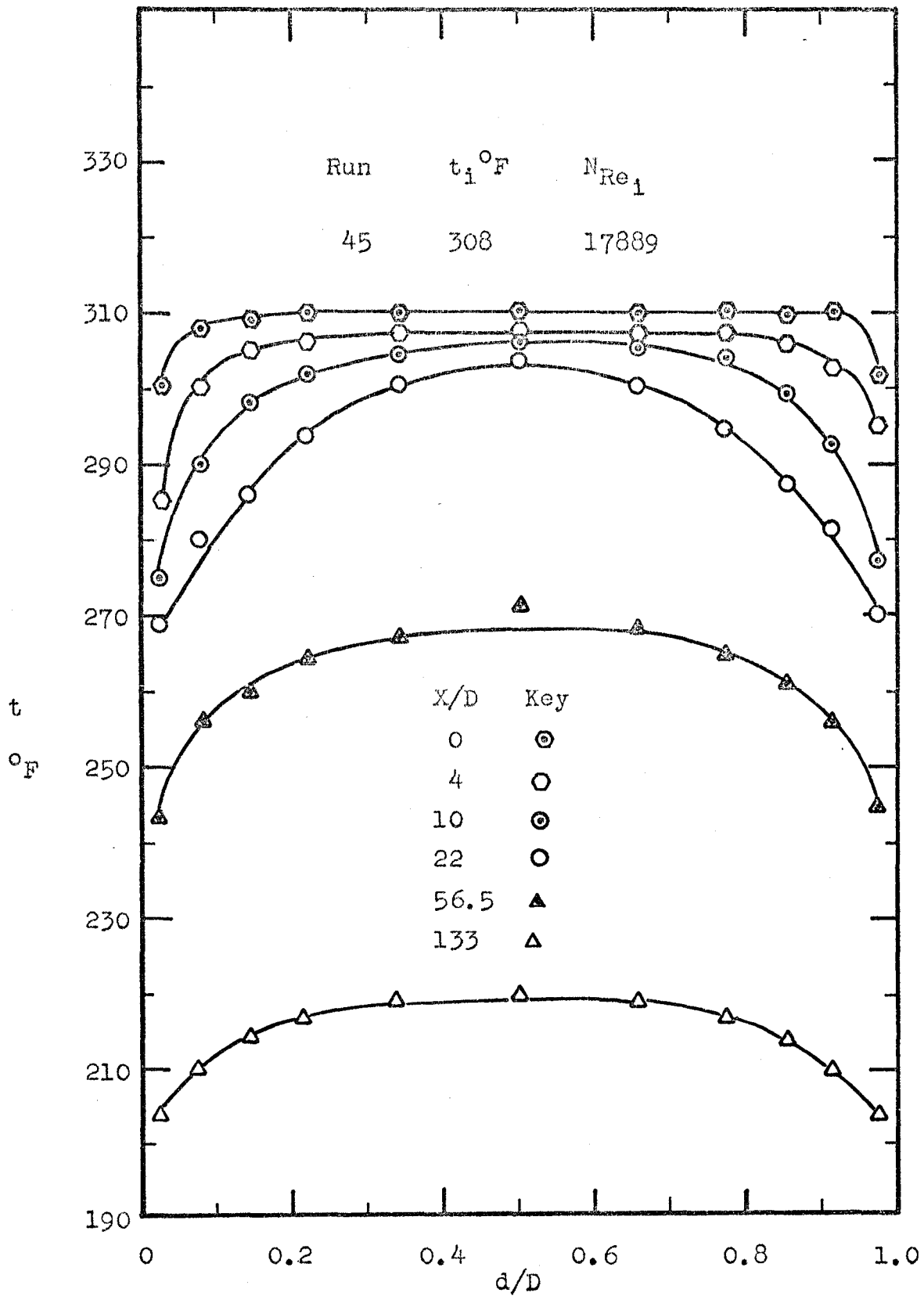


Fig. 47. Radial Horizontal Temperature Profiles at Various X/D Ratios.

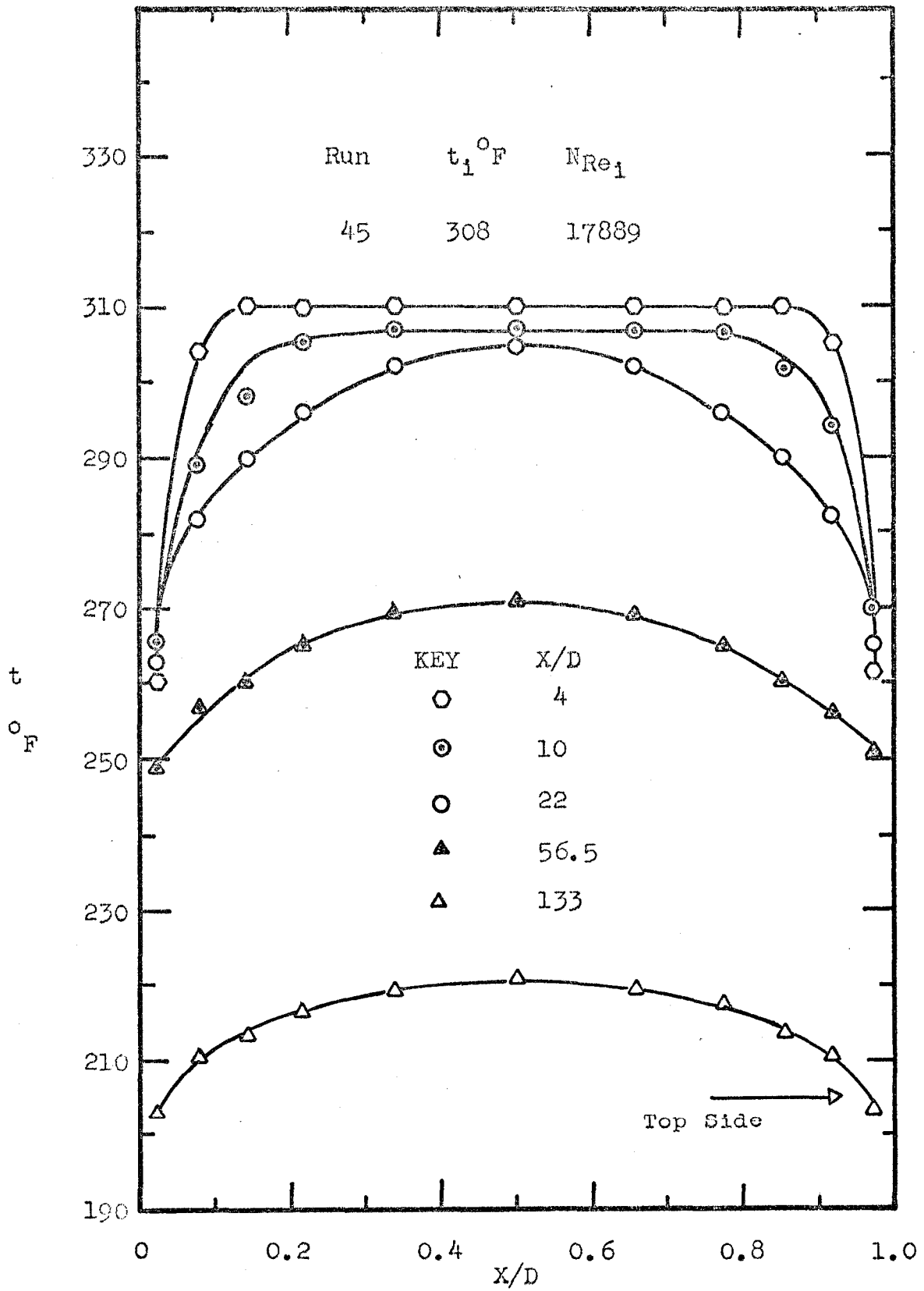


Fig. 48. Radial Perpendicular Temperature Profiles at Various X/D Ratios.

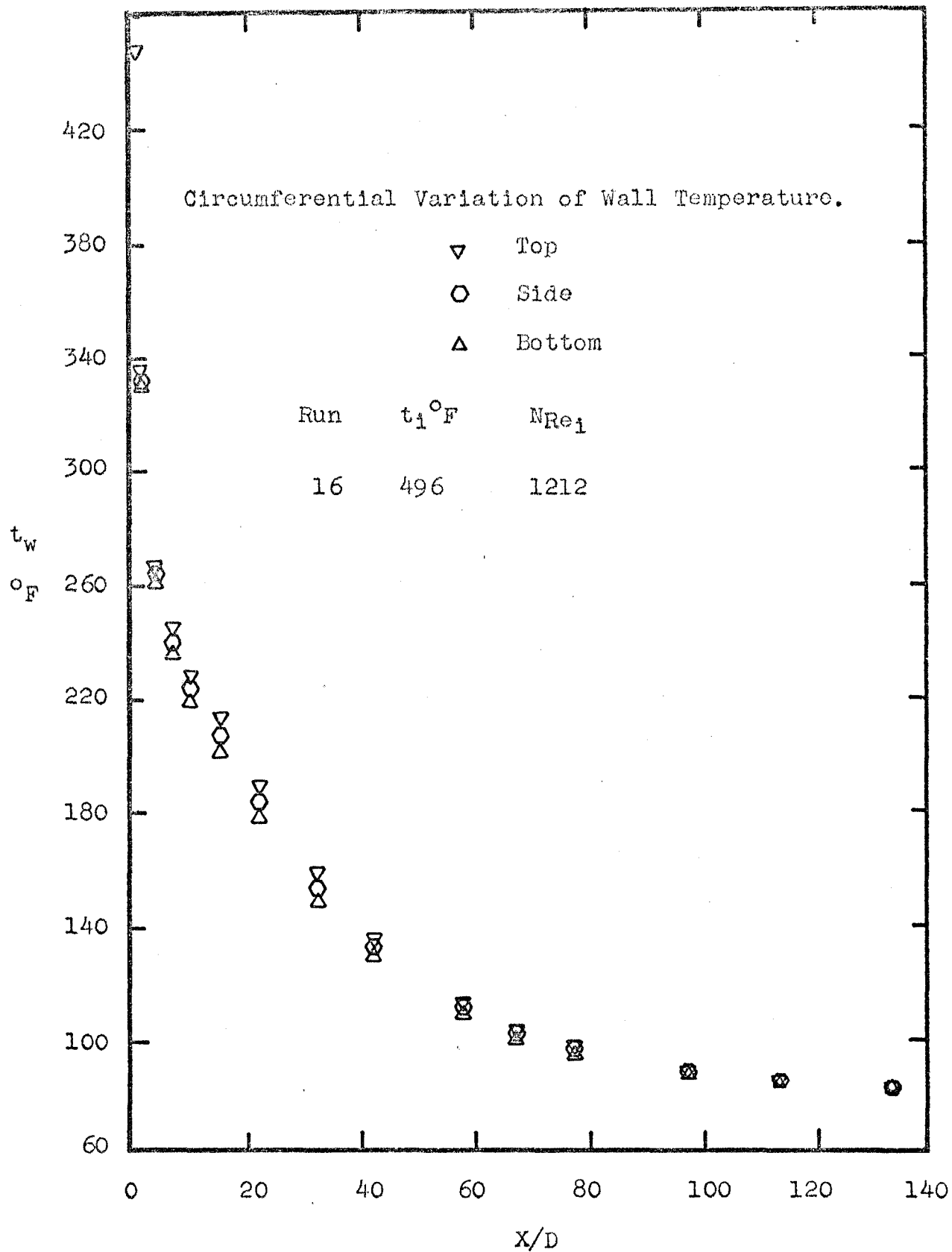


Fig. 49. Circumferential and Axial Variation of Wall Temperatures.

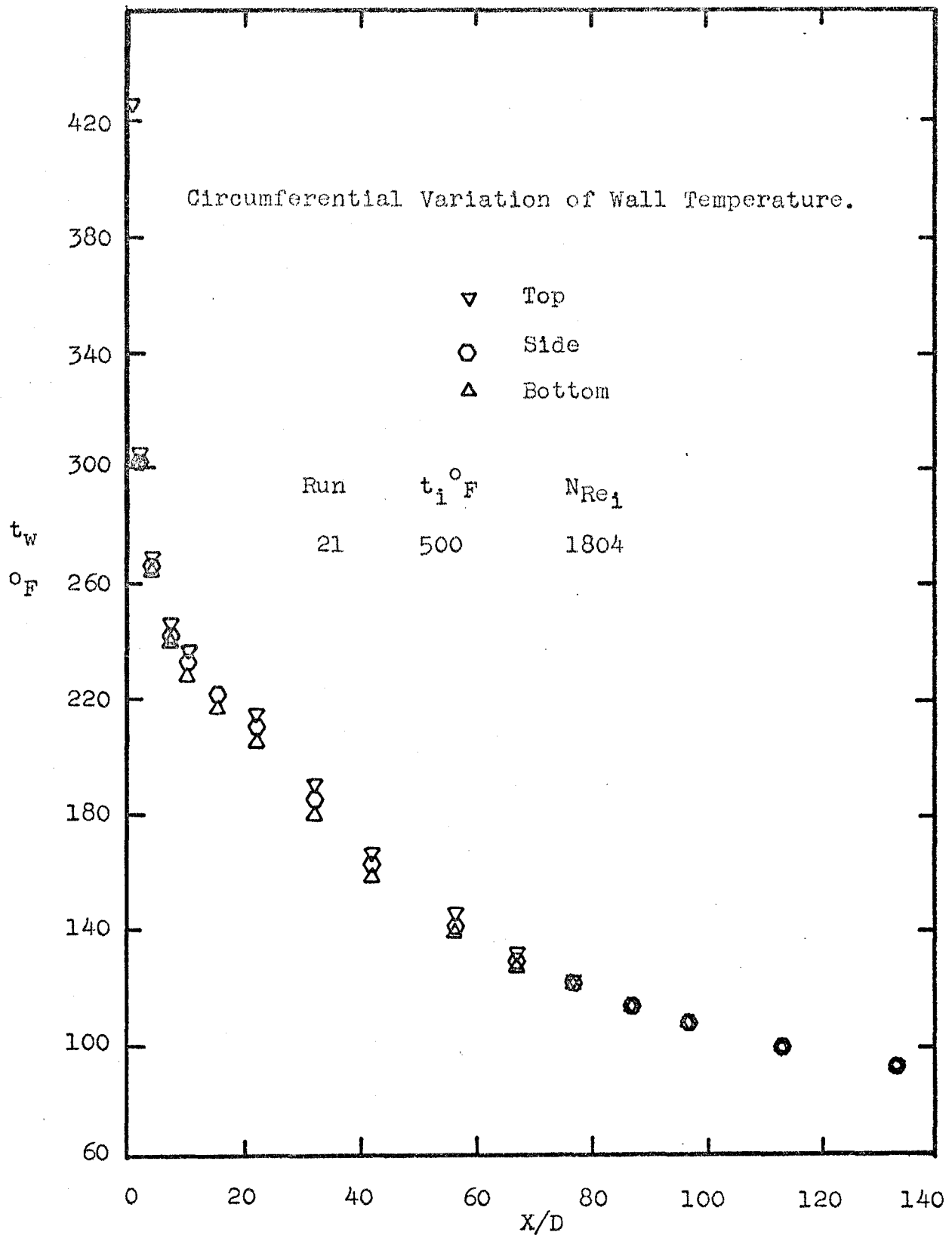


Fig. 50. Circumferential and Axial Variation of Wall Temperatures.

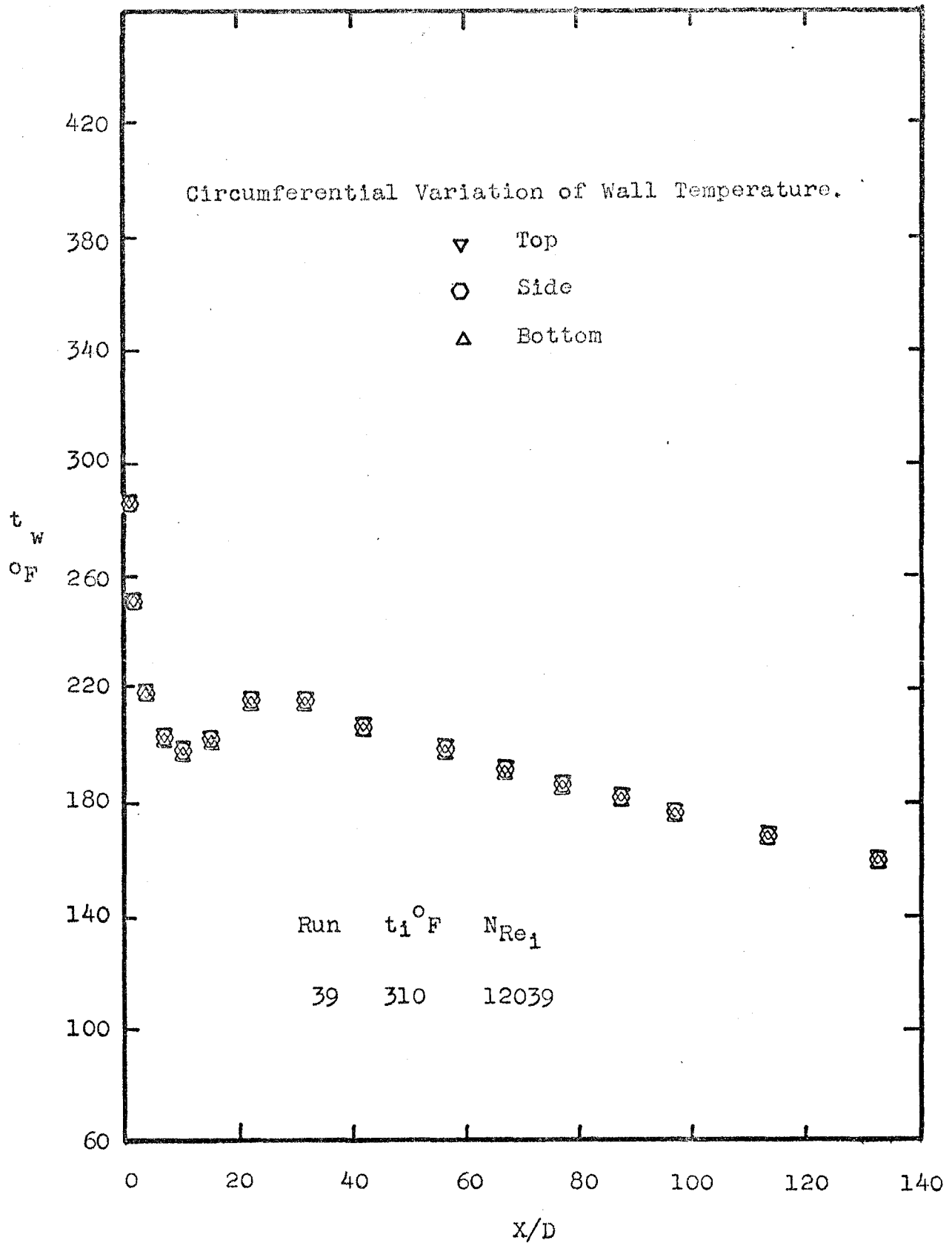


Fig. 51. Circumferential and Axial Variation of Wall Temperatures.

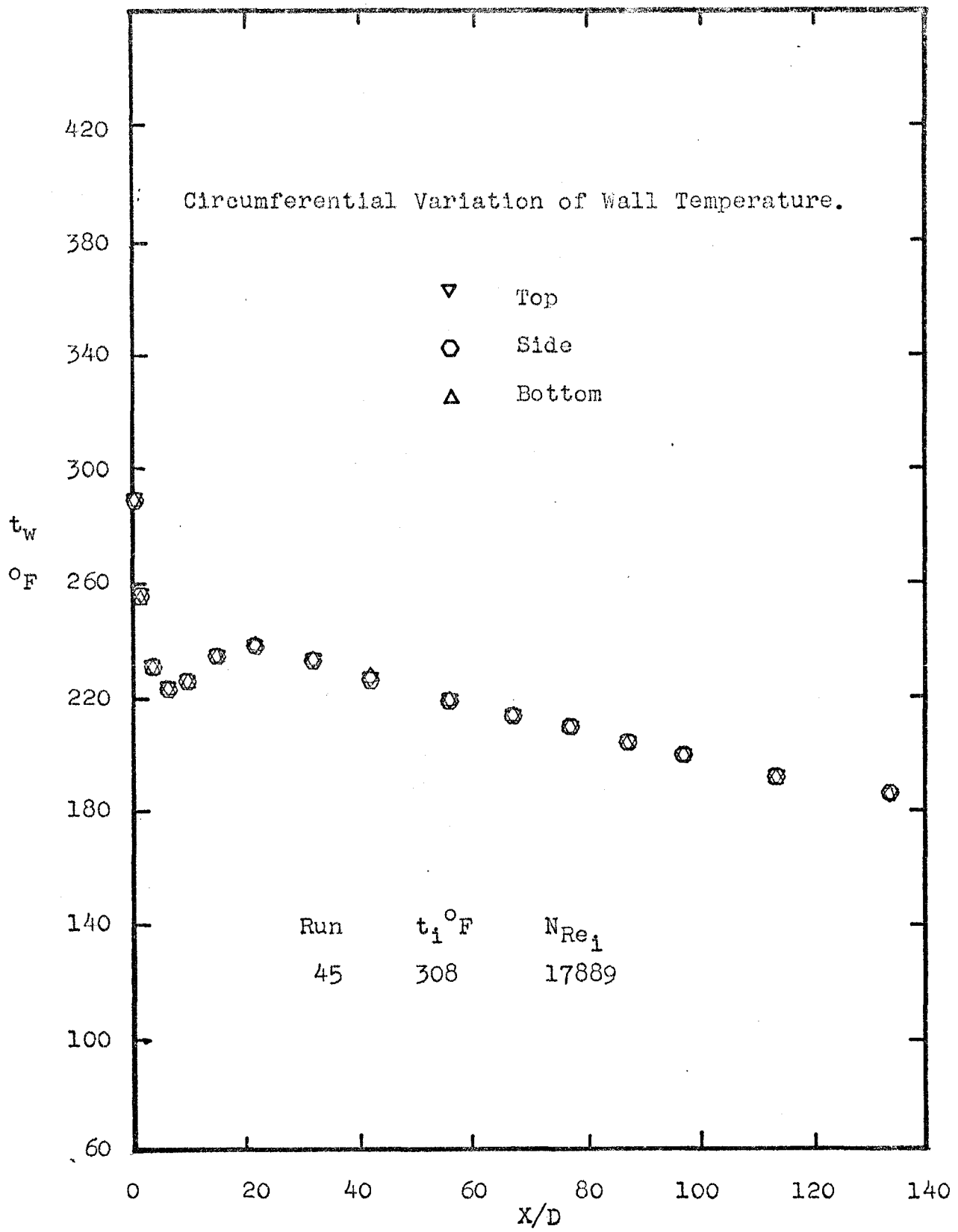


Fig. 52. Circumferential and Axial Variation of Wall Temperatures.

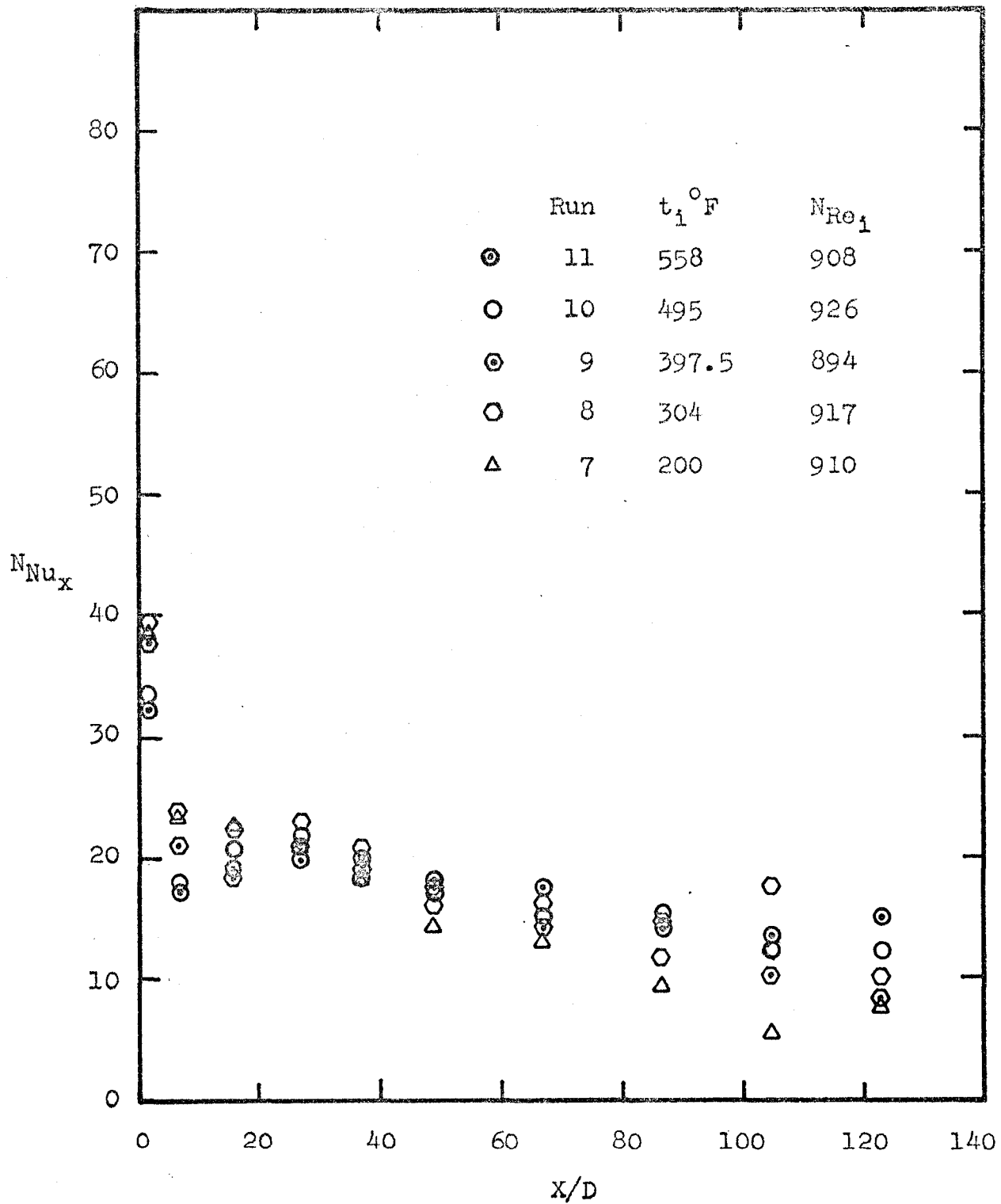


Fig. 53. Effect of Inlet Air Temperature on the Axial Variation of Local Nusselt Number.

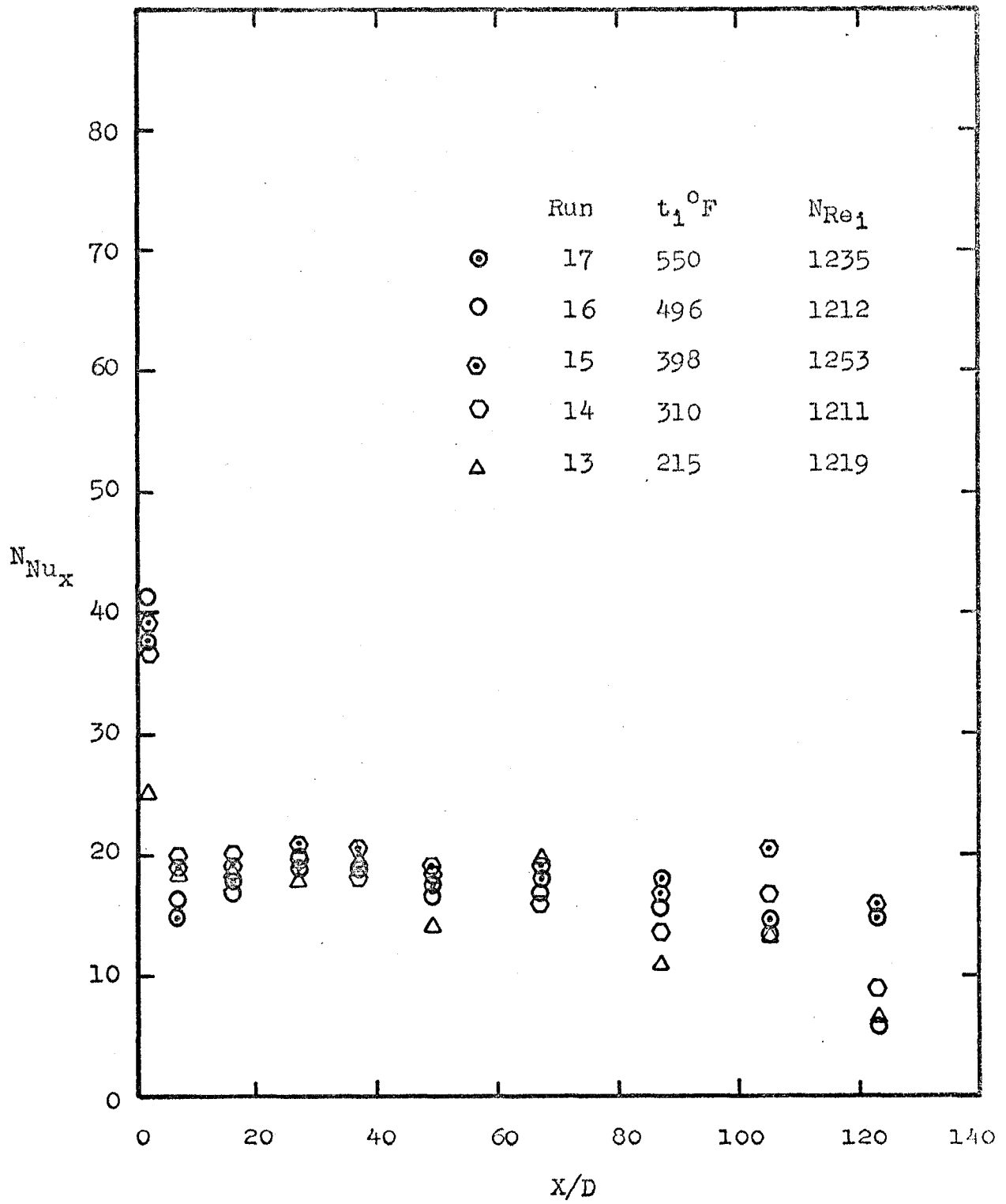


Fig. 54. Effect of Inlet Air Temperature on the Axial Variation of Local Nusselt Number.

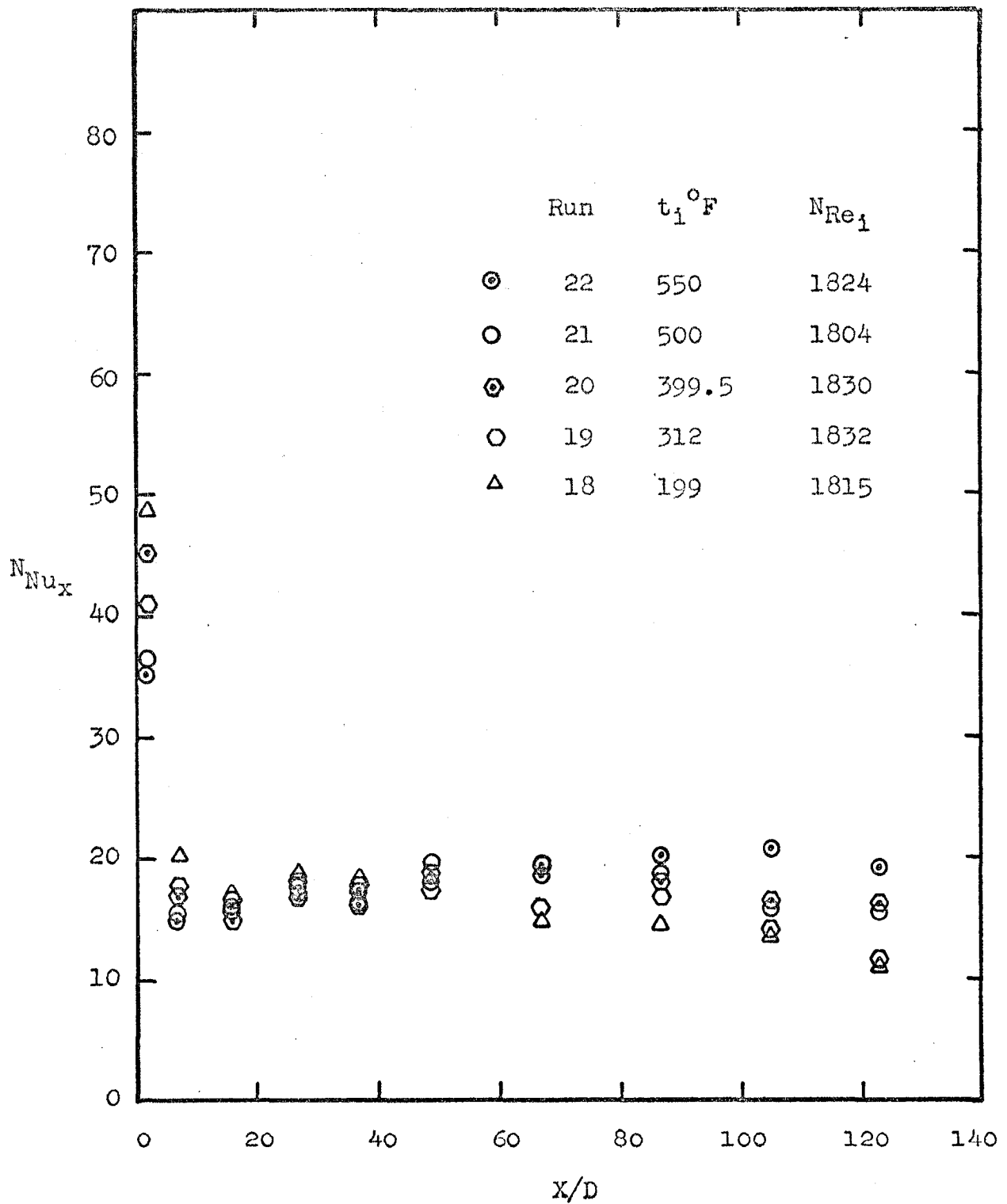


Fig. 55. Effect of Inlet Air Temperature on the Axial Variation of Local Nusselt Number.

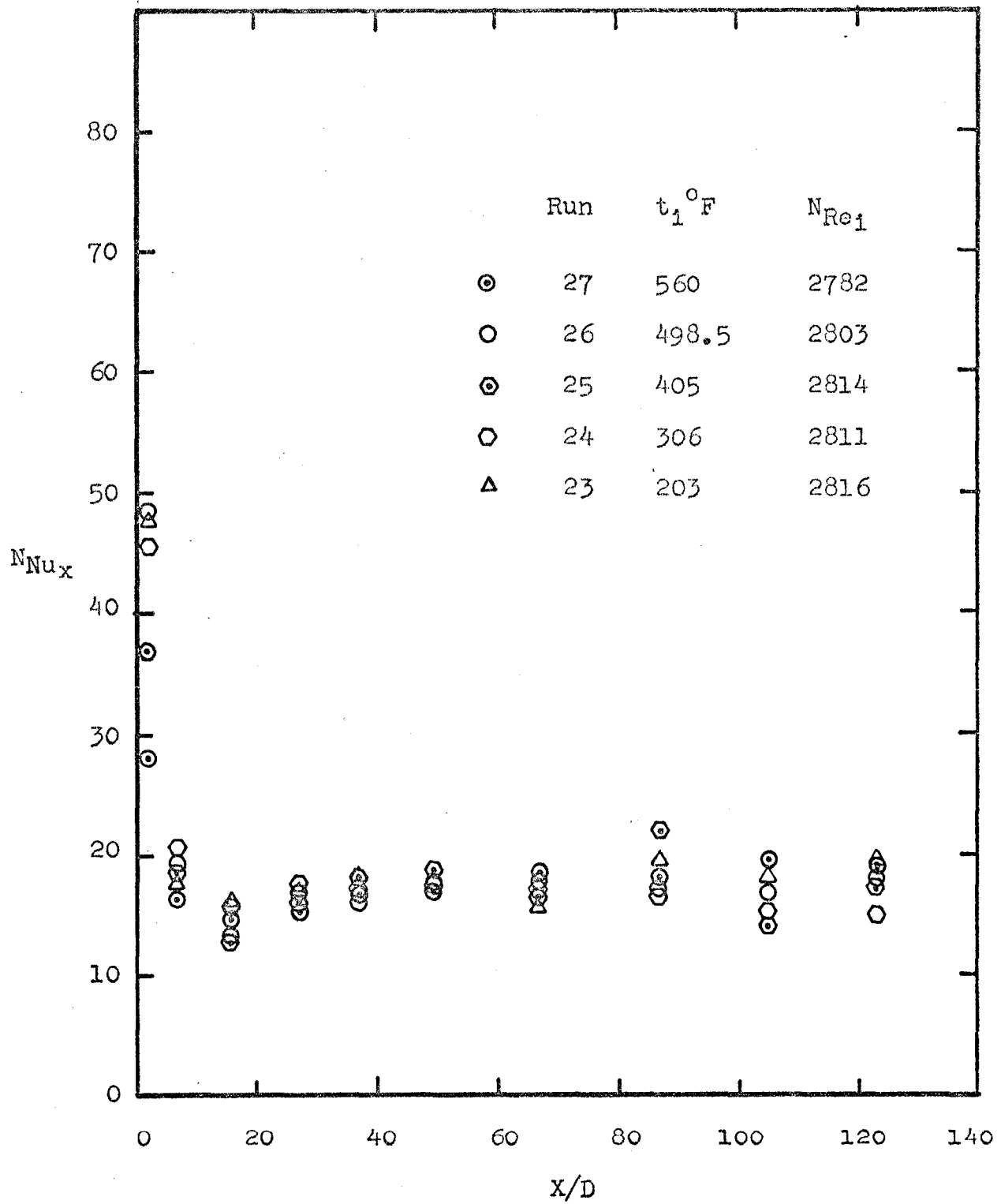


Fig. 56. Effect of Inlet Air Temperature on the Axial Variation of Local Nusselt Number.

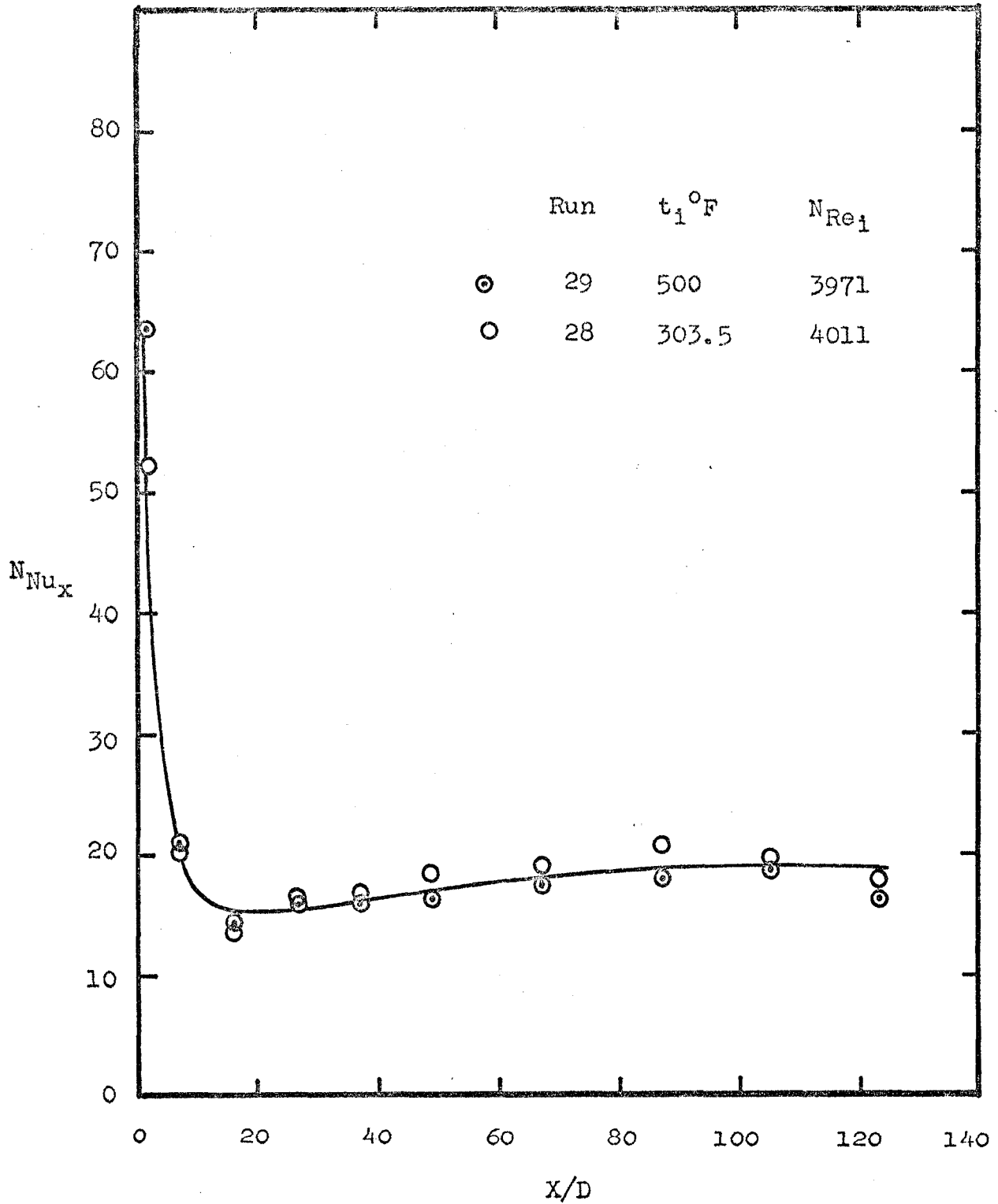


Fig. 57. Effect of Inlet Temperature on the Axial Variation of Local Nusselt Number.

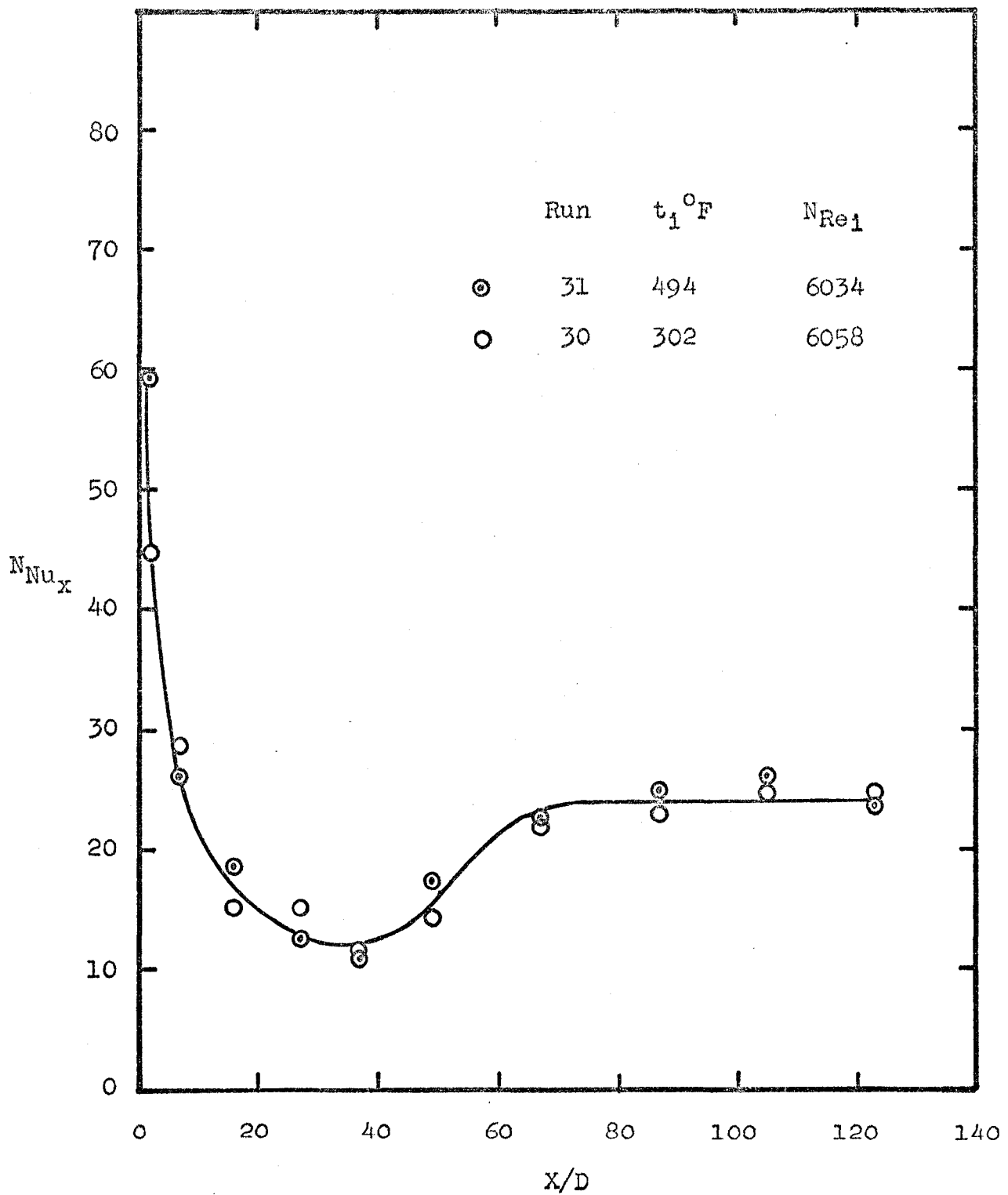


Fig. 58. Effect of Inlet Air Temperature on the Axial Variation of Local Nusselt Number.

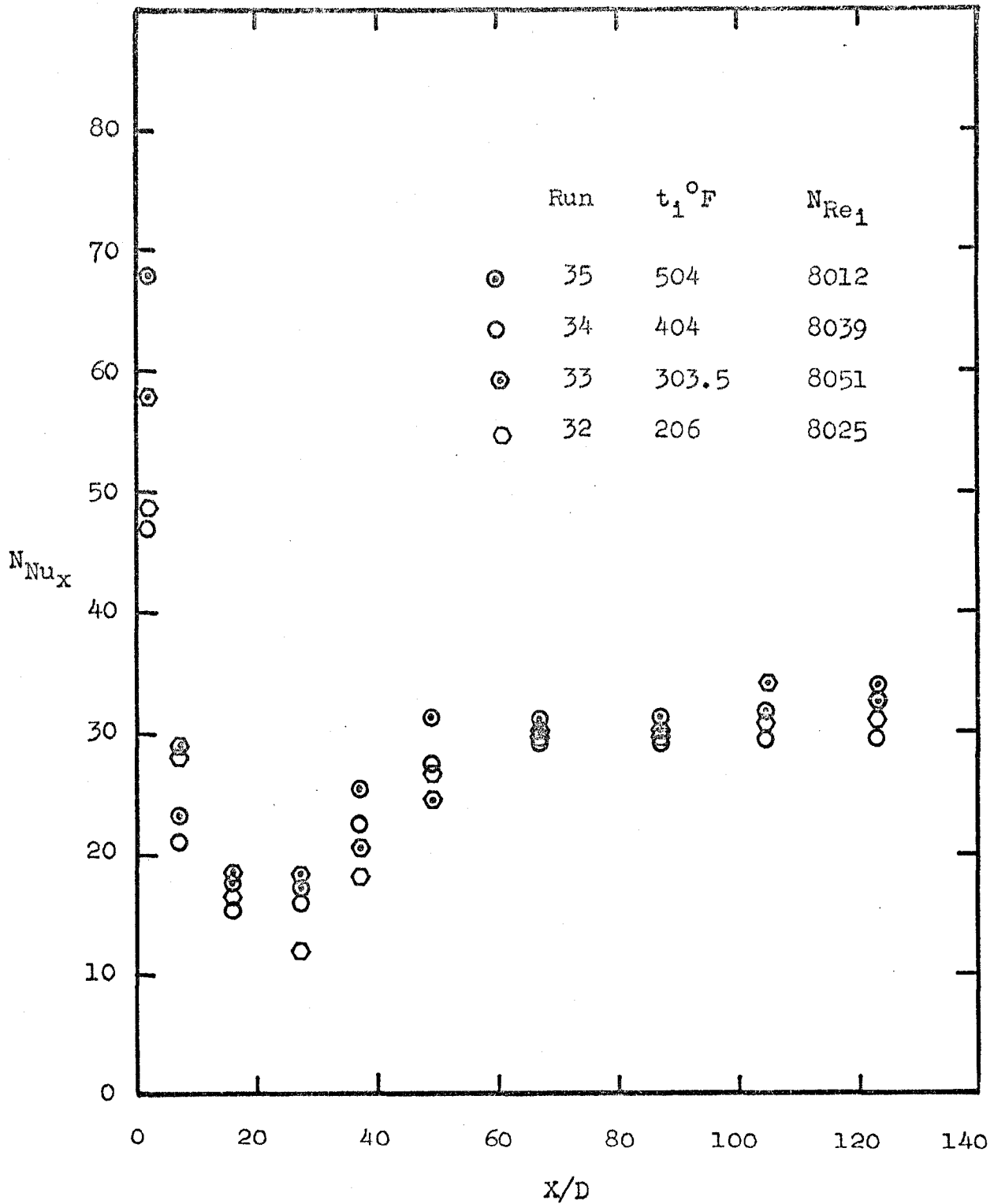


Fig. 59. Effect of Inlet Air Temperature on the Axial Variation of Local Nusselt Number.

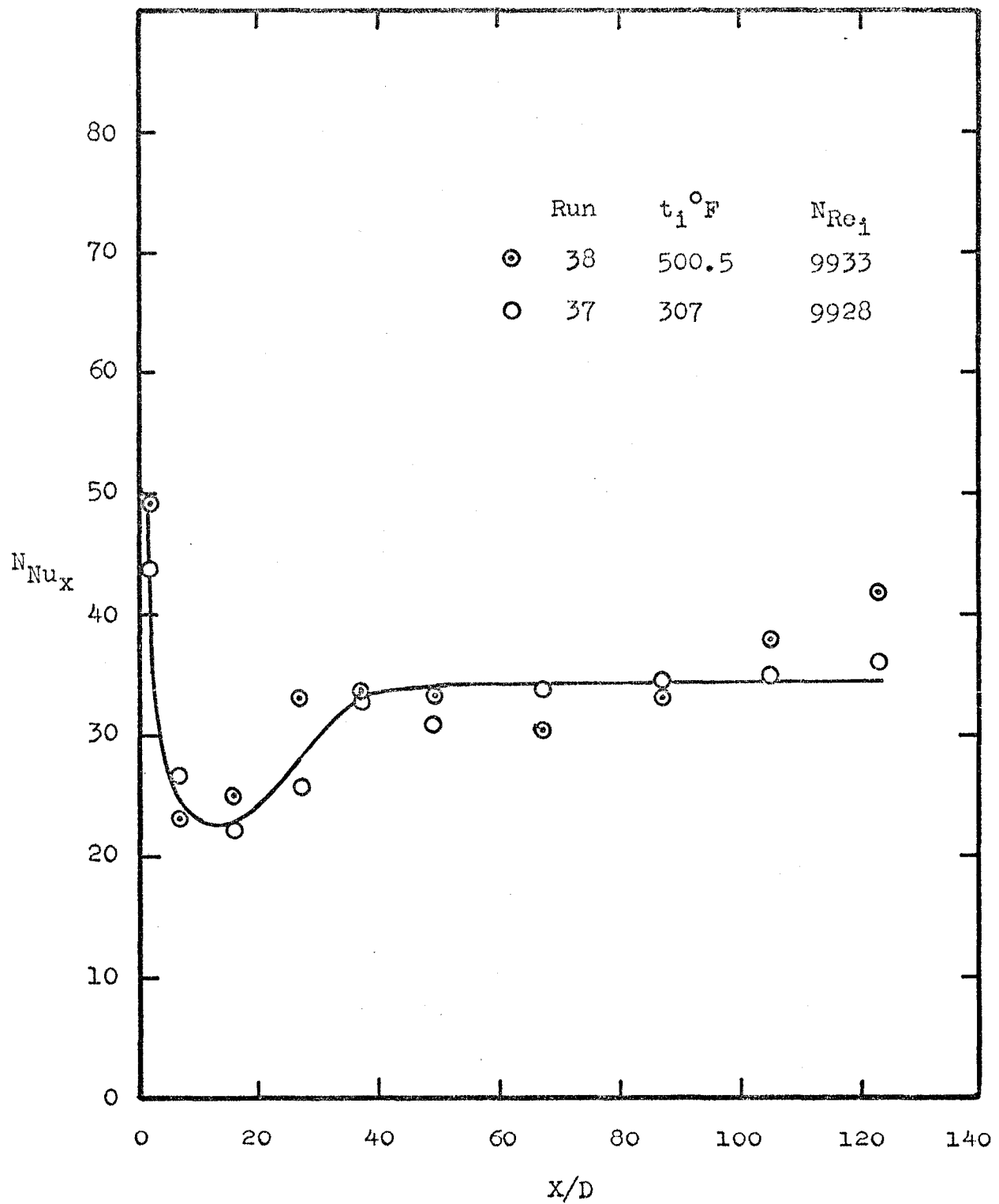


Fig. 60. Effect of Inlet Air Temperature on the Axial Variation of Local Nusselt Number.

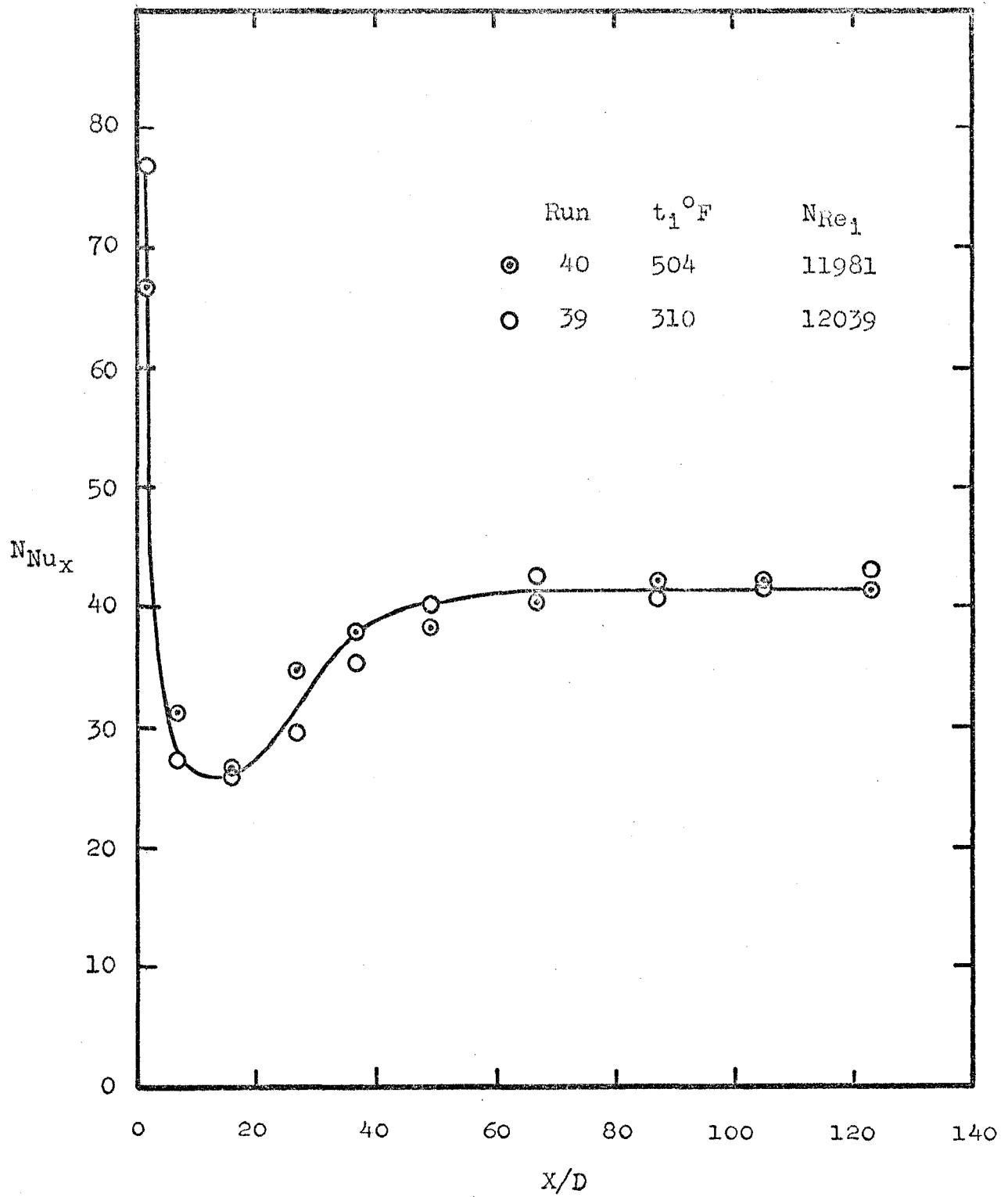


Fig. 61. Effect of Inlet Air Temperature on the Axial Variation of Local Nusselt Number.

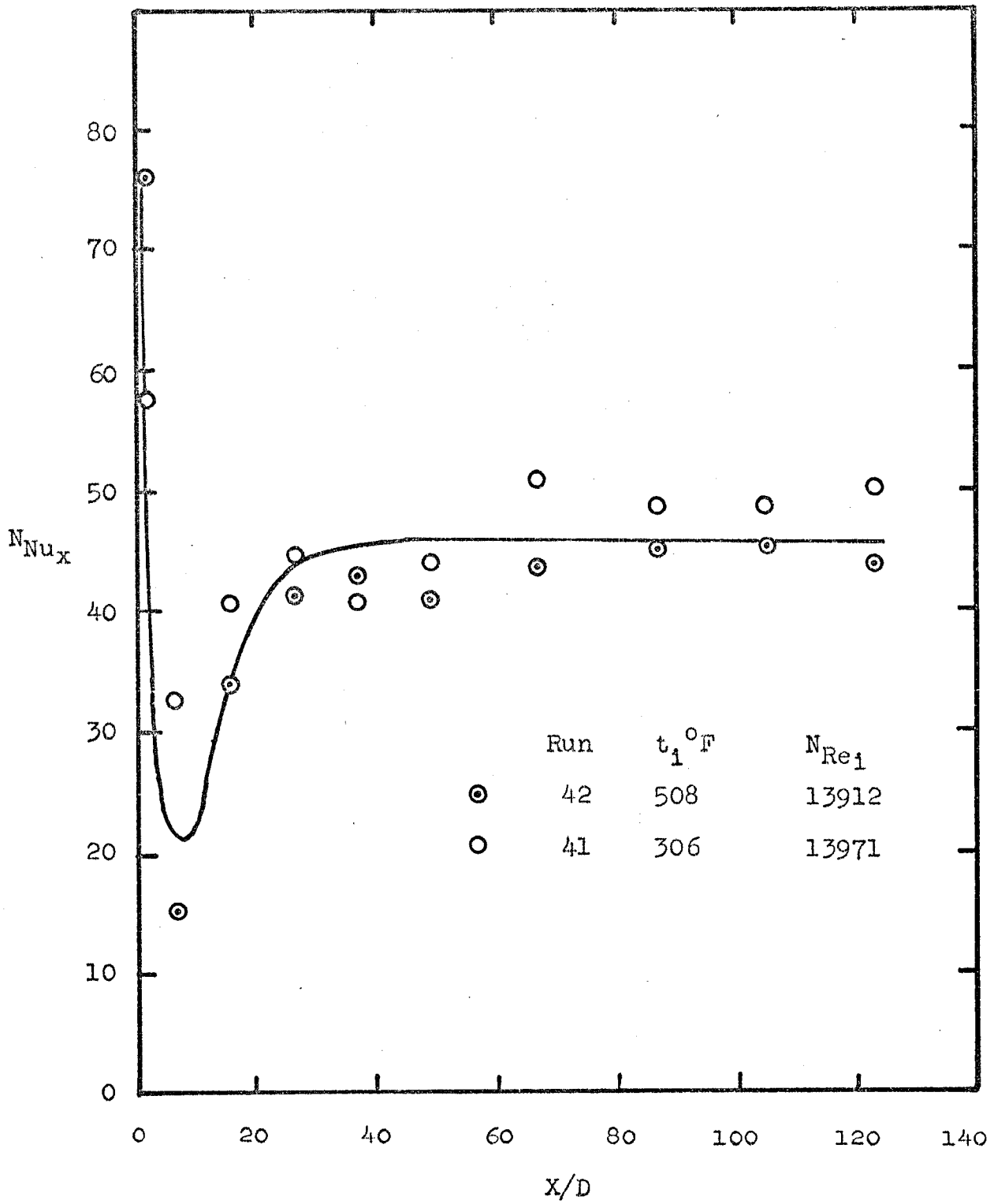


Fig. 62. Effect of Inlet Air Temperature on the Axial Variation of Local Nusselt Number.

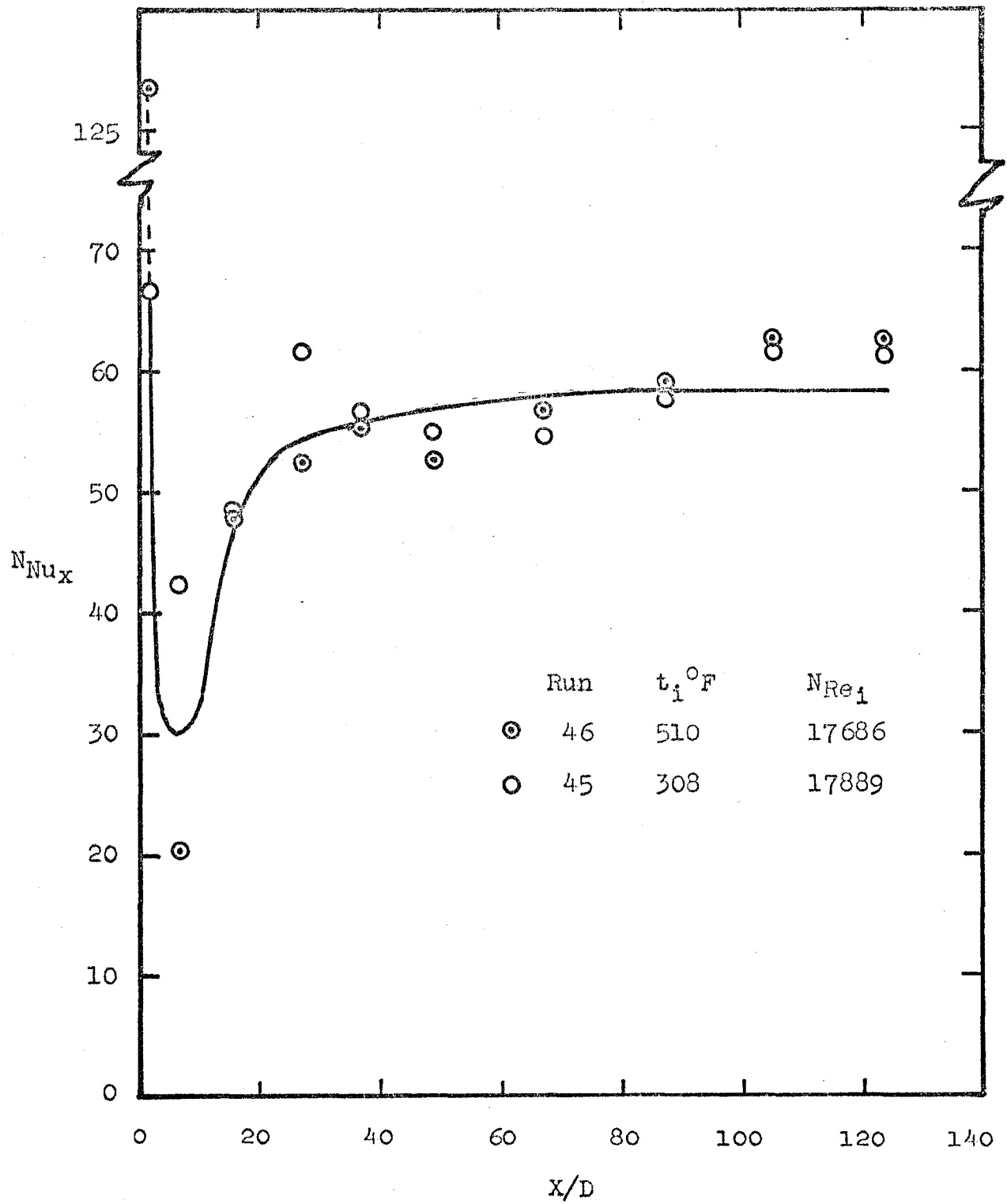


Fig. 63. Effect of Inlet Air Temperature on the Axial Variation of Local Nusselt Number.

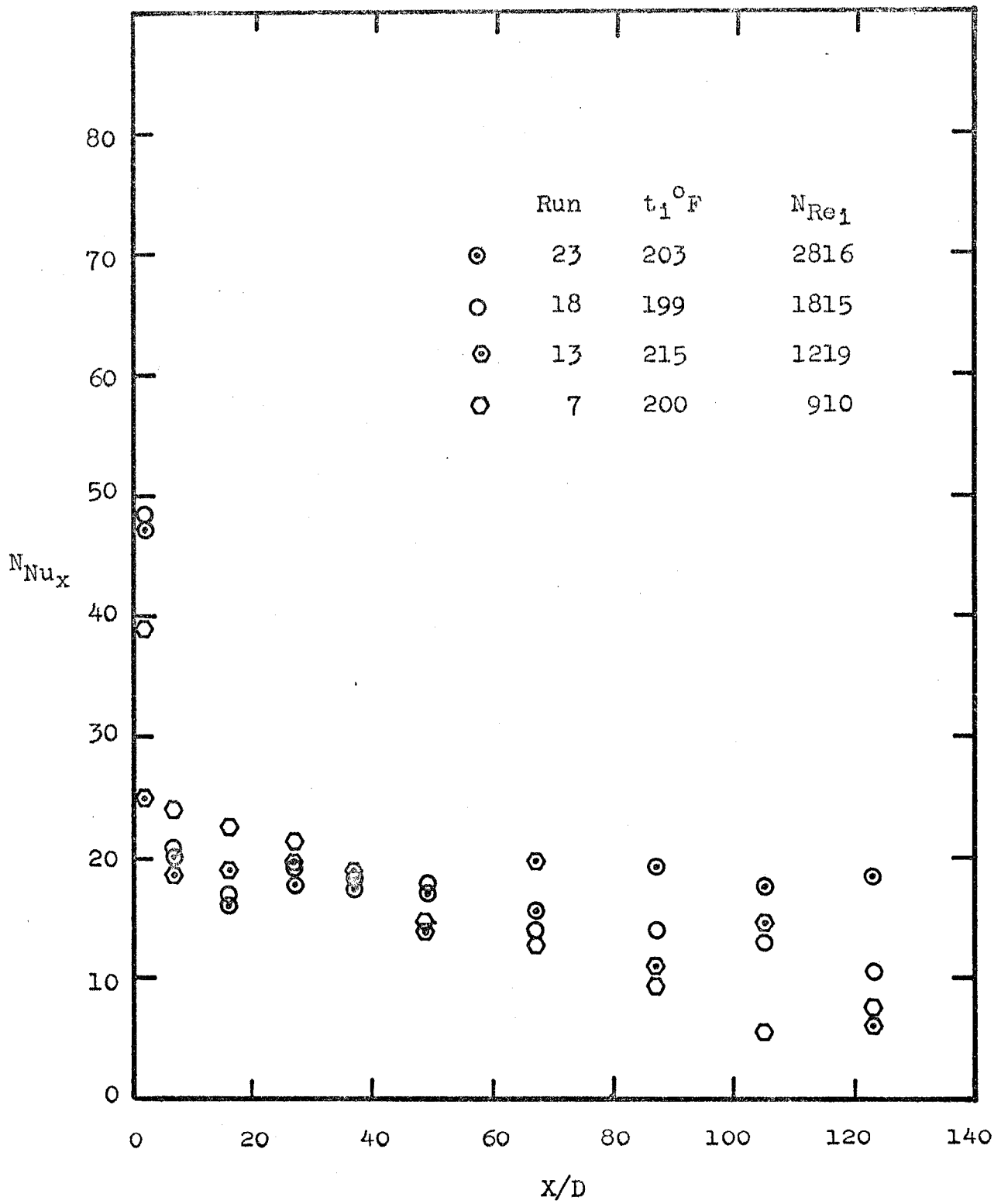


Fig. 64. Effect of Inlet Reynolds Number on the Axial Variation of Local Nusselt Number.

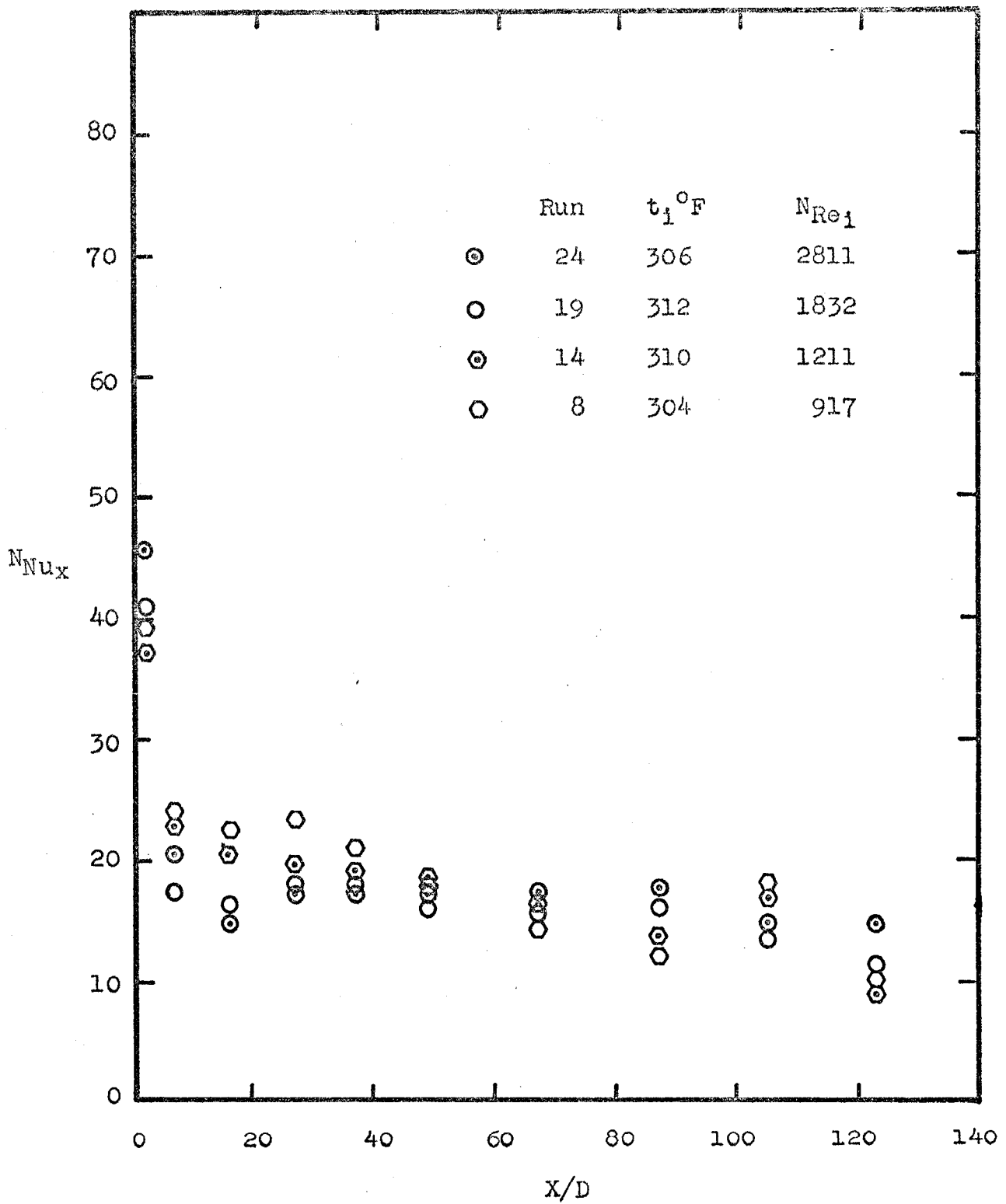


Fig. 65. Effect of Inlet Reynolds Number on the Axial Variation of Local Number.

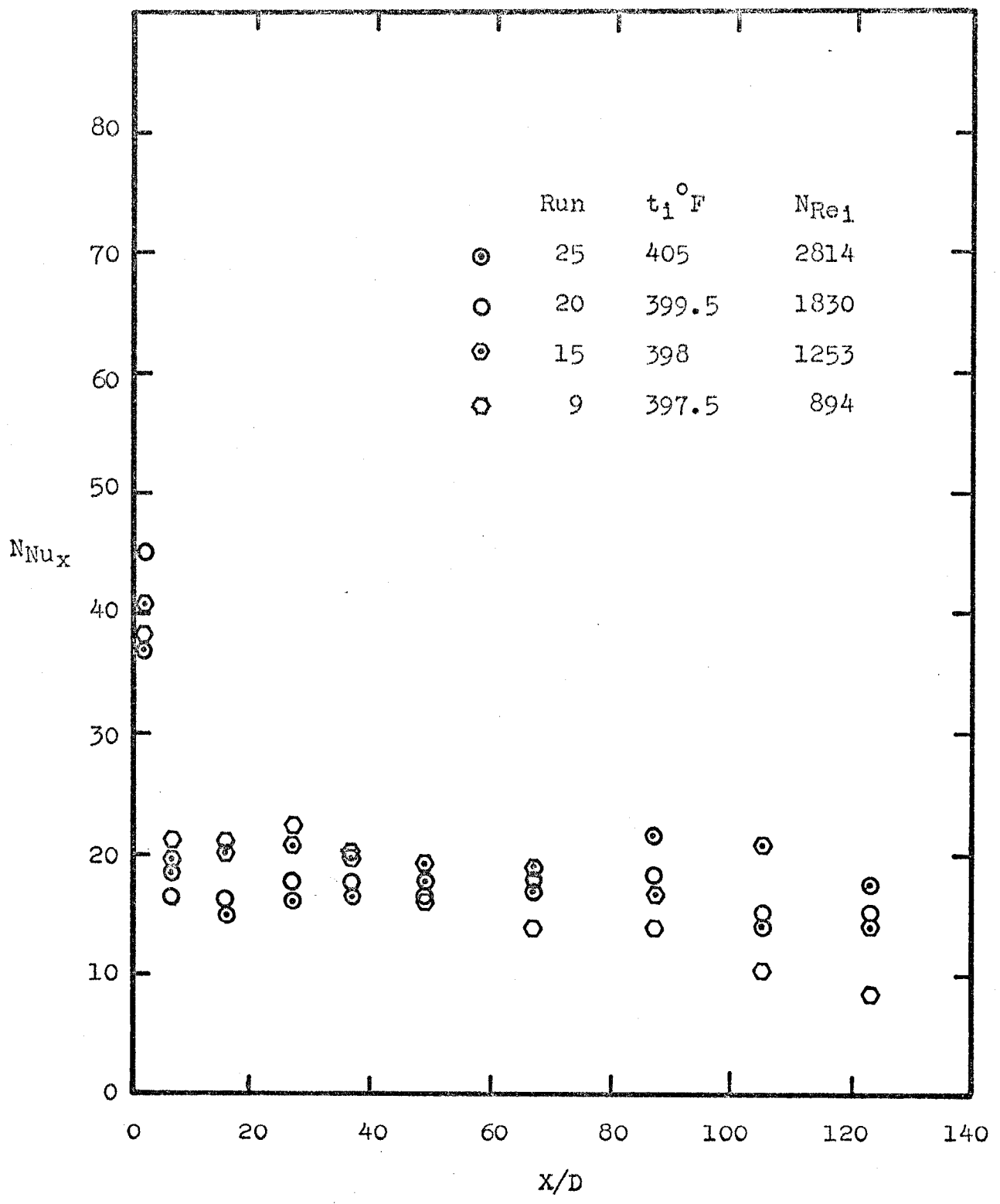


Fig. 66. Effect of Inlet Reynolds Number on the Axial Variation of Local Nusselt Number.

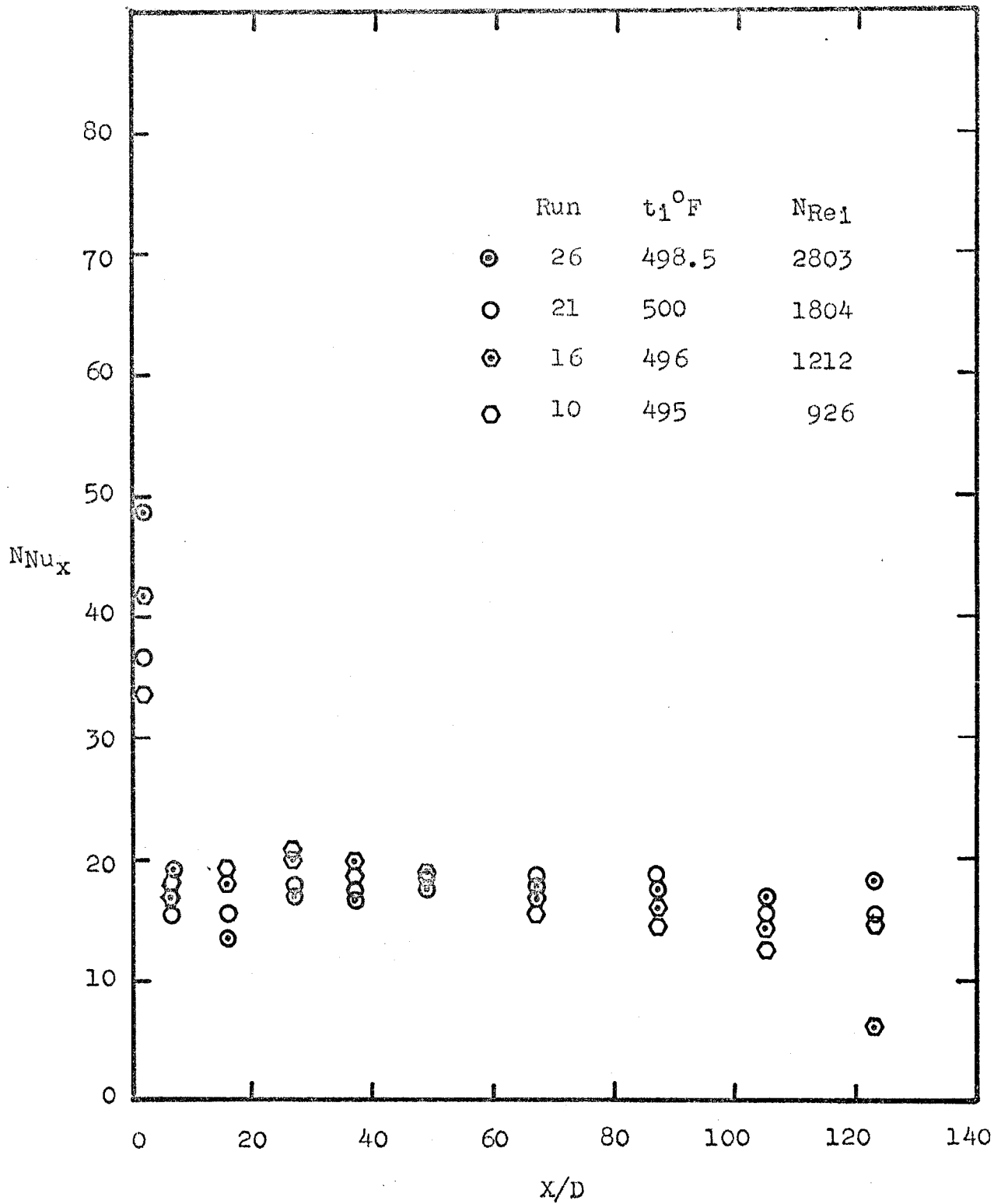


Fig. 67. Effect of Inlet Reynolds Number on the Axial Variation of Local Nusselt Number.

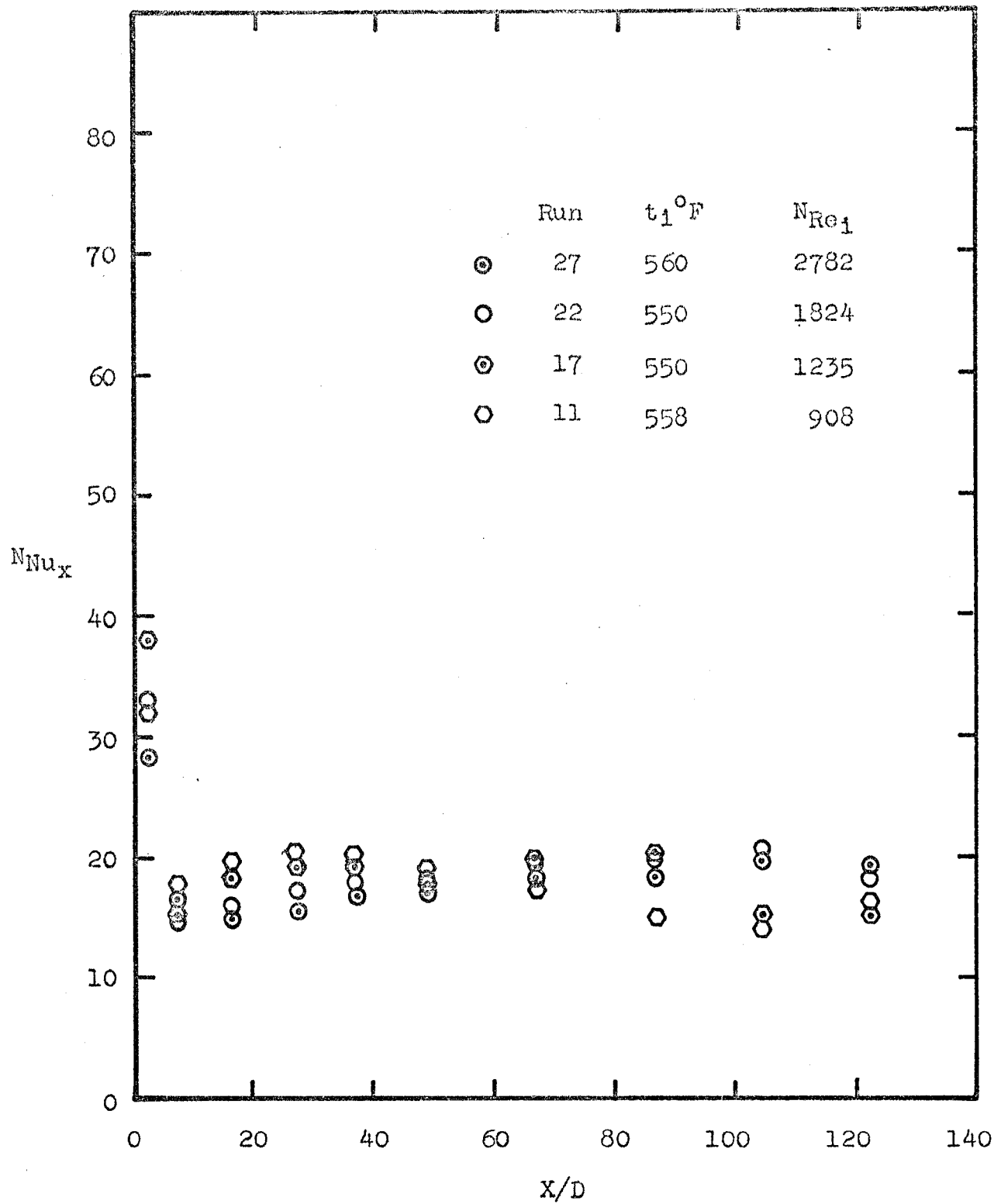


Fig. 68. Effect of Inlet Reynolds Number on the Axial Variation of Local Nusselt Number.

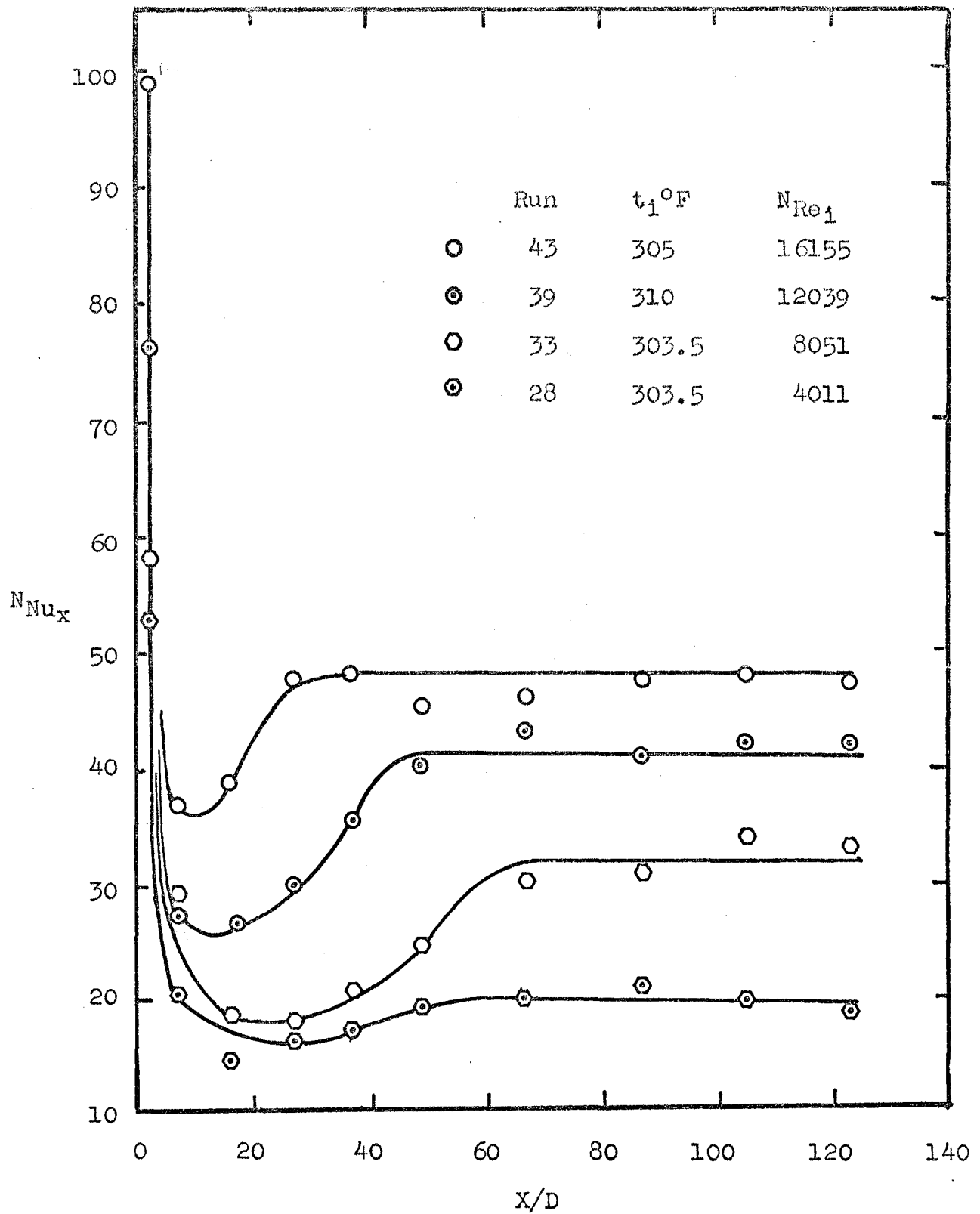


Fig. 69. Effect of Inlet Reynolds Number on the Axial Distribution of Local Nusselt Number.

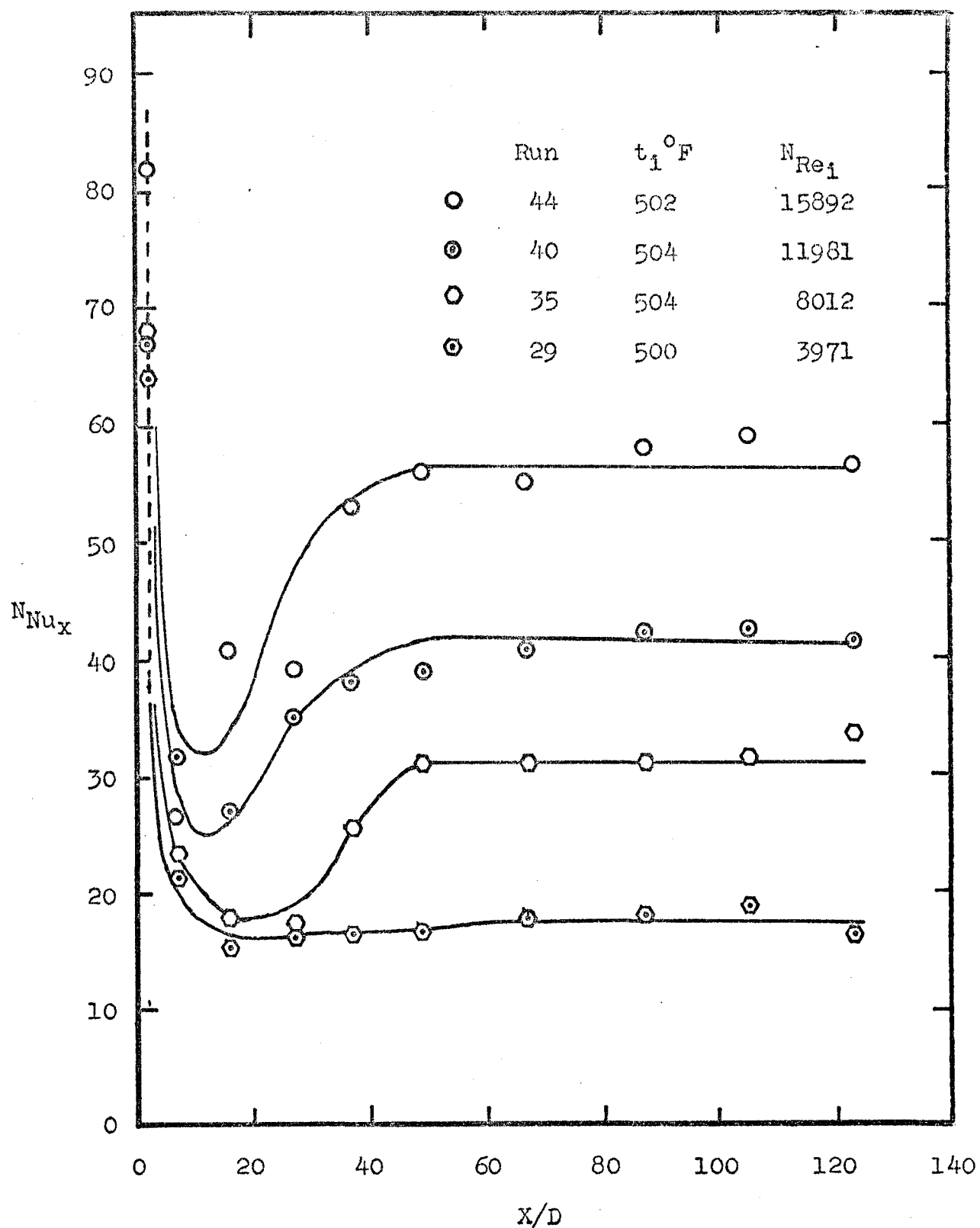


Fig. 70. Effect of Inlet Reynolds Number on the Axial Distribution of Local Nusselt Number.

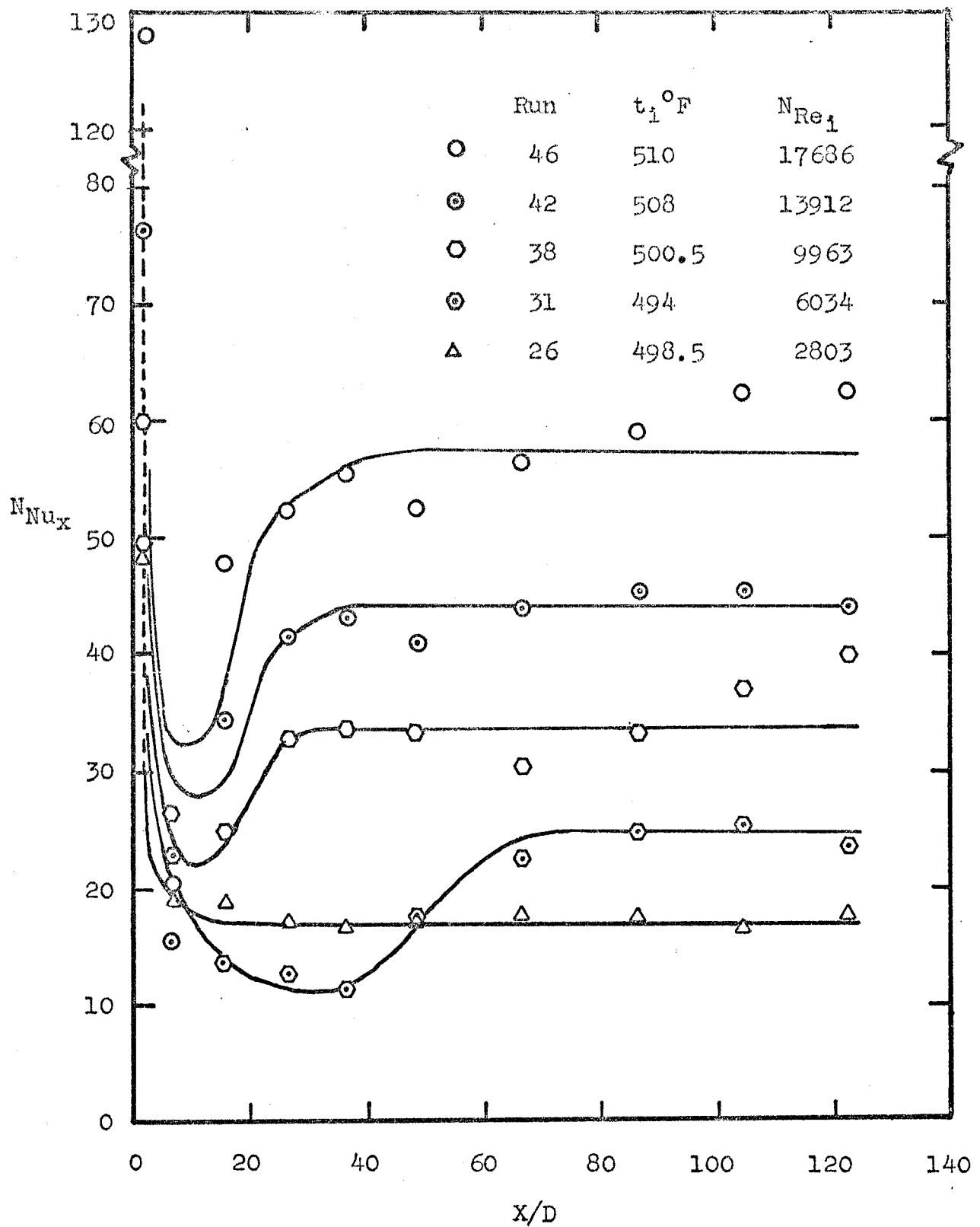


Fig. 71. Effect of Inlet Reynolds Number on the Axial Distribution of Local Number.

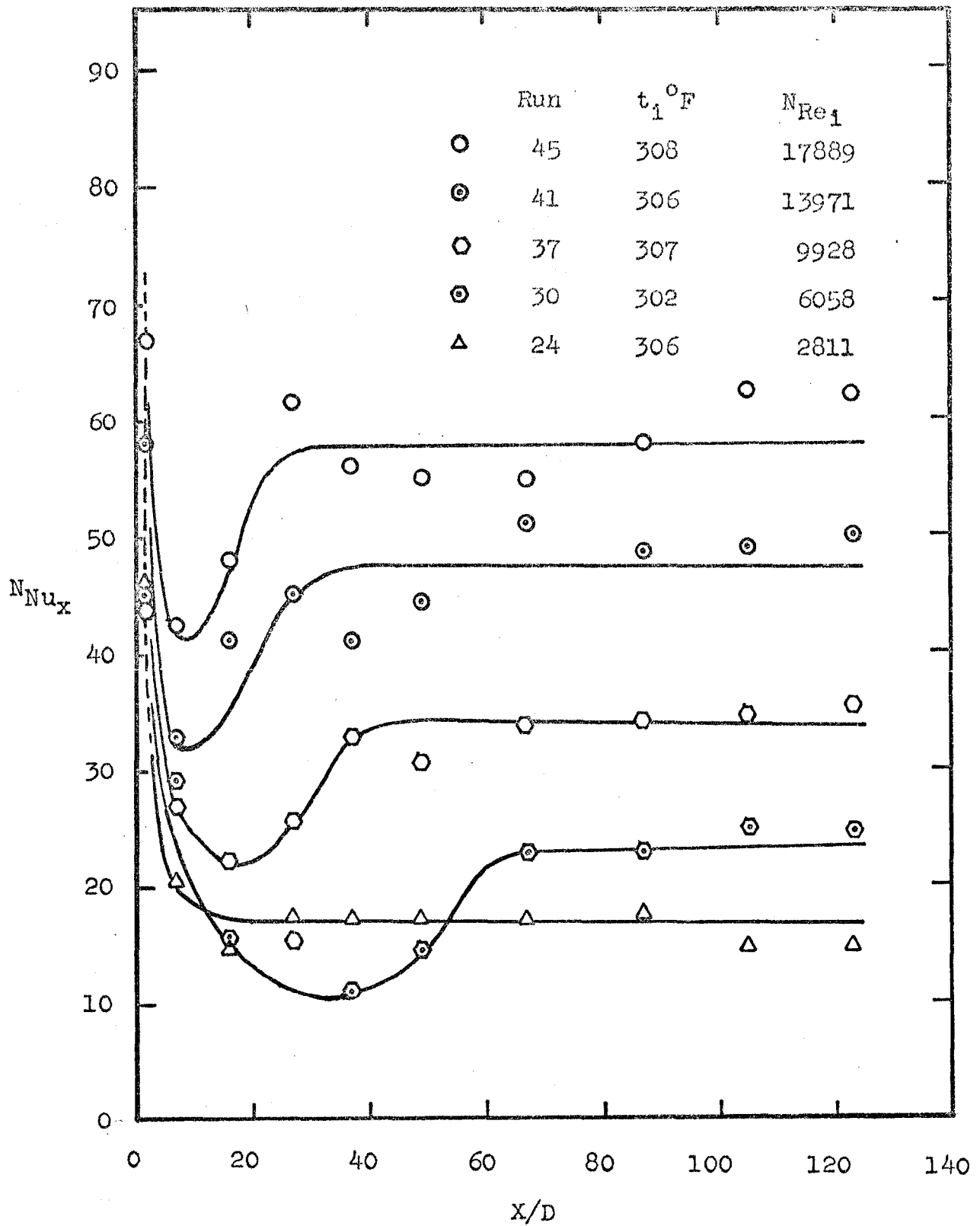


Fig. 72. Effect of Inlet Reynolds Number on the Axial Distribution of Local Nusselt Number.

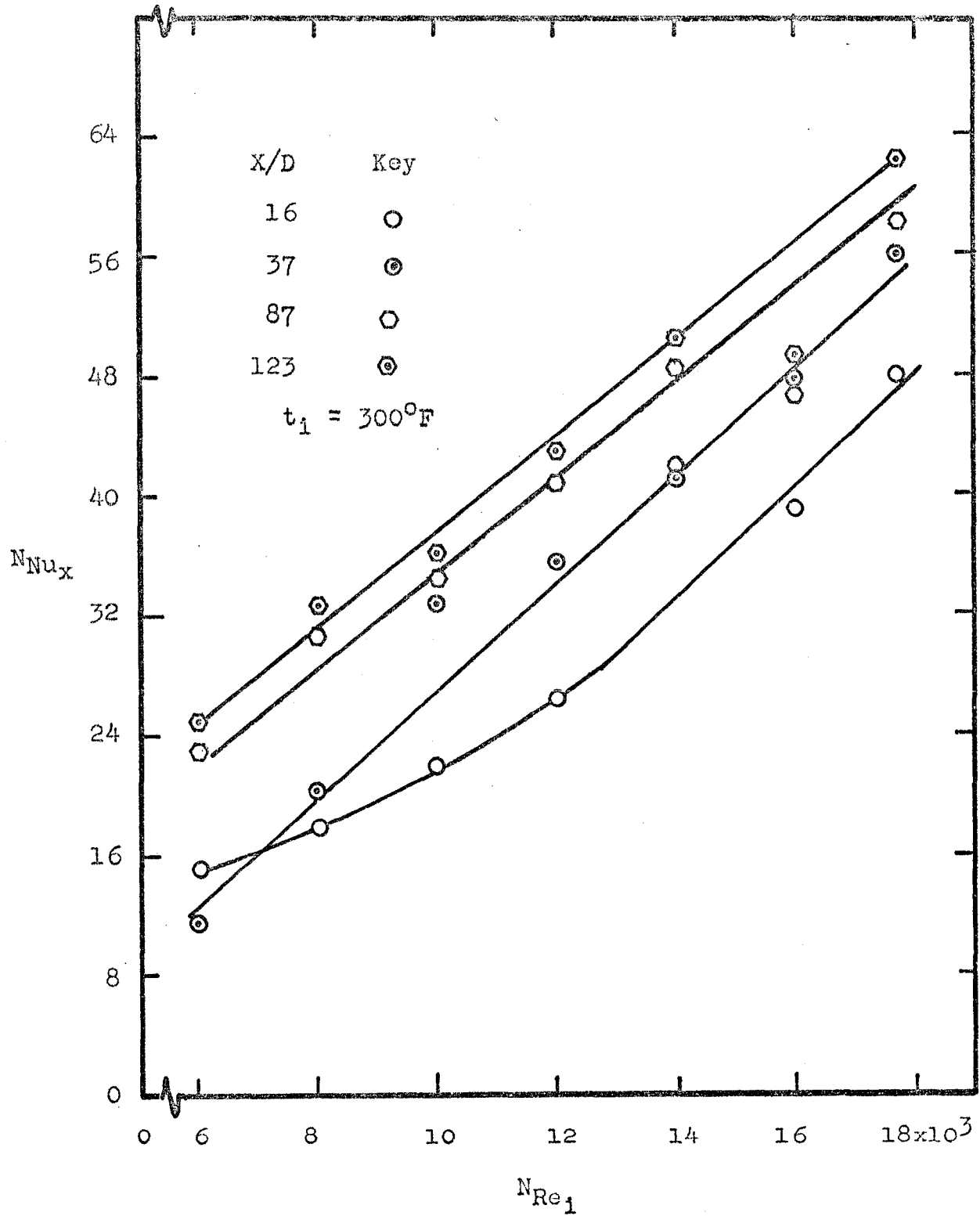


Fig. 73. Effect of Inlet Reynolds Number on the Local Nusselt Number.

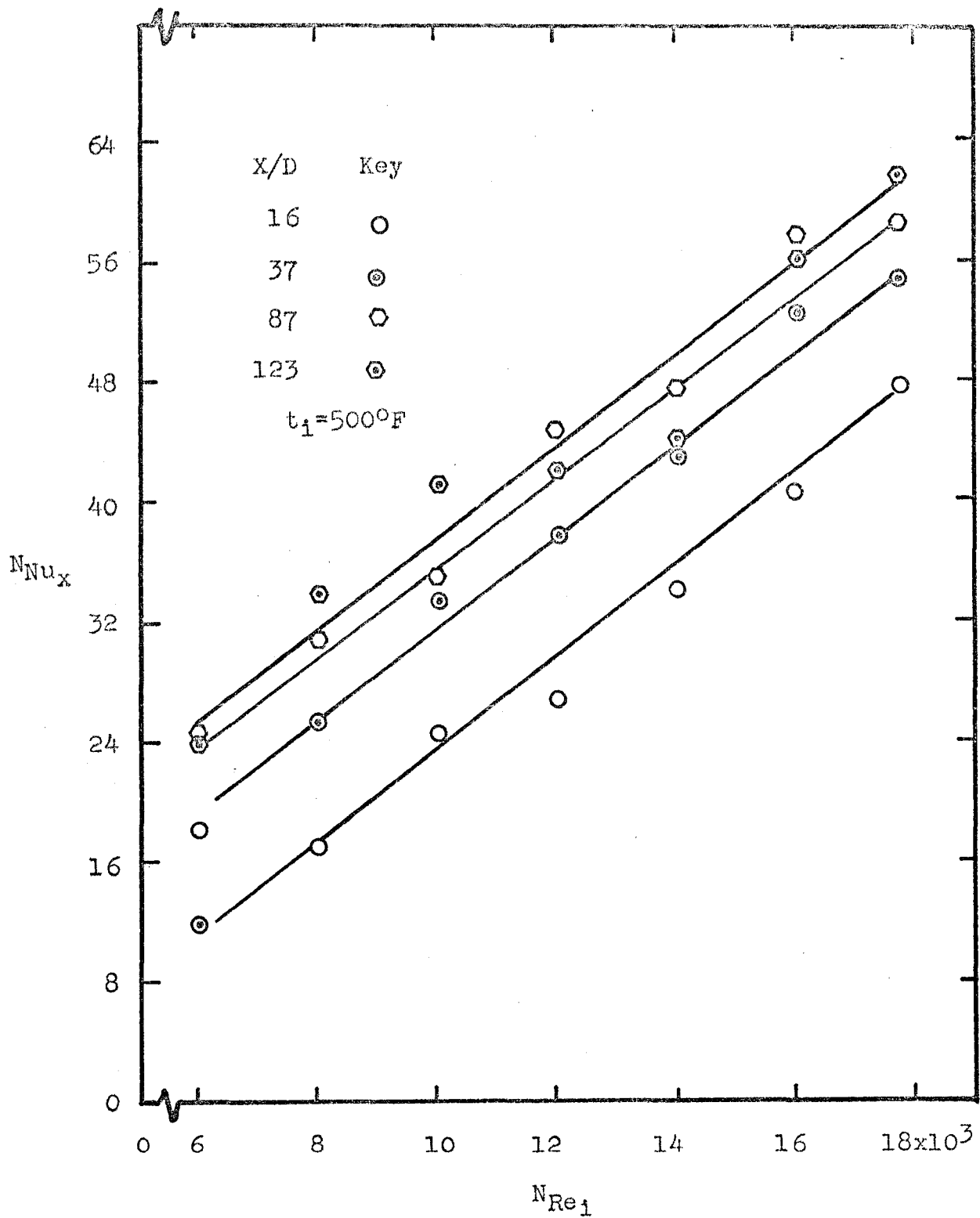


Fig. 74. Effect of Inlet Reynolds Number on the Local Nusselt Number.

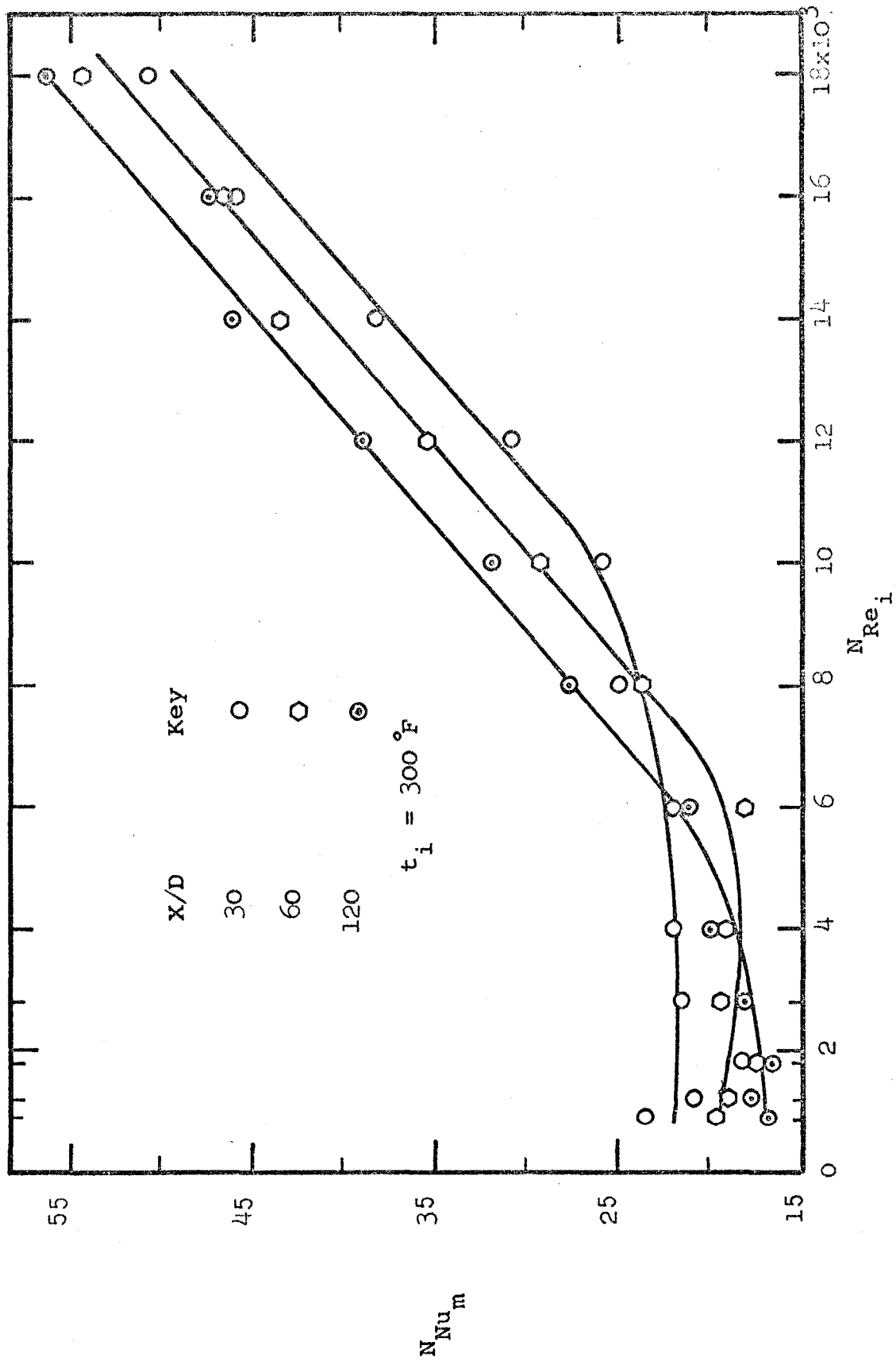


Fig. 75. Influence of X/D Ratios on the Mean Nusselt Number.

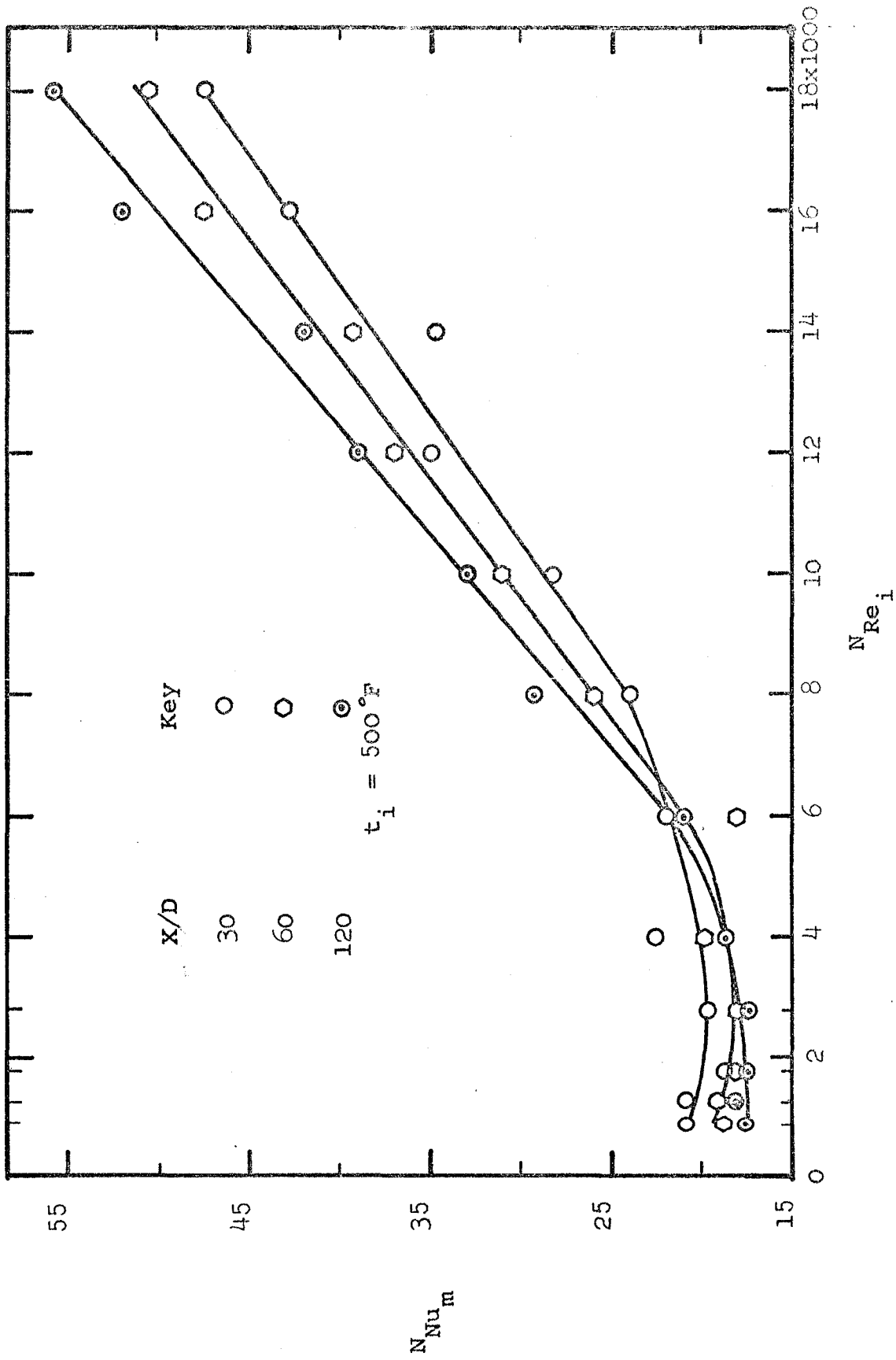


Fig. 76. Influence of X/D Ratios on the Mean Nusselt Number.

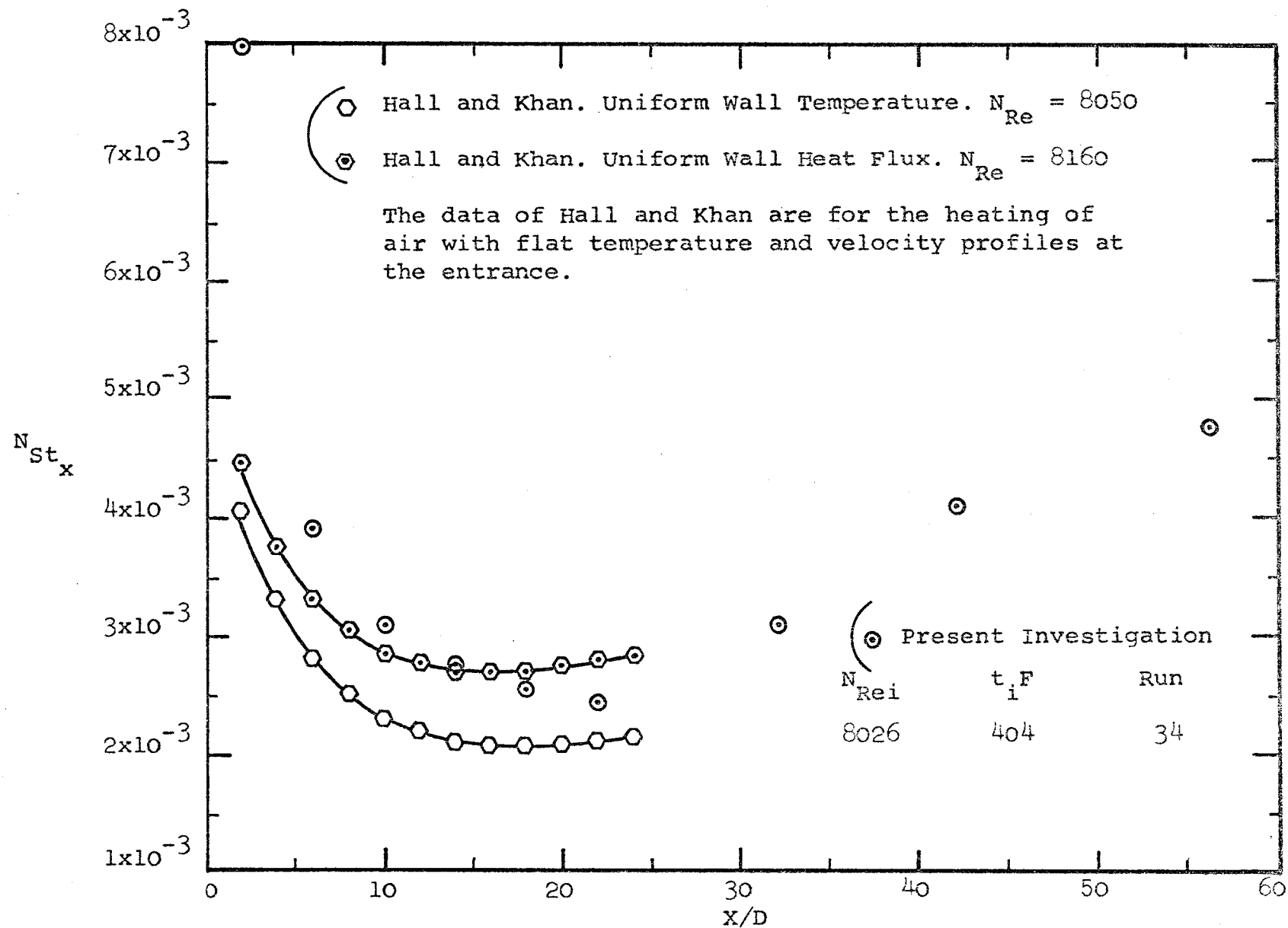


Fig. 77. Comparison with the experimental data of Hall and Khan.

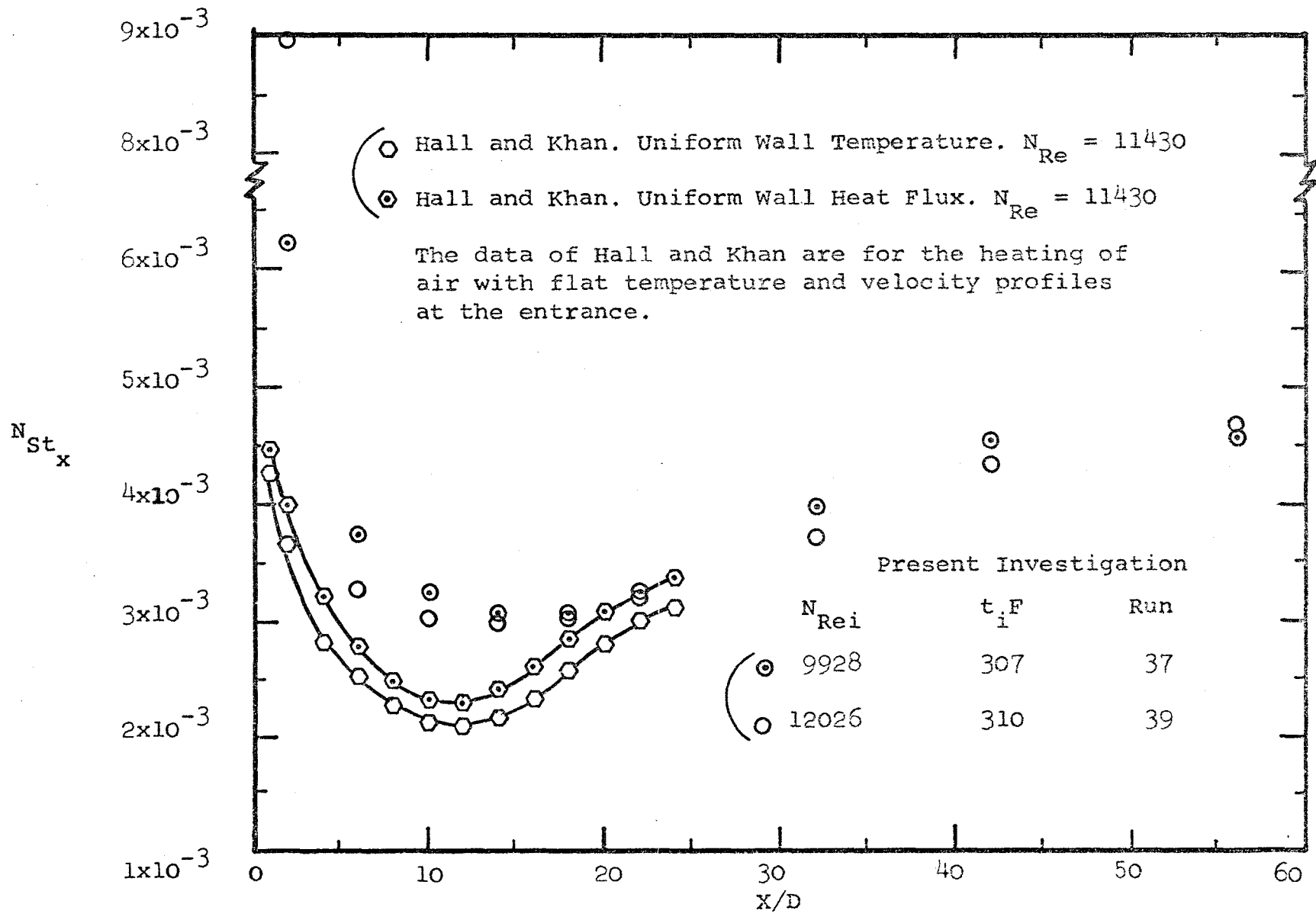


Fig. 78. Comparison with the experimental data of Hall and Khan.

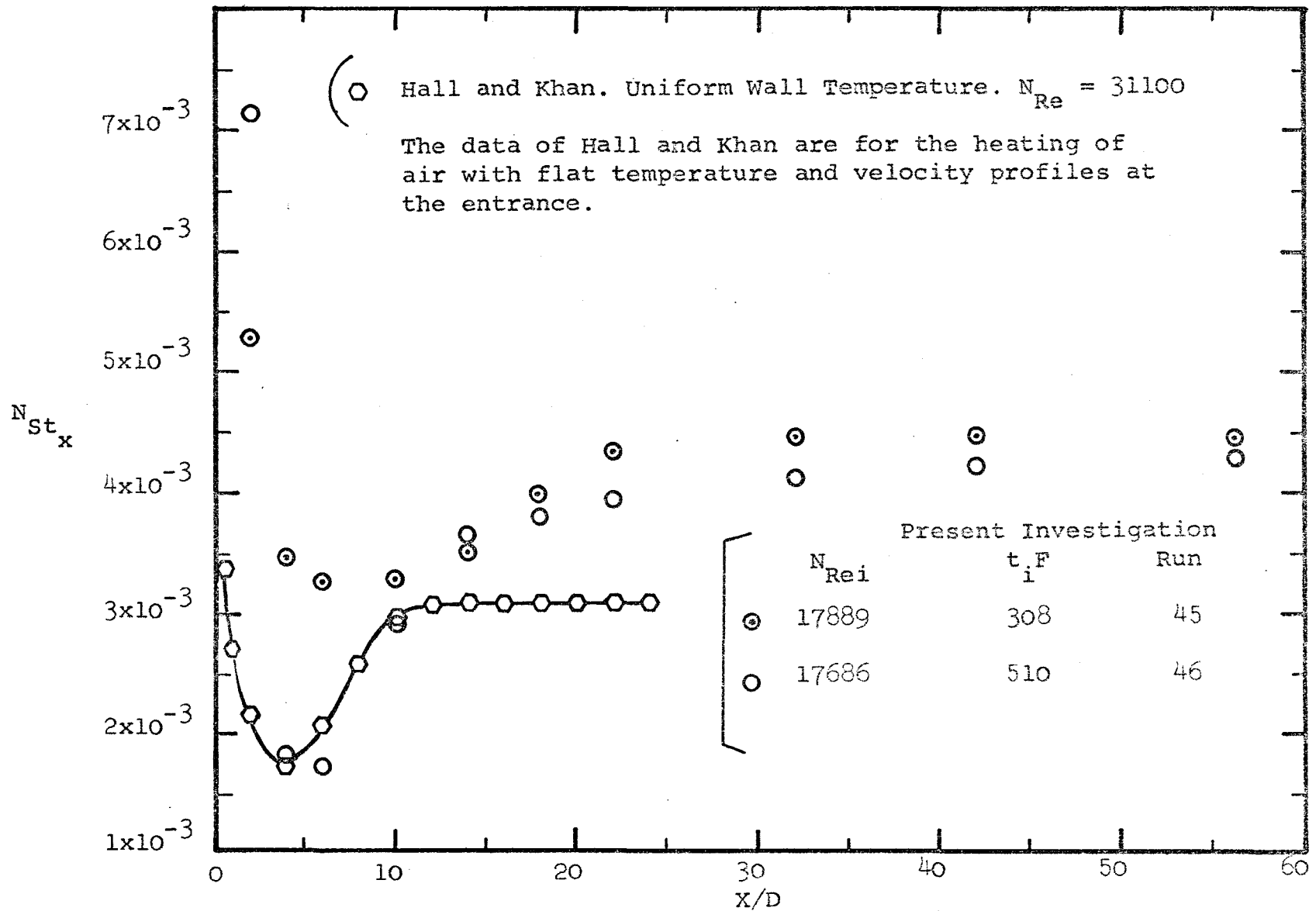


Fig. 79. Comparison with the experimental data of Hall and Khan.

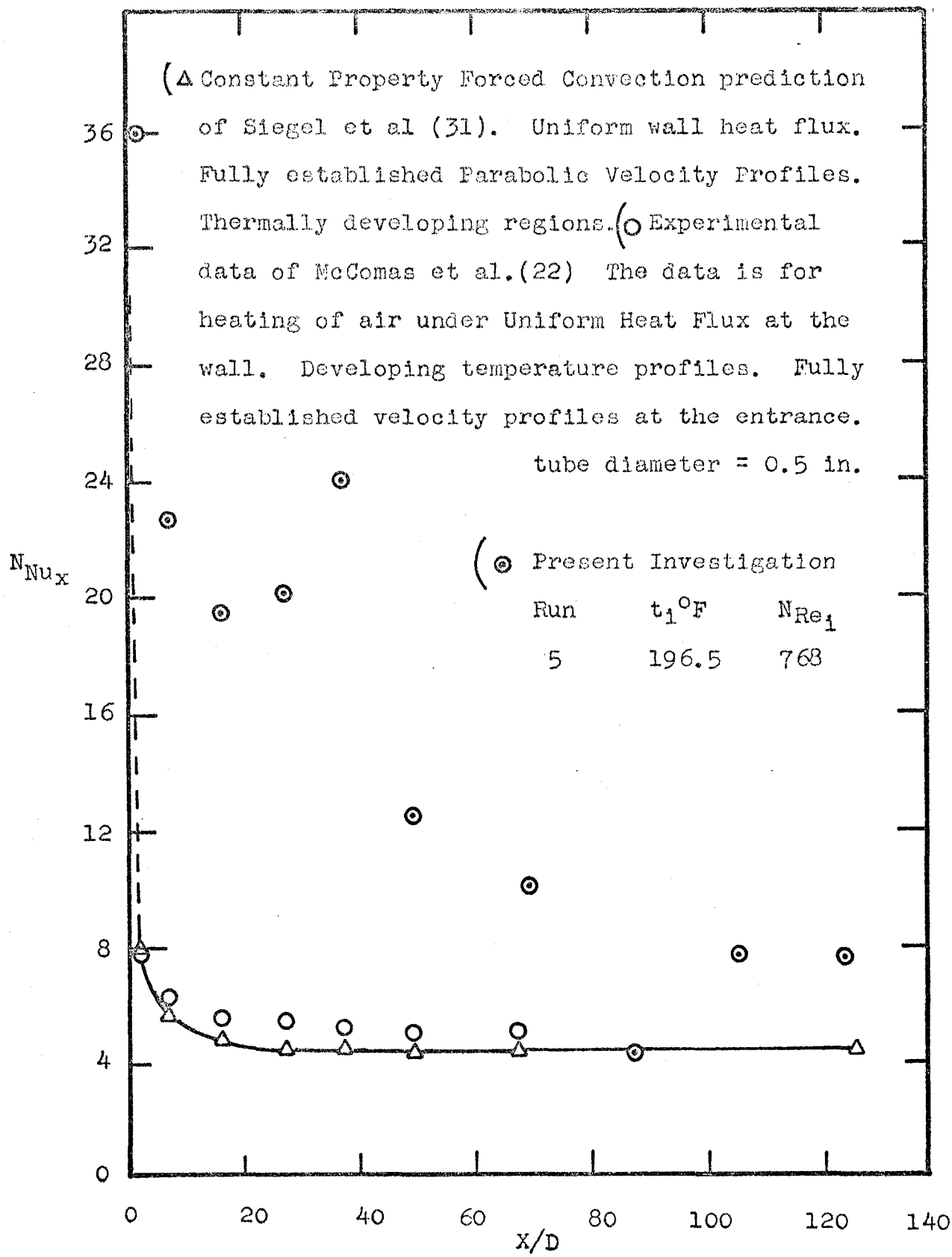


Fig. 80. Comparison with the Experimental data of McComas et al. and the Analytical Prediction of Siegel et al.

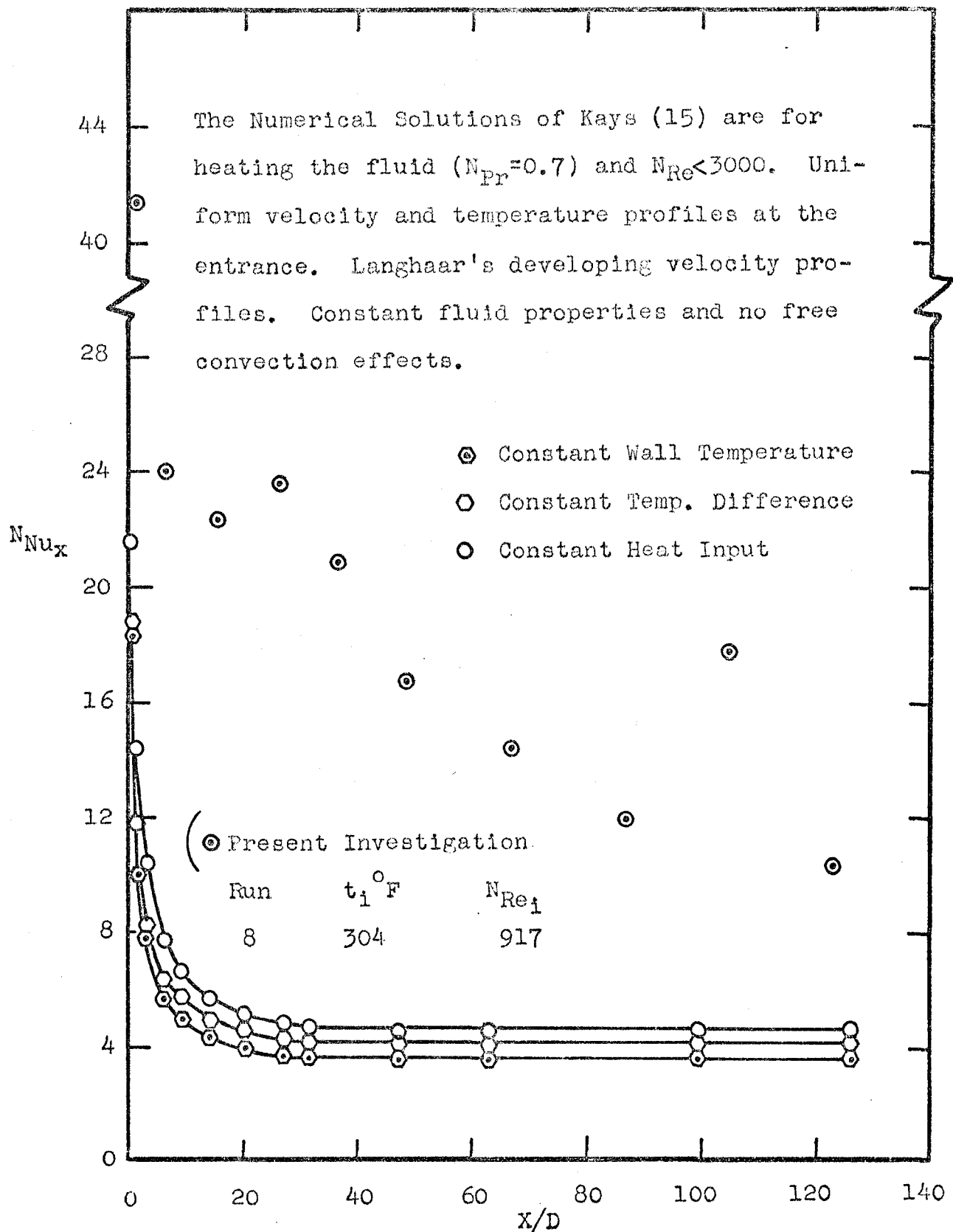


Fig. 81. Comparison with the Numerical Solutions of Kays for Various Heating Wall Boundary Conditions.

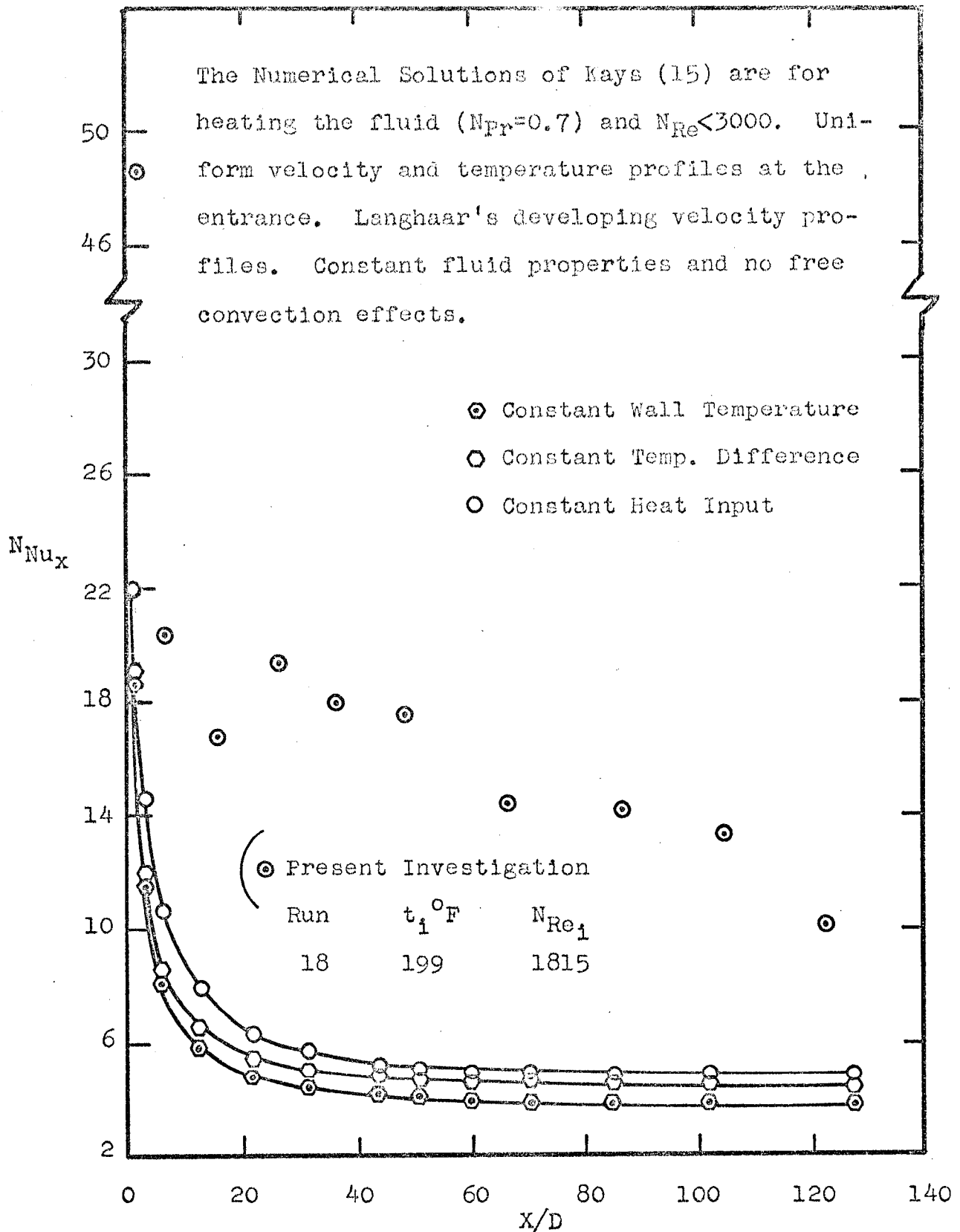


Fig. 82. Comparison with the Numerical Solutions of Kays for Various Heating Wall Boundary Conditions.

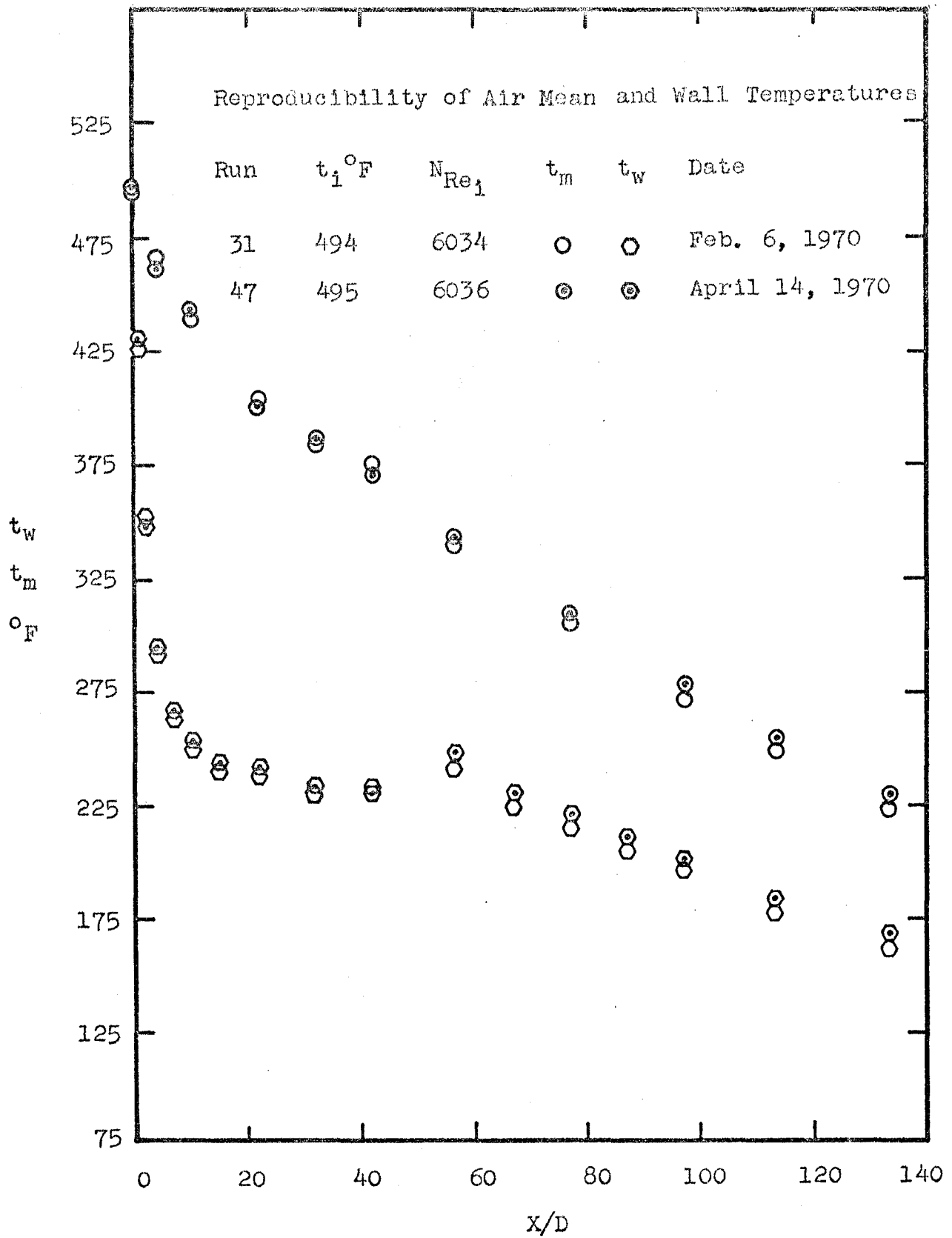


Fig. 83. Reproducibility of the Experimental Results.

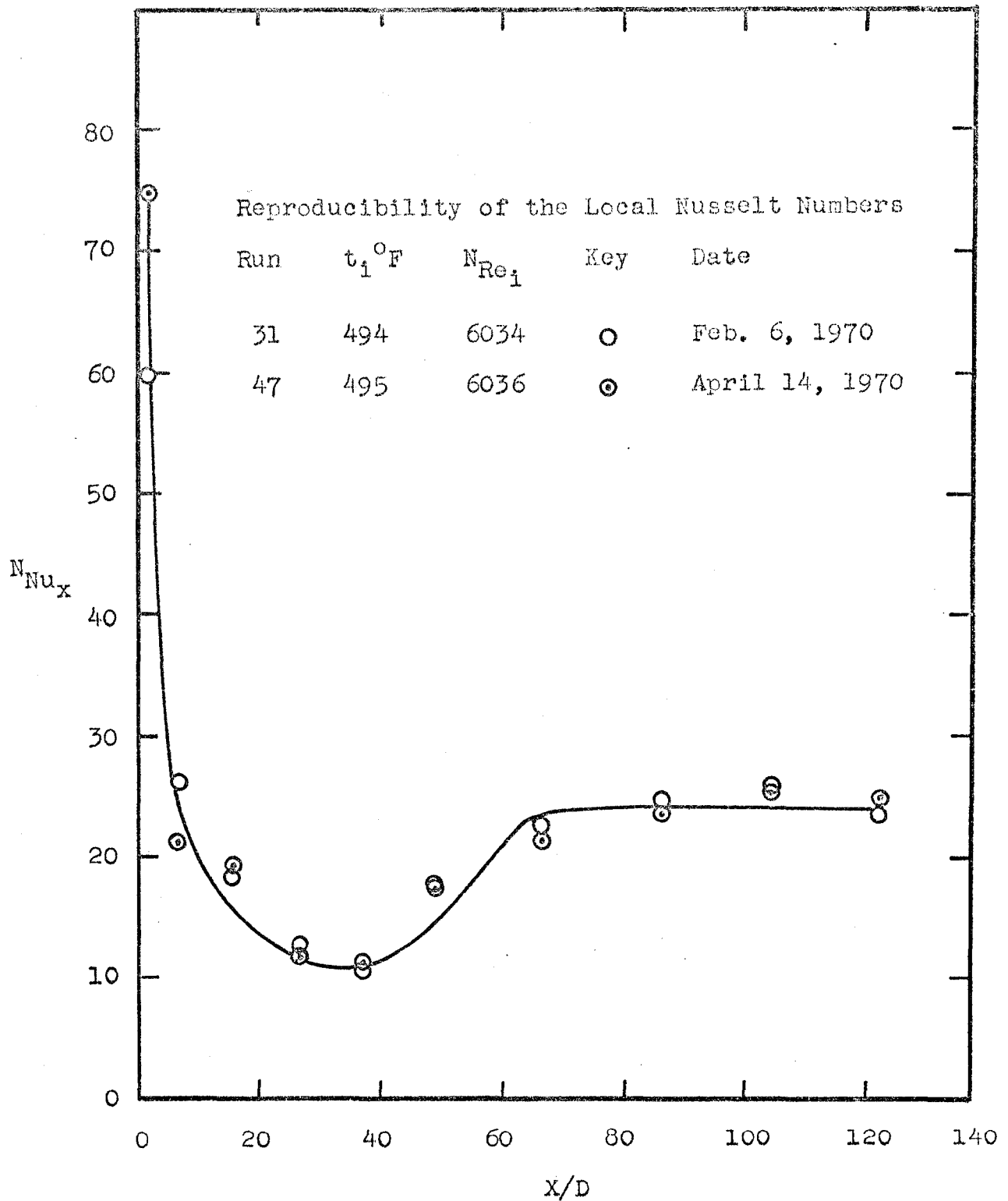


Fig. 84. Reproducibility of the Experimental Results.

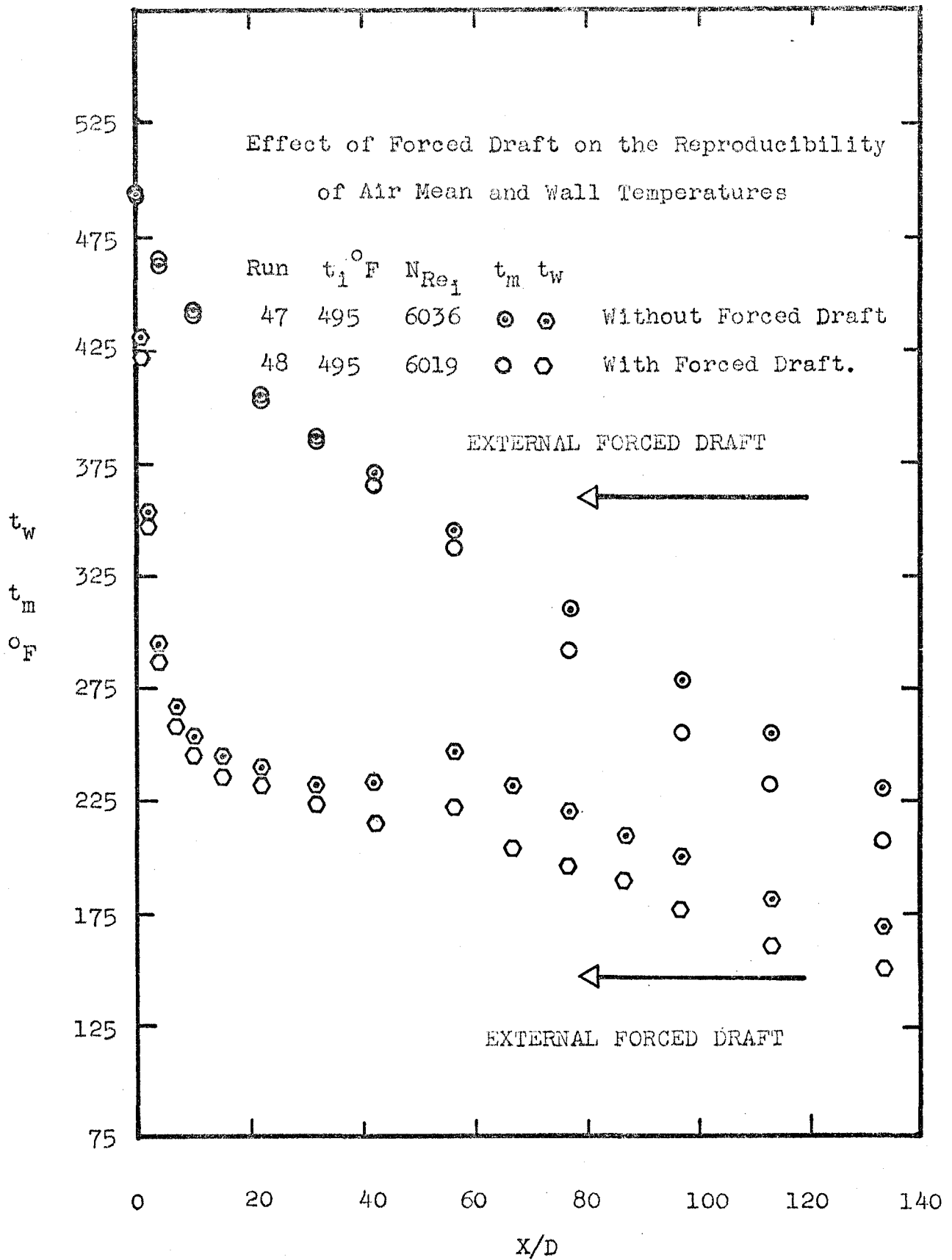


Fig. 85. Effect of Forced Draft on the Experimental Results.

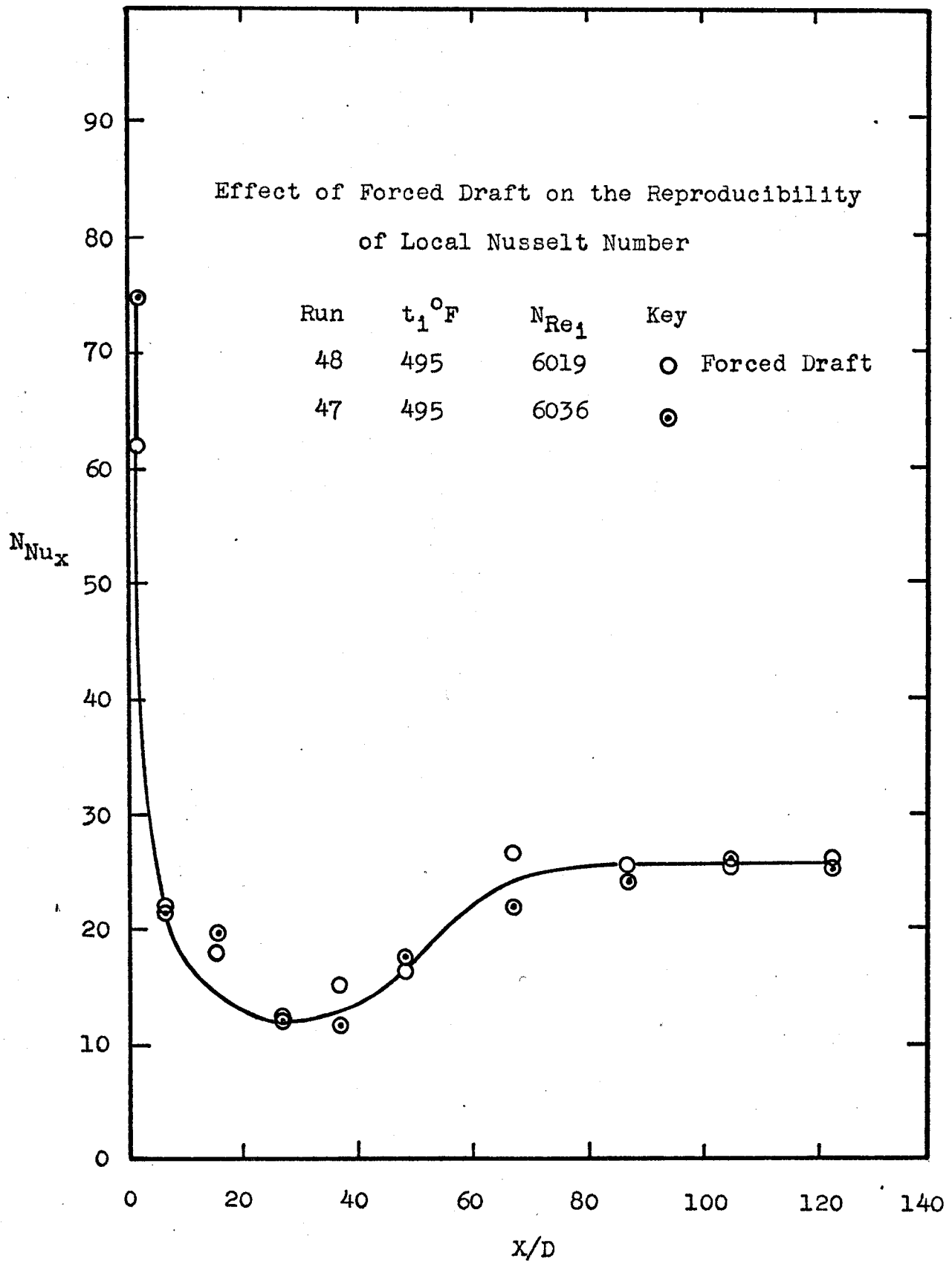


Fig. 86. Effect of Forced Draft on the Experimental Results.

## CHAPTER 5

## DISCUSSION

## 5.1 AXIAL VARIATION OF MEAN FLUID TEMPERATURE

From the curves shown in figures 2 to 9 and 15 to 30, it can be seen that the variation of mean air temperature  $t_m$  in the axial direction is changed markedly with an increasing flow rate. In the case of smaller mass flows ( $N_{Re_i} \leq 1800$ ), the distribution of  $t_m$  is very steep over the first 50 diameters and then tends to flatten out. At moderate flow rates ( $1800 < N_{Re_i} < 8000$ ), the rapid drop tendency of  $t_m$  in the initial part of the test-section disappears and is replaced by a gradual decrease along the full length of the pipe. Finally for higher mass flow rates ( $N_{Re_i} > 8000$ ), the trend is towards an almost linear distribution of  $t_m$  over the entire length of the test-section.

## 5.2 AXIAL VARIATION OF WALL TEMPERATURE

A careful examination of the variation of axial wall temperature curves in figures 10 to 32, reveals that:

- a. The inlet Reynolds number does not affect the axial wall temperature in the same manner as it affects the axial variation of fluid mean temperature.
- b. Under the axial wall temperature distribution

curves lies the phenomenon of the "gradual development" to "transition" of the laminar boundary layer in the test-section under the conditions of the present investigation.

- c. It appears as if the  $t_w$  curves establish two distinctive families probably due to two different phenomena taking place in the system. The family 1, shown in figures 10 to 14, prevails over flow Reynolds numbers  $< 6000$ , and is characterized on the basis of the free-Convection effects. The family 2, which is illustrated in figures 16 to 32, prevails over the flow Reynolds number  $\geq 6000$  and is attributed to the transition phenomenon of the laminar to turbulent boundary layer in the test-section.

The characteristic behaviour of these two families of curves is discussed briefly in the following:

A. Family of curves established for  $N_{Re} < 6000$ .

The following points are noteworthy regarding the behaviour of the curves shown in figures 10 to 14.

1. The Reynolds number has a marked influence on the axial wall temperature variation.
2. At low Reynolds numbers ( $N_{Re} \leq 1200$ ), it seems as if the laminar boundary layer is developing and the length occupied by it is very small (not more than

2 or 3 diameters). However, as the inlet Reynolds number increases, the section occupied by the laminar boundary layer also increases. For instance, when  $t_1 \simeq 300^\circ\text{F}$  and  $N_{\text{Re}} \simeq 1800$ , the length of this section is approximately 12 diameters, and for  $N_{\text{Re}} \simeq 2800$  and 4000, it becomes approximately 15 and 20 diameters respectively.

3. At some distance from the entrance (depending upon  $N_{\text{Re}_1}$ ), the rate of wall temperature drop is reduced comparatively over certain length of the pipe. This may be due to the effect of free convection which appears to oppose the drop in wall temperature over this region. Following this, the decrease in wall temperature becomes more gradual.

From the foregoing observations, three regions could possibly be identified over the total length of the heat transfer-section. They are:

1. Initial Section

This section is occupied by the laminar boundary layer. Wall temperature drops very rapidly. Buoyancy effects are not so pronounced.

2. Intermediate Section

In this section buoyancy effects seem to be dominant. Due to this, a secondary flow is established which brings

the hotter air from the centre of the pipe out to the walls resulting in a rise in wall temperature.

### 3. Exit Section

Over this section, the effect of buoyancy does not appear to be pronounced. The wall temperature decreases gradually.

It may be noted that the length of the initial section occupied by the laminar boundary layer attains its limiting value of approximately 30 diameters at  $N_{Re_i} \approx 6000$ , beyond which it starts decreasing again with an increasing inlet Reynolds number.

#### B. Family of Curves established for $N_{Re_i} \geq 6000$ .

Graphs showing the axial variation of wall temperature for this family of curves are presented in figures 16 to 32 for  $t_1 \approx 300$  and  $500^\circ\text{F}$ . Salient characteristics of this class of curves are discussed here.

It is seen from these curves that a viscous flow exists at the beginning of the tube (i.e., a laminar boundary layer is formed), the wall temperature falling off rapidly with the distance from the inlet. After passing the minimum point, a transition region is entered where laminar boundary layer turns into turbulent one. Within this region, the wall temperature increases along the length. Starting from certain value of  $X/D$ , subsequent turbulent cooling takes

place.

These figures show conclusively that the jump in the axial wall temperature curves is due to a boundary-layer effect and is caused by transition.

Again, the total heat transfer section could be divided into three distinctive zones each having different characteristics. They are:

### 1. Laminar Boundary-Layer Zone

This section of the pipe is occupied by a laminar boundary-layer which results in a rapid drop in wall temperature over it. At  $N_{Re_i} \geq 6000$ , the section occupied by the laminar boundary layer covers a considerable part of the tube; its length diminishes as the Reynolds number increases. For instance, at  $N_{Re_i} \approx 8000$ , the length of the laminar section is approximately 18 diameters whereas at  $N_{Re_i} \approx 17700$ , the length of this section does not exceed 7 diameters.

### 2. Transition Zone

Over this section of the pipe the wall temperature increases rapidly from the minimum to a new maximum value. As the inlet Reynolds number increases, the length occupied by this section decreases and the value of  $X/D$  where transition starts, moves towards the inlet of the pipe.

### 3. Turbulent Boundary-Layer Zone

This section of the pipe is occupied by the turbulent boundary-layer. Since increasing Reynolds number has the effect of diminishing both the laminar and transition zones,

consequently the turbulent zone increases proportionally. The slope of the  $t_w$  curves is very small as compared with the laminar boundary-layer section.

It follows from the above that the shares of the laminar section and of the transition region in the total heat transfer decrease as the  $N_{Re_i}$  and the relative length of the pipe increases. When values of  $N_{Re_i}$  or  $X/D$  are sufficiently larger, the influence of these section will become so small that it might be neglected.

### 5.3 RADIAL TEMPERATURE PROFILES

Typical horizontal and perpendicular temperature profiles, presented in figures 33 to 48 for various inlet Reynolds numbers, reveal the following noticeable features:-

1. The temperature profiles at the entrance to the test-section are nearly uniform.
2. The effects of natural convection are exceedingly severe and pronounced for  $N_{Re_i} < 8000$ . The horizontal and perpendicular temperature variations across the cross-section are significantly different from each other in the above mentioned range of Reynolds numbers and over a major portion of the test-section. The temperature profiles are practically symmetrical in the horizontal plane passing through the tube axis but not in a vertical plane.
3. For  $N_{Re_i} > 8000$ , the temperature distributions along the

horizontal and vertical diameters tend to be identical and are symmetrical about their respective axes.

4. Some starting length appears necessary for the establishment of the free convection effects.
5. The influence of natural convection tends to increase with increasing  $X/D$  ratio, attains its maximum value at some  $X/D$  beyond which it starts diminishing again.

#### 5.4 THE SECONDARY FLOW

By studying the horizontal and vertical temperature profiles in the test pipe it can be seen that a secondary flow exists which is superimposed on the axial flow. A brief description of the process is attempted below:

As the wall temperature gets lower than the fluid temperature, the fluid near the wall becomes cooler and therefore more dense than the fluid nearer the centre of the pipe. It therefore flows downward along the tube wall. The two downward flows along the both sides of the tube probably coincide with each other at the bottom part of the tube, change direction and come to the central part. The particle of the fluid caught in transverse circulation moves simultaneously in the longitudinal direction. The resultant path of the particle is a helical line. Therefore, it is considered that these flows form a pair of vortices one on each side of a vertical plane passing through the axis of the tube. Furthermore, it appears that the centres of these vortices change their position with (i) increasing  $X/D$  ratio,

and (ii) increasing flow rate. The flow of the hot fluid from the inner part towards the pipe wall to replace the cooled descending fluid probably explains the occurrence of two maximum temperatures on each side of the centre of the horizontal diameter.

Since the convective movement cannot start until some heat has been transferred from wall layers of the fluid, the effect on heat transfer must be small near the inlet, build up to a maximum when appreciable volumes of cooled fluid are present and finally die away when the bulk temperature of the fluid approaches the tube wall temperature. This seems to explain why: (i) some starting length appears to be necessary for the establishment of natural convection effects, and (ii) increase in the effects of the free convection to some limiting value along the pipe length.

### 5.5 CIRCUMFERENTIAL TEMPERATURE DISTRIBUTION

Figures 49 to 52 illustrate some of the typical circumferential temperature distributions along the pipe axis for both low and high flow rates. It can be seen that practically there is no difference between the top, side and bottom temperatures of the pipe circumference for  $N_{Re_t} \approx 12000$  and above. The temperature distributions for low Reynolds numbers however, show some difference. These curves show under what conditions of inlet Reynolds number and over what length of the pipe, the effect of the free convection are more pronounced.

### 5.6 EFFECT OF INCREASING $t_1$ ON $N_{Nu_x}$

Figures 53 to 63 are self explanatory and show the effect of increasing inlet air temperature on the local rate of heat transfer along the length of the pipe. The figures show that the inlet air temperature does not have any significant influence on the local Nusselt number at any of the Reynolds number studied in this investigation.

### 5.7 EFFECT OF INCREASING $N_{Re_1}$ ON $N_{Nu_x}$

From figures 64 to 74, the following observations can be made:

1. For the lower Reynolds numbers ( $800 < N_{Re_1} < 3000$ ), the local rate of heat transfer is not affected significantly by the increasing  $N_{Re_1}$ .
2. For the range of Reynolds numbers ( $6000 < N_{Re_1} < 18000$ ), the effect of increasing flow rate on local Nusselt number is highly significant. The local Nusselt number varies approximately linearly with the increasing inlet Reynolds numbers.
3. The established pattern of the  $N_{Nu_x}$  vs  $X/D$ , curves are very interesting and illustrate the growth of the boundary layer, that is, a laminar boundary layer giving way to a turbulent boundary layer. The local heat transfer rate decreases rapidly from a very high value in the laminar-flow region until a point of transition to a turbulent boundary layer is reached. It then rises to the corresponding value of turbulent flow.

## 5.8 EFFECT OF X/D RATIOS ON $N_{Num}$

The results of calculating the mean heat transfer for different tube lengths are given in figures 75 and 76. It may be noted that (i) for  $N_{Re_t} < 3000$ , the length of the tube does not affect the mean Nusselt numbers significantly but the trend of mean Nusselt number being higher at smaller values of X/D, is consistent, and (ii) for  $N_{Re_t} > 6000$ , the mean Nusselt number does show dependence on X/D and the trend of it being higher at larger values of X/D is also consistent.

## 5.9 COMPARISON WITH PREVIOUS INVESTIGATIONS

### 1. The Effect of Wall Boundary Condition

Figures 77 to 79 show the comparison of this work with the experimental data of Hall and Khan (12). Their results are for heating of air using the boundary condition of (i) uniform wall temperature and (ii) uniform wall heat flux. The velocity and temperature profiles were uniform at the inlet of the test-section.

Figure 77 shows that the local Stanton number for this study was higher than those of the other two wall boundary conditions over  $X/D < 14$ , and fell in between them over  $14 < X/D < 25$ . Under the comparison condition of figures 78 and 79, it can be observed that the present results are higher than the other boundary conditions over  $X/D < 20$  (fig 78) and  $X/D > 10$  (fig 79) respectively. Unfortunately, non-availability of experimental data for the cooling of air in horizontal tubes does not permit any conclusive remarks as to the effect

of wall boundary condition on the local rate of heat transfer.

## 2. The Effect of Free-Convection

Figure 80 compares the results of the present investigation with the experimental data of McComas and Eckert (22), and the analytical prediction of Siegel et al. (31).

The experimental data of McComas and Eckert is for (i) heating of air under uniform wall heat flux, (ii) developing temperature profiles, (iii) fully established velocity profiles at the entrance of the heated section, (iv) test-section of 0.5" diameter.

The figure shows that the values of local Nusselt number for the present work are far higher than their experimental results. This could be due to (i) tube diameter effect, (ii) hydrodynamic entrance effect, and (iii) wall boundary condition.

The analytical prediction of Siegel et al. is valid for (i) uniform heat flux at the wall, (ii) fully established parabolic velocity profiles, (iii) thermally developing region, and (iv) longitudinal heat conduction negligible and (v) constant fluid properties. The values of local Nusselt number are higher for this work than those of the prediction (Fig 80). This could be attributed to (i) free convection effect, (ii) wall boundary condition, (iii) hydrodynamic entry effect, and (iv) temperature dependent fluid properties. According to Kays (15), the effect of the temperature dependent fluid properties could be up to 10 per cent and those of hydrodynamic entry effect 12 to 25 per cent.

The numerical solutions of Kays (15) are compared with the present work in figures 81 and 82. These solutions are valid for the heating of fluids having  $N_{Pr} \geq 0.7$  and  $N_{Re} < 3000$ , using the boundary conditions of (i) constant wall temperature, (ii) constant wall heat flux, and (iii) constant wall to fluid temperature difference. Also, these solutions assume, (i) uniform velocity and temperature profiles at the entrance, (ii) constant fluid properties, Langhaar's developing velocity profiles, and (iv) no free convection effects. The graphs (Fig. 81 & 82) show that the local Nusselt number for this study are substantially higher than those calculated from the numerical solutions. This may be due to (i) free convection effects, (ii) wall boundary conditions, and (iii) temperature dependent properties.

## 5.10 RELIABILITY OF THE EXPERIMENTAL RESULTS

### 1. Reproducibility

Figures 83 and 84 show the reproducibility of the experimental results. Curves in figure 83 show that the axial variation of wall and fluid mean temperatures are not affected appreciably by unknown and uncontrolled variables. Figure 74 shows that the local rate of heat transfer also remains practically unaffected.

### 2. Effect of External Forced Draft

Run 48 was especially conducted to explore the effect of external forced draft on the surface of the pipe. A large fan was used to produce an artificial draft over the test section and to upset the normal conditions of the room.

The results of various measurements are shown in figures 85 and 86. Figure 85 shows that the  $t_w$  and  $t_m$  curves are affected almost in an identical manner. Consequently in figure 86 the rate of local heat transfer remains practically unaffected by the external forced draft.

We close the discussion with the remarks that in nonisothermal flow of fluid the phenomenon acquires a number of peculiarities. Many of the above discussed considerations regarding the nature of the nonisothermal flow, the effect of free convection on heat transfer, etc, cannot yet be expressed in the form of precise quantitative relationships. Nevertheless these considerations may be successfully employed to evaluate phenomena qualitatively; they show what aspects of the process merit attention and permit correct evaluation of test results.

## CHAPTER 6

### CONCLUSIONS

Under the condition and range of the investigation, following are the main conclusions arrived at :

1. The increasing inlet air temperature has no significant effect on the local rate of heat transfer along the length of the tube.
2. The local Nusselt number is not affected significantly by the increasing inlet Reynolds number for  $N_{Re_i} < 3000$ . For the range of Reynolds numbers ( $6000 \leq N_{Re_i} \leq 18000$ ), the effect of the increasing flow rate on the local and mean Nusselt numbers is highly significant. In this range, both the local and the mean Nusselt numbers vary approximately linearly with an increasing inlet Reynolds number.
3. For  $N_{Re_i} \geq 6000$ , the phenomenon of laminar, transition and turbulent boundary-layer is encountered which has pronounced effects on the axial wall temperature variation and the distribution of local Nusselt number along the tube length.
4. The  $X/D$  ratio seems to have some effect on the mean Nusselt number in conditions of a mixed boundary layer.
5. Free-Convection has a pronounced effect on the radial horizontal and perpendicular temperature

profiles up to approximately  $N_{Re_1} = 6000$ . Above this value of Reynolds number, the effects of free convection are diminished and the temperature distributions tend to be symmetrical about their respective axes.

6. As indicated by the axial and circumferential variation of wall temperatures and the radial temperature profiles, the effect of the free convection appear to be dominant over flow Reynolds numbers up to approximately 6000.
7. Some starting length appears necessary for the establishment of the free convection effect.

## BIBLIOGRAPHY

1. Back, L. H., Cuffel, R. F., and Massier, P. F., "Laminar, Transition, and Turbulent Boundary-Layer Heat Transfer Measurements with Wall Cooling in Turbulent Airflow Through a Tube," Trans. ASME, paper no. 69-HT-39, (September 1969).
2. Bajaj, J. K. L., "Non-Isothermal Flow of Air in a Vertical Pipe," M.A.Sc. Thesis, University of Windsor, Windsor, Ontario, Canada, (1969).
3. Boelter, L. K. M., Young, G., and Iversen, H. W., "An Investigation of Air Craft Heaters - XXVII," NACA TN 1451, (July 1948).
4. Brown, A. R., and Thomas, M. A., "Combined Free and Forced Convection Heat Transfer from Laminar Flow in Horizontal Tubes," Journal of Mechanical Engineering Science, Vol. 7, no. 4, p. 440, (1965).
5. Chapman, A. J., "Heat Transfer," The MacMillan Co., N.Y., (1960).
6. Colburn, A. P., "A Method of Correlating Forced Convection Heat Transfer Data and a Comparison with Fluid Friction," Trans. A.I.Ch.E., Vol. 29, p. 174, (1933).

7. Deissler, R. G., "Turbulent Heat Transfer and Friction in the Entrance Regions of Smooth Passages," Trans. ASME, Vol. 77, p. 1221, (November 1955).
8. Del Casal, E. P., and Gill, W. N., "A Note on Natural Convection Effects in Fully Developed Horizontal Tube Flow," A.I.Ch.E. Journal, Vol. 8, p. 570, (September 1962).
9. Drew, T. B., "Heat Transfer in Laminar Flow," Trans. A.I.Ch.E., Vol. 27, p. 81, (1931).
10. Drobitch, A. J., "Non-Isothermal Flow of Air in a Vertical Tube," M.A.Sc. Thesis, University of Windsor, Windsor, Ontario, (1965).
11. Gulati, U. S., "Non-Isothermal Flow of Air in a Vertical Pipe at Low Velocities," M.A.Sc. Thesis, University of Windsor, Windsor, Ontario, (1965).
12. Hall, W. B., Khan, S. A., "Experimental Investigation into the Effects of Thermal Boundary Condition on Heat Transfer in the Entrance Region of a Pipe," Journal of Mechanical Engineering Science, Vol. 6, no. 3, p. 250, (1964).
13. Jackson, T. W., Spurlock, J. M., and Purdy, K. R., "Combined Free and Forced Convection in a Constant

- Temperature Horizontal Tube," A.I.Ch.E. Journal, Vol. 7, p. 38, (March 1961).
14. Kays, W. M., "Numerical Solutions for Laminar-Flow Heat Transfer in Circular Tubes," Trans. ASME, Vol. 58, p. 1265, (November 1955).
  15. Kays, W. M., "Convective Heat and Mass Transfer," McGraw-Hill Series in Mechanical Engineering, N.Y., (1966).
  16. Knudsen, J. G., and Katz, D. L., "Fluid Dynamics and Heat Transfer," McGraw-Hill Book Co., Inc., N.Y., (1959).
  17. Kreith, F., "Principals of Heat Transfer," International Textbook Co., Scranton, Pennsylvania, (1962).
  18. Langhaar, H. L., "Steady Flow in the Transition Length of a Straight Tube," Journal of Applied Mechanics, Trans. ASME, Vol. 64, p. A-55, (June 1942).
  19. Latzko, H., "Heat Transfer in a Turbulent Liquid or Gas Stream," NACA, TM No. 1068, (1944).
  20. Martinelli, R. C., and Boelter, L. K. M., University of California Publications in Engineering, " Vol. 5, No. 2, p. 23, (1942).

21. McAdams, W. H., "Heat Transmission," McGraw-Hill Series in Chemical Engineering, N.Y., (1954).
22. McComas, S. T., and Eckert, E. R. G., "Combined Free and Forced Convection in a Horizontal Circular Tube," Journal of Heat Transfer, Trans. ASME, Series C, Vol. 88, p. 147, (1966).
23. Mills, A. F., "Experimental Investigation of Turbulent Heat Transfer in the Entrance Region of a Circular Conduit," Journal of Mechanical Engineering Science, Vol. 4, no. 1, p. 63, (1962).
24. Mori, Y., Futagami, K., Tokuda, S., and Nakamura, M., "Forced Convection Heat Transfer in Uniformly Heated Horizontal Tubes," Int. J. Heat Mass Transfer, Vol. 9, p. 453, (1966).
25. Mori, Y., and Futagami, K., "Forced Convection Heat Transfer in Uniformly Heated Horizontal Tubes," Int. J. Heat Mass Transfer, Vol. 10, p. 1801, (1967).
26. Morton, B. R., "Laminar Convection in Uniformly Heated Horizontal Pipes at Low Rayleigh Numbers," Quart. Jour. Mech. and Applied Math, Vol. 12, p. 410, (November 1959).
27. Newell Jr., P. H., and Bergless, A. E., "Analysis of

- Combined Free and Forced Convection for Fully Developed Laminar Flow in Horizontal Tubes," Trans. ASME, paper no. 69-HT-39, (September 1969).
28. Oliver, D. R., "The Effects of Natural Convection on Viscous Flow Heat Transfer in Horizontal Tubes," Chemical Engineering Science, Vol. 17, p. 335, (1962).
  29. Poppendick, H. F., "Forced Convection Heat Transfer in Thermal Entrance Regions - Part I," ORNL-913, Series A, Physics, Oak Ridge, Tenn., (May 1951).
  30. Poppendick, H. F., "Forced Convection Heat Transfer in Thermal Entrance Regions-Part II," ORNL-914, Met and Ceramics, Oak Ridge, Tenn., (May 1952).
  31. Siegel, R., Sparrow, E. M., and Hallman, T. M., "Steady Laminar Heat Transfer in a Circular Tube with Prescribed Wall Heat Flux," Applied Scientific Research, Section A, Vol. 7, p. 386, (1958).
  32. Shannon, R. L., and Depew, C. A., "Combined Free and Forced Laminar Convection in a Horizontal Tube with Uniform Heat Flux," Journal of Heat Transfer, Trans. ASME, Series C, Vol. 90, p. 353, (1968).
  33. Smith, R. H., and Wang, C., "Contracting Cones Giving Uniform Throat Speeds," J. Aero. Sci., Vol. 11, no. 4,

(1944).

34. Vissers, J. I., "Isothermal and Non-Isothermal Flow of Air in a Vertical Tube," M.A.Sc. Thesis, University of Windsor, Windsor, Ontario, (1965).

## APPENDIX A

Table A - 1

Variation of Temperature and Dimensionless  
Parameters with X/D Ratio

Run No. 1		Barometric Pressure	- 29.45" Hg				
		Ambient Air Temperature	- 84.5°F				
		Inlet Air Temperature	- 342.0°F				
		Mass Flow	-19.80 lbs/hr				
X/D	$t_m$ °F	$t_w$ °F	$N_{RE_x}$	$N_{GR_x}$ $\times 10^{-5}$	$N_{GZ_x}$	$N_{GZ}$	$N_{Nu}$
						(x + $\Delta x/2$ )	
0	342.0	290.0	1776	18.21		487.1	35.4
4	307.8	210.0	1833	18.34	247.8	143.6	15.3
10	280.0	184.5	1882	18.22	102.0	65.7	21.2
22	222.0	165.0	1992	16.91	49.4	41.0	22.1
32	190.0	145.0	2059	15.26	35.2	30.8	19.3
42	168.0	130.0	2108	13.55	27.5	23.9	21.6
56.5	142.0	118.0	2168	10.75	21.1	18.1	19.3
77	122.0	107.0	2217	7.84	15.9	14.2	18.5
97	110.0	99.5	2247	5.71	12.8	11.9	14.6
113	104.2	95.0	2262	4.56	11.1	10.2	9.5
133	100.0	91.5	2274	3.68	9.4		

Table A - 2

Variation of Temperature and Dimensionless  
Parameters with X/D Ratio

<u>Run No. 2</u>		Barometric Pressure		-29.44" Hg			
		Ambient Air Temperature		- 82.0°F			
		Inlet Air Temperature		- 387.5°F			
		Mass Flow		-19.46 lbs/hr			
X/D	$t_m$ °F	$t_w$ °F	$N_{RE_x}$	$N_{GR_x}$ $\times 10^{-5}$	$N_{GZ_x}$	$N_{GZ}$	$N_{Nu}$
						(x + $\Delta x/2$ )	
0	387.5	330.0	1677	17.92			
4	345.0	232.5	1741	18.43	234.7	460.0	36.6
10	302.0	202.5	1811	18.62	97.9	137.0	20.6
22	246.0	178.0	1912	18.01	47.2	63.0	17.9
32	210.0	156.0	1982	16.78	33.8	39.3	19.9
42	185.0	137.0	2035	15.35	26.5	29.7	17.1
56.5	155.0	122.5	2101	12.76	20.4	23.0	18.6
77	132.5	109.0	2154	9.99	15.4	17.5	14.6
97	114.0	99.5	2199	7.03	12.5	13.8	18.6
113	105.0	94.0	2222	5.33	10.9	11.6	17.2
133	98.5	89.0	2238	3.97	9.3	10.0	12.5

Table A - 3

Variation of Temperature and Dimensionless  
Parameters with X/D Ratio

Run No. 3		Barometric Pressure	-29.68"Hg				
		Ambient Air Temperature	-83.0°F				
		Inlet Air Temperature	-432.2°F				
		Mass Flow	-20.43 lbs/hr				
X/D	$t_m$ °F	$t_w$ °F	$N_{RE_x}$	$N_{GR_x}$ $\times 10^{-5}$	$N_{GZ_x}$	$N_{GZ}$	$N_{Nu}$
						$(x + \Delta x/2)$	
0	432.2	380.0	1695	17.37			
4	380.5	251.0	1771	18.22	238.2	465.3	42.2
10	335.7	217.0	1844	18.70	99.5	139.0	18.6
22	270.2	191.5	1960	18.59	48.3	64.2	18.1
32	227.0	164.5	2045	17.60	34.8	40.3	21.2
42	198.2	146.0	2107	16.27	27.4	30.6	18.1
56.5	165.7	133.0	2180	13.84	21.2	23.8	19.7
77	137.0	114.0	2250	10.57	16.1	18.2	19.5
97	118.0	104.0	2298	7.63	13.1	14.4	20.5
113	109.0	98.0	2322	5.97	11.4	12.2	18.3
133	100.2	93.0	2345	4.16	9.8	10.5	19.9

Table A - 4

Variation of Temperature and Dimensionless  
Parameters with X/D Ratio

Run No. 4		Barometric Pressure		-29.52" Hg			
		Ambient Air Temperature		-81.0°F			
		Inlet Air Temperature		-337.0°F			
		Mass Flow		-19.55 lbs/hr			
X/D	$t_m$ °F	$t_w$ °F	$N_{RE_x}$	$N_{GR_x}$ $\times 10^{-5}$	$N_{GZ_x}$	$N_{GZ}$	$N_{Nu}$
						(x + $\Delta x/2$ )	
0	337.0	290.0	1762	18.70		482.5	31.7
4	306.3	204.5	1812	18.84	245.0	142.6	20.4
10	269.7	181.0	1877	18.65	101.8	65.3	18.4
22	221.0	163.0	1969	17.50	48.8	40.4	20.4
32	190.5	144.5	2032	15.97	34.7	30.4	18.1
42	168.5	127.5	2080	14.33	27.2	23.5	17.8
56.5	144.5	117.0	2135	11.84	20.8	17.8	17.9
77	122.5	104.5	2188	8.75	15.7	14.0	16.5
97	109.5	97.0	2220	6.47	12.7	11.7	19.4
113	101.0	92.0	2242	4.77	11.0	10.1	13.9
133	95.3	88.0	2257	3.53	9.4		

Table A - 5

Variation of Temperature and Dimensionless  
Parameters with X/D Ratio

Run No. 5		Barometric Pressure		- 29.52" Hg			
		Ambient Air Temperature		- 77.3°F			
		Inlet Air Temperature		- 196.5°F			
		Mass Flow		- 7.44 lbs/hr			
X/D	$t_m$ °F	$t_w$ °F	$N_{RE_x}$	$N_{GR_x}$ $\times 10^{-5}$	$N_{GZ_x}$	$N_{GZ}$	$N_{Nu}$
						(x + $\Delta x/2$ )	
0	196.5	170.0	768	16.98			
4	164.8	132.0	794	14.71	109.0	214.0	36.4
10	137.3	113.0	819	11.72	45.1	63.4	22.7
22	107.7	95.0	847	7.03	21.3	28.7	19.5
32	94.3	87.0	860	4.25	14.9	17.5	20.2
42	85.6	82.0	869	2.19	11.5	13.0	24.4
56.5	82.2	80.0	872	1.32	8.6	9.8	12.5
77	79.8	78.4	875	0.68	6.3	7.3	10.1
97	79.0	77.5	876	0.47	5.0	5.6	4.3
113	78.0	77.0	877	0.19	4.3	4.6	7.8
133	77.0	76.0	878	0.08	3.7	4.0	7.8

Table A - 6

Variation of Temperature and Dimensionless  
Parameters with X/D Ratio

Run No. 6		Barometric Pressure		-29.72" Hg			
		Ambient Air Temperature		-78.8°F			
		Inlet Air Temperature		-306.0°F			
		Mass Flow		-8.78 lbs/hr			
X/D	$t_m$ °F	$t_w$ °F	$N_{RE_x}$	$N_{GR_x}$ $\times 10^{-5}$	$N_{GZ_x}$	$N_{GZ}$	$N_{Nu}$
						(x + $\Delta x/2$ )	
0	306.0	270.0	814	19.36		226.2	35.5
4	253.5	183.0	856	18.97	116.3	68.4	23.1
10	199.7	152.0	904	17.12	49.4	31.9	21.8
22	142.0	118.0	962	12.16	24.1	19.9	22.7
32	116.5	102.0	989	8.37	17.1	14.9	20.5
42	102.7	93.5	1005	5.75	13.2	11.4	20.1
56.5	91.5	87.0	1018	3.26	10.0	8.5	15.3
77	85.0	82.0	1026	1.66	7.4	6.6	16.5
97	81.2	80.0	1031	0.66	5.9	5.5	33.3
113	79.3	79.2	1033	0.14	5.1	4.7	54.9
133	79.0	79.0	1033	0.05	4.3		

Table A - 7

Variation of Temperature and Dimensionless  
Parameters with X/D Ratio

<u>Run No. 7</u>		Barometric Pressure	- 29.42" Hg				
		Ambient Air Temperature	- 62.9°F				
		Inlet Air Temperature	- 200.0°F				
		Mass Flow	- 8.85 lbs/hr				
X/D	$t_m$ °F	$t_w$ °F	$N_{RE_x}$	$N_{GR_x}$ $\times 10^{-5}$	$N_{GZ_x}$	$N_{GZ}$	$N_{Nu}$
						(x + $\Delta x/2$ )	
0	200.0	180.0	910	19.57		253.0	38.9
4	171.2	131.5	939	17.96	128.7	74.9	23.9
10	141.8	113.0	968	15.34	53.4	34.1	22.6
22	108.2	94.0	1006	10.66	25.3	20.9	21.4
32	94.2	85.0	1023	7.99	17.7	15.4	19.1
42	85.8	79.0	1033	6.15	13.7	11.7	14.5
56.5	79.2	74.5	1041	4.56	10.2	8.7	13.0
77	74.0	71.5	1048	3.20	7.6	6.7	9.5
97	71.8	70.0	1050	2.60	6.0	5.6	5.6
113	71.0	69.5	1051	2.38	5.2	4.8	7.5
133	70.0	69.0	1052	2.10	4.4		

Table A - 8

Variation of Temperature and Dimensionless  
Parameters with X/D Ratio

Run No. 8		Barometric Pressure	- 29.56" Hg				
		Ambient Air Temperature	- 71.5°F				
		Inlet Air Temperature	- 300.0°F				
		Mass Flow	- 9.83 lbs/hr				
X/D	$t_m$ °F	$t_w$ °F	$N_{RE_x}$	$N_{GR_x}$ $\times 10^{-5}$	$N_{GZ_x}$	$N_{GZ}$	$N_{Nu}$
						(x + $\Delta x/2$ )	
0	304.0	275.0	917	20.05		254.5	39.5
4	253.5	179.0	962	19.82	130.7	76.9	24.1
10	200.0	147.5	1016	18.22	55.5	35.9	22.4
22	141.8	115.0	1081	13.58	27.1	22.4	23.7
32	115.5	99.5	1113	9.86	19.2	16.8	20.9
42	101.0	89.5	1132	7.19	14.9	12.8	16.8
56.5	89.5	82.0	1147	4.69	11.3	9.6	14.5
77	81.5	78.0	1158	2.74	8.4	7.4	11.9
97	78.2	76.0	1163	1.87	6.7	6.2	17.7
113	76.0	75.0	1166	1.27	5.7	5.3	10.3
133	75.0	74.0	1167	0.99	4.9		

Table A - 9

Variation of Temperature and Dimensionless  
Parameters with X/D Ratio

<u>Run No. 9</u>		Barometric Pressure		-29.57"Hg			
		Ambient Air Temperature		-80.0°F			
		Inlet Air Temperature		-397.5°F			
		Mass Flow		-10.46 lbs/hr			
X/D	$t_m$ °F	$t_w$ °F	$N_{RE_x}$	$N_{GR_x}$ $\times 10^{-5}$	$N_{GZ_x}$	$N_{GZ}$	$N_{Nu}$
						(x + $\Delta x/2$ )	
0	397.5	360.0	894	18.10			
4	329.8	226.0	949	18.93	128.1	247.8	37.8
10	262.2	187.5	1011	18.76	54.9	75.7	21.3
22	182.8	143.0	1096	15.69	27.3	35.8	21.1
32	145.2	119.0	1141	12.17	19.6	22.7	22.3
42	123.5	105.0	1169	9.17	15.4	17.2	19.7
56.5	105.8	95.0	1193	6.02	11.7	13.3	17.3
77	94.0	87.5	1210	3.50	8.7	10.0	14.0
97	87.5	84.0	1219	1.95	7.0	7.7	14.0
113	85.0	82.0	1222	1.32	6.0	6.5	10.4
133	83.0	81.0	1225	0.80	5.1	5.5	8.7

Table A - 10

Variation of Temperature and Dimensionless  
Parameters with X/D Ratio

Run No. 10		Barometric Pressure		-29.40"Hg			
		Ambient Air Temperature		-78.0°F			
		Inlet Air Temperature		-495.0°F			
		Mass Flow		-11.75 lbs/hr			
X/D	$t_m$ °F	$t_w$ °F	$N_{RE_x}$	$N_{GR_x}$ $\times 10^{-5}$	$N_{GZ_x}$	$N_{GZ}$	$N_{Nu}$
						(x + $\Delta x/2$ )	
0	495.0	450.0	926	16.19			
4	415.5	267.0	988	17.76	132.7	256.3	33.5
10	335.2	221.0	1061	18.89	57.2	78.7	17.9
22	229.8	168.0	1173	18.12	29.0	37.7	19.2
32	179.5	138.0	1236	15.64	21.1	24.3	20.4
42	147.8	118.0	1278	12.75	16.7	18.6	19.4
56.5	120.7	101.0	1318	9.07	12.9	14.5	17.2
77	100.5	90.0	1348	5.37	9.7	11.0	15.3
97	90.7	85.0	1364	3.22	7.8	8.6	14.5
113	86.5	82.0	1371	2.21	6.7	7.2	12.4
133	82.5	80.5	1377	1.19	5.7	6.2	14.9

Table A - 11

Variation of Temperature and Dimensionless  
Parameters with X/D Ratio

<u>Run No. 11</u>		Barometric Pressure		-29.32"Hg			
		Ambient Air Temperature		-80.0°F			
		Inlet Air Temperature		-558.0°F			
		Mass Flow		-12.10 lbs/hr			
X/D	$t_m$ °F	$t_w$ °F	$N_{RE_x}$	$N_{GR_x}$ $\times 10^{-5}$	$N_{GZ_x}$	$N_{GZ}$	$N_{Nu}$
						$(x + \Delta x/2)$	
0	558.0	500.0	908	14.68		251.7	32.3
4	466.0	296.0	976	16.55	130.7	77.7	17.4
10	375.5	245.0	1054	18.13	56.7	37.6	19.4
22	254.5	185.5	1179	18.32	29.1	24.5	20.2
32	198.5	151.0	1247	16.40	21.3	18.8	19.8
42	161.8	127.0	1297	13.72	16.9	14.7	18.4
56.5	129.7	109.0	1343	9.94	13.1	11.3	17.7
77	105.8	95.0	1380	5.92	9.9	8.8	14.4
97	95.2	88.0	1397	3.71	8.0	7.4	13.7
113	90.0	85.5	1406	2.52	6.9	6.4	15.3
133	86.0	84.0	1412	1.55	5.9		

Table A - 12

Variation of Temperature and Dimensionless  
Parameters with X/D Ratio

Run No. 12		Barometric Pressure		- 29.45"Hg			
		Ambient Air Temperature		- 79.0°F			
		Inlet Air Temperature		- 2700°F			
		Mass Flow		- 14.81 lbs/hr			
X/D	$t_m$ °F	$t_w$ °F	$N_{RE_x}$	$N_{GR_x}$ $\times 10^{-5}$	$N_{GZ_x}$	$N_{GZ}$	$N_{Nu}$
						$(x + \Delta x/2)$	
0	270.0	240.0	1421	18.84			
4	241.3	173.0	1462	18.35	198.7	391.4	36.4
10	212.3	150.5	1505	17.38	82.1	115.4	19.1
22	172.0	133.0	1570	14.98	39.1	52.5	17.8
32	146.5	119.0	1614	12.44	27.7	32.4	21.3
42	132.5	108.0	1639	10.65	21.5	24.2	15.4
56.5	114.5	99.0	1673	7.83	16.4	18.5	18.1
77	100.2	91.5	1700	5.08	12.2	14.0	17.1
97	93.8	87.0	1713	3.68	9.8	10.8	12.4
113	89.3	85.0	1722	2.63	8.5	9.1	15.4
133	86.0	82.0	1728	1.82	7.2	7.8	12.1

Table A - 13

Variation of Temperature and Dimensionless  
Parameters with X/D Ratio

Run No. 13		Barometric Pressure		- 29.86"Hg			
		Ambient Air Temperature		- 73.5°F			
		Inlet Air Temperature		- 215.0°F			
		Mass Flow		- 12.03 lbs/hr			
X/D	$t_m$ °F	$t_w$ °F	$N_{RE_x}$	$N_{GR_x}$ $\times 10^{-5}$	$N_{GZ_x}$	$N_{GZ}$	$N_{Nu}$
						(x + $\Delta x/2$ )	
0	215.0	170.0	1219	18.91		336.7	25.0
4	192.8	142.5	1247	17.84	170.5	98.9	19.3
10	168.3	125.5	1280	16.12	70.2	44.8	19.3
22	134.0	109.0	1329	12.41	33.3	27.4	18.4
32	117.0	98.5	1355	9.82	23.4	20.4	18.8
42	104.5	91.0	1374	7.52	18.1	15.6	14.0
56.5	94.5	84.0	1390	5.41	13.6	11.6	20.1
77	82.7	79.0	1410	2.54	10.2	9.0	11.1
97	79.5	76.0	1415	1.69	8.1	7.5	14.3
113	77.0	75.0	1419	1.00	7.0	6.4	6.3
133	76.0	74.0	1421	0.72	5.9		

Table A - 14

Variation of Temperature and Dimensionless  
Parameters with X/D Ratio

<u>Run No. 14</u>		Barometric Pressure		- 29.81" Hg			
		Ambient Air Temperature		- 72.0°F			
		Inlet Air Temperature		- 310.0°F			
		Mass Flow		- 13.11 lbs/hr			
X/D	$t_m$ °F	$t_w$ °F	$N_{RE_x}$	$N_{GR_x}$ $\times 10^{-5}$	$N_{GZ_x}$	$N_{GZ}$	$N_{Nu}$
						(x + $\Delta x/2$ )	
0	310.0	273.0	1211	20.30		334.3	37.1
4	269.0	188.5	1259	20.26	170.8	99.7	19.8
10	229.3	161.6	1310	19.57	71.3	46.0	20.5
22	173.5	135.0	1388	16.78	34.6	28.6	19.8
32	146.5	118.0	1428	14.25	24.6	21.5	18.7
42	127.5	104.5	1459	11.80	19.2	16.5	18.6
56.5	109.0	96.5	1489	8.74	14.6	12.5	15.9
77	95.3	85.5	1513	5.97	10.9	9.7	13.7
97	87.5	82.0	1527	4.16	8.7	8.1	16.7
113	83.0	79.4	1535	3.03	7.5	6.9	8.9
133	81.0	78.5	1539	2.51	6.4		

Table A - 15

Variation of Temperature and Dimensionless  
Parameters with X/D Ratio

Run No. 15		Barometric Pressure	- 29.74"Hg				
		Ambient Air Temperature	- 72.0°F				
		Inlet Air Temperature	- 398.0°F				
		Mass Flow	- 14.68 lbs/hr				
X/D	$t_m$ °F	$t_w$ °F	$N_{RE_x}$	$N_{GR_x}$ $\times 10^{-5}$	$N_{GZ_x}$	$N_{GZ}$	$N_{Nu}$
						(x + $\Delta x/2$ )	
0	398.0	350.0	1253	19.04		346.1	40.2
4	339.7	228.0	1320	19.95	178.0	104.2	18.9
10	289.5	195.0	1383	20.25	74.9	48.6	20.0
22	216.8	161.0	1485	19.08	36.8	30.6	20.7
32	178.5	137.0	1545	17.07	26.4	23.2	19.4
42	152.3	120.0	1590	14.81	20.8	18.0	19.3
56.5	126.0	105.0	1636	11.52	16.0	13.7	18.4
77	105.0	93.5	1676	7.94	12.0	10.7	17.0
97	94.3	87.0	1697	5.72	9.7	9.0	21.0
113	88.0	84.0	1709	4.26	8.4	7.7	15.2
133	84.5	81.5	1716	3.99	7.2		

Table A - 16

Variation of Temperature and Dimensionless  
Parameters with X/D Ratio

<u>Run No. 16</u>		Barometric Pressure	- 29.53" Hg				
		Ambient Air Temperature	- 74.5°F				
		Inlet Air Temperature	- 496.0°F				
		Mass Flow	- 15.39 lbs/hr				
X/D	$t_m$ °F	$t_w$ °F	$N_{RE_x}$	$N_{GR_x}$ $\times 10^{-5}$	$N_{GZ_x}$	$N_{GZ}$	$N_{Nu}$
						(x + $\Delta x/2$ )	
0	496.0	450.0	1212	16.55			
4	417.8	263.0	1292	18.18	173.5	335.2	41.6
10	355.3	223.5	1364	19.21	73.5	102.0	16.5
22	261.5	182.0	1489	19.46	36.7	48.1	18.1
32	209.7	153.5	1568	18.11	26.7	30.8	20.2
42	175.0	131.0	1626	16.10	21.2	23.6	19.3
56.5	141.7	112.0	1686	12.89	16.4	18.5	18.0
77	113.5	96.5	1740	8.77	12.5	14.2	17.7
97	99.0	88.0	1769	5.99	10.1	11.2	16.0
113	92.0	84.0	1784	4.46	8.8	9.4	14.4
133	89.0	81.0	1790	3.76	7.5	8.1	15.9

Table A - 17

Variation of Temperature and Dimensionless  
Parameters with X/D Ratio

Run No. 17		Barometric Pressure		-29.74" Hg			
		Ambient Air Temperature		-75.50°F			
		Inlet Air Temperature		-550.0°F			
		Mass Flow		-16.36 lbs/hr			
X/D	$t_m$ °F	$t_w$ °F	$N_{RE_x}$	$N_{GR_x}$ $\times 10^{-5}$	$N_{GZ_x}$	$N_{GZ}$	$N_{Nu}$
						(x + $\Delta x/2$ )	
0	550.0	485.0	1235	15.54		341.6	37.8
4	464.8	284.5	1321	17.39	177.0	104.0	14.9
10	400.0	245.0	1395	18.68	74.9	49.0	17.9
22	293.5	200.0	1535	19.80	37.8	31.7	18.9
32	237.0	167.5	1622	19.13	27.6	24.4	19.0
42	196.3	142.5	1690	17.54	22.0	19.2	17.6
56.5	158.2	122.0	1760	14.67	17.1	14.8	18.3
77	123.7	102.0	1828	10.35	13.1	11.7	18.3
97	104.5	92.0	1869	6.96	10.7	9.9	14.7
113	96.5	86.5	1886	5.28	9.3	8.5	14.8
133	89.0	82.0	1903	3.55	7.9		

Table A - 18

Variation of Temperature and Dimensionless  
Parameters with X/D Ratio

<u>Run No. 18</u>		Barometric Pressure		-29.60"Hg			
		Ambient Air Temperature		-75.0°F			
		Inlet Air Temperature		-199.0°F			
		Mass Flow		-17.62 lbs/hr			
X/D	$t_m$ °F	$t_w$ °F	$N_{RE_x}$	$N_{GR_x}$ $\times 10^{-5}$	$N_{GZ_x}$	$N_{GZ}$	$N_{Nu}$
						(x + $\Delta x/2$ )	
0	199.0	183.5	1815	17.61			
4	18.07	136.0	1850	16.50	253.4	501.3	48.5
10	164.5	122.0	1883	15.22	103.3	146.2	20.2
22	143.3	115.0	1927	13.03	48.2	65.4	16.6
32	129.3	108.0	1957	11.20	33.7	39.6	19.2
42	119.0	100.5	1980	9.62	26.0	29.4	17.9
56.5	107.5	94.0	2006	7.60	19.6	22.4	17.9
77	97.9	88.0	2028	5.66	14.6	16.7	14.2
97	91.2	84.0	2044	4.17	11.7	13.0	14.1
113	87.5	82.0	2053	3.29	10.1	10.8	13.2
133	84.7	80.5	2060	2.59	8.6	9.3	10.5

Table A - 19

Variation of Temperature and Dimensionless  
Parameters with X/D Ratio

<u>Run No. 19</u>		Barometric Pressure		-29.44"Hg			
		Ambient Air Temperature		-77.0°F			
		Inlet Air Temperature		-312.0°F			
		Mass Flow		-19.86 lbs/hr			
X/D	$t_m$ °F	$t_w$ °F	$N_{RE_x}$	$N_{GR_x}$ $\times 10^{-5}$	$N_{GZ_x}$	$N_{GZ}$	$N_{Nu}$
						$(x + \Delta x/2)$	
0	312.0	275.0	1832	19.20			
4	279.0	186.0	1889	19.16	256.0	505.3	40.7
10	251.0	164.0	1941	18.83	105.5	148.4	17.2
22	209.5	151.0	2024	17.58	50.2	67.4	16.3
32	183.3	136.5	2080	16.13	35.6	41.5	17.7
42	162.5	123.0	2127	14.48	27.8	31.2	17.7
56.5	140.7	111.0	2188	12.15	21.2	24.0	16.4
77	120.3	100.5	2228	9.26	16.0	18.2	15.6
97	106.5	93.0	2263	6.84	13.0	14.3	16.4
113	99.5	88.0	2282	5.43	11.2	12.0	14.0
133	93.8	85.0	2297	4.19	9.6	10.3	11.4

Table A - 20

Variation of Temperature and Dimensionless  
Parameters with X/D Ratio

Run No. 20		Barometric Pressure	-29.53" Hg				
		Ambient Air Temperature	-76.4°F				
		Inlet Air Temperature	-400.0°F				
		Mass Flow	-21.46 lbs/hr				
X/D	$t_m$ °F	$t_w$ °F	$N_{RE_x}$	$N_{GR_x}$ $\times 10^{-5}$	$N_{GZ_x}$	$N_{GZ}$	$N_{Nu}$
						(x + $\Delta x/2$ )	
0	399.5	350.0	1830	18.34			
4	350.5	226.0	1911	19.07	257.5	503.1	45.0
10	314.7	199.0	1974	19.37	106.7	149.7	16.6
22	261.0	180.0	2077	19.19	51.3	68.5	15.9
32	225.5	160.0	2152	18.39	36.6	42.6	17.7
42	197.5	142.5	2214	17.20	28.8	32.2	17.6
56.5	167.3	127.0	2286	15.12	22.2	25.0	17.1
77	137.0	110.0	2363	11.89	16.9	19.1	17.9
97	117.5	100.0	2415	9.00	13.7	15.1	18.4
113	108.3	94.0	2441	7.37	12.0	12.8	15.5
133	99.5	89.0	2466	5.62	10.3	11.0	15.4

Table A - 21

Variation of Temperature and Dimensionless  
Parameters with X/D Ratio

<u>Run No. 21</u>		Barometric Pressure	- 29.52"Hg				
		Ambient Air Temperature	- 77.0°F				
		Inlet Air Temperature	- 500.0°F				
		Mass Flow	- 22.98 lbs/hr				
X/D	$t_m$ °F	$t_w$ °F	$N_{RE_x}$	$N_{GR_x}$ $\times 10^{-5}$	$N_{GZ_x}$	$N_{GZ}$	$N_{Nu}$
						(x + $\Delta x/2$ )	
0	500.0	425.0	1804	16.28			
4	442.0	267.0	1891	17.48	253.5	494.5	36.5
10	395.0	233.0	1967	18.35	105.8	147.9	15.3
22	322.5	210.5	2099	19.25	51.5	68.4	15.4
32	275.0	186.0	2195	19.24	37.2	43.0	17.5
42	238.5	163.5	2274	18.66	29.5	32.8	17.2
56.5	197.0	143.0	2373	17.06	23.0	25.7	17.9
77	158.0	122.0	2473	14.14	17.6	19.9	17.9
97	132.3	108.0	2545	11.12	14.4	15.9	18.7
113	120.0	100.0	2579	9.27	12.6	13.5	15.6
133	108.3	93.5	2614	7.21	10.9	11.7	15.4

Table A - 22

Variation of Temperature and Dimensionless  
Parameters with X/D Ratio

Run No. 22		Barometric Pressure		-29.45"Hg			
		Ambient Air Temperature		-74.0°F			
		Inlet Air Temperature		-550.0°F			
		Mass Flow		-24.15 lbs/hr			
X/D	$t_m$ °F	$t_w$ °F	$N_{RE_x}$	$N_{GR_x}$ $\times 10^{-5}$	$N_{GZ_x}$	$N_{GZ}$	$N_{Nu}$
						$(x + \Delta x/2)$	
0	550.0	475.0	1824	15.33		499.1	35.1
4	495.0	293.5	1911	16.63	255.7	149.2	14.6
10	440.3	260.0	1990	17.68	106.7	69.2	15.8
22	358.3	233.5	2135	19.12	52.3	43.7	17.1
32	306.8	205.5	2238	19.58	37.8	33.4	17.3
42	265.5	179.0	2328	19.47	30.1	26.3	17.9
56.5	218.5	156.0	2439	18.44	23.5	20.4	18.5
77	172.8	130.5	2558	15.94	18.2	16.4	19.9
97	142.0	114.0	2645	12.96	15.0	14.0	20.5
113	125.0	104.5	2695	10.69	13.2	12.2	18.9
133	111.0	96.0	2738	8.40	11.4		

Table A - 23

Variation of Temperature and Dimensionless  
Parameters with X/D Ratio

Run No. 23		Barometric Pressure	- 29.48" Hg				
		Ambient Air Temperature	- 74.5°F				
		Inlet Air Temperature	- 203.0°F				
		Mass Flow	- 27.45 lbs/hr				
X/D	$t_m$ °F	$t_w$ °F	$N_{RE_x}$	$N_{GR_x}$ $\times 10^{-5}$	$N_{GZ_x}$	$N_{GZ}$	$N_{Nu}$
						$(x + \Delta x/2)$	
0	203.0	180.0	2816	17.75			
4	188.7	137.0	2859	16.97	391.0	775.5	47.3
10	176.3	125.0	2896	16.14	158.7	225.1	20.1
22	159.3	120.0	2950	14.72	73.6	100.2	16.0
32	147.2	116.0	2989	13.48	51.4	60.4	17.8
42	137.3	110.0	3022	12.30	39.6	44.7	17.8
56.5	125.8	103.0	3061	10.72	29.9	34.0	16.9
77	114.0	97.0	3102	8.83	22.3	25.5	15.7
97	103.7	91.5	3138	6.93	17.9	19.8	19.4
113	98.0	88.0	3159	5.76	15.5	16.6	17.8
133	92.5	86.0	3180	4.56	13.3	14.3	18.7

Table A - 24

Variation of Temperature and Dimensionless  
Parameters with X/D Ratio

<u>Run No. 24</u>		Barometric Pressure		- 29.48"Hg			
		Ambient Air Temperature		- 76.5°F			
		Inlet Air Temperature		- 306.0°F			
		Mass Flow		- 30.31 lbs/hr			
X/D	$t_m$ °F	$t_w$ °F	$N_{RE_x}$	$N_{GR_x}$ $\times 10^{-5}$	$N_{GZ_x}$	$N_{GZ}$	$N_{Nu}$
						$(x + \Delta x/2)$	
0	306.0	265.0	2811	19.33			
4	280.3	183.0	2880	19.29	390.2	770.0	45.6
10	257.2	166.5	2945	19.05	159.9	225.7	20.6
22	229.0	156.0	3029	18.43	74.9	101.5	14.8
32	208.3	154.0	3093	17.66	52.7	61.8	17.3
42	191.2	137.0	3148	16.77	41.0	46.1	17.1
56.5	169.7	127.5	3221	15.25	31.3	35.4	17.1
77	147.2	117.0	3300	13.06	23.6	26.8	17.3
97	130.5	106.0	3362	10.95	19.11	21.1	17.8
113	121.3	99.5	3397	9.57	16.6	17.8	14.8
133	111.6	94.0	3434	7.92	14.3	15.3	14.8

Table A -

Variation of Temperature and Dimensionless  
Parameters with X/D Ratio

Run No. 25		Barometric Pressure		- 29.64" Hg			
		Ambient Air Temperature		- 74.0°F			
		Inlet Air Temperature		- 405.0°F			
		Mass Flow		- 33.15 lbs/hr			
X/D	$t_m$ °F	$t_w$ °F	$N_{RE_x}$	$N_{GR_x}$ $\times 10^{-5}$	$N_{GZ_x}$	$N_{GZ}$	$N_{Nu}$
						(x + $\Delta x/2$ )	
0	405.0	350.0	2814	18.60			
4	375.5	235.0	2887	19.11	388.4	766.2	36.8
10	344.7	207.0	2967	19.54	160.0	225.2	18.5
22	302.0	193.5	3086	19.85	75.9	102.1	15.0
32	272.2	182.5	3174	19.78	53.8	62.8	16.2
42	246.3	166.0	3256	19.43	42.1	47.2	16.9
56.5	213.8	151.0	3364	18.50	32.5	36.6	18.0
77	181.0	132.5	3480	16.75	24.7	28.0	17.1
97	155.2	119.0	3590	14.28	20.3	22.3	21.7
113	140.7	109.0	3635	12.97	17.7	18.9	14.0
133	125.7	103.0	3697	10.94	15.3	16.4	17.7

Table A - 26

Variation of Temperature and Dimensionless  
Parameters with X/D Ratio

Run No. 26		Barometric Pressure		-29.22"Hg			
		Ambient Air Temperature		-75.0°F			
		Inlet Air Temperature		-498.5°F			
		Mass Flow		-35.66 lbs/hr			
X/D	$t_m$ °F	$t_w$ °F	$N_{RE_x}$	$N_{GR_x}$ $\times 10^{-5}$	$N_{GZ_x}$	$N_{GZ}$	$N_{Nu}$
						(x + $\Delta x/2$ )	
0	498.5	435.0	2803	16.12		765.2	48.5
4	450.5	273.0	2914	17.11	390.5	227.0	19.1
10	411.0	239.0	3012	17.88	161.7	103.3	13.4
22	363.5	224.0	3138	18.65	76.8	63.8	16.9
32	324.5	211.0	3251	19.07	54.8	48.2	16.4
42	293.5	192.0	3346	19.18	43.1	37.5	17.2
56.5	254.7	173.0	3473	18.89	33.4	28.9	17.9
77	212.2	152.0	3624	17.76	25.7	23.1	17.5
97	182.5	134.0	3738	16.20	21.1	19.7	16.7
113	164.2	122.5	3812	14.81	18.5	17.2	18.2
133	144.0	111.0	3896	12.78	16.1		

Table A - 27

Variation of Temperature and Dimensionless  
Parameters with X/D Ratio

<u>Run No. 27</u>		Barometric Pressure		-29.78"Hg			
		Ambient Air Temperature		-75.5°F			
		Inlet Air Temperature		-560.0°F			
		Mass Flow		-37.11 lbs/hr			
X/D	$t_m$ °F	$t_w$ °F	$N_{RE_x}$	$N_{GR_x}$ $\times 10^{-5}$	$N_{GZ_x}$	$N_{GZ}$	$N_{Nu}$
						(x + $\Delta x/2$ )	
0	560.0	490.0	2782	15.37		753.0	27.9
4	526.0	304.0	2855	16.11	381.6	221.8	16.2
10	483.2	269.5	2953	17.04	158.1	101.5	14.5
22	419.3	252.5	3112	18.37	75.9	63.1	15.3
32	376.0	236.5	3230	19.14	54.3	47.8	16.5
42	337.7	215.0	3343	19.64	42.9	37.5	16.8
56.5	291.8	193.5	3488	19.85	33.4	29.0	18.0
77	240.5	167.0	3666	19.27	25.9	23.4	18.0
97	204.0	147.0	3804	17.99	21.4	20.1	19.5
113	179.7	132.0	3902	16.53	18.9	17.6	18.9
133	157.1	122.5	3997	14.60	16.5		

Table A - 28

Variation of Temperature and Dimensionless  
Parameters with X/D Ratio

<u>Run No. 28</u>		Barometric Pressure		- 29.58 <sup>''</sup> Hg			
		Ambient Air Temperature		- 78.5 <sup>°</sup> F			
		Inlet Air Temperature		- 303.5 <sup>°</sup> F			
		Mass Flow		- 43.15 lbs/hr			
X/D	$t_m$ °F	$t_w$ °F	$N_{RE_x}$	$N_{GR_x}$ $\times 10^{-5}$	$N_{GZ_x}$	$N_{GZ}$	$N_{Nu}$
						(x + $\Delta x/2$ )	
0	303.5	268.0	4011	19.22		1095.6	52.6
4	283.8	189.5	4086	19.18	553.4	318.9	20.3
10	267.4	169.0	4151	19.04	225.2	142.4	14.3
22	246.0	163.0	4239	18.69	104.7	86.1	16.3
32	229.0	157.5	4312	18.24	73.4	64.0	17.1
42	213.8	151.0	4379	17.68	56.9	49.1	19.0
56.5	193.2	141.0	4473	16.65	43.3	37.2	19.6
77	169.4	128.0	4587	14.94	32.7	29.2	21.0
97	150.3	118.0	4682	13.08	26.5	24.7	19.4
113	139.2	112.3	4740	11.75	23.1	21.4	18.3
133	128.7	107.5	4796	10.31	19.9		

Table A - 29

Variation of Temperature and Dimensionless  
Parameters with X/D Ratio

Run No. 29		Barometric Pressure	-29.20" Hg				
		Ambient Air Temperature	-80.0°F				
		Inlet Air Temperature	-500.0°F				
		Mass Flow	-50.58 lbs/hr				
X/D	$t_m$ °F	$t_w$ °F	$N_{RE_x}$	$N_{GR_x}$ $\times 10^{-5}$	$N_{GZ_x}$	$N_{GZ}$	$N_{Nu}$
						(x + $\Delta x/2$ )	
0	500.0	445.0	3971	15.73		1081.4	63.9
4	457.5	283.3	4109	16.57	550.6	318.9	21.3
10	425.8	248.0	4219	17.17	226.4	144.1	15.0
22	385.8	237.0	4365	17.83	106.7	88.2	16.3
32	355.9	226.5	4482	18.22	75.5	66.1	16.4
42	330.0	213.0	4588	18.46	59.0	51.1	16.7
56.5	297.5	200.0	4728	18.55	45.3	39.1	17.7
77	258.7	178.8	4907	18.24	34.6	31.1	18.2
97	228.0	162.0	5059	17.52	28.4	26.6	18.9
113	206.8	148.5	5170	16.68	25.0	23.2	16.4
133	186.9	135.0	5278	15.57	21.7		

Table A - 30

Variation of Temperature and Dimensionless  
Parameters with X/D Ratio

<u>Run No. 30</u>		Barometric Pressure		- 29.53" Hg			
		Ambient Air Temperature		- 78.0°F			
		Inlet Air Temperature		- 302.0°F			
		Mass Flow		- 65.09 lbs/hr			
X/D	$t_m$ °F	$t_w$ °F	$N_{RE_x}$	$N_{GR_x}$ $\times 10^{-5}$	$N_{GZ_x}$	$N_{GZ}$	$N_{Nu}$
						(x + $\Delta x/2$ )	
0	302.0	273.0	6058	19.22		1647.5	44.8
4	291.5	197.5	6119	19.21	828.2	477.2	28.9
10	275.5	173.0	6213	19.12	336.8	212.4	15.5
22	259.0	169.0	6313	18.94	155.8	127.8	15.3
32	247.0	164.5	6388	18.72	108.5	94.3	11.1
42	239.2	165.0	6438	18.54	83.4	71.6	14.5
56.5	226.8	168.5	6518	18.19	62.8	53.9	22.7
77	204.5	153.0	6668	17.28	47.3	42.3	23.0
97	185.8	142.0	6800	16.22	38.4	35.7	25.0
113	172.0	133.5	6900	15.20	33.5	31.0	24.9
133	157.2	123.5	7010	13.86	29.0		

Table A - 31

Variation of Temperature and Dimensionless  
Parameters with X/D Ratio

<u>Run No. 31</u>		Barometric Pressure		- 29.92"Hg			
		Ambient Air Temperature		- 80.0°F			
		Inlet Air Temperature		- 494.0°F			
		Mass Flow		- 76.50 lbs/hr			
X/D	$t_m$ °F	$t_w$ °F	$N_{RE_x}$	$N_{GR_x}$ $\times 10^{-5}$	$N_{GZ_x}$	$N_{GZ}$	$N_{Nu}$
						(x + $\Delta x/2$ )	
0	494.0	426.0	6034	16.64		1633.8	59.7
4	466.2	292.0	6171	17.23	826.5	477.8	26.4
10	439.2	250.0	6309	17.77	338.4	214.9	18.7
22	403.0	239.0	6505	18.44	158.9	130.5	12.8
32	384.8	230.0	6608	18.74	111.1	96.5	11.1
42	370.5	232.5	6665	18.88	85.4	74.0	17.5
56.5	344.0	240.0	6875	19.29	65.6	56.5	22.8
77	305.8	214.0	7096	19.48	49.8	44.9	25.1
97	271.8	195.5	7328	19.34	41.0	38.3	26.3
113	247.8	178.0	7502	18.94	36.0	33.6	23.7
133	224.0	161.5	7683	18.25	31.5		

Table A - 32

Variation of Temperature and Dimensionless  
Parameters with X/D Ratio

<u>Run No. 32</u>		Barometric Pressure		- 29.48" Hg			
		Ambient Air Temperature		- 77.0 °F			
		Inlet Air Temperature		- 206.0 °F			
		Mass Flow		- 78.45 lbs/hr			
X/D	$t_m$ °F	$t_w$ °F	$N_{RE_x}$	$N_{GR_x}$ $\times 10^{-5}$	$N_{GZ_x}$	$N_{GZ}$	$N_{Nu}$
						(x + $\Delta x/2$ )	
0	206.0	188.5	8025	17.47		2196.6	48.9
4	201.2	150.0	8064	17.23	1101.3	631.8	28.7
10	194.5	136.0	8121	16.87	444.0	278.8	17.1
22	186.5	134.0	8189	16.39	203.7	166.4	11.9
32	182.5	139.0	8224	16.12	140.7	122.0	18.1
42	177.5	141.5	8267	15.76	107.8	92.5	26.5
56.5	168.5	136.5	8347	15.05	81.0	69.1	29.5
77	156.2	128.5	8459	13.92	60.4	53.7	30.1
97	145.8	122.0	8549	12.88	48.5	45.0	30.0
113	138.5	116.5	8624	11.91	42.0	38.8	31.2
133	130.0	110.5	8711	10.69	36.1		

Table A - 33

Variation of Temperature and Dimensionless  
Parameters with X/D Ratio

Run No. 33							
		Barometric Pressure		- 29.50"Hg			
		Ambient Air Temperature		- 77.5°F			
		Inlet Air Temperature		- 303.5°F			
		Mass Flow		- 86.61 lbs/hr			
X/D	$t_m$ °F	$t_w$ °F	$N_{RE_x}$	$N_{GR_x}$ $\times 10^{-5}$	$N_{GZ_x}$	$N_{GZ}$	$N_{Nu}$
						(x + $\Delta x/2$ )	
0	303.5	271.0	8051	19.24			
4	293.2	202.0	8129	19.23	1100.1	2188.6	58.0
10	281.1	177.0	8223	19.19	445.6	632.5	29.1
22	266.1	175.0	8343	19.06	205.7	280.7	18.3
32	256.1	186.0	8425	18.92	143.0	168.5	18.0
42	247.0	186.5	8500	18.76	110.0	124.3	20.4
56.5	233.0	176.5	8620	18.42	83.0	94.5	24.5
77	211.8	164.5	8807	17.67	62.4	71.1	30.1
97	194.3	153.8	8967	16.79	50.5	55.8	30.8
113	181.0	145.0	9094	15.95	44.1	47.0	34.2
133	167.5	138.0	9225	14.89	38.1	40.8	32.9

Table A - 34

Variation of Temperature and Dimensionless  
Parameters with X/D Ratio

<u>Run No. 34</u>		Barometric Pressure		- 29.60"Hg			
		Ambient Air Temperature		- 80.0°F			
		Inlet Air Temperature		- 404.0°F			
		Mass Flow		- 94.62 lbs/hr			
X/D	$t_m$ °F	$t_w$ °F	$N_{RE_x}$	$N_{GR_x}$ $\times 10^{-5}$	$N_{GZ_x}$	$N_{GZ}$	$N_{Nu}$
						(x + $\Delta x/2$ )	
0	404.0	370.0	8093	18.03		2170.9	47.0
4	392.5	257.5	8119	18.22	1091.2	627.4	21.3
10	379.2	223.5	8213	18.42	441.9	279.1	15.6
22	360.0	224.0	8374	18.71	205.1	167.8	15.8
32	346.7	240.0	8441	18.81	142.2	124.0	22.9
42	331.0	237.0	8574	18.96	110.2	95.1	27.5
56.5	307.2	223.0	8765	19.06	83.9	72.1	29.4
77	276.7	205.5	9022	18.96	63.5	57.0	29.2
97	252.0	189.5	9241	18.62	51.8	48.3	29.7
113	234.2	176.0	9405	18.19	45.3	42.1	29.6
133	214.2	161.0	9598	17.48	39.4		

Table A - 35

Variation of Temperature and Dimensionless  
Parameters with X/D Ratio

Run No. 35		Barometric Pressure		-29.53" Hg			
		Ambient Air Temperature		-82.0°F			
		Inlet Air Temperature		-504.0°F			
		Mass Flow		-102.37 lbs/hr			
X/D	$t_m$ °F	$t_w$ °F	$N_{RE_x}$	$N_{GR_x}$ $\times 10^{-5}$	$N_{GZ_x}$	$N_{GZ}$	$N_{Nu}$
						(x + $\Delta x/2$ )	
0	504.0	440.0	8012	15.87		2163.9	68.1
4	480.8	310.0	8161	16.34	1092.5	629.1	23.4
10	462.5	267.0	8283	16.70	443.8	280.6	17.8
22	435.5	270.5	8469	17.22	206.5	169.6	17.4
32	418.0	290.0	8595	17.53	144.2	125.9	25.5
42	397.2	283.0	8748	17.88	111.9	96.9	31.3
56.5	365.2	265.0	8996	18.33	85.7	73.9	30.9
77	327.8	242.5	9304	18.67	65.2	58.6	31.2
97	297.2	223.0	9572	18.73	53.4	49.9	31.7
113	275.3	205.3	9774	18.60	46.9	43.7	34.0
133	250.2	194.0	10015	18.21	40.9		

Table A - 36

Variation of Temperature and Dimensionless  
Parameters with X/D Ratio

<u>Run No. 36</u>		Barometric Pressure		- 29.38" Hg			
		Ambient Air Temperature		- 80.0°F			
		Inlet Air Temperature		- 310.0°F			
		Mass Flow		- 93.57 lbs/hr			
X/D	$t_m$ °F	$t_w$ °F	$N_{RE_x}$	$N_{GR_x}$ $\times 10^{-5}$	$N_{GZ_x}$	$N_{GZ}$	$N_{Nu}$
						$(x + \Delta x/2)$	
0	310.0	277.0	8645	18.77		2348.2	57.6
4	300.2	206.0	8725	18.78	1180.0	677.7	25.0
10	290.2	183.0	8807	18.76	476.9	300.4	20.1
22	274.8	187.0	8938	18.66	220.3	180.2	14.8
32	267.3	198.0	9003	18.58	152.6	132.7	22.9
42	257.5	193.2	9089	18.44	117.5	101.1	28.1
56.5	241.8	184.0	9231	18.13	88.8	76.1	32.0
77	220.2	171.5	9433	18.46	66.8	59.6	26.7
97	205.0	160.0	9566	17.87	53.8	50.2	31.7
113	192.0	151.0	9711	16.09	47.0	43.5	33.2
133	177.0	141.0	9843	15.23	40.5		

Table A - 37

Variation of Temperature and Dimensionless  
Parameters with X/D Ratio

<u>Run No. 37</u>		Barometric Pressure		-29.70" Hg			
		Ambient Air Temperature		-80.0°F			
		Inlet Air Temperature		-307.0°F			
		Mass Flow		-107.16 lbs/hr			
X/D	$t_m$ °F	$t_w$ °F	$N_{RE_x}$	$N_{GR_x}$ $\times 10^{-5}$	$N_{GZ_x}$	$N_{GZ}$	$N_{Nu}$
						(x + $\Delta x/2$ )	
0	307.0	280.0	9928	19.19			
4	301.0	210.0	9984	19.19	1350.3	2692.3	43.6
10	292.0	188.0	10069	19.18	545.1	775.1	26.6
22	278.2	199.3	10203	19.10	251.4	343.1	22.0
32	268.0	206.0	10303	19.00	174.7	205.9	25.6
42	257.0	199.0	10414	18.84	134.6	152.0	32.8
56.5	243.2	188.5	10557	18.56	101.6	115.7	30.6
77	224.0	176.0	10762	17.98	76.2	86.9	33.7
97	207.7	166.0	10942	17.30	61.6	68.0	34.2
113	196.0	157.0	11076	16.68	53.6	57.3	34.7
133	182.5	148.0	11233	15.81	46.2	49.6	35.7

Table A - 38

Variation of Temperature and Dimensionless  
Parameters with X/D Ratio

Run No. 38		Barometric Pressure		-29.64" Hg			
		Ambient Air Temperature		-79.0°F			
		Inlet Air Temperature		-500.5°F			
		Mass Flow		-126.57 lbs/hr			
X/D	$t_m$ °F	$t_w$ °F	$N_{RE_x}$	$N_{GR_x}$ $\times 10^{-5}$	$N_{GZ_x}$	$N_{GZ}$	$N_{Nu}$
						(x + $\Delta x/2$ )	
0	500.5	450.0	9933	16.27			
4	488.0	323.4	10032	16.53	1342.0	2671.3	49.4
10	473.8	285.0	10148	16.82	543.5	771.8	23.0
22	445.7	306.0	10383	17.39	253.1	343.8	25.0
32	423.0	315.8	10582	17.83	177.5	208.3	32.9
42	403.8	302.5	10755	18.17	137.6	154.8	33.6
56.5	378.5	283.6	10993	18.58	104.7	118.7	33.1
77	348.9	262.0	11286	18.96	79.0	89.8	30.3
97	321.0	242.0	11576	19.18	64.5	70.9	33.0
113	298.2	225.5	11824	19.24	56.6	60.2	37.8
133	271.8	213.0	12125	19.10	49.4	52.7	41.5

Table A - 39

Variation of Temperature and Dimensionless  
Parameters with X/D Ratio

Run No. 39		Barometric Pressure		- 29.45" Hg			
		Ambient Air Temperature		- 78.0°F			
		Inlet Air Temperature		- 310.0°F			
		Mass Flow		- 130.06 lbs/hr			
X/D	$t_m$ °F	$t_w$ °F	$N_{RE_x}$	$N_{GR_x}$ $\times 10^{-5}$	$N_{GZ_x}$	$N_{GZ}$	$N_{Nu}$
						(x + $\Delta x/2$ )	
0	310.0	286.0	12039	19.10		3262.0	76.9
4	302.5	218.0	12089	19.11	1634.5	937.8	27.2
10	295.0	199.5	12177	19.11	659.0	414.7	26.4
22	282.8	215.5	12328	19.07	303.6	248.6	29.8
32	274.0	215.0	12442	19.00	210.8	183.1	35.5
42	264.5	208.5	12535	18.92	161.9	139.2	40.5
56.5	250.0	198.5	12714	18.70	122.3	104.6	43.0
77	231.0	186.5	12952	18.26	91.6	81.6	40.7
97	216.0	177.0	13149	17.75	73.9	68.7	42.2
113	205.0	169.0	13315	17.22	64.3	59.5	42.6
133	192.5	160.0	13496	16.53	55.5		

Table A - 40

Variation of Temperature and Dimensionless  
Parameters with X/D Ratio

Run No. 40		Barometric Pressure		-29.42"Hg			
		Ambient Air Temperature		-82.0°F			
		Inlet Air Temperature		-504.0°F			
		Mass Flow		-152.60 lbs/hr			
X/D	$t_m$ °F	$t_w$ °F	$N_{RE_x}$	$N_{GR_x}$ $\times 10^{-5}$	$N_{GZ_x}$	$N_{GZ}$	$N_{Nu}$
						(x + $\Delta x/2$ )	
0	504.0	450.0	11981	15.84		3213.0	66.9
4	490.0	330.0	12072	16.03	1615.4	926.0	31.5
10	475.0	306.5	12146	16.18	650.3	411.3	27.0
22	453.0	336.0	12425	16.73	302.7	248.9	34.9
32	435.0	331.0	12643	17.12	212.0	184.6	38.0
42	417.0	315.0	12814	17.40	163.8	141.2	38.3
56.5	392.5	299.0	13079	17.80	124.4	106.9	40.6
77	360.0	276.0	13458	18.24	94.1	84.4	42.2
97	332.0	260.5	13785	18.49	76.7	71.6	42.4
113	312.0	242.0	14070	18.59	67.3	62.6	41.5
133	290.0	230.0	14383	18.56	58.6		

Table A - 41

Variation of Temperature and Dimensionless  
Parameters with X/D Ratio

Run No. 41		Barometric Pressure		-29.50"Hg			
		Ambient Air Temperature		-81.0°F			
		Inlet Air Temperature		-306.0°F			
		Mass Flow		-150.65 lbs/hr			
X/D	$t_m$ °F	$t_w$ °F	$N_{RE_x}$	$N_{GR_x}$ $\times 10^{-5}$	$N_{GZ_x}$	$N_{GZ}$	$N_{Nu}$
						(x + $\Delta x/2$ )	
0	306.0	280.0	13971	18.82			
4	300.8	218.5	14039	18.81	1898.6	3787.3	57.9
10	294.0	206.8	14129	18.80	764.7	1088.7	32.9
22	279.6	223.5	14324	18.73	352.8	481.5	41.1
32	270.0	220.0	14457	18.63	245.0	289.0	45.0
42	262.0	214.0	14570	18.53	188.3	212.8	41.0
56.5	250.2	205.0	14739	18.32	141.7	161.6	44.3
77	233.0	194.0	14993	17.88	106.0	121.1	51.3
97	219.2	184.0	15203	17.41	85.4	94.5	48.7
113	209.2	176.5	15359	16.98	74.2	79.4	48.9
133	197.5	167.6	15546	16.37	63.9	68.6	50.2

Table A - 42

Variation of Temperature and Dimensionless  
Parameters with X/D Ratio

Run No. 42		Barometric Pressure		- 29.68" Hg			
		Ambient Air Temperature		- 86.0°F			
		Inlet Air Temperature		- 508.0°F			
		Mass Flow		- 178.31 lbs/hr			
X/D	$t_m$ °F	$t_w$ °F	$N_{RE_x}$	$N_{GR_x}$ $\times 10^{-5}$	$N_{GZ_x}$	$N_{GZ}$	$N_{Nu}$
						(x + $\Delta x/2$ )	
0	508.0	450.0	13912	15.69			
4	494.1	335.4	14065	15.96	1881.9	3742.3	76.4
10	487.8	318.5	14136	16.08	756.7	1078.2	15.4
22	463.7	348.5	14414	16.55	351.0	477.7	34.4
32	445.5	344.0	14630	16.89	245.1	288.3	41.6
42	428.3	330.0	14841	17.19	189.6	213.6	43.3
56.5	406.0	312.5	15124	17.56	143.8	163.3	41.1
77	375.8	293.5	15524	17.99	108.5	123.4	44.0
97	349.4	275.0	15892	18.27	88.3	97.2	45.4
113	330.5	262.0	16182	18.41	77.3	82.4	45.5
133	310.0	247.5	16453	18.45	66.9	71.7	43.9

Table A - 43

Variation of Temperature and Dimensionless  
Parameters with X/D Ratio

Run No. 43		Barometric Pressure		-29.37" Hg			
		Ambient Air Temperature		-84.0°F			
		Inlet Air Temperature		-305.0°F			
		Mass Flow		-174.04 lbs/hr			
X/D	$t_m$ °F	$t_w$ °F	$N_{RE_x}$	$N_{GR_x}$ $\times 10^{-5}$	$N_{GZ_x}$	$N_{GZ}$	$N_{Nu}$
						(x + $\Delta x/2$ )	
0	305.0	286.0	16155	18.30			
4	298.6	227.5	16252	18.29	2198.4	4382.4	99.1
10	293.0	220.8	16339	18.27	884.4	1259.8	36.6
22	283.0	232.5	16494	18.21	406.2	555.8	38.5
32	275.0	229.0	16621	18.14	281.6	332.3	47.4
42	267.0	223.0	16758	18.03	216.5	244.6	47.7
56.5	257.6	214.0	16904	17.88	162.5	185.5	45.1
77	244.0	202.0	17132	17.59	121.0	138.5	45.6
97	231.3	193.0	17350	17.23	97.4	107.8	47.2
113	222.0	186.5	17514	16.90	84.5	90.4	47.6
133	211.7	180.0	17699	16.46	72.6	78.1	46.9

Table A - 44

Variation of Temperature and Dimensionless  
Parameters with X/D Ratio

Run No. 44		Barometric Pressure	-29.66" Hg				
		Ambient Air Temperature	-84.0°F				
		Inlet Air Temperature	-502.0°F				
		Mass Flow	-202.73 lbs/hr				
X/D	$t_m$ °F	$t_w$ °F	$N_{RE_x}$	$N_{GR_x}$ $\times 10^{-5}$	$N_{GZ_x}$	$N_{GZ}$	$N_{Nu}$
						(x + $\Delta x/2$ )	
0	502.0	450.0	15892	15.92		4275.7	91.8
4	488.2	335.5	16067	16.19	2150.2	1233.3	26.5
10	479.5	331.0	16179	16.37	866.4	546.5	40.8
22	457.6	357.0	16469	16.79	401.2	328.8	39.0
32	444.0	347.4	16654	17.05	279.1	243.2	52.9
42	426.5	333.6	16899	17.37	215.9	186.1	55.9
56.5	402.3	321.0	17249	17.78	164.0	140.7	55.1
77	373.7	303.7	17683	18.19	123.6	110.7	58.2
97	348.7	287.2	18080	18.46	100.5	93.6	58.9
113	331.0	275.0	18380	18.60	87.8	81.5	56.5
133	311.8	259.5	18727	18.66	76.1		

Table A - 45

Variation of Temperature and Dimensionless  
Parameters with X/D Ratio

Run No. 45		Barometric Pressure		-29.24" Hg			
		Ambient Air Temperature		-85.0°F			
		Inlet Air Temperature		-308.0°F			
		Mass Flow		-193.26 lbs/hr			
X/D	$t_m$ °F	$t_w$ °F	$N_{RE_x}$	$N_{GR_x}$ $\times 10^{-5}$	$N_{GZ_x}$	$N_{GZ}$	$N_{Nu}$
						(x + $\Delta x/2$ )	
0	308.0	286.0	17889	18.02		4846.0	66.7
4	303.9	231.0	17958	18.02	2428.0	1391.6	42.4
10	298.0	227.0	18057	18.01	977.1	614.1	47.9
22	286.9	237.0	18248	17.95	449.2	367.8	61.5
32	277.7	233.0	18409	17.88	311.8	270.7	56.0
42	270.0	227.0	18546	17.79	239.5	205.4	54.9
56.5	259.6	218.5	18734	17.63	180.0	153.4	54.7
77	246.0	208.0	18986	17.35	134.0	119.5	57.9
97	233.2	198.0	19230	16.99	107.9	100.2	62.6
113	223.2	191.5	19424	16.64	93.7	86.6	62.3
133	212.5	186.0	19637	16.19	80.5		

Table A - 46

Variation of Temperature and Dimensionless  
Parameters with X/D Ratio

Run No. 46		Barometric Pressure		- 29.30"Hg			
		Ambient Air Temperature		- 86.0°F			
		Inlet Air Temperature		- 510.0°F			
		Mass Flow		- 227.05 lbs/hr			
X/D	$t_m$ °F	$t_w$ °F	$N_{RE_x}$	$N_{GR_x}$ $\times 10^{-5}$	$N_{GZ_x}$	$N_{GZ}$	$N_{Nu}$
						(x + $\Delta x/2$ )	
0	510.0	469.0	17686	15.25			
4	495.0	358.8	17897	15.54	2394.5	4759.5	128.4
10	489.6	357.0	17974	15.64	962.1	1371.4	20.5
22	468.4	373.0	18283	16.04	445.2	606.7	47.9
32	453.0	364.0	18514	16.33	310.1	365.1	52.4
42	437.7	351.0	18784	16.64	240.0	270.3	55.4
56.5	417.9	337.0	19064	17.93	181.2	206.2	52.6
77	391.2	320.0	19504	17.33	136.2	155.2	56.5
97	367.5	303.0	19877	17.61	110.3	121.7	59.0
113	349.5	290.0	20225	17.81	96.5	102.8	62.5
133	329.5	277.0	20604	17.94	83.6	89.5	62.6

Table A - 47

Variation of Temperature and Dimensionless  
Parameters with X/D Ratio

Run No. 47		Barometric Pressure		- 29.29" Hg			
		Ambient Air Temperature		- 82.0°F			
		Inlet Air Temperature		- 495.0°F			
		Mass Flow		- 76.58 lbs/hr			
X/D	$t_m$ °F	$t_w$ °F	$N_{RE_x}$	$N_{GR_x}$ $\times 10^{-5}$	$N_{GZ_x}$	$N_{GZ}$	$N_{Nu}$
						$(x + \Delta x/2)$	
0	495.0	430.0	6036	15.79		1638.0	75.1
4	461.5	293.8	6201	16.45	830.7	478.5	21.5
10	440.0	252.0	6296	16.80	337.6	214.9	19.8
22	402.1	240.5	6517	17.51	159.2	130.7	12.0
32	385.5	233.8	6611	17.76	111.1	96.7	11.5
42	370.8	232.0	6697	17.96	85.8	74.1	17.6
56.5	345.0	249.2	6861	18.25	65.5	56.3	21.6
77	310.5	220.0	7072	18.43	49.6	44.7	23.7
97	278.5	201.8	7289	18.32	40.7	38.1	25.6
113	254.9	185.0	7458	18.01	35.8	33.4	25.1
133	230.0	170.0	7636	17.42	31.3		

Table A - 48

Variation of Temperature and Dimensionless  
Parameters with X/D Ratio

<u>Run No. 48</u>		Barometric Pressure	-29.60"Hg				
		Ambient Air Temperature	-81.0°F				
		Inlet Air Temperature	-495.0°F				
		Mass Flow	-76.36 lbs/hr				
X/D	$t_m$ °F	$t_w$ °F	$N_{RE_x}$	$N_{GR_x}$ $\times 10^{-5}$	$N_{GZ_x}$	$N_{GZ}$	$N_{Nu}$
						(x + $\Delta x/2$ )	
0	495.0	421.0	6019	16.20		1630.9	61.8
4	465.0	287.0	6166	16.81	825.9	476.7	22.2
10	441.5	245.0	6286	17.27	337.1	214.1	17.7
22	405.5	233.0	6479	17.91	158.2	130.0	12.3
32	387.0	224.0	6583	18.21	110.6	96.6	15.2
42	365.5	207.0	6709	18.51	86.0	74.3	16.5
56.5	337.5	223.0	6879	18.80	65.7	56.9	26.5
77	290.5	196.0	7185	18.92	50.5	45.5	25.4
97	255.5	176.0	7432	18.55	41.6	38.9	25.4
113	232.0	161.0	7607	17.97	36.6	34.1	26.3
133	207.0	151.0	7803	16.99	32.0		

APPENDIX B  
DEFINITIONS AND EVALUATION OF DIMENSIONLESS  
PARAMETERS

The purpose of this appendix is to provide the reader the definitions and method of evaluation of some measured quantities and various dimensionless parameters encountered in this study.

a. Mean wall temperature,  $t_w$

Mean wall temperature at any particular station along the pipe refers to the mean temperature of the circumference at that position. At every station the temperature of the top, side and bottom of the pipe wall was measured and the mean wall temperature  $t_w$  was evaluated as:

$$t_w = \left( \frac{t_{\text{top}} + 2t_{\text{side}} + t_{\text{bottom}}}{4} \right)$$

b. Mean fluid temperature,  $t_m$

This is the mean fluid temperature over a cross-section area of the pipe and is determined from the temperature profiles across the vertical and horizontal diameters.

$$t_m = \frac{(t_{mv} + t_{mH})}{2}$$

where

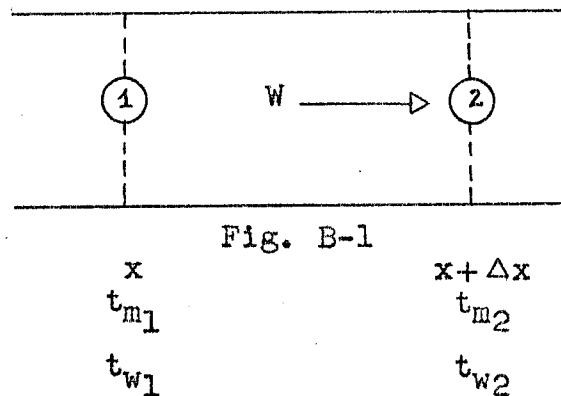
$t_{mv}$  = Mean fluid temperature on the vertical diameter.

$t_{mH}$  = Mean fluid temperature on the horizontal diameter.

and

$$t_{mv} \text{ or } t_{mH} = \frac{2}{R^2} \int_0^R t_r r dr$$

Figure B-1 represents a typical pipe section



$t_{m1}$  and  $t_{w1}$  are the mean fluid and mean wall temperatures at  $x$ .

$t_{m2}$  and  $t_{w2}$  are the mean fluid and mean wall temperatures at  $(x + \Delta x)$ ,

and  $w$  is the mass flow (lbs./hr.).

c. Nusselt number,  $N_{Nu_x}$

The Nusselt number between any two consecutive stations was considered as the local nusselt number and is given by

$$N_{Nu_x} = \frac{hD}{k}$$

where the film coefficient,  $h$  is given by

$$h = \frac{q}{A \cdot \Delta t}$$

where

$$\Delta t = (t_{m1} + t_{m2})/2 - (t_{w1} + t_{w2})/2$$

and

$$q = WC_p(t_{m1} - t_{m2})$$

Therefore

$$N_{Nu_x} = \frac{hD}{k} = \frac{WC_p(t_{m1} - t_{m2})D}{A k \Delta t}$$

$C_p$  and  $k$  are evaluated at  $(t_{m1} + t_{m2})/2$ .

d. Mean Nusselt number,  $N_{Num}$

The average or mean Nusselt number was evaluated by the following equation:

$$N_{Num} = \frac{1}{L} \int_0^L N_{Nu_x} dx$$

e. Grashof number,  $N_{Gr_x}$

The Grashof number at any position  $x$  was defined by

$$N_{Gr_x} = \frac{D^3 \cdot \rho_x^2 \cdot \epsilon \cdot \beta \cdot \Delta t}{\mu_x^2}$$

where

$$\beta = \frac{1}{t_o} \left( \frac{1}{\sigma_R} \right)$$

$$\Delta t = (t_{m1} - t_0) \text{ (}^\circ\text{R or }^\circ\text{F)}$$

$\rho_x$  and  $\mu_x$  are the properties of air evaluated at  $t_{m_x}$ .

f. Reynolds number,  $N_{Re_x}$

The Reynolds number at any position  $x$  was defined as:

$$N_{Re_x} = \frac{\rho_x D \bar{U}_x}{\mu_x}$$

where

$\rho_x$ ,  $\mu_x$  and  $\bar{U}_x$  are determined at  $t_{m_x}$ .

g. Prandtl number,  $N_{Pr_x}$

The Prandtl number was defined as :

$$N_{Pr_x} = \frac{c_p \mu}{k}$$

It is assumed to constant at 0.71 (for air).

h. Graetz number,  $N_{Gz_x}$

The Graetz number at any position was evaluated by the following equation :

$$N_{Gz_x} = \frac{W C_{px}}{K_x X}$$

$X$  is the length of the pipe from the entrance to the position where Graetz number is to be evaluated;  $C_{px}$  and  $K_x$  are evaluated at  $t_{m_x}$ .

In the appendix A, two values of Graetz number are given, one at  $(x + \frac{\Delta x}{2})$  and the other at  $(x + \Delta x)$ . They are to be used for the plot of local Nusselt number and mean Nusselt number vs. Graetz number.

## VITA AUCTORIS

- 1942 Born in Amritsar, India on November 1.
- 1958 Matriculated from Government High School Daska, Sialkot, Pakistan.
- 1963 Received Higher Secondary School Certificate from Islamia College Peshawar, Peshawar, Pakistan.
- 1966 Graduated in Mechanical Engineering from Peshawar University, Peshawar, Pakistan.
- 1970 Candidate for the Degree of Master of Applied Science in Mechanical Engineering at the University of Windsor, Ontario, Canada